

Hydrogen production through biocatalyzed electrolysis

René Alexander Rozendal

Promotor:

Prof.dr.ir. C.J.N. Buisman
Hoogleraar Biologische Kringlooptechnologie
Sectie Milieutechnologie

Co-promotor:

Dr.ir. H.V.M. Hamelers
Universitair Docent bij de sectie Milieutechnologie

Promotiecommissie:

Prof.dr. B.E. Logan

Dr. R. Mulder

Prof.dr.ir. A.J.M. Stams

Prof.dr.ing. M. Wessling

Pennsylvania State University, USA

Paques bv, Balk

Wageningen Universiteit

Universiteit Twente

Dit onderzoek is uitgevoerd binnen de onderzoekschool SENSE (Socio-Economic and Natural Sciences of the Environment).

Hydrogen production through biocatalyzed electrolysis

René Alexander Rozendal

Proefschrift

ter verkrijging van de graad van doctor
op gezag van de rector magnificus
van Wageningen Universiteit,
Prof.dr. M.J. Kropff,
in het openbaar te verdedigen
op woensdag 24 oktober 2007
des namiddags te vier uur
in het Auditorium van
Hogeschool Van Hall Larenstein
te Leeuwarden

Rozendal, R.A., 2007.

Hydrogen production through biocatalyzed electrolysis.

PhD thesis Wageningen University, Wageningen, the Netherlands – with references – with summary in Dutch.

ISBN 978-90-8504-731-5

“Imagination is more important than knowledge. For knowledge is limited to all we now know and understand, while imagination embraces the entire world, and all there ever will be to know and understand.”

Albert Einstein

Opgedragen aan Agnes Catharina Rozendal-Sjamaar
(12/05/1917 - 04/08/2000)

Abstract

Rozendal, R.A., 2007. *Hydrogen production through biocatalyzed electrolysis*. PhD thesis Wageningen University, Wageningen, The Netherlands.

Up till now, many wastewaters were unsuitable for biological hydrogen production due to the slightly endothermic nature of many of the involved reactions. This PhD thesis describes the first steps in the development of a novel technology for hydrogen production that is capable of overcoming this thermodynamic barrier. This bioelectrochemical technology, referred to as biocatalyzed electrolysis, was invented and developed within this PhD project. Biocatalyzed electrolysis is capable of overcoming thermodynamic barriers through the application of electrochemically active microorganisms in combination with a small input of electrical energy. Electrochemically active microorganisms are capable of using an electrode as an electron acceptor for the oxidation of organic matter. This turns the electrode into a bioanode. Biocatalyzed electrolysis couples this bioanode to a conventional proton reducing cathode by means of a power supply. Consequently, the organic matter is electrolyzed and hydrogen is generated. The theoretically required applied voltage for biocatalyzed electrolysis of organic material is about 0.12 V, which equals a theoretical energy requirement of about 0.26 kWh/Nm³ H₂. Microbial metabolic losses and other potential losses (e.g., ohmic loss and electrode overpotentials) will increase this energy requirement under practical conditions, but the energy requirement of biocatalyzed electrolysis is expected to remain far below that of commercial water electrolysis (4.4 to 5.4 kWh/Nm³ H₂).

The scope of this thesis is to investigate the feasibility of hydrogen production through biocatalyzed electrolysis of organic material. The principle of the biocatalyzed electrolysis concept is proven and it is shown that biocatalyzed electrolysis is a promising technology for hydrogen production from wastewater with a wide range of possible applications in wastewater treatment, transportation, and industry. It is expected that volumetric hydrogen production rates can be improved to over 10 Nm³ H₂/m³ reactor volume/day at an energy input of below 1 kWh/Nm³ H₂ by improving the performance of the critical biocatalyzed electrolysis system components (bioanode, membrane, and cathode). However, to get to a mature hydrogen production technology, it is also important to realize a cost-effective scale-up that considers ohmic losses and material costs.

Keywords: Biocatalyzed electrolysis, BEAMR, microbial fuel cell, MFC, electrochemically active microorganisms, bioanode, ion exchange membrane, biocathode, hydrogen, wastewater, fermentation

Preface

In the first half of 2003 I was doing my MSc graduation work at Paques bv, a Dutch company specialized in the field of industrial wastewater treatment. At that time, Cees Buisman was Technology Manager at Paques bv and was soon to start as a professor at the Sub-Department of Environmental Technology of Wageningen University. In an afternoon lunch walk I asked him whether he was going to initiate new PhD projects in Wageningen that he thought I would find interesting to apply for. Then he told me about microbial fuel cells and I was inspired.

In the weeks after this conversation, I collected and studied all the microbial fuel cell literature that was available at the time. The topic was in my mind all the time and on one night, just before falling asleep, I experienced a true “*Eureka!*” moment. I jumped out of bed and made a few process schemes of biocatalyzed electrolysis. Clearly, this “*Eureka!*” moment has changed my life as after a little more than 4 years I have now finished my PhD thesis on biocatalyzed electrolysis.

Table of Contents (Abbreviated)

T

Chapter 1.....	1
General Introduction	
Chapter 2.....	43
Principle and Perspectives of Hydrogen Production through Biocatalyzed Electrolysis	
Chapter 3.....	65
Effects of Membrane Cation Transport on pH and Microbial Fuel Cell Performance	
Chapter 4.....	87
Effect of the Type of Ion Exchange Membrane on Ion Transport and pH in Biocatalyzed Electrolysis of Wastewater	
Chapter 5.....	101
Performance of Single Chamber Biocatalyzed Electrolysis with Different Types of Ion Exchange Membranes	
Intermezzo.....	129
Understanding Cathode pH Increase from the Nernst-Planck Flux Equation	
Chapter 6.....	143
Hydrogen Production with a Microbial Biocathode	
Chapter 7.....	165
Concluding Remarks and Outlook	
Summary/Samenvatting.....	187

1

2

3

4

5

I

6

7

S

Table of Contents

(Extended)



Chapter 1.....	1
General Introduction	
1.1 Background.....	4
1.1.1 Global warming & crude oil scarcity	4
1.1.2 Renewable energy.....	6
1.1.3 Wastewater treatment – biogas or hydrogen?	9
1.1.4 Objective.....	11
1.2 Fermentative hydrogen production	11
1.2.1 Dark fermentation & thermodynamic limit	11
1.2.2 Second stage processes	15
1.3 Biocatalyzed electrolysis	16
1.3.1 Basic characteristics of biocatalyzed electrolysis.....	16
1.3.2 Exocellular electron transfer by electrochemically active microorganisms	17
1.3.3 Thermodynamics & fundamentals of bioelectrochemical conversions	21
1.3.4 Microbial fuel cells	27
1.3.5 Biocatalyzed electrolysis	31
1.4 Thesis scope & outline.....	34
1.5 References	36
 Chapter 2.....	 43
Principle and Perspectives of Hydrogen Production through Biocatalyzed Electrolysis	
2.1 Introduction.....	46
2.2 Materials and methods.....	49
2.2.1 Electrochemical cell.....	49
2.2.2 Medium preparation	49
2.2.3 Electrochemically active microorganisms.....	50
2.2.4 Experimental procedures	50
2.2.5 Electrochemical calculations	51
2.3 Results and discussion.....	52
2.4 Perspectives.....	57
2.5 Acknowledgments	60
2.6 References	61

Chapter 3.....	65
Effects of Membrane Cation Transport on pH and Microbial Fuel Cell Performance	
3.1 Introduction.....	68
3.2 Materials and methods.....	69
3.2.1 Electrochemical cell.....	69
3.2.2 Medium and microorganisms	70
3.2.3 Experimental procedures and calculations	71
3.3 Results and discussion.....	73
3.3.1 Membrane cation transport	73
3.3.2 Sulfonate group occupation.....	78
3.3.3 Effects on pH and MFC performance.....	79
3.3.4 Implications for MFC application on wastewaters	80
3.4 Acknowledgments	83
3.5 References	83
 Chapter 4.....	 87
Effect of the Type of Ion Exchange Membrane on Ion Transport and pH in Biocatalyzed Electrolysis of Wastewater	
4.1 Introduction.....	90
4.2 Materials and methods.....	92
4.2.1 Electrochemical cell.....	92
4.2.2 Experimental procedures and calculations	92
4.3 Results and discussion.....	94
4.4 Conclusions	98
4.5 Acknowledgments	98
4.6 References	99
 Chapter 5.....	 101
Performance of Single Chamber Biocatalyzed Electrolysis with Different Types of Ion Exchange Membranes	
5.1 Introduction.....	104
5.1.1 Biocatalyzed electrolysis	104
5.1.2 Performance	104
5.1.3 Single chamber configuration.....	105
5.1.4 Membrane ion transport	105
5.1.5 Anion exchange membrane	106
5.1.6 Objective.....	106

5.2	Materials and methods.....	107
5.2.1	Electrochemical cell.....	107
5.2.2	MEA preparation.....	108
5.2.3	Experimental procedures and calculations	109
5.3	Results and discussion.....	112
5.3.1	Applied voltage scans	112
5.3.2	Hydrogen yield tests.....	114
5.3.3	Electrochemical impedance spectroscopy	117
5.3.4	Permeated water analysis.....	118
5.3.5	Scanning electron microscopy	120
5.3.6	Potential losses	121
5.3.7	Outlook	123
5.4	Conclusions	125
5.5	Acknowledgments.....	126
5.6	References	126

Intermezzo.....129

Understanding Cathode pH Increase from the Nernst-Planck Flux Equation

I.1	Nernst-Planck flux equation	132
I.2	Why does pH increase?	133
I.3	What is the effect of membrane type?	137
I.4	What is the effect of cathode chamber pH increase?.....	140
I.5	References.....	142

Chapter 6.....143

Hydrogen Production with a Microbial Biocathode

6.1	Introduction.....	146
6.2	Materials and methods.....	148
6.2.1	Biocatalyzed electrolysis cell.....	148
6.2.2	Experimental set-up.....	149
6.2.3	Experimental procedures	150
6.2.4	Scanning electron microscopy (SEM)	152
6.3	Results and discussion.....	152
6.3.1	Biocathode start up.....	152
6.3.2	Polarization curves.....	154
6.3.3	Hydrogen yield tests.....	155
6.3.4	Indications for the microbial origin of the biocathode.....	157
6.3.5	Future research and outlook	159

6.4	Acknowledgments	161
6.5	References	161

Chapter 7..... 165

Concluding Remarks and Outlook

7.1	General conclusion	168
7.2	Applications	169
7.2.1	Wastewater treatment	169
7.2.2	Transportation	170
7.2.3	Industry	171
7.3	Performance – status & objective	172
7.4	Outlook – scale up & future research	173
7.4.1	Scale up issues	173
7.4.2	Critical biocatalyzed electrolysis system components	178
7.5	To summarize,	184
7.6	References	184

Summary/Samenvatting..... 187

Summary	189
----------------------	------------

Samenvatting	193
---------------------------	------------

Dankwoord/Acknowledgments	199
--	------------

Curriculum Vitae.....	202
------------------------------	------------

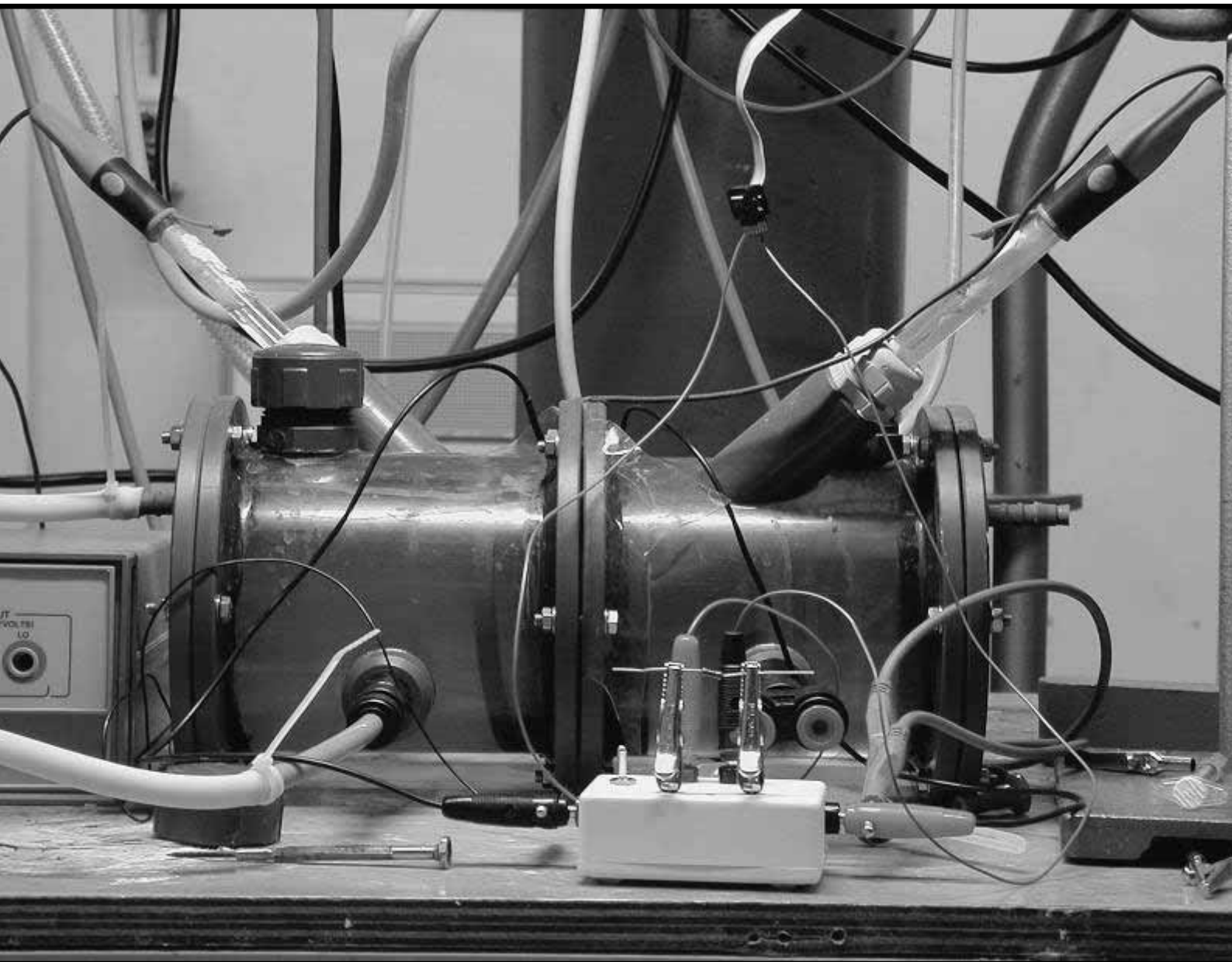
List of publications.....	203
----------------------------------	------------

List of patents	203
------------------------------	------------

SENSE education activities	204
---	------------

General Introduction

1



Paragraph 1.3.3 of this chapter has been published in:

Logan, B. E.; Hamelers, B.; Rozendal, R.; Schröder, U.; Keller, J.; Freguia, S.; Aelterman, P.; Verstraete, W.; Rabaey, K. Microbial fuel cells: methodology and technology. *Environ. Sci. Technol.* **2006**, *40*, 5181-5192.

General Introduction

1

This PhD thesis describes the first steps in the development of a promising new technology for hydrogen production from wastewaters. This bioelectrochemical technology, referred to as biocatalyzed electrolysis, was invented and developed within this PhD project.

Up till now, many wastewaters were unsuitable for biological hydrogen production due to the slightly endothermic nature of many of the involved reactions. Biocatalyzed electrolysis, however, is capable of overcoming this thermodynamic barrier through the application of electrochemically active microorganisms in combination with a small input of electrical energy. By doing this, biocatalyzed electrolysis can significantly increase hydrogen production from wastewaters compared to the current “state of the art” technologies, such as dark fermentation. Furthermore, the innovative design makes a much wider variety of wastewaters than before suitable for hydrogen production. Therefore, biocatalyzed electrolysis can be regarded as a potential breakthrough technology in the field of biological hydrogen production from wastewaters.

This chapter introduces the technology by first discussing the background of hydrogen production from wastewaters from the viewpoint of the global need for novel renewable energy processes. Secondly, this chapter discusses the “state of the art” technologies that are currently available for hydrogen production from wastewaters. Finally, this chapter describes the basic principles of biocatalyzed electrolysis.

1.1 Background

1.1.1 Global warming & crude oil scarcity

1 In 2007 the UN's Intergovernmental Panel on Climate Change (IPCC) presented their fourth assessment report (1), which speaks about a *very high confidence* (>90%) that the globally averaged net effect of human activities since pre-industrial times has been one of global warming. According to the report this global warming effect has been caused by a human induced, dramatic increase of atmospheric concentrations of greenhouse gasses, such as carbon dioxide, methane, and nitrous oxide (Figure 1.1). For a large part, this increase has been the result of the exploitation and combustion of fossil fuels (coal, oil, and natural gas).

The IPCC report states that the increase of atmospheric greenhouse gas concentrations has caused a worldwide temperature increase of 0.56 to 0.92 °C in the last 100 years, which resulted in a sea level rise of about 17 cm due to the thermal expansion of sea water and the melting of ice over land (e.g., glaciers). Moreover, the IPCC report predicts that before the end of the 21st century the worldwide temperatures will increase with another 1.1 to 6.4 °C (with respect to 1990) and the sea level will rise with another 18 to 59 cm (with respect to 1990). Even if the atmospheric greenhouse gas concentrations would stabilize, temperature increase and sea level rise will continue for centuries as a result of the timescales associated with climate change. Furthermore, stabilization of the greenhouse gas concentrations seems highly improbable at the moment as current projections estimate that the total world primary energy demand will expand by almost 60% in 2030 of which fossil fuels will still account for 80-85% (2).

Other predicted side-effects of the increasing atmospheric greenhouse gas concentrations and global warming include the increasing frequency of extreme weather events (e.g., storms, floods), changes in amount and pattern of precipitation, acidification of the oceans, dramatic changes of ecosystems, expansion of tropical diseases, and change of global agricultural patterns. Although the severity of many of these side-effects is uncertain, the threat alone already urges for an increase of political attention.

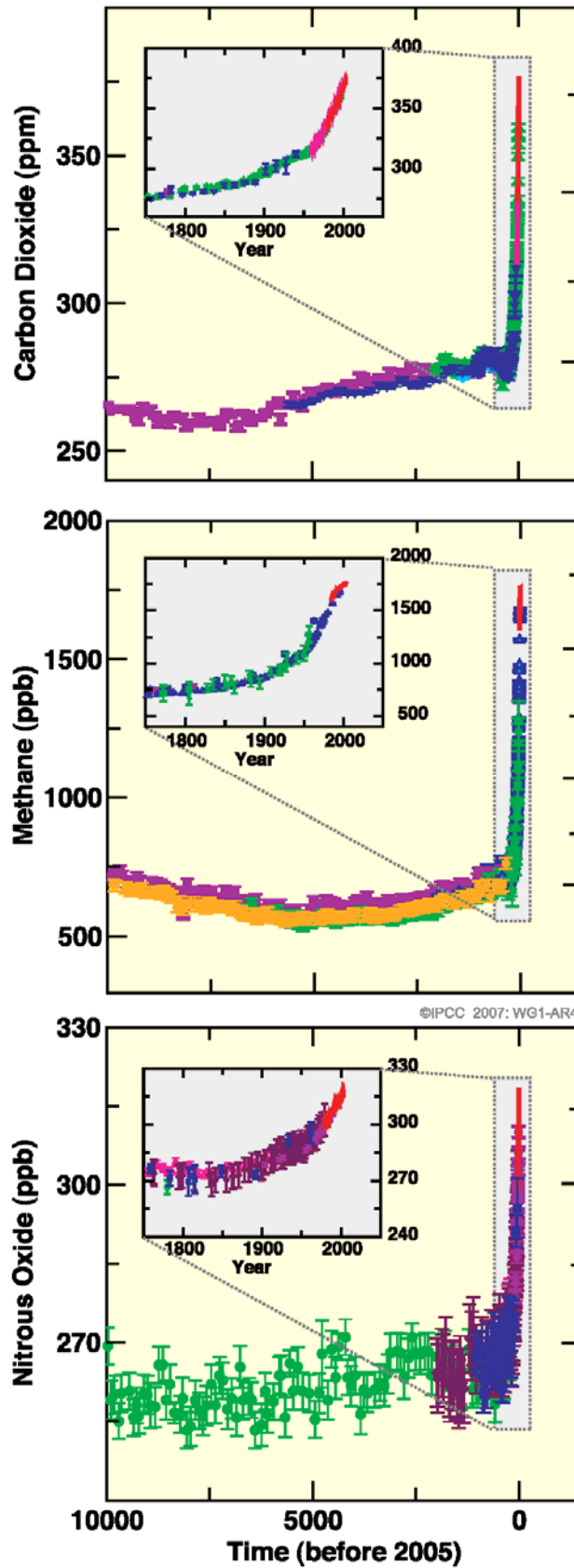


Figure 1.1. Historic increase of the global atmospheric concentrations of the three most important greenhouse gases from ice core and modern data (from *(1)*, reprinted with permission of the IPCC).

Besides global warming, also the growing oil scarcity and security of supply are important issues related to fossil fuel consumption (3). Fossil fuels show an uneven distribution across the world, which is especially true for crude oil. Most of the remaining crude oil reserves are concentrated in the Middle East region. Furthermore, oil production is expected to peak in the near future as a result of depletion of the easily extractable oil reserves, the rapid increase of demand from newly industrialized countries (e.g., China, India), and underinvestment in the development of new production capacity.

Due to the uneven distribution of fossil fuels and crude oil scarcity, the crude oil market price is subject to large unpredictable fluctuations. For example, the International Energy Agency in their world energy outlook 2004 predicted that 2003 “high” crude oil price (in real year-2000 dollars) of 27 \$/barrel would soon fall back to about 22 \$/barrel in 2006, remain more or less constant until 2010, and then steadily increase to a price of about 29 \$/barrel in 2030. History has shown, however, that this prediction was far from the truth. In the period 2004-2006 a decrease in oil supply due to growing turbulence in the Middle east (e.g., war in Iraq, Iranian nuclear energy program, the crisis between Israel and Lebanon) and many other reasons (e.g., hurricane Katrina (New Orleans), strikes in Venezuela), caused the crude oil price to increase to market prices far above 70 \$/barrel in 2006. Furthermore, as the prices of other fossil fuels (e.g., natural gas) are linked to the crude oil price, these enormous fluctuations also influenced other energy prices and consequently the world economy as a whole.

1.1.2 Renewable energy

The increasing awareness of the possible anthropogenic effect on climate change in combination with the instabilities in the fossil fuel market are leading to an increasing political drive to reduce greenhouse gas emissions and to stimulate renewable energy. In 1997, the first international steps in this direction were made in the Kyoto Protocol. This protocol, signed by more than 160 countries and covering over 55% of the global greenhouse gas emissions, obligates the participating industrialized countries to reduce their greenhouse gas emissions by 5% (with respect to 1990) in the period

2008 to 2012. Unfortunately, the Kyoto Protocol was not ratified by the United States, the world's largest emitter of greenhouse gases. Still, the Kyoto Protocol has created a worldwide awareness and many new developments in the field of renewable energy have taken place since then. For example, in March 2007 the European Union committed itself to a 20% renewable energy target and a minimum target of 10% for transport biofuels by 2020.

Although these measures are important steps in the right direction, much more of these steps will be required before society is completely based on renewable energy. On the long term solar energy is the ideal energy source in such a society, as it is earth's primary input of energy and available in large excess (Figure 1.2).

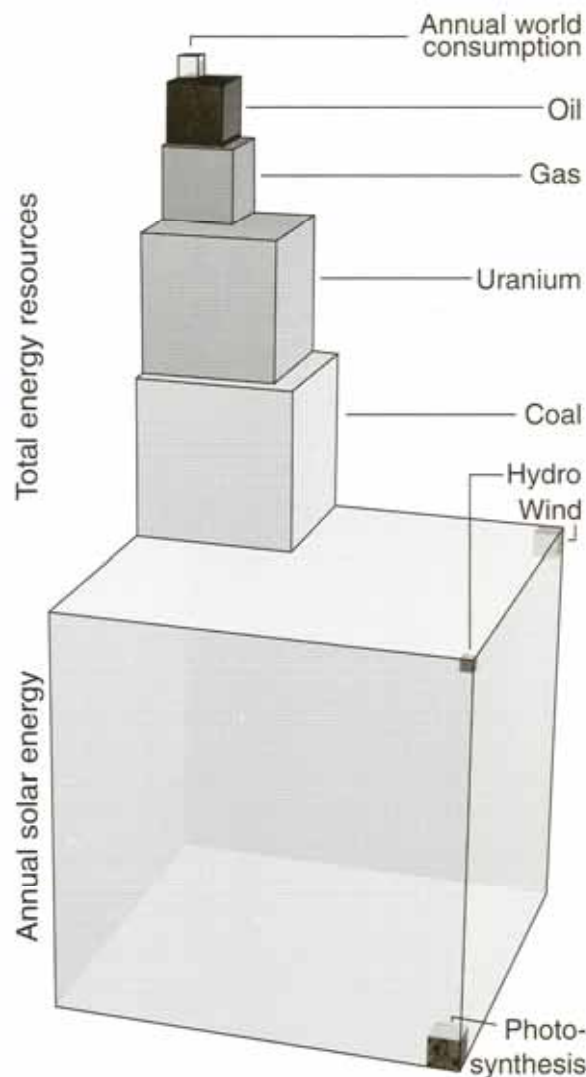


Figure 1.2. Annual solar energy compared to the annual world consumption of energy and global reserves of non-renewable energy resources (from (4), reprinted with permission of Cambridge University Press).

The sun radiates more than 170000 TW to our planet (5), whereas the total world energy consumption in 2001 was around 13.5 TW and is expected to increase to between 27 and 40.8 TW in the year 2050 (6). This means that the total amount of solar energy reaching the earth in one hour is in the same order as the total world energy consumption in one year (6).

However, a society that is completely based on solar energy is not considered to be a realistic option on a short term due to technological and economic obstacles. Therefore, other renewable energy technologies are being developed in parallel to solar energy. About 2000 TW of the 170000 TW solar radiation flux is continuously transformed into wind power, 100 TW is continuously stored as biomass through photosynthesis (7), and 6 TW is continuously transformed into hydropower through the water cycle (Figure 1.2). Nowadays, these indirect forms of solar energy are exploited to some extent for electricity production through wind turbines, biomass gasification/combustion and hydroelectric dams. Although these indirect forms of solar energy can be exploited for electricity production on a much larger scale in the future, a renewable society will also require large amounts of renewably produced chemicals and fuels.

Biomass is the most preferred renewable resource for chemical and fuel production as it already consists of renewable energy stored in chemical bonds. Nowadays, many conversion processes are being developed or have already been developed for chemical and fuel production from relatively concentrated biomass streams, such as wood and agricultural (by)products (8-12). However, not many conversion processes currently exist for chemical and fuel production from diluted aqueous biomass streams, such as industrial, agricultural and municipal wastewaters. Still, wastewaters form a large potential resource for renewable chemical and fuel production as they contain large amounts of dissolved organic compounds (13).

Wastewaters are traditionally treated aerobically, which consumes a lot of energy. However, if chemical and fuel production technologies are used for wastewater treatment, a net amount of energy can be produced. Wastewaters typically have a negative market value, which benefits the economy of chemical and fuel production from wastewaters. Furthermore, as wastewater treatment is typically regulated by law, the complete logistics

around wastewater collection is often already arranged. However, wastewaters often consist of a complex mixture of dissolved organic compounds. Wastewater utilization for fuel and chemical production, therefore, will require flexible and robust technology. In this perspective biological treatment is the ideal candidate as biological conversions in natural ecosystems also commonly occur in dilute aqueous environments. Two biological technologies are of particular interest for this purpose: (i) methanogenic anaerobic digestion, and (ii) biological hydrogen production. Both technologies have their own interesting features, but have in common that they make use of a gas/liquid phase separation to remove the product from the wastewater.

1.1.3 Wastewater treatment – biogas or hydrogen?

Methanogenic anaerobic digestion is a mature technology with thousands of full scale references across the world. For example, Paques bv, the world market leader in anaerobic wastewater treatment, has installed over 600 of their proprietary Biopaq® installations, treating over 9 million kg of COD per day (14). This results in a yearly production of over 1.15 billion m³ of methane which equals the natural gas demand of 1.4 million people equivalents. The biogas (CH₄/CO₂ mixture) produced through anaerobic digestion is usually used as a fuel source for electricity and heat production or flared on site. Further, it is currently also investigated whether the injection of biogas (after CO₂ removal) into the natural gas grid is feasible.

Biological hydrogen production, on the other hand, is much less developed than methanogenic anaerobic digestion. No full scale installations currently exist and many technological hurdles still have to be overcome before biological hydrogen production can be regarded as a mature wastewater treatment technology. Still, hydrogen might prove to be a more interesting product than biogas in many cases as hydrogen is both interesting as chemical and fuel. Even in today's society there exists a large demand for hydrogen gas for applications such as fossil fuel upgrading in the petrochemical industry and fat saturation in the food industry. For this reason, hydrogen represents a much higher added value than methane from

biogas. On a COD basis hydrogen is about 7 times more valuable than methane (0.75 \$/kg H₂-COD vs. 0.11 \$/kg CH₄-COD - calculated from (15)). This means that the amount of hydrogen that can be produced from a certain amount of wastewater is about 7 times as valuable as the amount of methane that can be produced from the same amount of wastewater.

Furthermore, hydrogen has also got some interesting characteristics as a fuel. Hydrogen can be converted directly into electrical energy using fuel cell technology (e.g., in a fuel cell powered passenger cars), which is emission-free with water as the only byproduct. Fossil fuels, on the other hand, are typically combusted (e.g., in passenger cars with internal combustion engines), which emits large amounts of NO_x, SO_x, and particulate matter that can negatively affect air quality in urban regions (16).

Another interesting property of hydrogen is that it can be produced from almost any kind of renewable energy. Whereas biogas can only be produced renewably from biomass, hydrogen can be produced from renewable electricity through water electrolysis, directly from solar energy through photoelectrolysis, from dry biomass through gasification, and from wastewater through biological conversion. All these hydrogen production technologies can work complementary to each other, which creates much more flexibility in the supply of hydrogen than there is in the supply of biogas. Furthermore, in a transition period from fossil to renewable fuels, hydrogen could temporarily even be produced from fossil fuels in a carbon dioxide neutral way if the produced carbon dioxide is separated from hydrogen and stored underground or in the ocean, i.e., carbon dioxide capture and storage (CCS). In that case the hydrogen distribution infrastructure can already be developed before truly renewable hydrogen production technologies become available. Furthermore, on the long term, hydrogen might even provide a way to produce fuels with a carbon dioxide negative effect, i.e., when hydrogen is produced from biomass in combination with CCS there is a net consumption of carbon dioxide so that atmospheric greenhouse gas concentrations can be reduced.

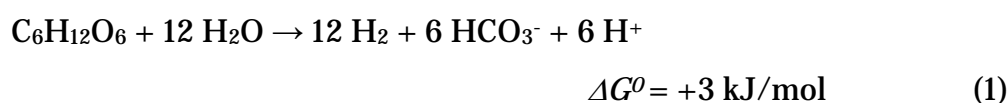
1.1.4 Objective

Whether hydrogen will ever become the fuel of the future remains uncertain and will depend on many political, societal, and technological issues. However, even without becoming the fuel of the future, there will always be a large future demand for renewably produced hydrogen (e.g., for industrial use). Hydrogen production from dissolved organic compounds in wastewater, therefore, is an interesting route to explore. For this reason, this PhD thesis investigates the principles and perspectives of biocatalyzed electrolysis as a new technology for biological hydrogen production from wastewater. Before discussing this new technology, however, we first discuss the technologies that are currently considered to be “state of the art” for biological hydrogen production from wastewaters.

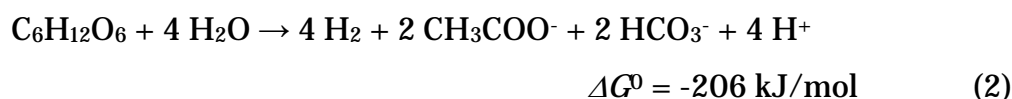
1.2 Fermentative hydrogen production

1.2.1 Dark fermentation & thermodynamic limit

The most promising of the currently known biological hydrogen production technologies from wastewaters is dark fermentation, which is characterized by high production rates of up to about 30 Nm³ H₂/m³ reactor volume/day (17). Dark fermentation, also referred to as heterotrophic hydrogen production, is carried out by a wide variety of microorganisms, such as *Clostridiaceae* and *Enterobacteriaceae* (17,18). In nature, hydrogen production is a way for these microorganisms to dispose of excess reducing equivalents that are produced under anaerobic conditions (e.g., in the form of reduced ferredoxin and NADH) (17,19). Carbohydrate-rich feedstocks are regarded to be the most suitable feedstock for dark fermentation (18,19). For this reason, glucose is most often studied as a model substrate for dark fermentation. Complete conversion of glucose to hydrogen gas theoretically yields 12 mol H₂/mol glucose:



Unfortunately, the Gibbs free energy of this reaction is only negative for very low hydrogen partial pressures. Therefore, this reaction is unfavorable to sustain microbial life under hydrogen accumulating conditions as there is not enough Gibbs free energy available for ATP generation (20). From a biochemical and thermodynamic point of view, the reaction that optimizes ATP generation under hydrogen accumulating conditions is the generation of 4 mol H₂/mol glucose with 2 mol acetate/mol glucose as a byproduct (20):



The metabolic pathway for achieving this optimal yield starts with the production of pyruvate from glucose through glycolysis (Figure 1.3). The conversion of glucose through glycolysis yields two pyruvate, 2 NADH, and 2 ATP (21). Subsequently, pyruvate is oxidized to acetyl-CoA, either catalyzed by pyruvate:ferredoxin oxidoreductase to form reduced ferredoxin (Fd_{red}) and carbon dioxide (*Clostridiaceae*), or catalyzed by pyruvate:formate lyase to form formate (*Enterobacteriaceae*) (21,22). Acetyl-CoA can be converted to acetate with additional ATP generation (21,23), which doubles the ATP formation from 2 mol ATP/mol glucose (from glycolysis) to 4 mol ATP/mol glucose.

However, before acetate formation can occur all produced reducing equivalents (NADH, Fd_{red}, and formate) first have to be disposed of properly. As both the Fd_{red}/Fd_{ox} ($E^0' = -0.420 \text{ V}$) and formate/HCO₃⁻ ($E^0' = -0.406 \text{ V}$) redox couples have a standard redox potential that is similar to that of proton reduction ($E^0' = -420 \text{ V}$) (13,21), Fd_{red} and formate can be readily converted to hydrogen gas at partial hydrogen pressures typically occurring in hydrogen producing reactors ($0 < p\text{H}_2 < 1 \text{ bar}$; Figure 1.4). The reoxidation of NADH, on the other hand, is much less straightforward under hydrogen accumulating conditions.

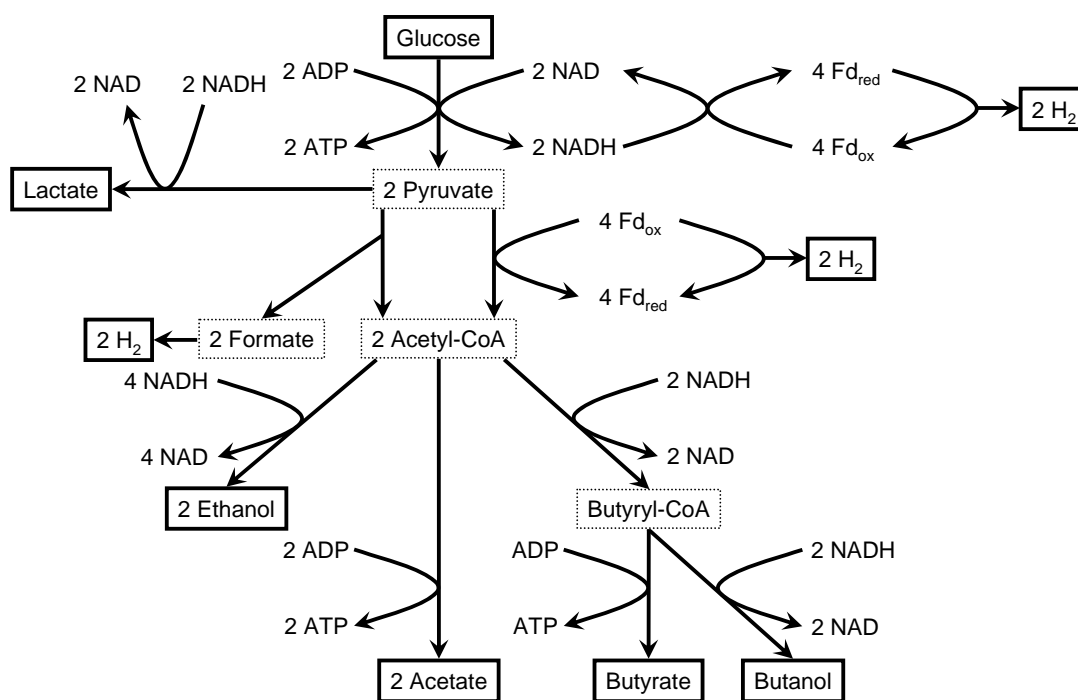


Figure 1.3. Overview of possible metabolic pathways during dark fermentation of glucose.

The redox couple NADH/NAD ($E^0' = -0.320$ V) has a standard redox potential that is significantly higher than that of proton reduction ($E^0' = -0.420$ V). This means that NADH can only be converted to hydrogen gas at low hydrogen partial pressures and/or high intracellular NADH/NAD ratios. Microbial intracellular NADH/NAD ratios are typically in the order of 0.1 to 10 (24-27), which means that the hydrogen partial pressure needs to be below 5 to 426 Pa respectively before NADH can be oxidized to form hydrogen gas (Figure 1.4).

If the hydrogen partial pressure is below these values, NADH can indeed be oxidized by the enzyme NADH:ferredoxin oxidoreductase. The oxidation of NADH by the enzyme NADH:ferredoxin oxidoreductase produces Fd_{red} that subsequently can be converted to hydrogen gas as described above. This increases the hydrogen yield to 4 mol H₂/mol glucose. Furthermore, as all of the reducing equivalents are now properly disposed of, acetyl-CoA can be converted to acetate with additional ATP generation.

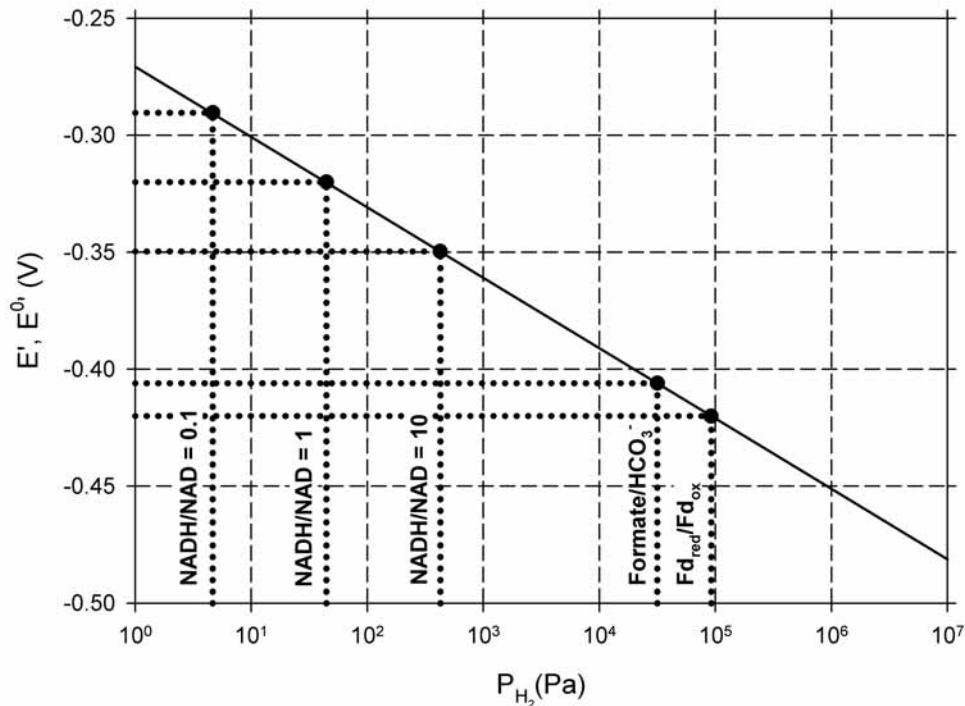


Figure 1.4. The redox potential at pH 7 (E') of the redox couple NADH/NAD (at a ratio of 0.1, 1 ($=E^0$), and 10) and the standard redox potential at pH 7 (E^0) of the redox couples formate/ HCO_3^- and Fd_{red}/F_{dox} , plotted against the hydrogen partial pressures below which these redox couples can be oxidized to produce hydrogen.

However, if the hydrogen partial pressures are insufficiently low to sustain an efficient NADH oxidation rate, alternative metabolic pathways are activated for NADH oxidation (18,23). In that case microorganisms start to oxidize NADH by producing more reduced fermentation byproducts instead of acetate, such as butyrate, lactate, ethanol, and butanol (Figure 1.3). These alternative metabolic pathways can also effectively consume the excess reducing equivalents in the form of NADH, but generate less than the 4 ATP/mol glucose that are generated when acetate is the end product. Furthermore, no additional hydrogen is produced, which limits the hydrogen yield to a maximum of 2 mol H_2 /mol glucose.

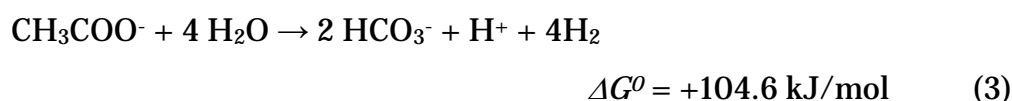
In literature many strategies have been described for lowering the hydrogen partial pressure to prevent the production of these more reduced fermentation byproducts. Some of these strategies include inert gas sparging, stream stripping, and continuous hydrogen removal through hydrogen selective membranes (23). Alternative strategies have focused on blocking the metabolic pathways towards the alternative fermentation end products so that intracellular NADH levels increase and more hydrogen is

produced (23). Although all of these strategies to increase hydrogen yields have been successful to some extent, the overall effect is relatively small as they only aim at the additional 2 mol H₂/mol glucose coming from NADH oxidation. This increases the hydrogen yield to a maximum of 4 mol H₂/mol glucose, while stoichiometrically 12 mol H₂/mol glucose can be produced.

Due to the biochemical and thermodynamic reasons explained above, dark fermentations in practice only yield a maximum of about 2.5 mol H₂/mol glucose under mesophilic conditions (13,18) and up to 4 mol H₂/mol glucose under thermophilic conditions (28). To achieve economic feasibility of hydrogen production from wastewaters, however, hydrogen yields will have to increase dramatically to about 10 mol H₂/mol glucose (29).

1.2.2 Second stage processes

As discussed in the previous paragraph, a well performing dark fermentation will produce acetate as the main byproduct, but other more reduced fermentation byproducts are also formed. Theoretically, at sufficiently low hydrogen partial pressures even acetate can be converted to hydrogen gas by means of dark fermentations. In that case acetate conversion would yield 4 mol H₂/mol acetate:



However, in order for this reaction to yield a minimum of -20 kJ of Gibbs free energy, i.e., the minimum amount of Gibbs free energy for ATP synthesis (30), the hydrogen partial pressure needs to be below 1 Pa (298.15 K, pH 7, [CH₃COO⁻]=[HCO₃⁻]=10 mM). Such a low hydrogen partial pressure is impossible to establish in practical hydrogen producing fermentations, but does occur in nature in acetate-oxidizing methanogenic cocultures (30-32). In these cocultures the hydrogen partial pressure is kept very low through the mechanism of interspecies hydrogen transfer (30,33). It is not surprising, therefore, that many research groups have been looking at anaerobic digestion to methane as an interesting second stage technology to convert the byproducts of dark fermentation (15,18).

However, if hydrogen and not methane is the product of choice, second stage hydrogen production technologies are required that are capable to deal with the endothermic nature of the byproduct conversion reactions at practical hydrogen partial pressures. For this purpose researchers have been looking at photoheterotrophic fermentations (18,34-36). Photoheterotrophic fermentations use the input of sunlight to deal with the endothermic nature of the byproduct conversion reactions. These fermentations typically apply pure cultures from the genera *Rhodopseudomonas*, *Rhodobacter*, and *Rhodospirillum* (37-39), but also mixed culture fermentations have recently been described (40). Furthermore, photoheterotrophic fermentations have been described for many types of substrates, including typical fermentation byproducts like lactate, acetate, and butyrate (37,40). Unfortunately, there are several drawbacks that so far have severely limited the practical application of photoheterotrophic fermentations. (i) The nitrogenase enzyme, which catalyzes hydrogen production in photoheterotrophic bacteria, is strongly inhibited by the presence of ammonia. This limits the application of photoheterotrophic fermentations to ammonium free wastewaters (36). (ii) As the process is dependent on sunlight there will be no production at night. (iii) The solar energy conversion efficiencies (i.e., solar energy \rightarrow hydrogen energy) of photoheterotrophic fermentations under practical conditions are low as they are typically far below 10% (36). (iv) Photoheterotrophic fermentations require enormous reactor surface areas due to the low surface intensity of solar radiation (22).

1.3 Biocatalyzed electrolysis

1.3.1 Basic characteristics of biocatalyzed electrolysis

Because it is doubtful whether dark fermentations and photoheterotrophic fermentations will ever become economically feasible (22), there exists a demand for alternative processes for hydrogen production from wastewaters. Such a new process should ideally combine the following characteristics: (i) amongst others it should be capable of converting dissolved organic compounds that are regarded to be dark fermentation byproducts, (ii) it should be capable of dealing with the

endothermic nature of the conversion reactions of many dissolved organic compounds to hydrogen in a more practical way than using sunlight (as used in photoheterotrophic fermentations), (iii) it should be robust and flexible, as it will be designed for hydrogen production from wastewaters, (iv) it should ideally be based on mesophilic mixed cultures that grow into the process through natural selection and are capable of converting a wide range of organic substrates.

All these characteristics are combined in biocatalyzed electrolysis, i.e., the technology that is described in this PhD thesis. Biocatalyzed electrolysis is indeed capable of dealing with the endothermic nature of the conversion reactions of many dissolved organic compounds to hydrogen. It establishes the required energy input by means of electrical energy instead of sunlight. Essential to the working principle of biocatalyzed electrolysis systems is the application of mixed consortia of electrochemically active microorganisms. Electrochemically active microorganisms are capable of exocellular electron transfer, i.e., electron transfer from the inside to the outside of the cell. This enables them to grow on an electrode surface while using the electrode as an electron acceptor for the oxidation of dissolved organic compounds (e.g., in wastewater). As the electrochemically active microorganisms release the electrons at a high energy level, a low electrode potential is established at the electrode, which can be utilized for hydrogen production in the biocatalyzed electrolysis process. To understand the principle of biocatalyzed electrolysis, therefore, it is necessary to understand the basic principles of exocellular electron transfer by electrochemically active microorganisms.

1.3.2 Exocellular electron transfer by electrochemically active microorganisms

Exocellular electron transfer is an important mechanism in anaerobic microbial communities to sustain microbial metabolism when electron donors are physically separated from electron acceptors (33). This situation commonly occurs in environments that contain large amounts of oxidized forms of iron and manganese, i.e., Fe(III) and Mn(IV). Fe(III)- and Mn(IV)-minerals form an interesting electron acceptor in anaerobic environments,

but they are poorly soluble in most natural environments (e.g., near neutral pH conditions). To be able to utilize these insoluble electron acceptors microorganisms have evolved several mechanisms through which electrons can be directed towards these exocellular electron acceptors (41). These strategies can be subdivided into two main categories: (i) exocellular electron transfer mediated by soluble electron shuttles (redox mediators), and (ii) exocellular electron transfer through direct contact with insoluble electron acceptors (mediator-less electron transfer) (Figure 1.5).

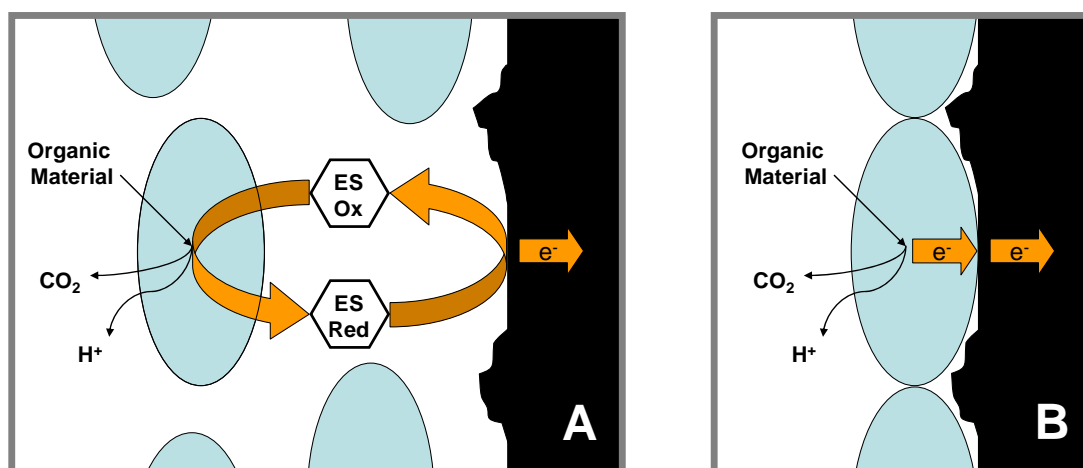


Figure 1.5. Exocellular electron transfer mechanisms to insoluble electron acceptors: (A) exocellular electron transfer mediated by soluble electron shuttles (ES), and (B) exocellular electron transfer through direct contact with insoluble electron acceptors (mediator-less electron transfer).

The first of these categories, i.e., exocellular electron transfer mediated by soluble electron shuttles, involves the redox cycling of the electron shuttles in between the microorganisms and insoluble electron acceptors. During this redox cycling the electron shuttles are continuously reduced by the microorganism and re-oxidized again by the insoluble electron acceptor. The electron shuttles involved in this process can be naturally present redox-active organic compounds, such as humic acids (42-44), but are also often produced by the microorganisms themselves, such as quinones (45-48). Furthermore, this exocellular electron transfer mechanisms in Fe(III)- and Mn(IV)-respiring microbial communities can also be artificially enhanced by adding artificial electron shuttles, such as thionine, iron chelates, and neutral red (49-52).

As electron shuttles also interact with electrode surfaces, microbial communities that respire according to this exocellular electron transfer mechanism are electrochemically active. This has formed the basis of the first generation of microbial fuel cells (MFCs; Paragraph 1.3.4). Unfortunately, in open environments such as MFCs that are continuously supplied with wastewater, electron shuttles are not retained in the system. This limits the applicability of this first generation of MFCs, as continuous addition of artificial electron shuttles is costly and imposes environmental risks due to the toxic nature of most artificial electron shuttles.

Renewed interest in MFC technology, however, emerged when researchers at the end of the last century realized the implication of the second category of exocellular electron transfer to insoluble electron acceptors, i.e., exocellular electron transfer through direct contact. In most other types of microorganisms the non-conductive cell wall of intact microbial cells prevents the contact of insoluble electron-acceptors with the redox proteins present in these cells. However, some Fe(III)- and Mn(IV)-respiring microorganisms have managed to overcome this problem by using membrane-bound redox proteins. These membrane-bound redox proteins include inner-membrane, periplasmic, and outer-membrane redox proteins (i.e., cytochromes), which allow for the transfer of electrons from the inside to the outside of the microorganism (41).

It was hypothesized that if insoluble Fe(III)- and Mn(IV)-minerals can be in direct electrochemical contact with the microbial metabolism, it should also be possible with an electrode surface. This hypothesis was tested and confirmed by Kim and co-workers in an experiment with the gram-negative metal-reducing bacterium *Shewanella oneidensis* growing on lactate in the presence of an electrode at a controlled potential (53). In the experiment Kim and co-workers confirmed that *Shewanella oneidensis* cells were indeed electrochemically active and could use the electrode as an electron acceptor. The activity seemed to be caused by a direct physical contact between the microorganism and the electrode, which was confirmed with electron microscopy. Furthermore, Kim and co-workers were able to generate electricity from lactate in an MFC setup (54).

In the same period other researchers discovered that the voltage gradient across the water-sediment interface occurring in many marine environments could be used for electricity generation (55-58). In the top few millimeters to centimeters of these sediments a voltage drop of up to 0.75 V can exist due to the anaerobic activity of sediment-dwelling microorganisms (57). These microorganisms anaerobically convert the organic material (0.1-10% by weight) in the sediment that is naturally present as a result of decaying plankton (58). During long-term *in situ* experiments with underwater fuel cells a pronounced enrichment of microorganisms was observed on the anode of the fuel cell (56,58). A large fraction of this enrichment was found to belong to a single cluster of bacteria in the family of *Geobacteraceae*, a group of anaerobic bacteria known to be able to couple the oxidation of organic material to the reduction of insoluble Fe(III)-minerals (55). A control electrode that was not electrically connected to a cathode and was placed in the same sediment over the same length of time did not show this enrichment. MFC and controlled potential experiments with pure culture members of the *Geobacteraceae* family (*Geobacter sulfurreducens*, *Geobacter metallireducens*, *Desulfuromonas acetooxidans*) indeed confirmed the mediator-less electron transfer ability of these Fe(III)-reducing bacteria (55,59).

Since these discoveries many more species of microorganisms have been identified that are electrochemically active through the mechanism of direct contact (60-65). Furthermore, several studies have recently reported that many of these electrochemically active species are capable of producing electrically conductive pili or nanowires, which enable direct electron transfer to electrode surfaces over longer distances (66,67). This is an interesting phenomenon as it implies that multilayered biofilms can grow on electrode surfaces that still rely on electron transfer through direct contact (63).

Because of its advantages compared to electron shuttle mediated exocellular electron transfer, exocellular electron transfer through direct contact became the basis of most present-day MFC systems. Electrochemically active microorganisms that are capable of exocellular electron transfer through direct contact are nowadays also referred to as

anodophilic microorganisms (13,68), electrigenes (50), or exoelectrogens (63). Basically, these electrochemically active microorganisms are the catalysts of the electrode that enable the electrochemical reactions to proceed. This is very much like the function of precious metal catalysts in non-biological electrochemical systems (e.g., platinum in hydrogen fuel cells). However, unlike precious metal catalysts, electrochemically active microorganisms are able to regenerate themselves, which is an important advantage in potentially poisoning environments like wastewaters.

Electrodes covered with electrochemically active microorganisms are referred to as biological electrodes or bioelectrodes. These biological electrodes behave similar to conventional chemical electrodes and can be understood through the same thermodynamic principles.

1.3.3 Thermodynamics & fundamentals of bioelectrochemical conversions

Bioelectrochemical reactions can be evaluated in terms of Gibbs free energy, which is a measure of the maximal work that can be derived from a reaction or the minimum work that has to be delivered to drive a reaction (69,70). The Gibbs free energy of a reaction is calculated as:

$$\Delta G_r = \Delta G_r^0 + RT \ln (\Pi) \quad (4)$$

with ΔG_r (J) the Gibbs free energy of a reaction at specific conditions, ΔG_r^0 (J) the Gibbs free energy of a reaction at standard conditions (298.15 K, 1 bar, 1 M concentration for all species), R the universal gas constant (8.3145 J/mol/K), T (K) the absolute temperature, and $\Pi(-)$ the reaction quotient. For a reaction $\nu_A A + \nu_B B \rightarrow \nu_C C + \nu_D D$, the reaction quotient is defined as:

$$\Pi = \frac{a_C^{\nu_C} a_D^{\nu_D}}{a_A^{\nu_A} a_B^{\nu_B}} \quad (5)$$

with a_i the activity of a specific product or reactant i and ν_i the reaction coefficient of a specific product or reactant. In dilute systems calculations

can be conveniently simplified by replacing the activities in the reaction quotient Π with concentrations (71):

$$\Pi = \frac{[C]^{v_C} [D]^{v_D}}{[A]^{v_A} [B]^{v_B}} \quad (6)$$

The standard Gibbs free energy of a reaction can be calculated from tabulated Gibbs free energies of formation for organic compounds in water, which are available from several sources (20,72-74).

For bioelectrochemical conversion processes, it is convenient to evaluate the reaction in terms of the electromotive force (emf) of a reaction, which is expressed in Volts (V) instead of Joules (J). The emf of a reaction is related to the Gibbs free energy of a reaction, according to:

$$-\Delta G_r = QE_{emf} = nFE_{emf} \quad (7)$$

with Q (C) the charge transferred in the reaction, E_{emf} (V) the emf of a reaction at specific conditions, n (mol) the number of electrons per reaction, and F Faraday's constant (96485.3 C/mol). Rearranging Equation 7 yields:

$$E_{emf} = -\frac{\Delta G_r}{nF} \quad (8)$$

If all reactions are evaluated at standard conditions, i.e., $I=1$, then

$$E_{emf}^0 = -\frac{\Delta G_r^0}{nF} \quad (9)$$

with E_{emf}^0 (V) the emf of a reaction at standard conditions.

Combining Equation 4, 8, and 9 yields the following expressing for the emf:

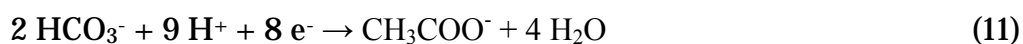
$$E_{emf} = E_{emf}^0 - \frac{RT}{nF} \ln(\Pi) \quad (10)$$

Galvanic processes have a positive value for the emf, whereas electrolytic processes have a negative value for the emf. Two types of bioelectrochemical conversion technologies are currently being studied in great detail: (i) MFC technology for electricity production (Paragraph 1.3.4; Table 1.1), and (ii) biocatalyzed electrolysis (Paragraph 1.3.5; Table 1.1) for hydrogen production. MFC technology is a galvanic process in which a biological anode that oxidizes organic material (e.g., acetate) is coupled to a cathode that reduces oxygen. Biocatalyzed electrolysis, on the other hand, is an electrolytic process in which a biological anode that oxidizes organic material (e.g., acetate) is coupled to a cathode that produces hydrogen.

Table 1.1. Electromotive force of bioelectrochemical processes: MFC and biocatalyzed electrolysis ([HCO₃⁻]=[CH₃COO⁻]=5 mM, pH 7, 298.15 K, pO₂=0.2 bar, pH₂=1 bar).

Bioelectrochemical process	Overall Reaction	E _{emf} (V)
<u>MFC</u>	CH ₃ COO ⁻ + 2 O ₂ → 2 HCO ₃ ⁻ + H ⁺	1.101
<u>Biocatalyzed Electrolysis</u>	CH ₃ COO ⁻ + 4 H ₂ O → 2 HCO ₃ ⁻ + H ⁺ + 4 H ₂	-0.118

Another way to look at bioelectrochemical systems is to evaluate them in terms of the potentials of the half cell reactions, i.e., the separate anode and cathode potentials. According to the IUPAC convention, standard electrode potentials (at 298.15 K, 1 bar, 1 M concentration for all species) are reported as a reduction potential, i.e., the reaction is written as consuming electrons (69). For example, if acetate is oxidized by electrochemically active microorganisms at the anode, the reaction is still written as:



The calculation of a theoretical electrode potential at specific conditions is similar to that of the electromotive force and proceeds according to the following equation:

$$E = E^0 - \frac{RT}{nF} \ln(\Pi) \quad (12)$$

with $E(V)$ the theoretical electrode potential at specific conditions and $E^0(V)$ the electrode potential at standard conditions, i.e., the standard potential. Standard potentials in literature are reported relative to the normal hydrogen electrode (NHE), which is defined to be zero at standard conditions (i.e., 298 K, $pH_2 = 1$ bar, $[H^+] = 1$ M).

For an anode that oxidizes acetate the theoretical electrode potential at specific conditions (E_{an}) can be calculated according to (Table 1.2):

$$E_{An} = E_{An}^0 - \frac{RT}{8F} \ln \left(\frac{[CH_3COO^-]}{[HCO_3^-]^2 [H^+]^9} \right) \quad (13)$$

Table 1.2. Standard potentials E^0 from (69) and theoretical potentials at pH 7 for typical conditions in bioelectrochemical systems E_{pH7} . E_{pH7} was calculated using Equation 12. All potentials are reported against NHE.

Electrode	Reaction	E^0 (V)	Conditions	E_{pH7} (V)
<u>Anode</u>	$2 HCO_3^- + 9 H^+ + 8 e^- \rightarrow$ $CH_3COO^- + 4 H_2O$	0.187 ^a	$[HCO_3^-]=5$ mM $[CH_3COO^-]=5$ mM	-0.296 ^b
<u>Cathode</u>	$O_2 + 4 H^+ + 4 e^- \rightarrow 2 H_2O$	1.229	$pO_2=0.2$	0.805 ^{b,d}
	$O_2 + 2 H_2O + 4 e^- \rightarrow 4 OH^-$	0.401	$pO_2=0.2$	0.805 ^{b,d}
	$Fe(CN)_6^{3-} + e^- \rightarrow Fe(CN)_6^{4-}$	0.361	$[Fe(CN)_6^{3-}]=[Fe(CN)_6^{4-}]$	0.361
	$2 H^+ + 2 e^- \rightarrow H_2$	0	$pH_2 = 1$ bar	-0.414 ^{c,e}
	$2 H_2O + 2 e^- \rightarrow 2 OH^- + H_2$	-0.828	$pH_2 = 1$ bar	-0.414 ^{c,e}

- Calculated from Gibbs free energy data (20).
- Note that the theoretical potential for the oxygen reduction reaction is the same when protons are consumed or when hydroxide is produced.
- Note that the theoretical potential for the hydrogen production reaction is the same when protons are consumed or when hydroxide is produced.
- Note that an MFC with an acetate oxidizing anode ($HCO_3^-=5$ mM, $CH_3COO^-=5$ mM, pH 7) and an oxygen reducing cathode ($pO_2=0.2$, pH 7) has a cell emf of $0.805 - -0.296 = 1.101$ V (Table 1.1).
- Note that a biocatalyzed electrolysis cell with an acetate oxidizing anode ($HCO_3^-=5$ mM, $CH_3COO^-=5$ mM, pH 7) and a hydrogen producing cathode ($pH_2=1$, pH 7) has a cell emf of $-0.414 - -0.296 = -0.118$ V (Table 1.1).

For a cathode that reduces oxygen the theoretical electrode potential at specific conditions (E_{cat_O2}) can be calculated according to (Table 1.2):



$$E_{cat_O2} = E_{cat_O2_H^+}^0 - \frac{RT}{4F} \ln \left(\frac{1}{pO_2 [H^+]^4} \right) \quad (15)$$

Or:



$$E_{cat_O2} = E_{cat_O2_OH^-}^0 - \frac{RT}{4F} \ln \left(\frac{[OH^-]^4}{pO_2} \right) \quad (17)$$

For a cathode that produces hydrogen the theoretical electrode potential at specific conditions (E_{cat_H2}) can be calculated according to (Table 1.2):



$$E_{cat_H2} = E_{cat_H2_H^+}^0 - \frac{RT}{2F} \ln \left(\frac{pH_2}{[H^+]^2} \right) \quad (19)$$

Or:



$$E_{cat_H2} = E_{cat_H2_OH^-}^0 - \frac{RT}{2F} \ln (pH_2 [OH^-]^2) \quad (21)$$

The electromotive force of the cell can be calculated from the separate anode and cathode potential according to:

$$E_{emf} = E_{cat} - E_{an} \quad (22)$$

When the pH in the anode and cathode are equal, the result of Equation 22 equals that of Equation 10.

The electromotive force represents a theoretical value for the cell voltage. The actual value for the cell voltage under practical conditions, however, will usually be lower due to various potential losses. An example is the potential loss that results from the microbial metabolic activity. This potential loss results from the fact that the electrochemically active microorganisms require energy themselves for growth and maintenance purposes. Consequently, the electrochemically active microorganisms will take some of the energy of the organic substrates and will release the electrons on a slightly lower energy level. Experiments have shown that a well-performing biological anode will release its electrons around -0.2 to -0.25 V. In the case of an acetate oxidizing anode ($E_{\text{pH}7}$ -0.296 V; Table 1.2) this means that about 0.05-0.10 V of the theoretical potential is lost to microbial metabolic activity (Figure 1.6). As a result of this loss the theoretical voltage of MFCs decreases and the theoretically required applied voltage of biocatalyzed electrolysis increases.

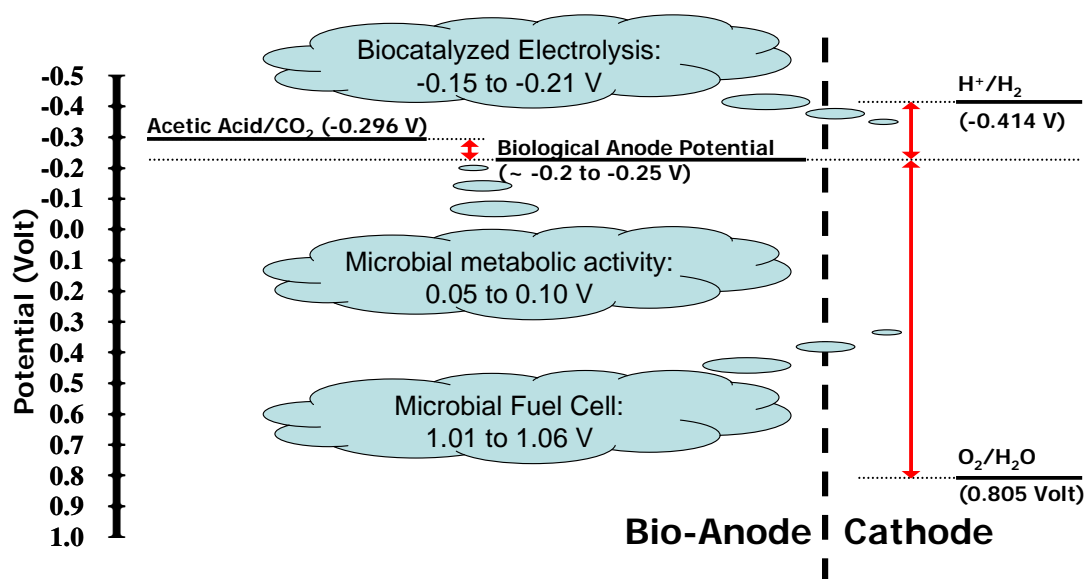


Figure 1.6. The effect of microbial metabolic activity on the theoretical voltage of MFCs and the theoretically required applied voltage of biocatalyzed electrolysis.

Besides the potential loss that results from microbial metabolic activity, also other potential losses (i.e., overpotentials) can be expected under practical operating conditions, including ohmic losses, activation losses, and concentration losses (75-77). These potential losses increase with increasing current densities and can have significant negative effects on the performance of the bioelectrochemical process. Decreasing these potential

losses, therefore, is one of the most important goals of the research in the field of bioelectrochemical conversion technologies.

1.3.4 Microbial fuel cells

Fuel cell technology already dates back from the time that Sir William Grove (1811-1896) built his first “gas voltaic battery” in 1839, a chemical hydrogen/oxygen fuel cell (75,76). The MFC, however, is more recent, but already from as early as 1911 recordings can be found on microbial electricity production (78). Compared to combustion technology, fuel cell technology has the advantage that it does not use heat as an intermediate form of energy for electricity production. When heat is used as an intermediate form of energy in an electricity production process (e.g., fossil fuel combustion), the process is limited by Carnot’s theorem. This theorem states that the theoretical maximum conversion efficiency of heat to work is determined by the absolute temperature $T_{\text{high}}(\text{K})$ of the process (i.e., the process) and the absolute temperature $T_{\text{low}}(\text{K})$ of the cold sink (i.e., the environment): $\eta_{\text{ideal}} = 1 - T_{\text{low}}/T_{\text{high}}$. As heat- and corrosion-resisting properties of construction materials of combustion processes (e.g., furnaces) are limited to a certain maximum temperature, this implies that the overall yield of combustion processes is usually not higher than 35-45%.

However, Carnot’s theorem does not apply for electrochemical electricity production as there is no intermediate heat step involved. For electrochemical electricity production the maximum efficiency is given by the ratio of the Gibbs free energy and enthalpy of a reaction ($\eta_{\text{ideal}} = \Delta G/\Delta H$). This means that theoretically the efficiency of an electrochemical electricity production can even exceed 100% (i.e., if heat is extracted from the environment during reaction).

MFC technology, therefore, is an interesting technology to explore for electricity production from wastewaters as it can theoretically increase the efficiency of electricity production from wastewaters significantly compared to traditional technologies (e.g., anaerobic digestion). MFC technology further offers the advantage that electricity can be produced in a single process step, whereas traditional electricity production from wastewater involves at least three process steps, i.e., (i) biogas production in an

anaerobic biological reactor, (ii) gas cleaning (i.e., H_2S removal), and (iii) biogas combustion in a gas motor.

Developing MFC technology, however, implies that microbial metabolic conversion routes somehow have to be “electrically connected” to an electrode. In the first generation of microbial fuels cells this “electrical connection” was established through the application of soluble electron shuttles (Paragraph 1.3.2). Unfortunately, practical limitations of the application of these soluble electron shuttles for large scale electricity production from wastewaters (e.g., cost, toxicity) prevented commercialization of this type of MFCs. However, from 1999 a renewed interest in MFC technology emerged when Kim and co-workers (53,54) and later also others (55-59) demonstrated that exocellular electron transfer was also possible without soluble electron shuttles, i.e., mediator-less electron transfer (Paragraph 1.3.2). Since this rediscovery of MFC technology, more and more research groups have started to work on MFC technology. Although MFC technology is not yet commercialized, much progress has been made in the last decade and it is generally agreed upon that MFC technology holds great promise as a future electricity production technology from wastewaters.

An MFC is a galvanic cell that connects the oxidation of organic material at a biological anode to the reduction of an electron acceptor at a cathode. To establish electricity production, this electron acceptor needs to be reduced at a higher electrode potential than that of the biological anode. For sustainable electricity production from wastewater the ideal terminal electron acceptor is oxygen from air as it is available in large excess (77,79). However, as oxygen reducing cathodes for MFCs are still under development, ferricyanide has often been used as an electron acceptor for research purposes to simulate a well-performing, oxygen reducing cathode (Table 1.2). The maximum MFC voltage (emf) of an MFC with an oxygen reducing cathode is theoretically in the order of 1.1 V (Table 1.1). Due to various potential losses, however, the practical MFC voltage is typically below 0.8 V under open circuit conditions and below 0.6 V under operating conditions (77). For a large part, these potential losses are suffered at the

oxygen reducing cathode as electrochemical oxygen reactions generally show slow kinetics (80).

In its standard configuration, an MFC consists of two chambers, i.e., one for the biological anode and one for the cathode (Figure 1.7). The anode is typically made of graphite, which is available in many forms, such as graphite felts, graphite paper, granular graphite, and graphite foam. The oxygen reducing cathode typically consists of platinum-catalyzed graphite. In a standard MFC configuration a cation exchange membrane separates the MFC chambers. This cation exchange membrane facilitates the transport of ions (preferably protons) through the membrane in order to maintain electroneutrality in the system, but does not allow for the transport of electrons. In order to reach the cathode, therefore, electrons have to go through an electrical circuit from which electrical power can be extracted.

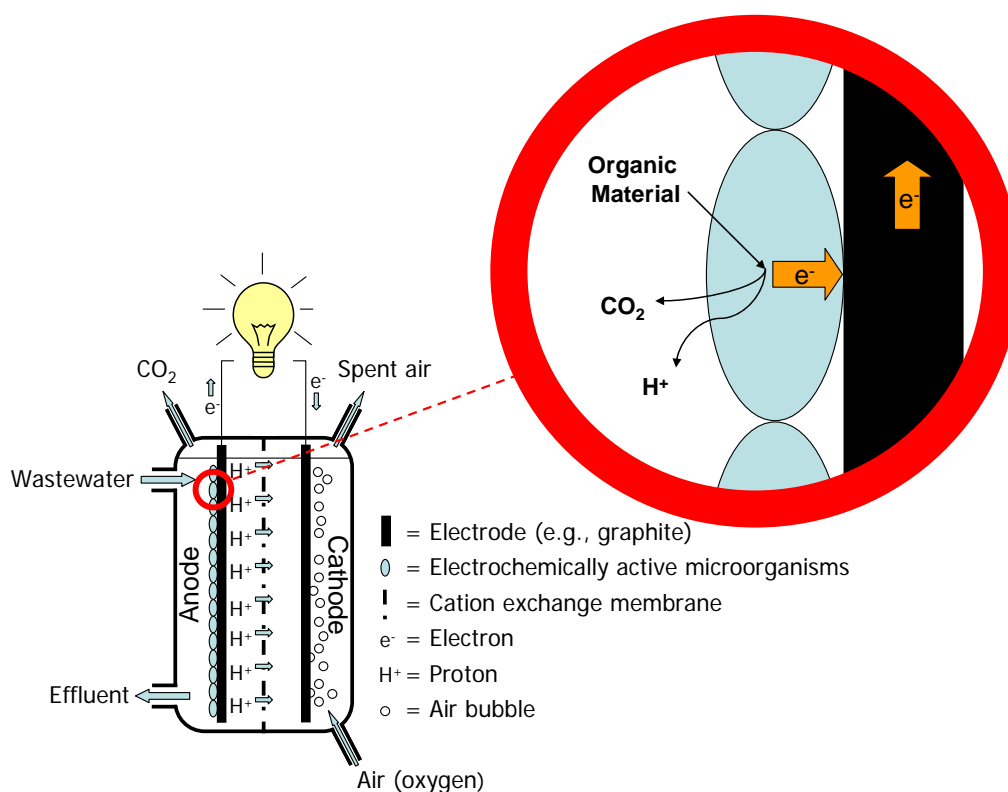


Figure 1.7. Schematic representation of a standard MFC configuration. At the anode dissolved organic compounds from wastewater are oxidized by electrochemically active microorganisms. These electrochemically active microorganisms transfer the electrons from the oxidation of the dissolved organic compounds to the anode through the mechanism of exocellular electron transfer. Subsequently, the electrons are transported to the cathode via an electrical circuit, where they are consumed in the oxygen reduction reaction. Electroneutrality is maintained in the system by the transport of cations (ideally protons) from the anode to the cathode through the cation exchange membrane. The Gibbs free energy of the overall reaction is negative, which means that electrical energy can be extracted from the electrical circuit.

Most of the MFC research in the last years has focused on two aspects: (i) reducing the costs of the MFC system, both in terms of material use and operation, and (ii) on improving the power output of the MFC system.

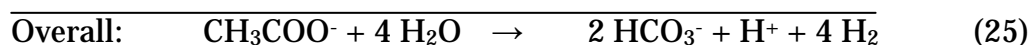
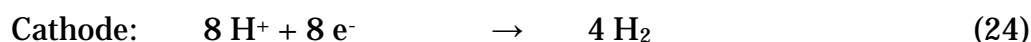
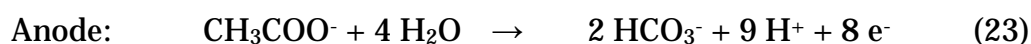
To reduce material cost, many studies aimed at finding alternatives for platinum as the catalyst for the oxygen reduction at the cathode (81-85). Other researchers have looked at the possibilities of membrane-less operation of MFCs in order to save the costs of the cation exchange membrane (86,87). To reduce operation costs, some studies have investigated single chamber operation of MFCs (88,89). In a single chamber MFC the oxygen reducing cathode is directly exposed to air so that no electrical energy needs to be invested for the aeration.

Also in terms of power output many improvements were made. These improvements predominantly have been the result of a better understanding of the MFC system. Most progress was made by reducing the ohmic resistance of the system (e.g., by reducing electrode spacing) and by better choice of anode and cathode materials. Early systems based on mediator-less electron transfer did not produce more than 0.1-1 mW/m² of anode surface area, but within a decade power output increased to more than 1000 mW/m² of anode surface area (63). As a result of this progress, MFC technology has evolved from a microbial curiosity to a promising wastewater treatment technology. To achieve the status of a mature wastewater treatment technology, however, more progress is required in the field of cost reduction and power increase. Furthermore, MFCs have to be benchmarked against conventional wastewater treatment systems in terms of efficiencies and volumetric loading rates (kg COD/m³ reactor volume/day). Nowadays, MFCs have already approached the volumetric loading rates of aerobic systems (77), but they have the potential to improve towards the volumetric loading rates of high rate anaerobic systems. At these volumetric loading rates power output is expected to increase to about 1 kW/m³ reactor volume (90).

1.3.5 Biocatalyzed electrolysis

The electrical energy harvested in MFCs can be used for hydrogen production by coupling MFCs to water electrolysis. This coupling was demonstrated by Kreysa et al. in a setup that coupled 10 electron shuttle (HNQ) mediated MFCs to a water electrolyzer (91). Although hydrogen production was indeed observed, the energy efficiency based on Gibbs free energy calculations (added substrate and produced hydrogen) was calculated to be only 11%. One of the reasons that this efficiency was observed to be so low is the fact that this configuration involved two electrochemical oxygen reactions, i.e., oxygen reduction in the MFCs and oxygen production in the water electrolyzer. Electrochemical oxygen reactions generally have slow kinetics and therefore suffer from large potential losses (80). From an energetic point of view, therefore, it would be much wiser to eliminate the electrochemical oxygen reactions by directly coupling the oxidation of organic material to the reduction of protons to form hydrogen gas. This is exactly what is done in biocatalyzed electrolysis.

Biocatalyzed electrolysis is a novel hydrogen production process and was developed within this PhD project (92,93). In parallel to this development and independent of our work, Bruce Logan and co-workers developed the same technology and refer to it as the bioelectrochemically assisted microbial reactor process or BEAMR-process (94,95). Biocatalyzed electrolysis is an electrolytic process that electrically connects the oxidation of organic material at a biological anode to the reduction of protons at the cathode so that hydrogen gas is formed. The conversion of organic material to hydrogen is thus split up into two half reactions: (i) the conversion of organic material into bicarbonate, protons, and electrons, and (ii) the conversion of protons and electrons to hydrogen gas. E.g., for acetate:



The theoretical cell voltage (emf) of biocatalyzed electrolysis of organic material is about -0.12 V (Table 1.1). The negative value of this theoretical cell voltage indicates that electrical energy needs to be supplied to the system to drive the biocatalyzed electrolysis reactions. This supply of electrical energy is accomplished by including a power supply into the electrical circuit. Essentially, dissolved organic material is thus *electrolyzed* into bicarbonate and hydrogen gas during the process with the electrochemically active microorganisms acting as the catalyst; hence the name biocatalyzed electrolysis. Overall, biocatalyzed electrolysis carries out the same endothermic conversion reactions as photoheterotrophic fermentations (Paragraph 1.2.2), but establishes the required energy input by means of an input of electrical energy instead of sunlight.

A typical biocatalyzed electrolysis configuration will be very much like that of MFCs (Figure 1.7), i.e., two chambers separated by a cation exchange membrane. Compared to MFCs, however, there are two important alterations required to start the biocatalyzed electrolysis reactions: (i) oxygen needs to be kept away from the cathode so that it is completely anaerobic, and (ii) a power supply needs to be included into the electrical circuit so that the required electrical energy can be supplied (Figure 1.8).

The theoretically required applied voltage of biocatalyzed electrolysis of about 0.12 V equals a theoretical energy requirement of about 0.26 kWh/Nm³ H₂. This is low compared to the 4.4 to 5.4 kWh/Nm³ H₂ required for commercial water electrolyzers (96). Undoubtedly, microbial metabolic losses (Figure 1.6) and other potential losses (e.g., ohmic loss and electrode overpotentials) will also increase the energy requirement of biocatalyzed electrolysis under practical conditions, but it is expected that the future energy requirement will remain below 1 kWh/Nm³ H₂. This low energy requirement is an important advantage of biocatalyzed electrolysis compared to water electrolysis, as the electricity price is a significant part of the price of hydrogen that is produced through water electrolysis (96).

Also compared to other biological hydrogen production processes biocatalyzed electrolysis has some important advantages. Various studies have shown that biological anodes can easily be operated under non-sterile conditions as electrochemically active consortia can be naturally selected

from a wide range of inocula. Moreover, these consortia are capable of converting a wide range of substrates (e.g., sugars, fatty acids, proteins) at high efficiencies (68,97-100). Other biological hydrogen production processes often suffer from low efficiencies when operated under non-sterile conditions and are more restricted with respect to the kinds of substrates they can convert (e.g., dark fermentation). Furthermore, the biocatalyzed electrolysis process does not suffer from product inhibition like dark and photoheterotrophic fermentations and the hydrogen can theoretically be produced as a pure gas in the cathode chamber instead of a hydrogen/carbon dioxide mixture in conventional hydrogen producing bioreactors. So besides acting as an efficient second stage process to dark fermentation, biocatalyzed electrolysis could potentially even replace dark fermentation in many cases (e.g., for complex wastewaters).

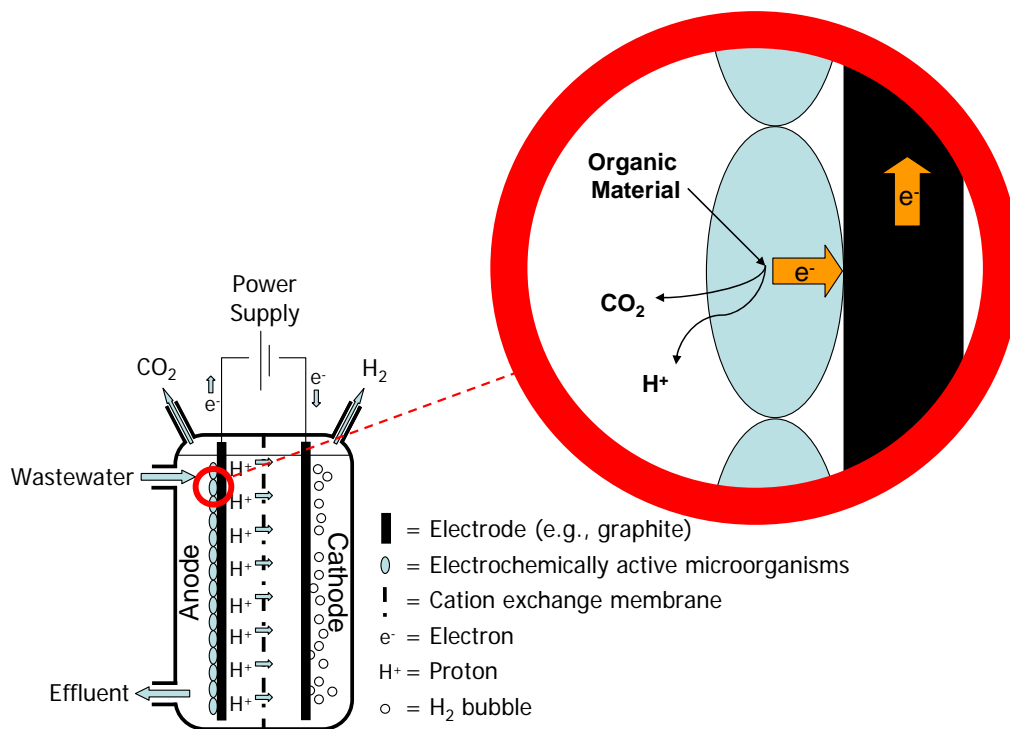


Figure 1.8. Schematic representation of a standard biocatalyzed electrolysis configuration. At the anode dissolved organic compounds from wastewater are oxidized by electrochemically active microorganisms. These electrochemically active microorganisms transfer the electrons from the oxidation of the dissolved organic compounds to the anode through the mechanism of exocellular electron transfer. Subsequently, the electrons are transported to the cathode via an electrical circuit, where they are consumed in the hydrogen production reaction. Electroneutrality is maintained in the system by the transport of cations (ideally protons) from the anode to the cathode through the cation exchange membrane. The Gibbs free energy of the overall reaction is positive, which means that electrical energy needs to be supplied to the electrical circuit by means of a power supply.

However, as biocatalyzed electrolysis is a new process, many of these potential advantages are still to be experimentally confirmed. Biocatalyzed electrolysis needs to be thoroughly examined and progress needs to be monitored on the basis of performance indicators such as applied voltage, process efficiency (e.g., overall efficiency: COD to H_2), energy requirement ($\text{kWh/Nm}^3 \text{ H}_2$), and volumetric hydrogen production rate ($\text{Nm}^3 \text{ H}_2/\text{m}^3/\text{day}$). Further, also the optimal design of a biocatalyzed electrolysis system needs to be investigated and the use of materials (e.g., cathode catalysts) needs to be critically assessed and optimized. Many of these aspects will be discussed in this PhD thesis.

1.4 Thesis scope & outline

The scope of this thesis is to investigate the feasibility of hydrogen production through biocatalyzed electrolysis of organic material. As biocatalyzed electrolysis is a novel technology that was developed within this PhD project, **Chapter 2** describes the “proof of principle” of biocatalyzed electrolysis by demonstrating the process with acetate as a model substrate. For biochemical and thermodynamic reasons acetate cannot be converted to hydrogen through dark fermentation (Paragraph 1.2.1), which makes it an ideal model substrate for demonstrating biocatalyzed electrolysis.

In contrast to our initial expectations most of the bottlenecks that were observed in the process were not of a biological nature. The remaining chapters of this thesis, therefore, have focused on identifying these bottlenecks and testing alternative configurations. **Chapter 3** discusses the operational problems associated with the application of cation exchange membranes in bioelectrochemical systems operated on wastewater. In contrast to what was generally assumed by MFC researchers, cation exchange membranes in bioelectrochemical systems operated on wastewater also transport significant amounts of other cation species than protons. As the cathode reactions of MFCs and biocatalyzed electrolysis consume protons equimolarly with electrons, the transport of cation species other than protons causes a significant pH increase in the cathode chamber of these processes. This pH increase at the cathode creates a pH gradient

across the membrane, which negatively affects the performance of bioelectrochemical processes. To prevent these potential losses we have evaluated the possibilities of using alternative types of ion exchange membranes in **Chapter 4**. Unfortunately, these alternative types of ion exchange membranes were not capable of completely eliminating the pH increase in the cathode chamber either.

Chapter 5 shows that biocatalyzed electrolysis can also be operated with one liquid chamber instead of two. Producing hydrogen gas directly in the gas phase has possible advantages for volume reduction of the process, so that the volumetric hydrogen production rate can be improved. Single chamber biocatalyzed electrolysis was tested with both a cation and an anion exchange membrane in the configuration, which further increased insight into the ion transport characteristics of these types of ion exchange membranes. Again, the pH at the cathode increased dramatically during operation of both single chamber configurations and negatively affected the performance.

As cathode pH effects were observed in all the experiments of **Chapter 3, 4, and 5**, these effects seem to be inherent to the use of membranes in bioelectrochemical systems that are running on wastewater. This hypothesis was qualitatively investigated in a short **Intermezzo** by approaching the problem of the cathode chamber pH increase with the Nernst-Planck flux equation.

Chapter 6 looks at the possibilities of the application of a microbial biocathode for hydrogen production. In the initial biocatalyzed experiments a platinum catalyzed cathode was used, which unfortunately is too expensive for commercial application. Therefore, it was tested whether hydrogen production can also be catalyzed by an electrochemically active consortium on a cathode. A microbial biocathode consists of plain graphite, which can offer significant cost advantages for the biocatalyzed electrolysis process.

Finally, **Chapter 7** discusses the status and future potential of biocatalyzed electrolysis of wastewater. This is done by summarizing the insights that were gained in this PhD thesis, by evaluating the possible applications of biocatalyzed electrolysis, and by critically assessing which scale-up and research issues need to be addressed before biocatalyzed

electrolysis can be referred to as a mature technology for hydrogen production from wastewaters.

1.5 References

1

- (1) Solomon, S.; Qin, D.; Manning, M.; Chen, Z.; Marquis, M.; Averyt, K. B.; Tignor, M.; Miller, H. L., Eds. *Climate change 2007: the physical science basis. Contribution of working group I to the fourth assessment report of the Intergovernmental Panel on Climate Change (IPCC)*; Cambridge University Press: Cambridge, United Kingdom and New York, NY, USA., 2007.
- (2) International Energy Agency, 2004. World Energy Outlook 2004. Paris, France.
- (3) Dorian, J. P.; Franssen, H. T.; Simbeck, D. R. Global challenges in energy. *Energy Policy* **2006**, *34*, 1984-1991.
- (4) Lomborg, B. *The skeptical environmentalist: measuring the real state of the world*; Cambridge University Press: Cambridge, 2001.
- (5) Seboldt, W. Space- and Earth-based solar power for the growing energy needs of future generations. *Acta Astronaut.* **2004**, *55*, 389-399.
- (6) Lewis, N. S.; Nocera, D. G. Powering the planet: Chemical challenges in solar energy utilization. *PNAS* **2006**, *103*, 15729-15735.
- (7) Niele, F. *Energy: engine of evolution*; Elsevier: Amsterdam, 2005.
- (8) Hatti-Kaul, R.; Tornvall, U.; Gustafsson, L.; Borjesson, P. Industrial biotechnology for the production of bio-based chemicals - a cradle-to-grave perspective. *Trends Biotechnol.* **2007**, *25*, 119-124.
- (9) Petrus, L.; Noordermeer, M. A. Biomass to biofuels, a chemical perspective. *Green Chem.* **2006**, *8*, 861-867.
- (10) Ragauskas, A. J.; Williams, C. K.; Davison, B. H.; Britovsek, G.; Cairney, J.; Eckert, C. A.; Frederick, W. J.; Hallett, J. P.; Leak, D. J.; Liotta, C. L.; Mielenz, J. R.; Murphy, R.; Templer, R.; Tschaplinski, T. The path forward for biofuels and biomaterials. *Science* **2006**, *311*, 484-489.
- (11) Kamm, B.; Kamm, M. Principles of biorefineries. *Appl. Microbiol. Biotechnol.* **2004**, *64*, 137-145.
- (12) van Wyk, J. P. H. Biotechnology and the utilization of biowaste as a resource for bioproduct development. *Trends Biotechnol.* **2001**, *19*, 172-177.
- (13) Angenent, L. T.; Karim, K.; Al-Dahhan, M. H.; Wrenn, B. A.; Domiguez-Espinosa, R. Production of bioenergy and biochemicals from industrial and agricultural wastewater. *Trends Biotechnol.* **2004**, *22*, 477-485.
- (14) Paques bv. <http://www.paques.nl/>.
- (15) Logan, B. E. Extracting hydrogen and electricity from renewable resources. *Environ. Sci. Technol.* **2004**, *38*, 160a-167a.
- (16) Jacobson, M. Z.; Colella, W. G.; Golden, D. M. Cleaning the air and improving health with hydrogen fuel-cell vehicles. *Science* **2005**, *308*, 1901-1905.
- (17) Li, C. L.; Fang, H. H. P. Fermentative hydrogen production from wastewater and solid wastes by mixed cultures. *Crit. Rev. Environ. Sci. Technol.* **2007**, *37*, 1-39.

- (18) Hawkes, F. R.; Hussy, I.; Kyazze, G.; Dinsdale, R.; Hawkes, D. L. Continuous dark fermentative hydrogen production by mesophilic microflora: Principles and progress. *Int. J. Hydrogen Energy* **2007**, *32*, 172-184.
- (19) Hawkes, F. R.; Dinsdale, R.; Hawkes, D. L.; Hussy, I. Sustainable fermentative hydrogen production: challenges for process optimisation. *Int. J. Hydrogen Energy* **2002**, *27*, 1339-1347.
- (20) Thauer, R. K.; Jungermann, K.; Decker, K. Energy conservation in chemotrophic anaerobic bacteria. *Bacteriol. Rev.* **1977**, *41*, 100-180.
- (21) Schlegel, H. G. *General Microbiology*; 7th ed.; Cambridge University Press: Cambridge, United Kingdom, 1992.
- (22) Hallenbeck, P. C.; Benemann, J. R. Biological hydrogen production; fundamentals and limiting processes. *Int. J. Hydrogen Energy* **2002**, *27*, 1185-1193.
- (23) Nath, K.; Das, D. Improvement of fermentative hydrogen production: various approaches. *Appl. Microbiol. Biotechnol.* **2004**, *65*, 520-529.
- (24) Berrios-Rivera, S. J.; Bennett, G. N.; San, K. Y. The effect of increasing NADH availability on the redistribution of metabolic fluxes in *Escherichia coli* chemostat cultures. *Metab. Eng.* **2002**, *4*, 230-237.
- (25) Guedon, E.; Payot, S.; Desvaux, M.; Petitdemange, H. Carbon and electron flow in *Clostridium cellulolyticum* grown in chemostat culture on synthetic medium. *J. Bacteriol.* **1999**, *181*, 3262-3269.
- (26) Payot, S.; Guedon, E.; Cailliez, C.; Gelhaye, E.; Petitdemange, H. Metabolism of cellobiose by *Clostridium cellulolyticum* growing in continuous culture: evidence for decreased NADH reoxidation as a factor limiting growth. *Microbiology* **1998**, *144*, 375-384.
- (27) Meyer, C. L.; Papoutsakis, E. T. Increased Levels Of Atp And Nadh Are Associated With Increased Solvent Production In Continuous Cultures Of *Clostridium-Acetobutylicum*. *Appl. Microbiol. Biotechnol.* **1989**, *30*, 450-459.
- (28) Hallenbeck, P. C. Fundamentals of the fermentative production of hydrogen. *Water Sci. Technol.* **2005**, *52*, 21-29.
- (29) Benemann, J. Hydrogen biotechnology: progress and prospects. *Nat. Biotechnol.* **1996**, *14*, 1101-1103.
- (30) Schink, B. Energetics of syntrophic cooperation in methanogenic degradation. *Microbiol. Mol. Biol. Rev.* **1997**, *61*, 262-&.
- (31) Lee, M. J.; Zinder, S. H. Hydrogen partial pressures in a thermophilic acetate-oxidizing methanogenic coculture. *Appl. Environ. Microbiol.* **1988**, *54*, 1457-1461.
- (32) Zinder, S. H.; Koch, M. Non-aceticlastic methanogenesis from acetate: acetate oxidation by a thermophilic syntrophic coculture. *Arch. Microbiol.* **1984**, *138*, 263-272.
- (33) Stams, A. J. M.; de Bok, F. A. M.; Plugge, C. M.; van Eekert, M. H. A.; Dolfing, J.; Schraa, G. Exocellular electron transfer in anaerobic microbial communities. *Environ. Microbiol.* **2006**, *8*, 371-382.
- (34) Claassen, P. A. M.; van Lier, J. B.; Contreras, A. M. L.; van Niel, E. W. J.; Sijtsma, L.; Stams, A. J. M.; de Vries, S. S.; Weusthuis, R. A. Utilisation of biomass for the supply of energy carriers. *Appl. Microbiol. Biotechnol.* **1999**, *52*, 741-755.
- (35) Rupprecht, J.; Hankamer, B.; Mussnug, J. H.; Ananyev, G.; Dismukes, C.; Kruse, O. Perspectives and advances of biological H-2

- production in microorganisms. *Appl. Microbiol. Biotechnol.* **2006**, 72, 442-449.
- (36) Reith, J. H.; Wijffels, R. H.; Barten, H., Eds. *Bio-methane & bio-hydrogen: status and perspectives of biological methane and hydrogen production*; Dutch Biological Hydrogen Foundation: The Netherlands, 2003.
- (37) Barbosa, M. J.; Rocha, J. M. S.; Tramper, J.; Wijffels, R. H. Acetate as a carbon source for hydrogen production by photosynthetic bacteria. *J. Biotechnol.* **2001**, 85, 25-33.
- (38) Lee, C. M.; Chen, P. C.; Wang, C. C.; Tung, Y. C. Photohydrogen production using purple nonsulfur bacteria with hydrogen fermentation reactor effluent. *Int. J. Hydrogen Energy* **2002**, 27, 1309-1313.
- (39) Oh, Y. K.; Seol, E. H.; Kim, M. S.; Park, S. Photoproduction of hydrogen from acetate by a chemoheterotrophic bacterium *Rhodospseudomonas palustris* P4. *Int. J. Hydrogen Energy* **2004**, 29, 1115-1121.
- (40) Fang, H. H. P.; Liu, H.; Zhang, T. Phototrophic hydrogen production from acetate and butyrate in wastewater. *Int. J. Hydrogen Energy* **2005**, 30, 785-793.
- (41) Lovley, D. R.; Holmes, D. E.; Nevin, K. P. Dissimilatory Fe(III) and Mn(IV) reduction. *Adv. Microb. Physiol.* **2004**, 49, 219-286.
- (42) Straub, K. L.; Benz, M.; Schink, B. Iron metabolism in anoxic environments at near neutral pH. *FEMS Microbiol. Ecol.* **2001**, 34, 181-186.
- (43) Coates, J. D.; Ellis, D. J.; Blunt-Harris, E. L.; Gaw, C. V.; Roden, E. E.; Lovley, D. R. Recovery of humic-reducing bacteria from a diversity of environments. *Appl. Environ. Microbiol.* **1998**, 64, 1504-1509.
- (44) Hernandez, M. E.; Newman, D. K. Extracellular electron transfer. *Cell. Mol. Life Sci.* **2001**, 58, 1562-1571.
- (45) Rabaey, K.; Boon, N.; Siciliano, S. D.; Verhaege, M.; Verstraete, W. Biofuel cells select for microbial consortia that self-mediate electron transfer. *Appl. Environ. Microbiol.* **2004**, 70, 5373-5382.
- (46) Nevin, K. P.; Lovley, D. R. Mechanisms for accessing insoluble Fe(III) oxide during dissimilatory Fe(III) reduction by *Geothrix fermentans*. *Appl. Environ. Microbiol.* **2002**, 68, 2294-2299.
- (47) Newman, D. K.; Kolter, R. A role for excreted quinones in extracellular electron transfer. *Nature* **2000**, 405, 94-97.
- (48) Rabaey, K.; Boon, N.; Hofte, M.; Verstraete, W. Microbial phenazine production enhances electron transfer in biofuel cells. *Environ. Sci. Technol.* **2005**, 39, 3401-3408.
- (49) Tanaka, K.; Vega, C. A.; Tamamushi, R. Mediating effects of ferric chelate compounds in microbial fuel cells. *Bioelectrochem. Bioenerg.* **1983**, 11, 135-143.
- (50) Lovley, D. R. Bug juice: harvesting electricity with microorganisms. *Nat. Rev. Microbiol.* **2006**, 4, 497-508.
- (51) Tanaka, K.; Vega, C. A.; Tamamushi, R. Thionine and ferric chelate compounds as coupled mediators in microbial fuel cells. *Bioelectrochem. Bioenerg.* **1983**, 11, 289-297.
- (52) Park, D. H.; Zeikus, J. G. Electricity generation in microbial fuel cells using neutral red as an electronophore. *Appl. Environ. Microbiol.* **2000**, 66, 1292-1297.

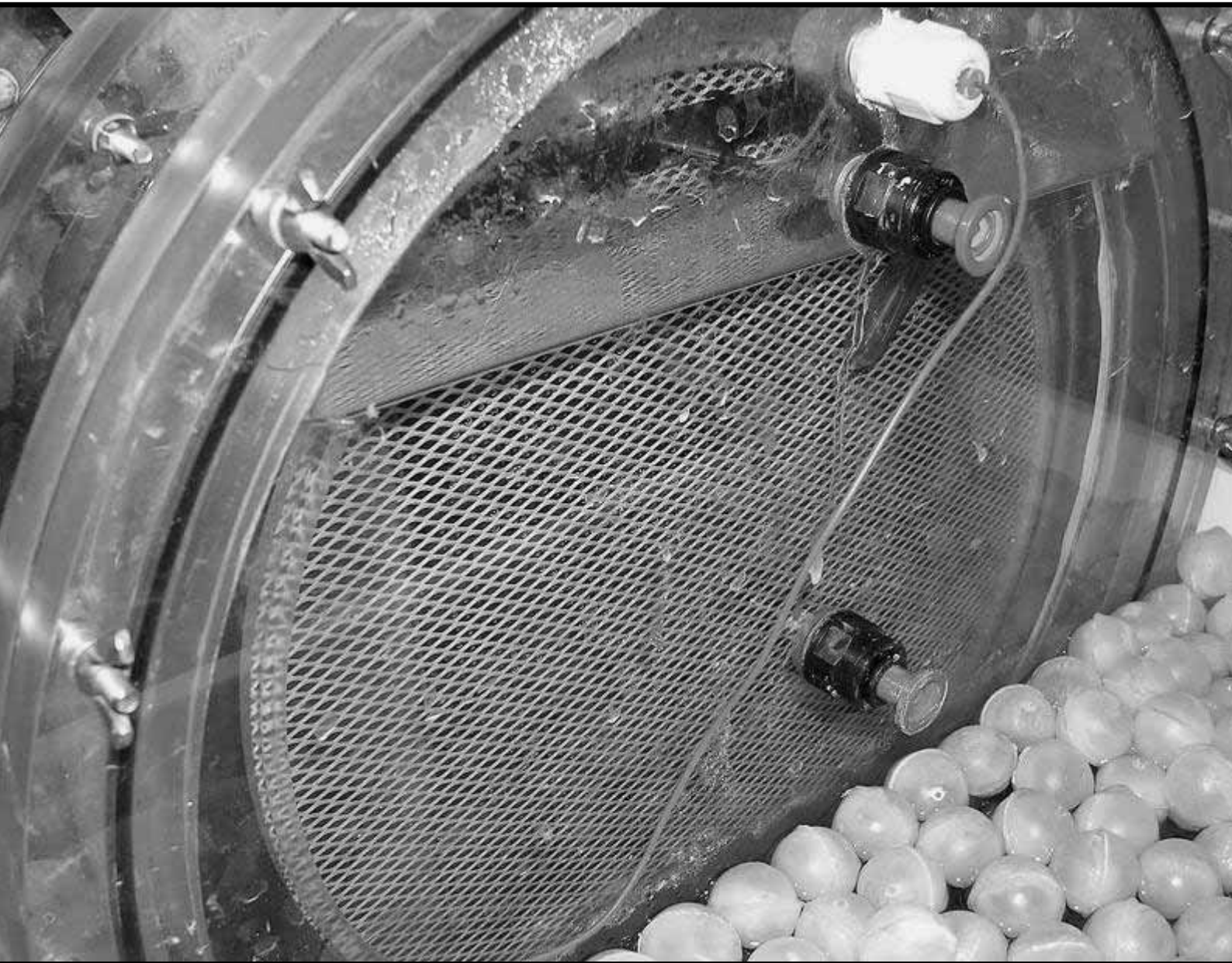
- (53) Kim, B. H.; Kim, H. J.; Hyun, M. S.; Park, D. H. Direct electrode reaction of Fe(III)-reducing bacterium, *Shewanella putrefaciens*. *J. Microbiol. Biotechnol.* **1999**, *9*, 127-131.
- (54) Kim, H. J.; Park, H. S.; Hyun, M. S.; Chang, I. S.; Kim, M.; Kim, B. H. A mediator-less microbial fuel cell using a metal reducing bacterium, *Shewanella putrefaciens*. *Enzyme Microb. Technol.* **2002**, *30*, 145-152.
- (55) Bond, D. R.; Holmes, D. E.; Tender, L. M.; Lovley, D. R. Electrode-reducing microorganisms that harvest energy from marine sediments. *Science* **2002**, *295*, 483-485.
- (56) DeLong, E. F.; Chandler, P. Power from the deep. *Nat. Biotechnol.* **2002**, *20*, 788-789.
- (57) Reimers, C. E.; Tender, L. M.; Fertig, S.; Wang, W. Harvesting energy from the marine sediment-water interface. *Environ. Sci. Technol.* **2001**, *35*, 192-195.
- (58) Tender, L. M.; Reimers, C. E.; Stecher, H. A.; Holmes, D. E.; Bond, D. R.; Lowy, D. A.; Pilobello, K.; Fertig, S. J.; Lovley, D. R. Harnessing microbially generated power on the seafloor. *Nat. Biotechnol.* **2002**, *20*, 821-825.
- (59) Bond, D. R.; Lovley, D. R. Electricity production by *Geobacter sulfurreducens* attached to electrodes. *Appl. Environ. Microbiol.* **2003**, *69*, 1548-1555.
- (60) Lee, J. Y.; Phung, N. T.; Chang, I. S.; Kim, B. H.; Sung, H. C. Use of acetate for enrichment of electrochemically active microorganisms and their 16S rDNA analyses. *FEMS Microbiol. Lett.* **2003**, *223*, 185-191.
- (61) Park, H. S.; Kim, B. H.; Kim, H. S.; Kim, H. J.; Kim, G. T.; Kim, M.; Chang, I. S.; Park, Y. K.; Chang, H. I. A novel electrochemically active and Fe(III)-reducing bacterium phylogenetically related to *Clostridium butyricum* isolated from a microbial fuel cell. *Anaerobe* **2001**, *7*, 297-306.
- (62) Pham, C. A.; Jung, S. J.; Phung, N. T.; Lee, J.; Chang, I. S.; Kim, B. H.; Yi, H.; Chun, J. A novel electrochemically active and Fe(III)-reducing bacterium phylogenetically related to *Aeromonas hydrophila*, isolated from a microbial fuel cell. *FEMS Microbiol. Lett.* **2003**, *223*, 129-134.
- (63) Logan, B. E.; Regan, J. M. Electricity-producing bacterial communities in microbial fuel cells. *Trends Microbiol.* **2006**, *14*, 512-518.
- (64) Holmes, D. E.; Bond, D. R.; Lovley, D. R. Electron transfer by *Desulfobulbus propionicus* to Fe(III) and graphite electrodes. *Appl. Environ. Microbiol.* **2004**, *70*, 1234-1237.
- (65) Chaudhuri, S. K.; Lovley, D. R. Electricity generation by direct oxidation of glucose in mediatorless microbial fuel cells. *Nat. Biotechnol.* **2003**, *21*, 1229-1232.
- (66) Gorby, Y. A.; Yanina, S.; McLean, J. S.; Rosso, K. M.; Moyses, D.; Dohnalkova, A.; Beveridge, T. J.; Chang, I. S.; Kim, B. H.; Kim, K. S.; Culley, D. E.; Reed, S. B.; Romine, M. F.; Saffarini, D. A.; Hill, E. A.; Shi, L.; Elias, D. A.; Kennedy, D. W.; Pinchuk, G.; Watanabe, K.; Ishii, S.; Logan, B.; Nealson, K. H.; Fredrickson, J. K. Electrically conductive bacterial nanowires produced by *Shewanella oneidensis* strain MR-1 and other microorganisms. *PNAS* **2006**, *103*, 11358-11363.
- (67) Reguera, G.; McCarthy, K. D.; Mehta, T.; Nicoll, J. S.; Tuominen, M. T.; Lovley, D. R. Extracellular electron transfer via microbial nanowires. *Nature* **2005**, *435*, 1098-1101.

- (68) Rabaey, K.; Lissens, G.; Siciliano, S. D.; Verstraete, W. A microbial fuel cell capable of converting glucose to electricity at high rate and efficiency. *Biotechnol. Lett.* **2003**, *25*, 1531-1535.
- (69) Bard, A. J.; Parsons, R.; Jordan, J., Eds. *Standard potentials in aqueous solution*; Marcel Dekker: New York, 1985.
- (70) Newman, J. S. *Electrochemical systems*; Prentice Hall: Englewood Cliffs, NJ, 1973.
- (71) Bard, A. J.; Faulkner, L. R. *Electrochemical methods: fundamentals and applications*; 2nd ed.; John Wiley & Sons: New York, 2001.
- (72) Alberty, R. A. *Thermodynamics of biochemical reactions*; John Wiley & Sons: New York, 2003.
- (73) Amend, J. P.; Shock, E. L. Energetics of overall metabolic reactions of thermophilic and hyperthermophilic Archaea and Bacteria. *FEMS Microbiol. Rev.* **2001**, *25*, 175-243.
- (74) Heijnen, J. J. Bioenergetics of Microbial Growth. In *Encyclopedia of Bioprocess Technology: Fermentation, Biocatalysis, and Bioseparation*; Flickinger, M. C., Drew, S. D., Eds.; John Wiley & Sons: Chichester, UK, 1999; pp 267-291.
- (75) Hoogers, G., Ed. *Fuel cell technology handbook*; CRC Press: Boca Raton, FL, 2003.
- (76) Larminie, J.; Dicks, A. *Fuel cell systems explained*; John Wiley & Sons: Chichester, 2000.
- (77) Logan, B. E.; Hamelers, B.; Rozendal, R.; Schröder, U.; Keller, J.; Freguia, S.; Aelterman, P.; Verstraete, W.; Rabaey, K. Microbial fuel cells: methodology and technology. *Environ. Sci. Technol.* **2006**, *40*, 5181-5192.
- (78) Potter, M. C. Electrical effects accompanying the decomposition of organic compounds. *Proc. Roy. Soc. London Ser. B* **1911**, *84*, 260-276.
- (79) Zhao, F.; Harnisch, F.; Schröder, U.; Scholz, F.; Bogdanoff, P.; Herrmann, I. Challenges and constraints of using oxygen cathodes in microbial fuel cells. *Environ. Sci. Technol.* **2006**, *40*, 5193-5199.
- (80) Kinoshita, K. *Electrochemical oxygen technology*; John Wiley & Sons, Inc.: New York, 1992.
- (81) Cheng, S.; Liu, H.; Logan, B. E. Power densities using different cathode catalysts (Pt and CoTMPP) and polymer binders (Nafion and PTFE) in single chamber microbial fuel cells. *Environ. Sci. Technol.* **2006**, *40*, 364-369.
- (82) Ter Heijne, A.; Hamelers, H. V. M.; Buisman, C. J. N. Microbial fuel cell operation with continuous biological ferrous iron oxidation of the catholyte. *Environ. Sci. Technol.* **2007**, *41*, 4130-4134.
- (83) Ter Heijne, A.; Hamelers, H. V. M.; De Wilde, V.; Rozendal, R. A.; Buisman, C. J. N. A bipolar membrane combined with ferric iron reduction as an efficient cathode system in microbial fuel cells. *Environ. Sci. Technol.* **2006**, *40*, 5200-5205.
- (84) Zhao, F.; Harnisch, F.; Schröder, U.; Scholz, F.; Bogdanoff, P.; Herrmann, I. Application of pyrolysed iron(II) phthalocyanine and CoTMPP based oxygen reduction catalysts as cathode materials in microbial fuel cells. *Electrochem. Commun.* **2005**, *7*, 1405-1410.
- (85) Bergel, A.; Feron, D.; Mollica, A. Catalysis of oxygen reduction in PEM fuel cell by seawater biofilm. *Electrochem. Commun.* **2005**, *7*, 900-904.

- (86) Jang, J. K.; Pham, T. H.; Chang, I. S.; Kang, K. H.; Moon, H.; Cho, K. S.; Kim, B. H. Construction and operation of a novel mediator- and membrane-less microbial fuel cell. *Process Biochem.* **2004**, *39*, 1007-1012.
- (87) Liu, H.; Logan, B. E. Electricity generation using an air-cathode single chamber microbial fuel cell in the presence and absence of a proton exchange membrane. *Environ. Sci. Technol.* **2004**, *38*, 4040-4046.
- (88) Liu, H.; Ramnarayanan, R.; Logan, B. E. Production of electricity during wastewater treatment using a single chamber microbial fuel cell. *Environ. Sci. Technol.* **2004**, *38*, 2281-2285.
- (89) Sell, D.; Kramer, P.; Kreysa, G. Use of an oxygen gas diffusion cathode and a three-dimensional packed-bed anode in a bioelectrochemical fuel cell. *Appl. Microbiol. Biotechnol.* **1989**, *31*, 211-213.
- (90) Rabaey, K.; Verstraete, W. Microbial fuel cells: novel biotechnology for energy generation. *Trends Biotechnol.* **2005**, *23*, 291-298.
- (91) Kreysa, G.; Schenck, K.; Sell, D.; Vuorilehto, K. Bioelectrochemical Hydrogen-Production. *Int. J. Hydrogen Energy* **1994**, *19*, 673-676.
- (92) Rozendal, R. A.; Buisman, C. J. N. Process for producing hydrogen. **2005**, *Patent WO2005005981*.
- (93) Rozendal, R. A.; Hamelers, H. V. M.; Euverink, G. J. W.; Metz, S. J.; Buisman, C. J. N. Principle and perspectives of hydrogen production through biocatalyzed electrolysis. *Int. J. Hydrogen Energy* **2006**, *31*, 1632-1640.
- (94) Liu, H.; Grot, S.; Logan, B. E. Electrochemically assisted microbial production of hydrogen from acetate. *Environ. Sci. Technol.* **2005**, *39*, 4317-4320.
- (95) Logan, B.; Grot, S. A bio-electrochemically assisted microbial reactor that generates hydrogen gas and methods of generating hydrogen gas. *Patent WO2006010149* **2006**.
- (96) Turner, J. A. Sustainable hydrogen production. *Science* **2004**, *305*, 972-974.
- (97) Freguia, S.; Rabaey, K.; Yuan, Z. G.; Keller, J. Electron and carbon balances in microbial fuel cells reveal temporary bacterial storage behavior during electricity generation. *Environ. Sci. Technol.* **2007**, *41*, 2915-2921.
- (98) Heilmann, J.; Logan, B. E. Production of electricity from proteins using a single chamber microbial fuel cell. *Water Environ. Res.* **2006**, *78*, 531-537.
- (99) Liu, H.; Cheng, S. A.; Logan, B. E. Production of electricity from acetate or butyrate using a single-chamber microbial fuel cell. *Environ. Sci. Technol.* **2005**, *39*, 658-662.
- (100) Rabaey, K.; Ossieur, W.; Verhaege, M.; Verstraete, W. Continuous microbial fuel cells convert carbohydrates to electricity. *Water Sci. Technol.* **2005**, *52*, 515-523.

Principle and Perspectives of Hydrogen Production through Biocatalyzed Electrolysis

2



This chapter has been published as:

Rozendal, R. A.; Hamelers, H. V. M.; Euverink, G. J. W.; Metz, S. J.; Buisman, C. J. N. Principle and perspectives of hydrogen production through biocatalyzed electrolysis. *Int. J. Hydrogen Energy* **2006**, 31, 1632-1640.

Principle and Perspectives of Hydrogen Production through Biocatalyzed Electrolysis

2

Biocatalyzed electrolysis is a novel biological hydrogen production process with the potential to efficiently convert a wide range of dissolved organic materials in wastewaters. Even substrates formerly regarded to be unsuitable for hydrogen production due to the endothermic nature of the involved conversion reactions can be converted with this technology. Biocatalyzed electrolysis achieves this by utilizing electrochemically active microorganisms that are capable of generating electrical current from the oxidation of organic matter. When this biological anode is coupled to a proton reducing cathode by means of a power supply, hydrogen is generated. In the biocatalyzed electrolysis experiments presented in this chapter acetate is used as a model compound. In theory, biocatalyzed electrolysis of acetate requires applied voltages that can be as low as 0.14 V, while hydrogen production by means of conventional water electrolysis, in practice, requires applied voltages well above 1.6 V. At an applied voltage of 0.5 V, the biocatalyzed electrolysis setup used in this study produces approximately 0.02 Nm³ H₂/m³ reactor liquid volume/day from acetate at an overall efficiency of 53±3.5%. This performance was mainly limited by the current design of the system, diffusional loss of hydrogen from the cathode to the anode chamber, and high overpotentials associated with the cathode reaction. In this chapter we show that optimization of the process will allow future volumetric hydrogen production rates above 10 Nm³ H₂/m³ reactor liquid volume/day at overall efficiencies exceeding 90% and applied voltages as low as 0.3–0.4 V. In the future, this will make biocatalyzed electrolysis an attractive technology for hydrogen production from a wide variety of wastewaters.

2.1 Introduction

Stimulated by the depletion of fossil fuels and the threat of global warming, society is widely considering renewably produced hydrogen as an alternative clean fuel for transportation (1). To deal with future hydrogen demands independent of fossil fuels, it will be necessary to consider all available renewable resources for hydrogen production (2). In theory, large amounts of renewable hydrogen can be produced from dissolved organic materials in wastewaters using fermentation technology. However, the efficiency of dark fermentation of carbohydrate-rich wastewater, the most promising of the currently known technologies, is generally less than 15% (3). Besides methanogenic consumption of hydrogen (4-6), thermodynamic limitations are an important reason for this low yield. Due to these thermodynamic limitations, the majority of the substrate is converted to byproducts (e.g., acetate, butyrate) instead of hydrogen. According to Benemann (7), economic feasibility can only be reached if hydrogen yields on dissolved organic material can approach 60–80%. This is only achievable if the produced byproducts can be converted to hydrogen as well. Dark fermentation is not capable of doing this, because the conversions involve endothermic reactions. Therefore, much research has been directed over the years towards photofermentations (8-10), which use sunlight to overcome this thermodynamic barrier. However, the diffuse nature of solar radiation and the limited conversion efficiencies severely limit the economic feasibility of these processes due to the enormous reactor surface areas that are required (11).

Alternatively, biocatalyzed electrolysis (12,13), a recently discovered technology that is related to the microbial fuel cell (14-22), overcomes this thermodynamic barrier by means of a small input of electrical energy. This makes the process independent of the reactor surface area, which benefits the economic feasibility. Biocatalyzed electrolysis achieves this by utilizing electrochemically active microorganisms, which convert dissolved organic material to bicarbonate, protons and electrons. Either by direct contact with an electrode surface (23,24) or aided by (excreted) redox mediators (21), these microorganisms release the produced electrons to an electrode

surface. In this way, a biological anode is created. By coupling this biological anode to a proton reducing cathode by means of a power supply, a direct conversion of dissolved organic material to hydrogen is accomplished. The complete process takes place in an electrochemical cell in which oxidation of dissolved organic material and proton reduction are separated in two chambers (Figure 2.1). The separation between these chambers is established by means of a cation exchange membrane (e.g., Nafion®). Externally, the anode and the cathode are connected to the power supply using an electrical circuit. While the power supply drives the released electrons from the anode to the cathode, an equal number of protons permeates through the membrane. At the cathode, protons and electrons combine to form pure hydrogen gas.

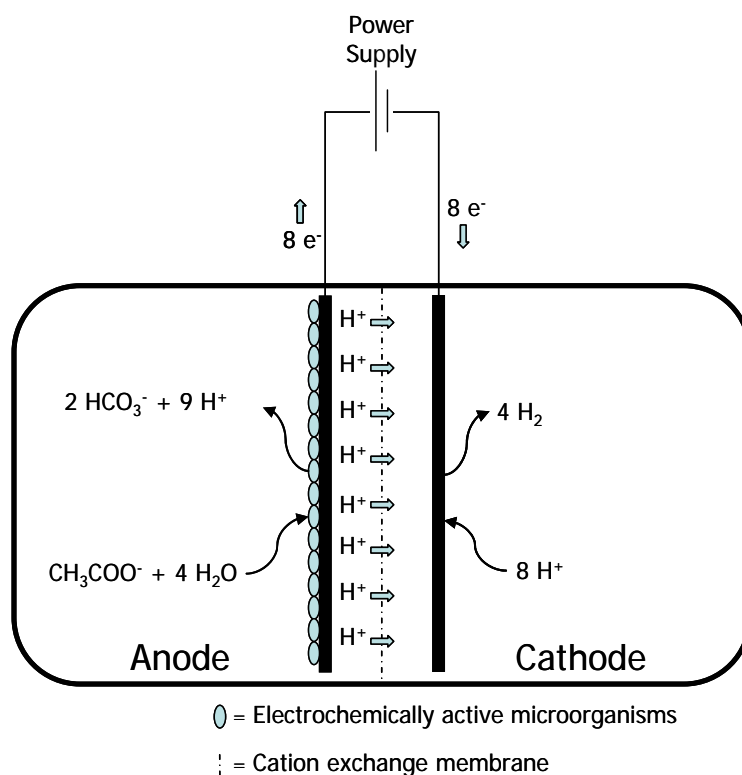
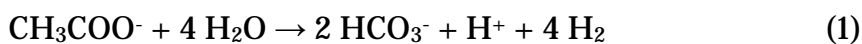


Figure 2.1. Schematic representation of hydrogen production through biocatalyzed electrolysis of acetate.

Acetate is used as a model compound for the biocatalyzed electrolysis experiments presented in this study, as acetate cannot be directly converted to hydrogen through dark fermentation:



Based on Gibbs free energy calculations, hydrogen production from acetate requires an energy input of 104.6 kJ/mol under standard conditions (25). Accordingly, in theory, an applied voltage of only 0.14 V is required for hydrogen production through biocatalyzed electrolysis of acetate. At pH 7, this corresponds to equilibrium potentials for the oxidation of acetate (1 mol/L) and proton reduction of -0.28 and -0.42 V (NHE), respectively. In practice, however, it can be expected that more than 0.14 V will be required for this reaction to proceed. Firstly, this is caused by the fact that electrochemically active microorganisms consume part of the available energy themselves for growth and maintenance purposes. Consequently, the microorganisms release the electrons at a higher potential than the equilibrium potential. Secondly, the required applied voltage is also expected to be affected by other losses in the cell as a consequence of the ohmic resistance of the electrochemical system and the occurrence of overpotentials. Nevertheless, at pH 7 anode potentials are found in literature that are typically around -0.2 V (NHE) or lower under operating conditions (17,18) and, therefore, it can be expected hydrogen production through biocatalyzed electrolysis will already be possible at applied voltages around 0.22 V. In comparison, hydrogen production through water electrolysis, in practice, operates at applied voltages that are well above 1.6 V (26-28).

Essentially, dissolved organic material is *electrolyzed* into carbon dioxide and hydrogen gas during the process with the electrochemically active microorganisms acting as the catalyst. Therefore, we call this technology “biocatalyzed electrolysis” (12). Independent of the work done by our laboratories, the researchers Liu et al. (13) recently published their preliminary findings on the same technology and refer to it as “electrochemically assisted microbial production of hydrogen”. In line with their work, this chapter aims to further elucidate the working principle, to pinpoint the possible bottlenecks of biocatalyzed electrolysis, and to evaluate what this technology implies for the future of hydrogen production from wastewaters.

2.2 Materials and methods

2.2.1 Electrochemical cell

Biocatalyzed electrolysis was studied in a two-chambered electrochemical cell made of poly(methylmethacrylate). The cylindrical chambers (290 mm inside diameter; length: 50 mm; wall thickness: 5 mm) had a total volume of 3.3 L each and were separated by a Nafion® 117 cation selective membrane (surface area: 256 cm²). Both the anode and the cathode chamber were equipped with an Ag/AgCl reference electrode (+0.2 V vs. NHE (29)) to be able to measure the separate electrode potentials. The anode consisted of a disc-shaped piece of graphite felt (diameter: 240 mm; thickness: 3 mm — FMI Composites Ltd., Galashiels, Scotland); the cathode of a disc-shaped titanium mesh electrode with a 50 g/m² platinum coating (diameter: 240 mm; thickness: 1 mm; specific surface area: 1.7 m²/m² — Magneto special anodes bv, Schiedam, The Netherlands). To minimize ohmic resistance, both electrodes were placed in direct contact with the membrane. During the experiments 400 cm² of the surface area of both electrodes was submerged in the respective media and regarded electrochemically active. The electrodes were connected to a potentiostat (μAutolabIII, Eco Chemie bv, Utrecht, The Netherlands) using an isolated electrical wire through a gas tight connection in the chamber wall. The potentiostat was used to control the applied voltage on the total system (as the power supply) or to control the anode potential during the growth of the microorganisms after inoculation. Prior to the experiments, the electrochemical cell was sterilized (1 h) with 6% hydrogen peroxide and rinsed with autoclaved Milli-Q water.

2.2.2 Medium preparation

The anode chamber was filled with 3 L of autoclaved anode medium (pH 7) containing (in Milli-Q): 2.22 g/L KCl, 0.61 g/L KH₂PO₄, 0.96 g/L K₂HPO₄, 0.28 g/L NH₄Cl, 0.1 g/L yeast extract, 0.1 g/L MgSO₄·7H₂O, 0.01 mg/L CaCl₂·2H₂O, and 1 mL/L of a trace element mixture (30). The cathode chamber was filled with 3 L of autoclaved cathode medium (pH 7) containing (in Milli-Q): 2.22 g/L KCl, 0.61 g/L KH₂PO₄, and 0.96 g/L

K₂HPO₄. The described amounts of acetate were added to the anode medium as an autoclaved concentrated (100 g/L) solution of NaCH₃COO·3H₂O in Milli-Q.

2.2.3 *Electrochemically active microorganisms*

The inoculation (3%) of the anode chamber was done with 90 ml of effluent from an identical electrochemical cell that had been running biocatalyzed electrolysis of acetate for over 5 months. That cell had previously been started up with sludge from a full scale UASB reactor treating sulfate-rich papermill wastewater (31) (Industriewater Eerbeek, Eerbeek, The Netherlands). The 5 month operation period had resulted in the natural selection of a consortium of electrochemically active microorganisms from this sludge.

Immediately after the inoculation, an applied voltage scan was recorded. After this, the microbial community was grown in the anode chamber by controlling the anode potential with the potentiostat. The anode potential was set to -0.1 V (vs. Ag/AgCl) for 3 days and then switched to -0.4 V (vs. Ag/AgCl) for 2 days. In this period, the current generation increased from ~1 to ~16 mA. Two applied voltage scans were then recorded. To check whether the microbial community had stabilized, the anode potential was set to -0.4 V (vs. Ag/AgCl) for 3 more days. During this period, the current remained stable. After this second growth period, two applied voltage scans were recorded again. During both growth periods, the pH was regularly checked and corrected to 7 if necessary.

2.2.4 *Experimental procedures*

During the applied voltage scans both chambers were flushed continuously with nitrogen gas. The applied voltage was gradually increased from 0 to 0.75 V at a rate of 0.1 V/h. This relatively low rate was chosen to reduce non-Faradaic currents to a negligible level. After every scan an equilibration time of 4 h at an applied voltage of 0 V was taken into account, preventing non-Faradaic currents from the potential switch back to 0 V to influence the next scan. All scans were taken in duplicate, except for the scan

taken just after inoculation of electrochemically active microorganisms (single scan).

During the constant applied voltage experiments (0.5 V, in duplicate) only the anode chamber was continuously flushed with nitrogen to enhance mixing; the cathode chamber was only flushed intensively prior to the experiment. The cathode chamber was kept closed during the experiment, thereby capturing all produced hydrogen in the headspace. To create equilibrium between the headspace volume and the bulk liquid, the headspace gas was continuously recycled through the cathode chamber at a recycle rate of 280 mL/min. Total cathode headspace volume was 275 mL.

During all experiments the temperature of the electrochemical cell was kept at 303 K. Current and applied voltage recordings were performed by the potentiostat. All reported potentials are against the NHE reference. An ion chromatograph (Metrohm 761 Compact IC) equipped with a conductivity detector and an ion exclusion column (Metrosep Organic Acids 6.1005.200) was used to measure the acetate concentrations. Gas samples were analyzed with a gas chromatograph (Shimadzu GC-2010) equipped with a thermal conductivity detector and a molesieve column (Varian molsieve 5A). Total hydrogen production was determined by measuring the hydrogen in the headspace and calculating the dissolved hydrogen from Henry's law (32). All reported hydrogen volumes refer to hydrogen at 303 K and 1 bar.

2.2.5 Electrochemical calculations

The theoretically required applied voltage was calculated from the Gibbs energy according to $\Delta G = -nF\Delta E$ (29). This calculation excludes all potential losses in a practical biocatalyzed electrolysis system caused by microbial energy consumption, ohmic resistances in the system, and overpotentials suffered at the electrodes. Including these potential losses will always lead to a higher required applied voltage. Consequently, the theoretically required applied voltage is also the minimally required applied voltage. The equilibrium cathode potential (proton reduction) at pH 7 was calculated by converting the potential of the NHE (by definition: 0 V) to its value at pH 7 by means of the Nernst equation (29). The Nernst equation was also used

for calculating other concentration effects. The equilibrium anode potential (acetate oxidation) at pH 7 was calculated from the difference between the theoretically required applied voltage and the equilibrium cathode potential at pH 7.

2.3 Results and discussion

2 The start-up of the biocatalyzed electrolysis process (10 mM acetate) was followed by evaluating the system performance by means of applied voltage scans (Figure 2.2). Without biocatalysis (open circles) and directly after inoculation of electrochemically active microorganisms (closed circles) no significant currents were generated as a result of the applied voltage. However, enhanced current generation was observed in the scans recorded after a 5-day (open squares) and after a subsequent 3-day growth period (closed squares) at controlled anode potential (see Materials and methods). The similarity of both of these scans indicates that the microbial community was stable.

From the scans it becomes clear that the presence of a developed culture of electrochemically active microorganisms is essential for the process; without biocatalysis no current is generated. The scans recorded after both growth periods also show that to enhance current generation an increasing voltage needs to be applied. This increasing voltage represents the additional energy that needs to be supplied at higher current densities to compensate for the increasing energy losses associated with the electrode reactions (i.e., overpotential/polarization) and the ohmic resistance in the system. The fact that current generation occurred below the theoretically required applied voltage of 0.16 V (at 10 mM acetate) can be explained from the continuous nitrogen purging of the cathode compartment during the scans. This constantly removed the generated hydrogen from the cathode, favoring new hydrogen formation.

To confirm that the current generation in the applied voltage scans indeed originated from acetate oxidation, the system was operated for 4 h at a constant applied voltage of 0.5 V without acetate in the anode medium. In this case, current generation was negligible ($<15 \text{ mA/m}^2$ anode surface) and

no hydrogen was detected in the cathode headspace. When the same procedure was repeated with acetate in the anode medium (2 mM), current generation and hydrogen production were significant. The average measured current density during this period was 470 ± 74.3 mA/m² anode surface (18.8 ± 3.0 mA). After 4 h 0.38 ± 0.034 mmol of acetate was consumed and 0.80 ± 0.13 mmol (20 ± 3.2 mL) of hydrogen was produced. This corresponded to a volumetric hydrogen production rate of approximately 0.02 Nm³ H₂/m³ reactor liquid volume/day.

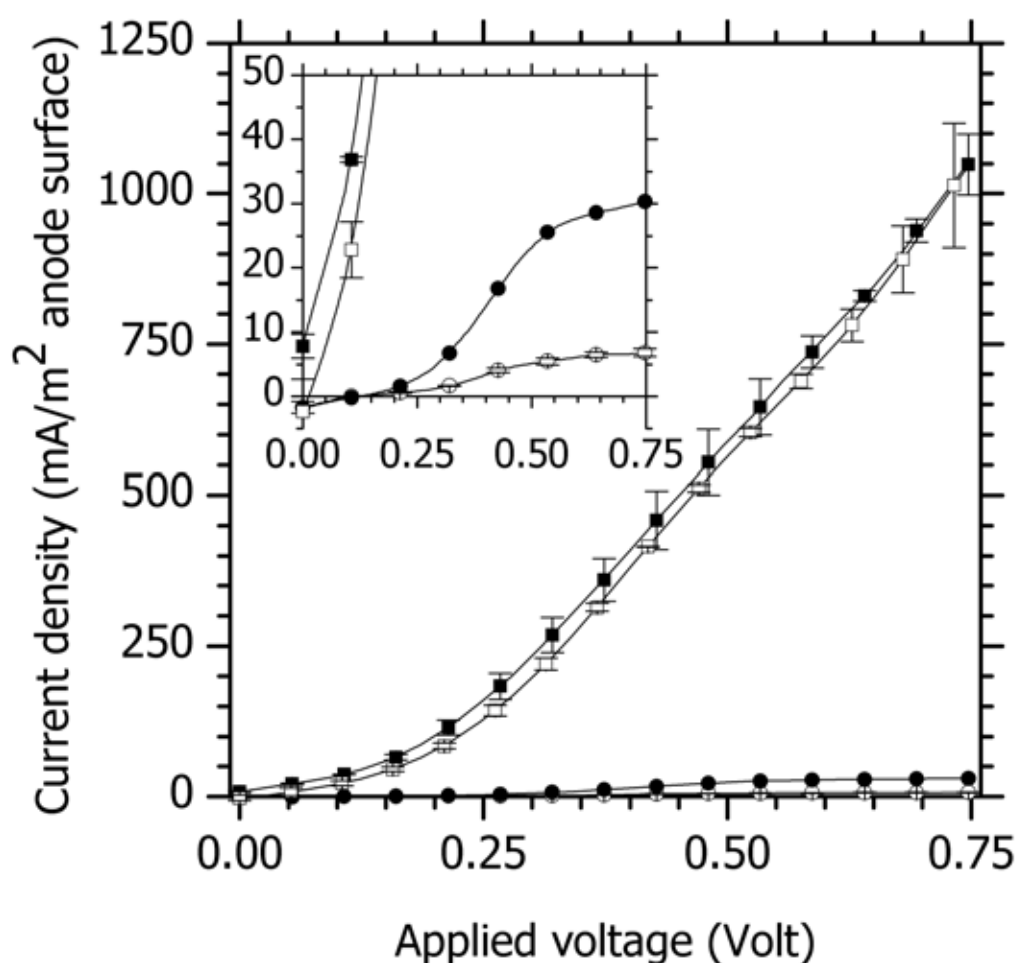


Figure 2.2. Applied voltage scans from 0 to 0.75 V for biocatalyzed electrolysis of acetate (10 mM). Current generation was measured in the absence of electrochemically active microorganisms (duplicate scans — open circles) and in the presence of electrochemically active microorganisms just after 3% inoculation (single scan — closed circles), after a 5-day growth period at controlled anode potential (duplicate scans — open squares) and after a subsequent 3-day growth period at controlled anode potential (duplicate scans — closed squares). See Materials and methods for details on the growth periods. The inset shows the same measurements on an adapted current density scale. Bars indicate minimum and maximum of the duplicate scans.

Further examination of these results, gave a clear indication of the current performance of the system and especially also pinpointed the bottlenecks that limit this performance. Table 2.1 shows the efficiencies that were calculated from these measurements.

Table 2.1. Calculated efficiencies^a of hydrogen production through biocatalyzed electrolysis of acetate

% Coulombic efficiency (acetate to e ⁻)	92 ± 6.3
% Cathodic hydrogen efficiency (e ⁻ to H ₂)	57 ± 0.1
% Overall hydrogen efficiency (acetate to H ₂)	53 ± 3.5

- a. Calculated from duplicate experiments that lasted for 4 h at a constant applied voltage of 0.5 V. The experiment started with an acetate concentration of 2 mM. 100% efficiency corresponds to: 1 acetate → 8 e⁻ → 4 H₂.

The Coulombic efficiency (92±6.3%), i.e., the conversion of acetate to electrons, compares well with that found for biological anodes that have been applied in microbial fuel cell systems (14,15,20,21) and even seem to be slightly higher. This is probably due to the fact that no coulombic efficiency losses are suffered by aerobic microbial conversion of substrate, as is the case in microbial fuel cells (18). In microbial fuel cells, oxygen can diffuse from the aerobic cathode chamber to the anaerobic anode chamber through the cation exchange membrane. In biocatalyzed electrolysis, this problem is circumvented as the cathode chamber is anaerobic as well. The small coulombic efficiency loss that is found for the biocatalyzed electrolysis system is partly caused by the presence of methane-producing bacteria in the anodic chamber, as confirmed by the presence of trace amounts of methane in the nitrogen purge flow. Furthermore, as in every microbial process, a few percent of the organic substrate is expected to be consumed for growth of the microbial consortium and thus lost for current generation. Nevertheless, all these losses are negligible compared to the loss of cathodic hydrogen efficiency, i.e., the conversion of electrons to hydrogen, suffered during the experiment. The cathodic hydrogen efficiency was found to be only 57±0.1%. Based on the generated current, 100% cathodic hydrogen efficiency would have yielded 35±5.6 mL of hydrogen gas. However, only 20 ± 3.2 mL was measured. Consequently, approximately 15 mL of hydrogen was lost during the experiment. This loss is likely caused by diffusion of

hydrogen from the cathode into the anode chamber through the Nafion® 117 membrane, as is the case with oxygen in microbial fuel cells. Hydrogen that enters the anode chamber is consumed by microorganisms or removed from the reactor with the nitrogen purge. Analysis indeed confirmed the presence of trace amounts of hydrogen in the nitrogen purge flow leaving the anode compartment. Assuming hydrogen saturation in the Nafion® 117 membrane, and using the hydrogen diffusion data as determined by other researchers (33), it was estimated (18) that during the experiment a maximum amount of hydrogen of between 19 and 26 mL could have diffused to the anode chamber. This is in the same order as the amount of hydrogen that was actually lost during the experiment. Although the hydrogen concentration in the headspace at the end of the experiment was only $6.1 \pm 0.9\%$, the hydrogen concentration at the membrane can still be close to saturation due the direct physical contact between the cathode and the membrane. During the experiment hydrogen bubble formation was clearly observed on the cathode surface, thus indicating hydrogen saturated conditions in proximity of these bubbles. Mainly due to the loss in cathodic hydrogen efficiency, the resulting overall hydrogen efficiency of biocatalyzed electrolysis system tested in this study was found not to be higher than $53 \pm 3.5\%$.

By analyzing the electrode potentials (Figure 2.3A) and comparing them with the equilibrium potentials, it was evaluated how the applied voltage of 0.5 V was consumed in the electrochemical cell during the 4 h experiment (Figure 2.3B). In this way, another bottleneck in the system was revealed. At an acetate concentration of 2 mM, the theoretically required applied voltage necessary to start hydrogen production is 0.16 V. The remaining 0.34 V was thus lost to irreversibilities in the system. From Figure 2.3B it can be clearly seen that in the current experimental setup, most of this overvoltage is consumed by the cathode. At the end of the experiment ($t=4$ h), for example, more than 0.28 V was lost by the cathode reaction (cathode potential -0.71 V). At the same time, only 0.04 V was lost in the anode reaction (anode potential -0.22 V) and 0.01 V to the other parts of the electrochemical cell (e.g., membrane and ohmic loss). So, despite the fact that platinum catalysis (50 g/m^2) is applied on the cathode, this part of the system still suffers from the largest potential losses. This is in contradiction to what is commonly

accepted for conventional polymer electrolyte water electrolysis, where the proton reduction step is known to be associated with low overvoltages. Even at a current density exceeding 10000 A/m^2 the overvoltage for the hydrogen evolution reaction can be as low as 0.025 V (27). Therefore, much lower potential losses should be possible at the relatively low current densities ($<10 \text{ A/m}^2$) as encountered in bioelectrochemical processes. One explanation might be the relatively mild conditions (pH 7, 303 K) under which the experiments have been conducted in this study. From literature not much is known about hydrogen evolution under those conditions (34).

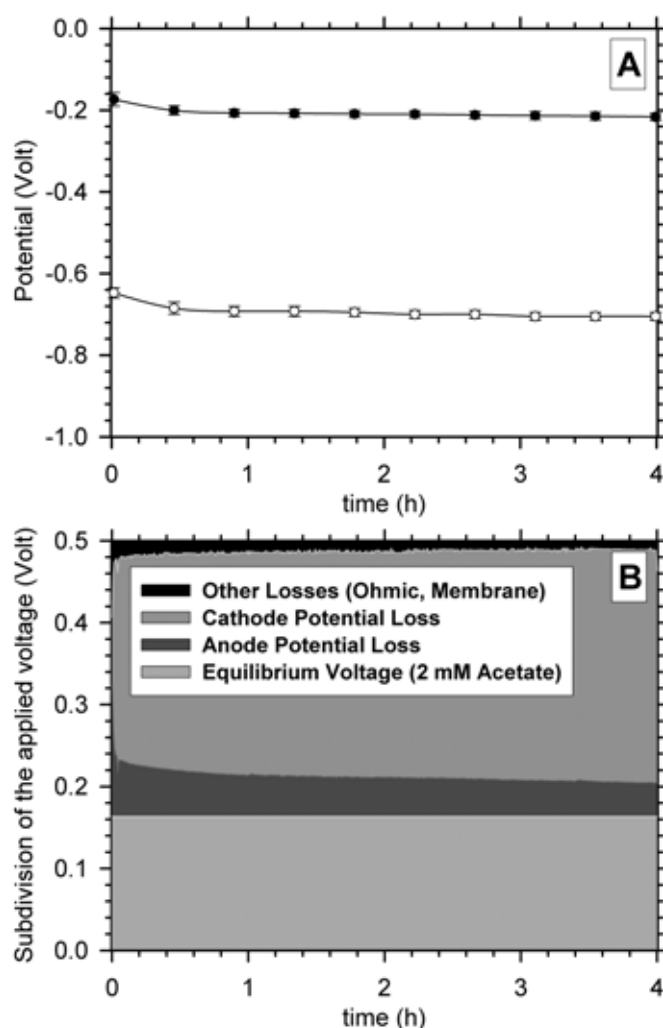


Figure 2.3. (A) Measured potential of the anode (closed circles) and cathode (open circles) during biocatalyzed electrolysis of acetate (2 mM) at an applied voltage of 0.5 V (duplicate experiments). The average measured current density during this period was $470 \pm 74.3 \text{ mA/m}^2$ anode surface. Bars indicate minimum and maximum of the duplicate experiments. (B) Subdivision of the applied voltage (0.5 V) during biocatalyzed electrolysis of acetate (2 mM).

2.4 Perspectives

The presented analysis of the experimental results has clearly indicated two important problems in the current biocatalyzed electrolysis setup, i.e., the cathodic hydrogen efficiency loss and the cathode potential loss. Together with the relatively low volumetric hydrogen production rate of approximately $0.02 \text{ Nm}^3 \text{ H}_2/\text{m}^3 \text{ reactor liquid volume/day}$ at an applied voltage of 0.5 V, it is clear that improvements are necessary to come to a mature hydrogen production technology. However, since this is one of the first studies describing biocatalyzed electrolysis, there is much room for improvements.

First of all, optimizations can be made with respect to the design of the electrochemical cell. The currently used system has a large liquid volume in relation to the anode surface area, while most of the generated current from acetate is believed to originate from the microorganisms that are directly attached to the anode (17). Assuming it is possible to reduce the anode liquid volume to a small layer around the anode (total compartment length: $\sim 5 \text{ mm}$) without influencing the current density and replacing the complete cathode chamber by a gas diffusion electrode as commonly applied in water electrolysis (35), the total reactor volume could be reduced to about 3% of its current size. This would already increase the volumetric hydrogen production rate to over $0.66 \text{ Nm}^3 \text{ H}_2/\text{m}^3 \text{ reactor liquid volume/day}$.

Furthermore, according to literature data on the performance of biological anodes in microbial fuel cell studies (21), current densities can be improved by at least one order of magnitude. However, in order to achieve this, much attention first needs to be spent towards lowering the above-mentioned cathode potential loss. When the cathode potential loss can be decreased, more of the applied voltage becomes available for other parts of the electrochemical cell, thus allowing higher current densities. At these higher current densities, the cathodic hydrogen efficiency is also expected to increase significantly, because the hydrogen diffusion through the membrane is only dependent on the hydrogen concentration gradient and not on the hydrogen production rate. This is schematically depicted in Figure 2.4 for the experimental setup that was used in this study. At higher

current densities, the absolute amount of hydrogen lost through the Nafion® membrane remains the same. However, in relative sense this loss becomes less significant, because more hydrogen is produced at the cathode at higher current densities. Furthermore, other cation selective membranes that are less hydrogen permeable might be available.

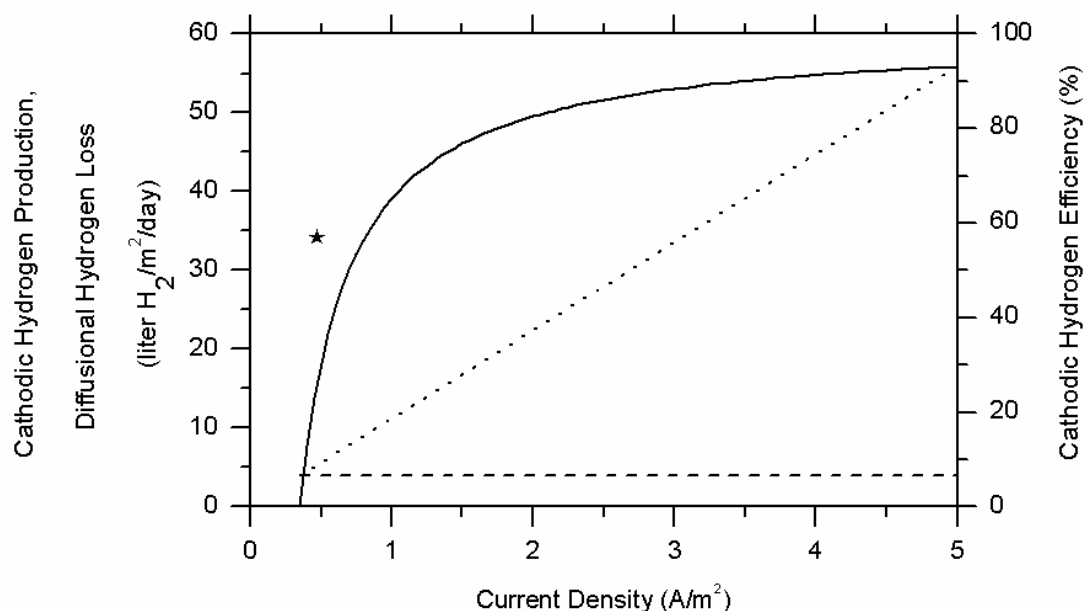


Figure 2.4. Estimation of the dependency of the cathodic hydrogen efficiency (solid line) on current density calculated for the experimental setup presented in this study. In the calculations it is assumed 100% H₂-saturated conditions apply in the cathode at all current densities. Therefore, a constant diffusional hydrogen loss is predicted of 4 L H₂/m²/day (dashed line — prediction based on (18,33)). The dotted line shows the hydrogen production at 100% cathodic hydrogen efficiency. The star indicates the cathodic hydrogen efficiency of the experiment presented in this study. The fact that the star is not on the line, is caused by the fact that the experiment was not conducted under 100% H₂-saturated conditions.

As can be seen from Figure 2.4, the current system was running the biocatalyzed electrolysis process in the lower part of the current density scale, explaining the relatively low cathodic hydrogen efficiency. If, on the other hand, a current density of 5 A/m² anode surface area is realized in an optimized system, the cathodic hydrogen efficiency and hence the overall hydrogen efficiency can reach values above 90%. This exceeds the mark for economic feasibility as mentioned by Benemann (7) by far. However, current densities of this magnitude can only be reached if the cathode potential loss can be reduced significantly (to <0.1 V at 5 A/m²). In combination with an optimized reactor design, volumetric hydrogen production rates will then become possible that exceed 10 Nm³ H₂/m³

reactor liquid volume/day at applied voltage of 0.3–0.4 V. The volumetric organic matter conversion rates associated with this increased performance are comparable to that of commercial anaerobic wastewater treatment plants. Therefore, next to being an efficient hydrogen generating process, the process then also functions as an efficient wastewater treatment process. Furthermore, with an expected required applied voltage of 0.3–0.4 V, biocatalyzed electrolysis achieves extremely low energy requirements for hydrogen production. Water electrolysis in practice operates at applied voltages well above 1.6 V (26-28), while biocatalyzed electrolysis requires at least four times less. The price of hydrogen produced through water electrolysis is strongly dependent on the electricity price (2). As this can be expected for biocatalyzed electrolysis as well, the reduced consumption of electrical energy per unit of hydrogen is a strong advantage of biocatalyzed electrolysis.

Besides acetate, a compound normally considered to be a byproduct of dark fermentation of glucose (3), many other substrates qualify for hydrogen production through biocatalyzed electrolysis. Recently, biological anodes have been studied in microbial fuel cells under various conditions. These conditions ranged from working with pure microbial cultures, e.g., with *Shewanella putrefaciens* (16), *Geobacter sulfurreducens* (14) and *Rhodospirillum rubrum* (15), on synthetic wastewater to mixed microbial cultures (17,21,22) on real wastewaters (18-20). These studies showed that electrochemically active microorganisms are able to generate current from many different substrates, varying from organic substrates like sugars (15,21,22) and fatty acids (14,17,36) to inorganic substrates, like elemental sulfur (23). By coupling comparable biological anodes to a proton reducing cathode many different kinds of substrates become available for hydrogen production. This diversity makes biocatalyzed electrolysis a robust and versatile hydrogen production process suitable for many kinds of wastewaters. Even more so, because this can be achieved by using a mixed culture of microorganisms. This obviously benefits the economics of the process, as no effort needs to be spent towards keeping the culture pure.

Another advantage of hydrogen that is produced through biocatalyzed electrolysis is its potential purity. Other biological hydrogen production

processes (e.g., dark fermentation, biomass gasification) produce a mixture of hydrogen, carbon dioxide and traces of other gases (e.g., H_2S , CO) and therefore require expensive gas treatment processes. Biocatalyzed electrolysis, on the other hand, produces the hydrogen separately in the cathode chamber. However, also with biocatalyzed electrolysis some contamination of the hydrogen can be expected due to the diffusion of gases produced in the anode chamber (e.g., CO_2) through the cation exchange membrane into the cathode chamber. As the biocatalyzed electrolysis experiments presented in this article were not optimized for the purity of the produced hydrogen, no definitive conclusion can yet be drawn about this. Hydrogen purity, therefore, needs to be subject for future research, as the product purity will eventually determine the application of this technology. PEM fuel cells, for example, which are considered to be most suitable for transportation purposes, require pure hydrogen as a fuel (37) and are irreversibly damaged by traces of H_2S and CO .

As a hydrogen production process, biocatalyzed electrolysis exhibits an enormous hydrogen production potential worldwide. In the case of the Netherlands, for example, all collected urban wastewater (38) already contains enough biodegradable material for the generation of 1.1 billion m^3 of hydrogen gas per year. Assuming a fuel efficiency of 0.5–1 kg hydrogen per 100 km for a fuel cell powered vehicle (39), this is already enough hydrogen for driving 9.4–19% of the total car km in the Netherlands (38). In its optimized configuration, biocatalyzed electrolysis will thus certainly proof its right of existence in a future hydrogen economy. However, also without a hydrogen economy biocatalyzed electrolysis is a promising technology for hydrogen production with a wide range of possible applications. For example, biocatalyzed electrolysis can be applied as a wastewater treatment process in hydrogen consuming industries (e.g., food-processing industry, petrochemical industry).

2.5 Acknowledgments

This work was financially supported by the NEO program of SenterNovem, agency of the Dutch Ministry of Economic Affairs. Project

title (translated from Dutch): Hydrogen production through biocatalyzed electrolysis (project number: 0268-03-04-04-002; granted: February 20, 2004).

2.6 References

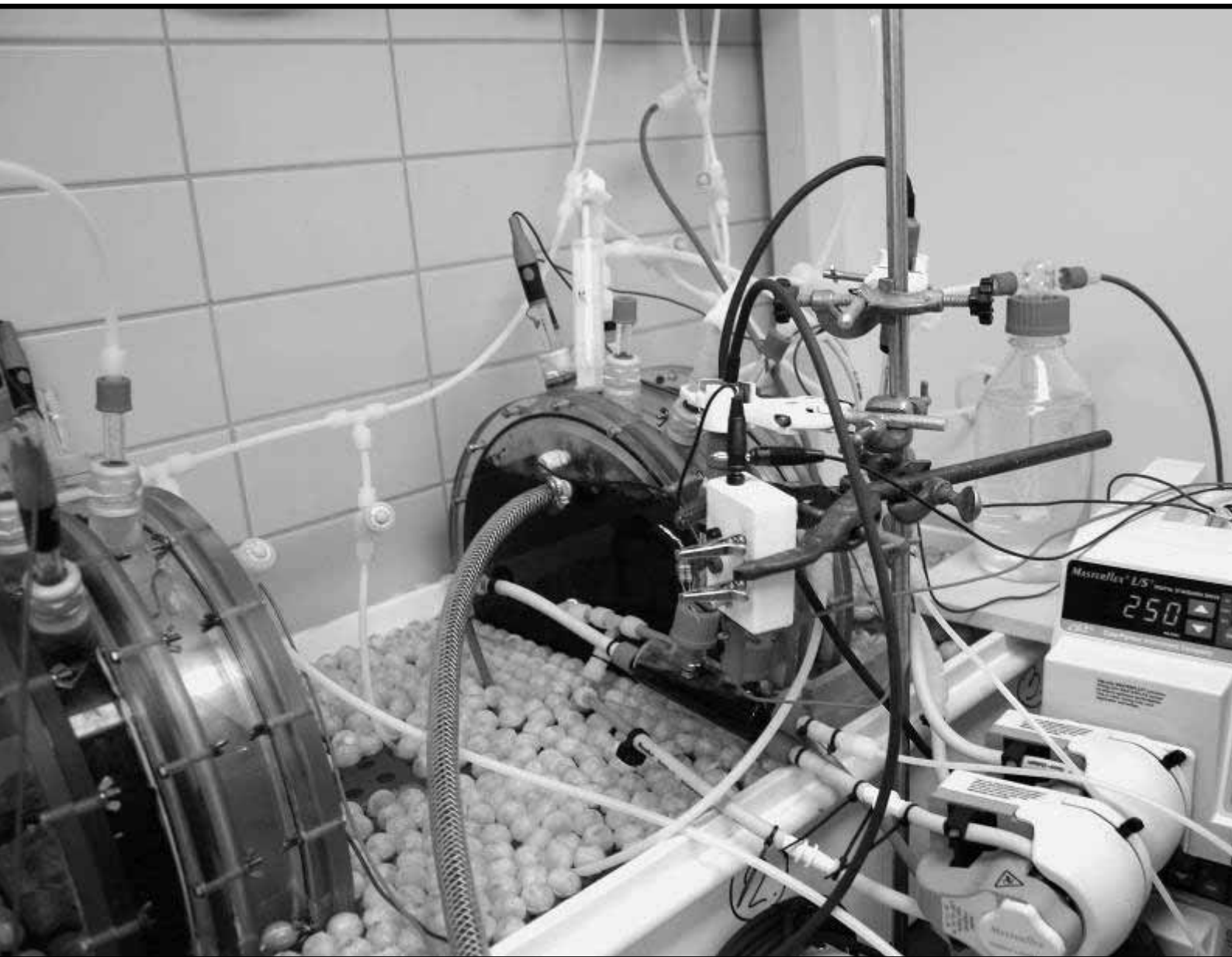
- (1) Schrope, M. Which way to energy utopia? *Nature* **2001**, *414*, 682-684.
- (2) Turner, J. A. Sustainable hydrogen production. *Science* **2004**, *305*, 972-974.
- (3) Angenent, L. T.; Karim, K.; Al-Dahhan, M. H.; Wrenn, B. A.; Domiguez-Espinosa, R. Production of bioenergy and biochemicals from industrial and agricultural wastewater. *Trends Biotechnol.* **2004**, *22*, 477-485.
- (4) Hawkes, F. R.; Dinsdale, R.; Hawkes, D. L.; Hussy, I. Sustainable fermentative hydrogen production: challenges for process optimisation. *Int. J. Hydrogen Energy* **2002**, *27*, 1339-1347.
- (5) Kim, I. S.; Hwang, M. H.; Jang, N. J.; Hyun, S. H.; Lee, S. T. Effect of low pH on the activity of hydrogen utilizing methanogen in bio-hydrogen process. *Int. J. Hydrogen Energy* **2004**, *29*, 1133-1140.
- (6) Oh, S. E.; Van Ginkel, S.; Logan, B. E. The relative effectiveness of pH control and heat treatment for enhancing biohydrogen gas production. *Environ. Sci. Technol.* **2003**, *37*, 5186-5190.
- (7) Benemann, J. Hydrogen biotechnology: progress and prospects. *Nat. Biotechnol.* **1996**, *14*, 1101-1103.
- (8) Barbosa, M. J.; Rocha, J. M. S.; Tramper, J.; Wijffels, R. H. Acetate as a carbon source for hydrogen production by photosynthetic bacteria. *J. Biotechnol.* **2001**, *85*, 25-33.
- (9) Lee, C. M.; Chen, P. C.; Wang, C. C.; Tung, Y. C. Photohydrogen production using purple nonsulfur bacteria with hydrogen fermentation reactor effluent. *Int. J. Hydrogen Energy* **2002**, *27*, 1309-1313.
- (10) Oh, Y. K.; Seol, E. H.; Kim, M. S.; Park, S. Photoproduction of hydrogen from acetate by a chemoheterotrophic bacterium *Rhodospseudomonas palustris* P4. *Int. J. Hydrogen Energy* **2004**, *29*, 1115-1121.
- (11) Hallenbeck, P. C.; Benemann, J. R. Biological hydrogen production; fundamentals and limiting processes. *Int. J. Hydrogen Energy* **2002**, *27*, 1185-1193.
- (12) Rozendal, R. A.; Buisman, C. J. N. Process for producing hydrogen. **2005**, *Patent WO2005005981*.
- (13) Liu, H.; Grot, S.; Logan, B. E. Electrochemically assisted microbial production of hydrogen from acetate. *Environ. Sci. Technol.* **2005**, *39*, 4317-4320.
- (14) Bond, D. R.; Lovley, D. R. Electricity production by *Geobacter sulfurreducens* attached to electrodes. *Appl. Environ. Microbiol.* **2003**, *69*, 1548-1555.

- (15) Chaudhuri, S. K.; Lovley, D. R. Electricity generation by direct oxidation of glucose in mediatorless microbial fuel cells. *Nat. Biotechnol.* **2003**, *21*, 1229-1232.
- (16) Kim, H. J.; Park, H. S.; Hyun, M. S.; Chang, I. S.; Kim, M.; Kim, B. H. A mediator-less microbial fuel cell using a metal reducing bacterium, *Shewanella putrefaciens*. *Enzyme Microb. Technol.* **2002**, *30*, 145-152.
- (17) Liu, H.; Cheng, S. A.; Logan, B. E. Production of electricity from acetate or butyrate using a single-chamber microbial fuel cell. *Environ. Sci. Technol.* **2005**, *39*, 658-662.
- (18) Liu, H.; Logan, B. E. Electricity generation using an air-cathode single chamber microbial fuel cell in the presence and absence of a proton exchange membrane. *Environ. Sci. Technol.* **2004**, *38*, 4040-4046.
- (19) Liu, H.; Ramnarayanan, R.; Logan, B. E. Production of electricity during wastewater treatment using a single chamber microbial fuel cell. *Environ. Sci. Technol.* **2004**, *38*, 2281-2285.
- (20) Oh, S.; Min, B.; Logan, B. E. Cathode performance as a factor in electricity generation in microbial fuel cells. *Environ. Sci. Technol.* **2004**, *38*, 4900-4904.
- (21) Rabaey, K.; Boon, N.; Siciliano, S. D.; Verhaege, M.; Verstraete, W. Biofuel cells select for microbial consortia that self-mediate electron transfer. *Appl. Environ. Microbiol.* **2004**, *70*, 5373-5382.
- (22) Rabaey, K.; Lissens, G.; Siciliano, S. D.; Verstraete, W. A microbial fuel cell capable of converting glucose to electricity at high rate and efficiency. *Biotechnol. Lett.* **2003**, *25*, 1531-1535.
- (23) Holmes, D. E.; Bond, D. R.; Lovley, D. R. Electron transfer by *Desulfobulbus propionicus* to Fe(III) and graphite electrodes. *Appl. Environ. Microbiol.* **2004**, *70*, 1234-1237.
- (24) Kim, B. H.; Kim, H. J.; Hyun, M. S.; Park, D. H. Direct electrode reaction of Fe(III)-reducing bacterium, *Shewanella putrefaciens*. *J. Microbiol. Biotechnol.* **1999**, *9*, 127-131.
- (25) Thauer, R. K.; Jungermann, K.; Decker, K. Energy conservation in chemotrophic anaerobic bacteria. *Bacteriol. Rev.* **1977**, *41*, 100-180.
- (26) Crow, D. R. *Principles and applications of electrochemistry*; 4th ed.; Stanley Thornes (Publishers) Ltd: Cheltenham, 1998.
- (27) Kinoshita, K. *Electrochemical oxygen technology*; John Wiley & Sons, Inc.: New York, 1992.
- (28) Rasten, E.; Hagen, G.; Tunold, R. Electrocatalysis in water electrolysis with solid polymer electrolyte. *Electrochim. Acta* **2003**, *48*, 3945-3952.
- (29) Bard, A. J.; Faulkner, L. R. *Electrochemical methods: fundamentals and applications*; 2nd ed.; John Wiley & Sons: New York, 2001.
- (30) Zehnder, A. J. B.; Huser, B. A.; Brock, T. D.; Wuhrmann, K. Characterization of an acetate-decarboxylating, non-hydrogen-oxidizing methane bacterium. *Arch. Microbiol.* **1980**, *124*, 1-11.
- (31) Oude Elferink, S. J. W. H.; Vorstman, W. J. C.; Sopjes, A.; Stams, A. J. M. Characterization of the sulfate-reducing and syntrophic population in granular sludge from a full scale anaerobic reactor treating papermill wastewater. *FEMS Microbiol. Ecol.* **1998**, *27*, 185-194.
- (32) Lide, R. L., Ed. *CRC Handbook of Chemistry and Physics*; 85th ed.; CRC Press: Boca Raton, 2004.

- (33) Jiang, J. H.; Kucernak, A. Investigations of fuel cell reactions at the composite microelectrode|solid polymer electrolyte interface. I. Hydrogen oxidation at the nanostructured Pt|Nafion[®] membrane interface. *J. Electroanal. Chem.* **2004**, *567*, 123-137.
- (34) Andersen, T. N.; Dandapani, B. S.; Berry, J. M. Hydrogen evolution studies in neutral media. *J. Electroanal. Chem.* **1993**, *357*, 77-89.
- (35) Motoo, S.; Furuya, N. Gas diffusion electrode for hydrogen evolution. *J. Electroanal. Chem.* **1984**, *161*, 189-191.
- (36) Bond, D. R.; Holmes, D. E.; Tender, L. M.; Lovley, D. R. Electrode-reducing microorganisms that harvest energy from marine sediments. *Science* **2002**, *295*, 483-485.
- (37) McNicol, B. D.; Rand, D. A. J.; Williams, K. R. Fuel cells for road transportation purposes - yes or no? *J. Power Sources* **2001**, *100*, 47-59.
- (38) Statistics Netherlands (CBS). <http://www.cbs.nl/en/>.
- (39) Schlapbach, L.; Züttel, A. Hydrogen-storage materials for mobile applications. *Nature* **2001**, *414*, 353-358.

Effects of Membrane Cation Transport on pH and Microbial Fuel Cell Performance

3



This chapter has been published as:

Rozendal, R. A.; Hamelers, H. V. M.; Buisman, C. J. N. Effects of membrane cation transport on pH and microbial fuel cell performance. *Environ. Sci. Technol.* **2006**, *40*, 5206-5211.

Effects of Membrane Cation Transport on pH and Microbial Fuel Cell Performance

3

Due to the excellent proton conductivity of Nafion® membranes in polymer electrolyte membrane fuel cells (PEMFCs), Nafion® has been applied also in microbial fuel cells (MFCs). In literature, however, application of Nafion® in MFCs has been associated with operational problems. Nafion® transports cation species other than protons as well, and in MFCs concentrations of other cation species (Na^+ , K^+ , NH_4^+ , Ca^{2+} , and Mg^{2+}) are typically 10^5 times higher than the proton concentration. The objective of this study, therefore, was to quantify membrane cation transport in an operating MFC and to evaluate the consequences of this transport for MFC application on wastewaters. We observed that during operation of an MFC mainly cation species other than protons were responsible for the transport of positive charge through the membrane, which resulted in accumulation of these cations and in increased conductivity in the cathode chamber. Furthermore, protons are consumed in the cathode reaction and, consequently, transport of cation species other than protons resulted in an increased pH in the cathode chamber and a decreased MFC performance. Membrane cation transport, therefore, needs to be considered in the development of future MFC systems.

3.1 Introduction

Chemical energy can be converted to electrical energy in a direct and efficient way by applying fuel cell technology. Due to their high power density, fast startup time, and flexible power output, polymer electrolyte membrane fuel cells (PEMFCs) have received much research attention (1). PEMFCs have been designed for conversion of relatively simple fuels, such as hydrogen. The electrochemical oxidation of hydrogen at the anode of PEMFCs produces protons and electrons. An electrical circuit transports the electrons to the cathode, where the electrons are consumed in the reduction reaction of oxygen. To sustain this process, electroneutrality needs to be observed, i.e., transport of electrons to the cathode needs to be compensated by transport of an equal amount of positive charge to the cathode chamber. In PEMFCs, electroneutrality is observed by transport of protons through a cation exchange membrane, which, therefore, is often referred to as proton exchange membrane (PEM). The cation exchange membrane is one of the most critical components in the PEMFC configuration. It provides a separation between fuel and oxidizer, but at the same time facilitates transport of positive charge to compensate for transport of electrons. The perfluorosulfonic acid membrane Nafion® (product of DuPont) has been known for its good performance as a cation exchange membrane in PEMFCs (2). The morphology and properties of Nafion® have extensively been reviewed by Mauritz and Moore (3). Nafion® consists of a hydrophobic fluorocarbon backbone to which hydrophilic sulfonate groups ($-\text{SO}_3^-$) are attached (4). The high cation conductivity of Nafion® can be explained from the high concentration of these negatively charged sulfonate groups in the membrane ($[-\text{SO}_3^-] \approx 1.13 \text{ mol/L}$) (5,6).

Due to its good reputation, Nafion® has recently become widely applied in microbial fuel cells (MFCs) as well (7-15). MFCs are considered a promising new technology for efficient production of electrical energy from wastewaters (16). In an MFC, electrons are generated from the oxidation of dissolved organic material by electrochemically active microorganisms (16). Current densities achieved in MFCs are typically 10^3 to 10^4 times lower than those achieved in PEMFCs, so the process is much less demanding with

respect to transport of positive charge through the cation exchange membrane. One would expect, therefore, that Nafion®, with its excellent cation conductivity, is more than suitable for application in MFCs.

In the literature, however, application of Nafion® in MFCs has been associated with operational problems. During operation of a two-chamber MFC, Gil et al. (9) observed a decreasing pH in the anode chamber and an increasing pH in the cathode chamber, because proton transport through the Nafion® seemed to be slower than the proton production rate in the anode chamber and the proton consumption rate in the cathode chamber. In another study, Liu and Logan (10) operated a single-chamber MFC in the presence and absence of a Nafion® 117 membrane and observed a reduced power output when Nafion® was present (262 ± 10 vs 494 ± 21 mW/m²). Potential measurements showed that the anode potential was identical in the presence and absence of a Nafion® 117, but that the cathode potential was 0.177 ± 0.012 V lower when Nafion® was present.

These results indicate that application of Nafion® in MFCs is not straightforward. Different working conditions in MFCs compared to those in PEMFCs might be an explanation for this. In PEMFCs, protons are the only cation species present in the system and protons, therefore, are the only cation species transported. In MFCs, however, operating with wastewater at pH neutral conditions, the proton concentration is about 10^{-4} mM, whereas concentrations of other cation species (e.g., Na⁺, K⁺, NH₄⁺, Ca²⁺, and Mg²⁺) are typically 10^5 times higher. Nafion®, like all other commercial cation exchange membranes, transports cation species other than protons as well (17,18). The objective of this study, therefore, was to quantify membrane cation transport in an operating MFC and to evaluate the consequences of this transport for MFC application on wastewaters.

3.2 Materials and methods

3.2.1 Electrochemical cell

Experimental runs were performed in a two-chamber electrochemical cell (total volume 6.6 L; total liquid volume 6 L; see Chapter 3 title page) as previously described (19). Graphite felt (surface area 400 cm², thickness 3

mm — FMI Composites Ltd., Galashiels, Scotland) was used as the anode; a platinum-coated (50 g/m²) titanium mesh electrode (surface area 400 cm², thickness 1 mm, specific surface area 1.7 m²/m² — Magneto Special Anodes bv, Schiedam, The Netherlands) was used as the cathode. The anode and cathode chamber were separated from each other by a Nafion® 117 membrane (surface area 256 cm²). Both chambers were equipped with an Ag/AgCl reference electrode and a pH electrode. To prevent interference of pH measurements with potential measurements, the pH electrodes were placed externally to the anode/cathode chamber in a flow cell through which the anolyte/catholyte was continuously pumped at a rate of 250 mL/min. If required, the anode and cathode chamber could be operated pH controlled (Liquisys M CPM 253, Endress+Hauser) by dosing 1 M KOH (anode) or 1 M HCl (cathode).

3.2.2 Medium and microorganisms

The anode chamber of the MFC was continuously fed at a rate of 4.5 mL/min with synthetic wastewater (i.e., anolyte; pH 7) containing (in deionized water) 1.36 g/L NaCH₃COO·3H₂O, 0.74 g/L KCl, 0.58 g/L NaCl, 0.68 g/L KH₂PO₄, 0.87 g/L K₂HPO₄, 0.28 g/L NH₄Cl, 0.1 g/L yeast extract, 0.1 g/L MgSO₄·7H₂O, 0.1 g/L CaCl₂·2H₂O, and 1 mL/L of a trace element mixture (20). The anode chamber was inoculated with 500 mL of effluent taken from an active bioelectrochemical cell (19) and operated in batch until a stable MFC system was established. Steady state conditions were achieved after 5 days of operation (cell voltage 0.14–0.2 V across a 10 Ω resistor). The anode chamber was operated pH controlled (pH 7) in all experimental runs. The cathode chamber was filled with 3.0 L of catholyte (Table 3.1) and was operated as a batch system in all experimental runs. The phosphate buffers that were used as catholyte were prepared as a mixture of KH₂PO₄ and K₂HPO₄. The catholyte was kept saturated with oxygen by continuously aerating with humidified air. Cathode chamber pH control varied per experimental run (Table 3.1).

Table 3.1. Experimental conditions

Run	Catholyte (in Milli-Q)	Cathode chamber pH control?	Resistor (Ω)
1/2	10 mM phosphate buffer (pH 7)	Yes (pH 7)	10
3/4	10 mM phosphate buffer (pH 7)	Yes (pH 7)	50
5/6	Anolyte without acetate + 10 mM NaCl	Yes (pH 7)	10
7/8	10 mM phosphate buffer (pH 7)	No	10
9/10	50 mM phosphate buffer (pH 7)	No	10

3.2.3 Experimental procedures and calculations

All experimental runs were performed at a temperature of 303 K. Experimental conditions that were varied are described in Table 3.1. An experimental run was started by closing the electrical circuit. Every experimental run lasted 96 h and was done in duplicate. Results are reported as means \pm standard deviation. Every 24 h a 15 mL sample was taken from the influent vessel, anode chamber, and cathode chamber and filtered across a 0.45 μ m filter. Anion concentrations were determined using an ion chromatograph (Metrohm 761 Compact IC) equipped with a conductivity detector and an anion column (Metrosep A Supp 5 6.1006.520). Ammonium concentrations were photometrically determined using standardized test kits (ammonium cuvette test LCK303, XION 500 spectrophotometer, Dr. Lange Nederland bv, The Netherlands). Other cation concentrations (Na^+ , K^+ , Ca^{2+} , and Mg^{2+}) were determined using inductively coupled plasma-optical emission spectroscopy (ICP-OES; Perkin-Elmer Optima 3000XL). Cell voltage and potentials of the anode and cathode were logged with a data logger (SQ800, Grant Instruments, England). The current through the electrical circuit was determined from the measured cell voltage according to

$$I = \frac{E}{R} \quad (1)$$

with I the current in amperes (A), E the cell voltage in volts (V), and R the electrical resistance in ohms (Ω).

Power output of the system was determined according to

$$P = E \cdot I = \frac{E^2}{R} \quad (2)$$

with P the power output in watts (W).

When calculating charge (Q) a distinction was made between transport of negative charge in the form of electrons through the electrical circuit (Q^-) and transport of positive charge in the form of the dominantly present cation species in the system (Na^+ , K^+ , NH_4^+ , Ca^{2+} , and Mg^{2+}) through the Nafion® membrane (Q^+). Transport of negative charge in the form of electrons through the electrical circuit (Q^-) in coulombs (C) was determined by integrating current over time. Transport of positive charge in the form of the dominantly present cation species in the system through the Nafion® membrane (Q^+) in coulombs (C) was determined from the ICP-OES measurements and ammonium tests as follows:

$$Q^+(t) = \sum_{\text{Na}^+, \text{K}^+, \text{NH}_4^+, \text{Ca}^{2+}, \text{Mg}^{2+}} ((x^{\text{cat},t} - x^{\text{cat},0}) \cdot V \cdot z^{\text{cat}} \cdot F) \quad (3)$$

with $x^{\text{cat},t}$ the molar concentration of the cation species at time t in moles per liter (M), $x^{\text{cat},0}$ the molar concentration of the cation species at the start of an experimental run in moles per liter (M), V the cathode chamber liquid volume in liters (L), z^{cat} the valence of the cation species, and F the Faraday constant (96485.3 C/mol). Calculated values were corrected for cathode chamber liquid volume reduction caused by sampling (~0.5% per day).

To evaluate the cation content of the Nafion® membrane after use in an MFC, membrane samples were taken after experimental runs 5/6. The membrane samples were first washed with Milli-Q water and then analyzed with energy dispersive X-ray spectrometry (EDX). For the EDX analysis a JEOL JSM-6480LV scanning electron microscope (SEM) equipped with a NORAN System SIX model 300 X-ray microanalysis system (Thermo Electron Corporation) was used. Measurements were done at an acceleration voltage of 10 kV. To test whether detected cation species could

be reversibly removed from the Nafion® membrane, samples were stored overnight in 35% H₂O₂, washed with Milli-Q water, boiled in 1 M HCl for 1 h, washed with Milli-Q water, and then analyzed again with EDX.

3.3 Results and discussion

3.3.1 *Membrane cation transport*

The synthetic wastewater, which was fed to the anode chamber of the MFC, contained 20 mM sodium, 25 mM potassium, 5.2 mM ammonium, 0.7 mM calcium, and 0.4 mM magnesium. At the start of the experimental runs the catholyte consisted of a 10 mM phosphate buffer solution (run 1/2 in Table 3.1). Both anode and cathode chamber were kept pH controlled at pH 7 and the proton concentration in the cathode chamber, therefore, remained constant (10⁻⁴ mM) throughout the experimental run. Under these conditions transport of cations to the cathode chamber was studied in an operating MFC in 96 h experimental runs. Average current during the experimental runs was 14.4±1.9 mA across a 10 Ω resistor (average current density 563±74 mA/m² membrane surface area). Figure 3.1 gives the development of the concentrations of the dominantly present cation species (Na⁺, K⁺, NH₄⁺, Ca²⁺, and Mg²⁺) and conductivity in the cathode chamber during the experimental run.

Figure 3.1 shows that all five dominantly present cation species in the anolyte were transported through the Nafion® 117 membrane resulting in an increased concentration of these cation species in the catholyte. Variations in the concentration of anion species in the cathode chamber during the experimental runs were negligible (<0.1 mM). An exception to this was the chloride concentration, which increased due to hydrochloric acid dosing for pH control. Increase in conductivity, therefore, was a combined effect of increased cation and chloride concentrations.

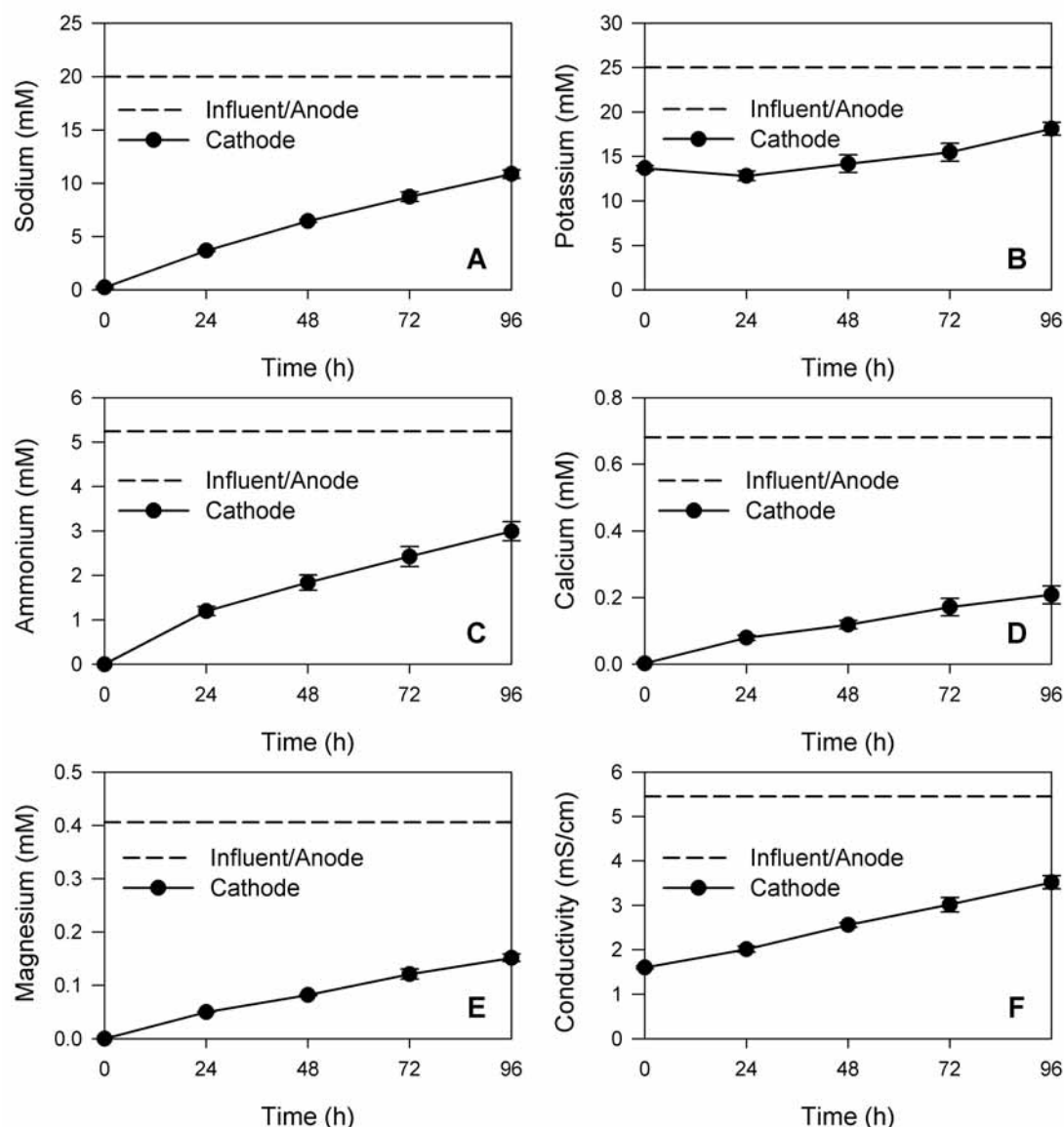


Figure 3.1. Development of the cation concentrations (Na^+ , K^+ , NH_4^+ , Ca^{2+} , and Mg^{2+}) and conductivity in a pH-controlled (pH 7) cathode chamber of a microbial fuel cell (catholyte at $t=0$ 10 mM phosphate buffer; resistor 10 Ω). Bars indicate standard deviations.

To quantify the contribution of the transport of cation species other than protons in relation to the total transport of positive charge to the cathode chamber, the total measured amounts of these cation species were expressed in coulombs (see Materials and methods) and plotted against the integrated current (Figure 3.2).

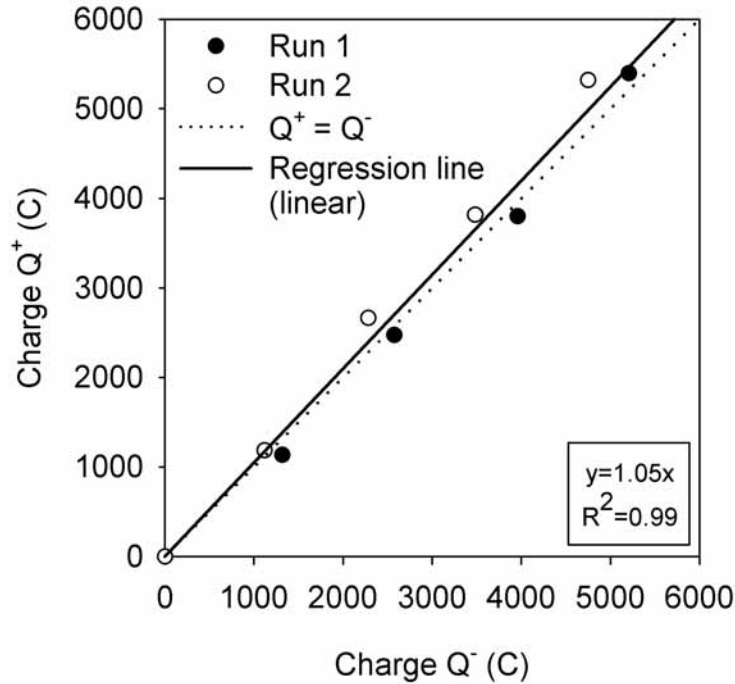


Figure 3.2. Transport of positive charge in the form of the dominantly present cation species (Na^+ , K^+ , NH_4^+ , Ca^{2+} , and Mg^{2+}) through the Nafion® 117 membrane (Q^+) to a pH-controlled (pH 7) cathode chamber of a microbial fuel cell (catholyte at $t=0$ 10 mM phosphate buffer; resistor 10 Ω) against the integrated current (Q^-). The box gives the result of the linear regression of Q^+ as a function of Q^- of all acquired data points of the duplicate runs.

As can be seen from Figure 3.2 a linear correlation exists between the transport of electrons through the electrical circuit and the transport of positive charge in the form of dominantly present cation species through the membrane. The slope close to unity (1.05) indicates that mainly cation species other than protons were responsible for the transport of positive charge through the membrane. This was also confirmed by chloride concentration measurements. The oxygen reduction reaction consumes protons equimolarly with electrons as follows:



To keep pH constant, therefore, one molecule of hydrochloric acid needs to be dosed for every positive charge in the form of cation species other than protons that is transported through the membrane. Indeed, the total amount of hydrochloric acid dosed was confirmed to be in the same range as the total amount of transported positive charge in the form of the

dominantly present cation species (49.7 ± 9.0 mmol vs 56.2 ± 0.6 mmol, respectively).

To exclude the possibility that the observed linear correlation was coincidental, the experimental runs were repeated with a 50Ω resistor in the electrical circuit (run 3/4 in Table 3.1; Figure 3.3). At this higher electrical resistance, less current flows (average current 6.0 ± 0.2 mA; average current density 234 ± 8 mA/m² membrane surface area) and consequently a reduced transport of the dominantly present cation species is expected.

Figure 3.3 shows that also when a 50Ω resistor was used, the transport of positive charge in the form of dominantly present cation species through the membrane was linearly related to the transport of electrons through the electrical circuit. Again, the slope of the linear regression line between Q^+ and Q^- was close to unity (0.84), which indicated that also in this case mainly cation species other than protons were responsible for the transport of positive charge through the Nafion® membrane.

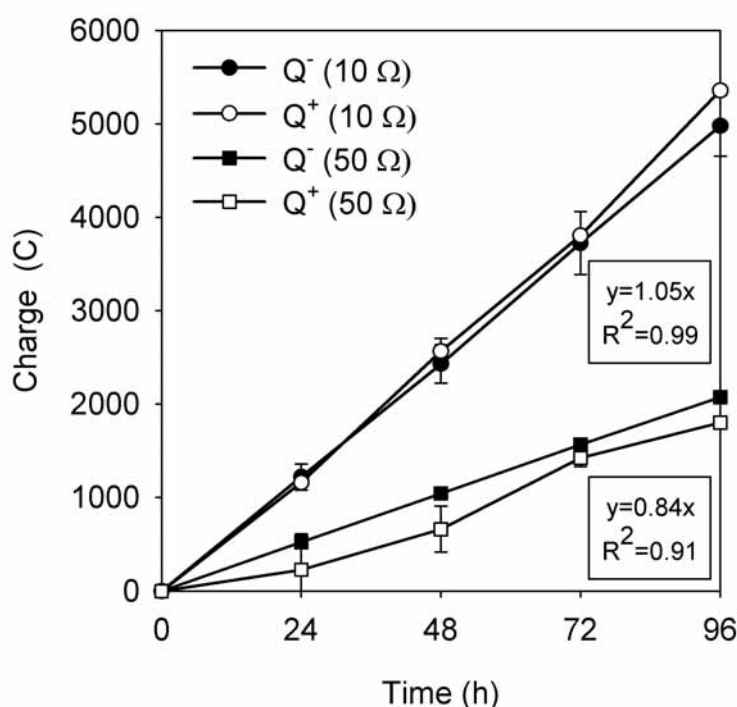


Figure 3.3. Influence of the electrical resistance on the integrated current (Q^-) and the transport of positive charge in the form of the dominantly present cation species (Na^+ , K^+ , NH_4^+ , Ca^{2+} , and Mg^{2+}) through the Nafion® 117 membrane (Q^+) to a pH-controlled (pH 7) cathode chamber of a microbial fuel cell (catholyte at $t=0$ 10 mM phosphate buffer). The boxes give the result of the linear regression of Q^+ as a function of Q^- of all acquired data points of the duplicate runs. Bars indicate standard deviations.

To test whether the transport of cation species other than protons would stop when cation concentrations in the catholyte become identical to those in the anolyte, membrane cation transport was quantified in case the cation concentrations in the catholyte at the start of the experimental runs were identical to those in the anolyte (run 5/6 in Table 3.1; Figure 3.4).

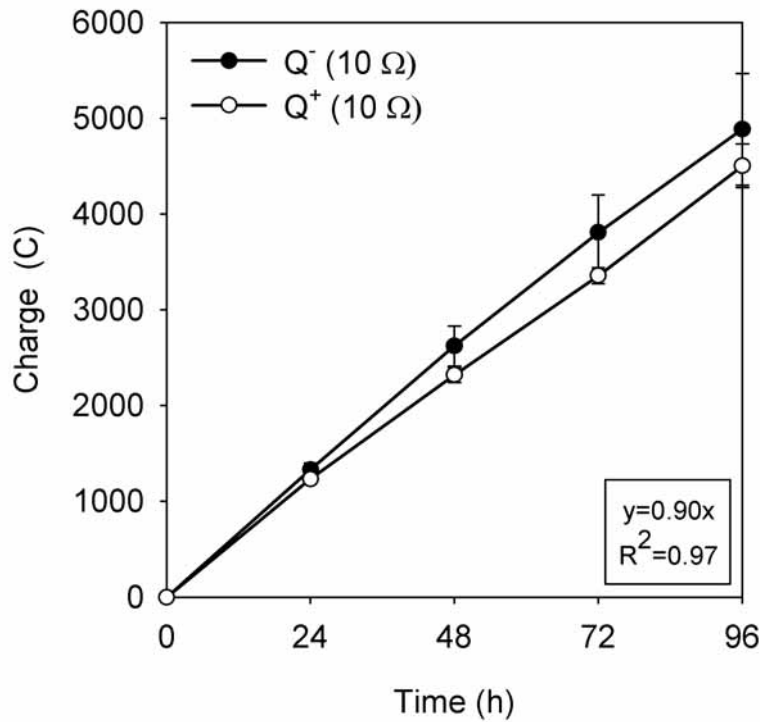


Figure 3.4. Development of the integrated current (Q^-) and the transport of positive charge in the form of the dominant cation species (Na^+ , K^+ , NH_4^+ , Ca^{2+} , and Mg^{2+}) through the Nafion® 117 membrane (Q^+) to a pH-controlled (pH 7) cathode chamber of a microbial fuel cell (resistor: $10\ \Omega$) when cation concentrations in the catholyte at $t=0$ are identical to those in the anolyte. The box gives the result of the linear regression of Q^+ as a function of Q^- of all acquired data points of the duplicate runs. Bars indicate standard deviations.

Figure 3.4 shows that even under these conditions mainly cation species other than protons were responsible for the transport of positive charge through the membrane. During the experimental runs (average current 14.2 ± 2.0 mA across a $10\ \Omega$ resistor; average current density 555 ± 78 mA/m² membrane surface area) the sodium concentration in the catholyte increased with $24 \pm 7\%$, potassium with $51 \pm 3\%$, ammonium with $25 \pm 2\%$, and conductivity with $36 \pm 2\%$. Again, the slope of the linear regression line between Q^+ and Q^- was close to unity (0.90). This shows that membrane transport of cation species other than protons to the cathode chamber does

not even stop when the cation concentrations of the anolyte are reached. This means that the MFC is performing electrodialysis (21). In electrodialysis processes liquid streams are concentrated or desalinated under the influence of an electric field. In case of the MFC this electrical field is generated internally.

3.3.2 Sulfonate group occupation

The experimental runs described above have demonstrated that under typical MFC working conditions, electroneutrality is observed mainly by transport of cation species other than protons through the Nafion® membrane. This can be explained from the relative abundance of these other cation species compared to protons in the system. In the MFC, the Nafion® membrane equilibrates with the cation species present in the anolyte and catholyte. This equilibration rapidly turns the membrane from its proton form into a form in which mainly other cation species (Na^+ , K^+ , NH_4^+ , Ca^{2+} , and Mg^{2+}) occupy the negatively charged sulfonate groups. Considering that concentrations of other cation species in (synthetic) wastewaters (~pH 7) are typically 10^5 times higher than the proton concentration (~ 10^{-7} vs ~ 10^{-4} mM) and that the sulfonate groups in Nafion® have a higher affinity for most other cation species than for protons (5,6,22), it can be calculated that over 99.999% of the sulfonate groups will be occupied by cation species other than protons. Although the diffusion coefficient of protons in Nafion® is up to 4.4 times (17) higher than that for sodium and up to 6.2 times (18) higher than that for potassium, the low proton concentration in solution and in the membrane cause the transport rate of protons to be about 10^4 times lower than the transport rate of other cation species. This makes proton transport negligibly small compared to the transport of other cation species, which explains the observed results.

To confirm that cation species other than protons indeed mainly occupied the negatively charged sulfonate groups, the Nafion® membrane used in experimental runs 5/6 (Table 3.1) was subjected to EDX analysis (Figure 3.5A). A quantitative analysis of this spectrum identified 1.33% of the atoms as sulfur (S), which originate from the negatively charged sulfonate groups in Nafion®. Sodium and potassium represented 0.30% and

0.68% of the atoms respectively, which indicated that these two cation species alone already occupied an important fraction (74%) of the negatively charged sulfonate groups. The other dominantly present cation species in the system (NH_4^+ , Ca^{2+} , and Mg^{2+}) were below the detection limit of the EDX analysis, but were expected to occupy most of the remaining sulfonate groups. All detectable cation species could be reversibly replaced by protons by storing the membrane overnight in 35% hydrogen peroxide and boiling it for 1 h in 1 M HCl (Figure 3.5B).

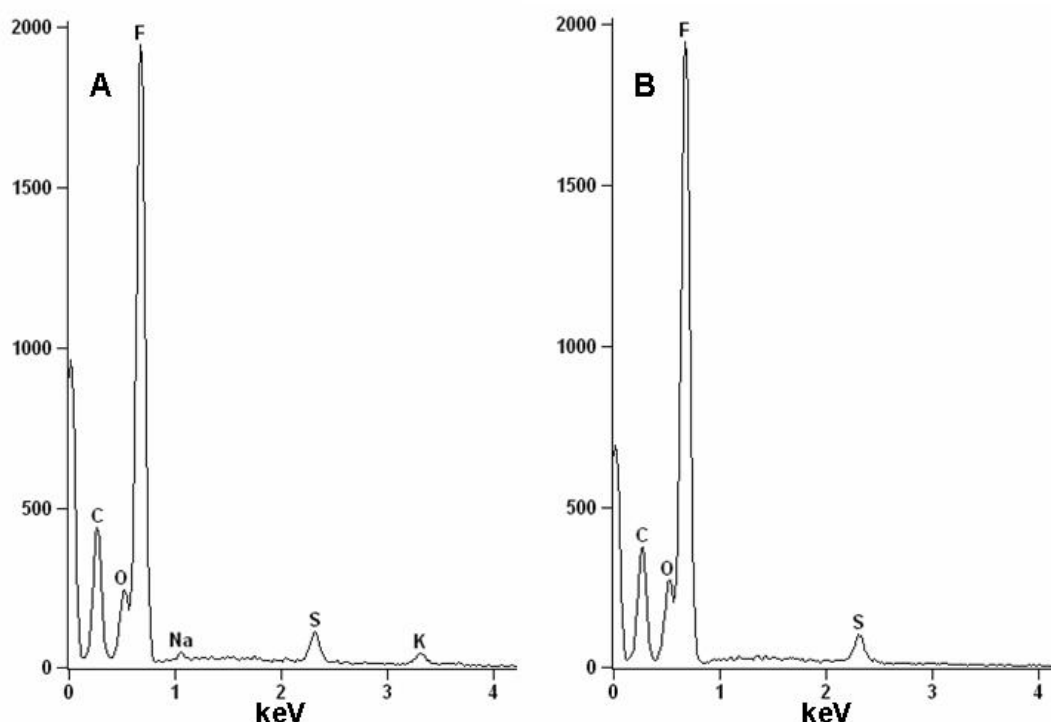


Figure 3.5. EDX spectrum of a Nafion® 117 membrane. (A) after use in an MFC (experimental runs 5/6 - Table 3.1), and (B) after subsequently treating it with 35% H_2O_2 (overnight) and 1 M HCl (boiling for 1 hour).

3.3.3 Effects on pH and MFC performance

Protons are consumed equimolarly with electrons in the oxygen reduction reaction in the cathode chamber (Equation 4). Consequently, in the absence of pH control, the pH will increase in the cathode chamber if protons are not replenished through the membrane. This was tested in the MFC (resistor 10 Ω) with a 10 mM phosphate buffer (pH 7) as the catholyte (run 7/8 in Table 3.1; Figure 3.6A and C) and with a 50 mM phosphate buffer (pH 7) as the catholyte (run 9/10 in Table 3.1; Figure 3.6B and D).

As predicted, the pH in the cathode chamber started to increase straight from the beginning of the experimental runs due to transport of cation species other than protons through the Nafion® membrane. Due to the higher buffer capacity of the catholyte with 50 mM phosphate buffer, pH increase was slower than when the catholyte with 10 mM phosphate buffer was used. Figure 3.6A and B show that an increase of pH in the cathode chamber was associated with a decrease in power output of the MFC. From Figure 3.6C and D it becomes clear that this decrease in performance was mainly caused by the decrease of the cathode potential. The anode potential, on the other hand, remained constant throughout all experimental runs and was close to the theoretical potential for acetate oxidation of -0.28 V at pH 7 (19).

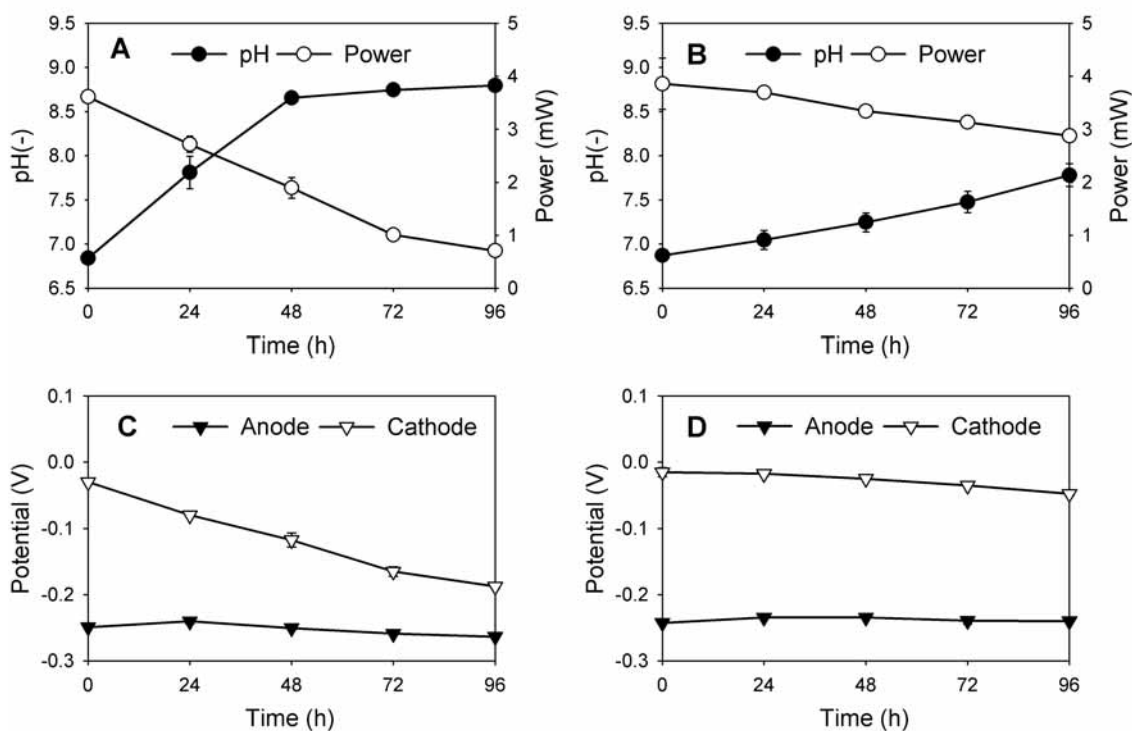


Figure 3.6. Development of the pH in the cathode chamber, power output, and anode and cathode potentials (vs NHE) during operation of a microbial fuel cell (resistor 10 Ω). (A/C) 10 mM phosphate buffer (pH 7) as the catholyte; (B/D) 50 mM phosphate buffer (pH 7) as the catholyte. Bars indicate standard deviations.

3.3.4 Implications for MFC application on wastewaters

By quantifying membrane cation transport, this study has provided an explanation for the operational problems, mentioned in the literature, associated with the application of Nafion® in MFCs. The pH effects as

mentioned by Gil et al. (9), i.e., a decreasing anode pH and an increasing cathode pH, can now be explained from membrane cation transport. In an operating MFC, electroneutrality is observed mainly by transport of cation species other than protons through the membrane, because these other cation species are more dominantly present. As suggested by Gil et al. (9), buffers can indeed compensate for lack of proton transport. This compensation, however, can be only temporary. The buffer strengths as applied in the catholytes in our experimental runs are similar to those used in many other MFC studies (9,12,13,23). In short experiments these buffers are sufficiently strong to keep a reasonably constant performance. However, as our results show, if experiments take longer than a few days, i.e., which is more comparable to practical conditions, the cathode chamber will suffer from an increasing pH. In our experiments this increasing pH was associated with a decrease of the MFC performance. Furthermore, if also the anode chamber is operated in batch, a decrease of the anode chamber pH can be expected as well. A decrease of the anode chamber pH can inhibit the microbial consortium, which will also negatively influence MFC performance (9).

This study also provides an explanation for the cathode potential loss as reported by Liu and Logan in their study on a single-chamber MFC operated in the presence and absence of a Nafion® 117 membrane (10). At open circuit conditions, the cathode potential loss caused by the presence of the Nafion® 117 membrane was 0.177 ± 0.012 V and remained constant over the complete measuring range (up to 1.4 A/m^2). This potential loss is too high to be explained from the area resistance of the membrane. The reported area resistances for Nafion® 117 are in the range 0.09 to $0.35 \text{ } \Omega\text{cm}^2$ (4) for protons and $1.5 \text{ } \Omega\text{cm}^2$ for cations in general (24). Assuming the highest value applies to Nafion® in MFCs, the cathode potential loss due to the area resistance of the Nafion® at the current densities, as reported by Liu and Logan, cannot have been higher than 0.00021 V ($=1.4 \times 10^{-4} \text{ A/cm}^2 \times 1.5 \text{ } \Omega\text{cm}^2$). Alternatively, the results of this study suggest that lack of protons in the membrane due to equilibration with the anolyte (pH 7.3-7.6), was the most important reason for the cathode potential loss. Transport of protons through Nafion® markedly decreases when the amount of cation species

other than protons occupy over 50% of the sulfonate groups (5,6,25). In an MFC, over 99.999% of the sulfonate groups are expected to be occupied by cation species other than protons. This lack of protons, therefore, is likely to limit proton transport through the membrane. In a single-chamber MFC, the cathode chamber is omitted by applying a gas diffusion electrode (GDE). Consequently, the protons required for the oxygen reduction reaction need to be supplied from the anolyte through the Nafion® membrane. As lack of protons in the membrane limits the proton transport through the membrane, a pH increase at the cathode side of the membrane can be expected. From the Nernst equation (26) it can be calculated that this negatively influences cathode potential. If the pH at the cathode side of the membrane increases only 3 pH units (e.g., from pH 7 to 10) the cathode potential will already decrease 0.18 V, which comes close to the value reported by Liu and Logan.

Despite the excellent performance of Nafion® in PEMFCs, application of Nafion® as a cation exchange membrane in MFCs is not straightforward, because the membrane transports cation species other than protons as well. Although not demonstrated for other types of cation exchange membranes, such as Ultrex (27-29), similar results can be expected there. In the literature, operational problems associated with the use of cation exchange membranes in MFCs are not generally acknowledged, but this study shows that the effects for long-term operation of MFCs on wastewater can be dramatic. Buffers offer only a temporary solution and permanent cathode chamber pH control is too costly as for every mole of electrons transported, close to one mole of acid needs to be dosed. In principle, only membranes that are truly 100% proton selective can prevent the described pH effects, but these types of membranes are currently not commercially available. Alternatively, membranes can be omitted from the MFC configuration, but only at the cost of a reduced coulombic efficiency (10). None of the available solutions seem to be optimal and membrane cation transport, therefore, is an important issue for the development of future MFC systems.

3.4 Acknowledgments

This work was performed at Wetsus, Centre for Sustainable Water Technology. Wetsus is funded by the city of Leeuwarden, the Province of Fryslân, the European Union European Regional Development Fund and by the EZ/KOMPAS program of the “Samenwerkingsverband Noord-Nederland”. We thank the participants of the theme “Energy from Water” for their input and contributions: Nuon, Paques bv, Frisia Zout bv, Magneto Special Anodes bv, Triqua bv, Landustrie Sneek bv, Hubert Stavoren bv, Waterbedrijf Groningen, Waterleidingmaatschappij Drenthe, and Waterlab Noord. We further thank Dr. G. J. W. Euverink for critical reading of the manuscript.

3.5 References

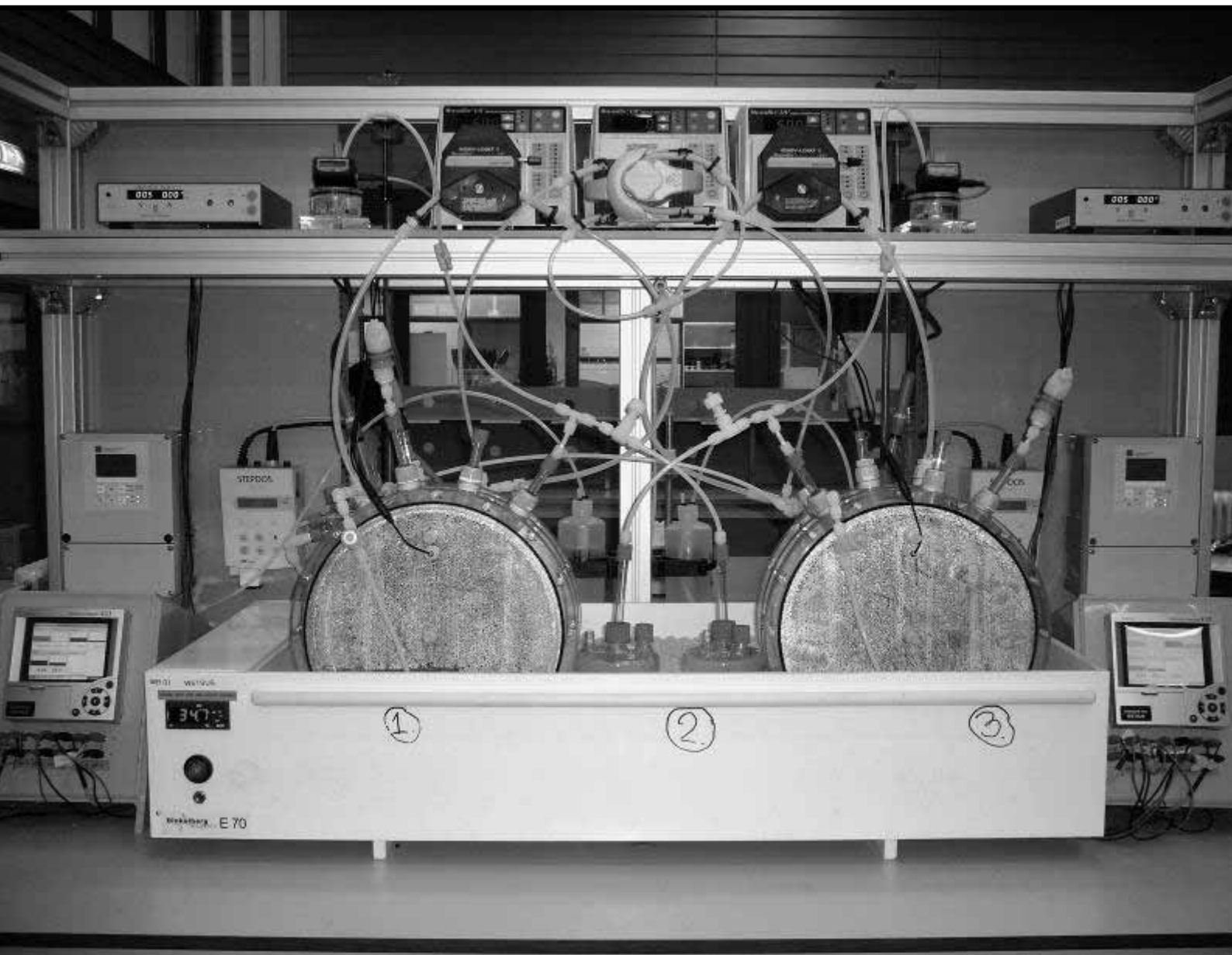
- (1) McNicol, B. D.; Rand, D. A. J.; Williams, K. R. Fuel cells for road transportation purposes - yes or no? *J. Power Sources* **2001**, *100*, 47-59.
- (2) Banerjee, S.; Curtin, D. E. Nafion® perfluorinated membranes in fuel cells. *J. Fluorine Chem.* **2004**, *125*, 1211-1216.
- (3) Mauritz, K. A.; Moore, R. B. State of understanding of Nafion. *Chem. Rev.* **2004**, *104*, 4535-4585.
- (4) Slade, S.; Campbell, S. A.; Ralph, T. R.; Walsh, F. C. Ionic conductivity of an extruded Nafion 1100 EW series of membranes. *J. Electrochem. Soc.* **2002**, *149*, A1556-A1564.
- (5) Okada, T.; Møller-Holst, S.; Gorseth, O.; Kjelstrup, S. Transport and equilibrium properties of Nafion® membranes with H⁺ and Na⁺ ions. *J. Electroanal. Chem.* **1998**, *442*, 137-145.
- (6) Okada, T.; Nakamura, N.; Yuasa, M.; Sekine, I. Ion and water transport characteristics in membranes for polymer electrolyte fuel cells containing H⁺ and Ca²⁺ cations. *J. Electrochem. Soc.* **1997**, *144*, 2744-2750.
- (7) Bond, D. R.; Lovley, D. R. Electricity production by *Geobacter sulfurreducens* attached to electrodes. *Appl. Environ. Microbiol.* **2003**, *69*, 1548-1555.
- (8) Chaudhuri, S. K.; Lovley, D. R. Electricity generation by direct oxidation of glucose in mediatorless microbial fuel cells. *Nat. Biotechnol.* **2003**, *21*, 1229-1232.
- (9) Gil, G. C.; Chang, I. S.; Kim, B. H.; Kim, M.; Jang, J. K.; Park, H. S.; Kim, H. J. Operational parameters affecting the performance of a mediatorless microbial fuel cell. *Biosens. Bioelectron.* **2003**, *18*, 327-334.
- (10) Liu, H.; Logan, B. E. Electricity generation using an air-cathode single chamber microbial fuel cell in the presence and absence of a proton exchange membrane. *Environ. Sci. Technol.* **2004**, *38*, 4040-4046.

- (11) Liu, H.; Ramnarayanan, R.; Logan, B. E. Production of electricity during wastewater treatment using a single chamber microbial fuel cell. *Environ. Sci. Technol.* **2004**, *38*, 2281-2285.
- (12) Min, B.; Cheng, S.; Logan, B. E. Electricity generation using membrane and salt bridge microbial fuel cells. *Water Res.* **2005**, *39*, 1675-1686.
- (13) Min, B.; Kim, J. R.; Oh, S. E.; Regan, J. M.; Logan, B. E. Electricity generation from swine wastewater using microbial fuel cells. *Water Res.* **2005**, *39*, 4961-4968.
- (14) Niessen, J.; Schröder, U.; Scholz, F. Exploiting complex carbohydrates for microbial electricity generation - a bacterial fuel cell operating on starch. *Electrochem. Commun.* **2004**, *6*, 955-958.
- (15) Schröder, U.; Niessen, J.; Scholz, F. A generation of microbial fuel cells with current outputs boosted by more than one order of magnitude. *Angew. Chem., Int. Ed.* **2003**, *42*, 2880-2883.
- (16) Rabaey, K.; Verstraete, W. Microbial fuel cells: novel biotechnology for energy generation. *Trends Biotechnol.* **2005**, *23*, 291-298.
- (17) Samec, Z.; Trojanek, A.; Langmaier, J.; Samcova, E. Diffusion coefficients of alkali metal cations in Nafion® from ion-exchange measurements - an advanced kinetic model. *J. Electrochem. Soc.* **1997**, *144*, 4236-4242.
- (18) Stenina, I. A.; Sistat, P.; Rebrov, A. I.; Pourcelly, G.; Yaroslavl'tsev, A. B. Ion mobility in Nafion-117 membranes. *Desalination* **2004**, *170*, 49-57.
- (19) Rozendal, R. A.; Hamelers, H. V. M.; Euverink, G. J. W.; Metz, S. J.; Buisman, C. J. N. Principle and perspectives of hydrogen production through biocatalyzed electrolysis. *Int. J. Hydrogen Energy* **2006**, *31*, 1632-1640.
- (20) Zehnder, A. J. B.; Huser, B. A.; Brock, T. D.; Wuhrmann, K. Characterization of an acetate-decarboxylating, non-hydrogen-oxidizing methane bacterium. *Arch. Microbiol.* **1980**, *124*, 1-11.
- (21) Pilat, B. Practice of water desalination by electrodialysis. *Desalination* **2001**, *139*, 385-392.
- (22) Kelly, M. J.; Fafilek, G.; Besenhard, J. O.; Kronberger, H.; Nauer, G. E. Contaminant absorption and conductivity in polymer electrolyte membranes. *J. Power Sources* **2005**, *145*, 249-252.
- (23) Kim, H. J.; Park, H. S.; Hyun, M. S.; Chang, I. S.; Kim, M.; Kim, B. H. A mediator-less microbial fuel cell using a metal reducing bacterium, *Shewanella putrefaciens*. *Enzyme Microb. Technol.* **2002**, *30*, 145-152.
- (24) Xu, T. Ion exchange membranes: state of their development and perspective. *J. Membr. Sci.* **2005**, *263*, 1-29.
- (25) Okada, T.; Ayato, Y.; Satou, H.; Yuasa, M.; Sekine, I. The effect of impurity cations on the oxygen reduction kinetics at platinum electrodes covered with perfluorinated ionomer. *J. Phys. Chem. B* **2001**, *105*, 6980-6986.
- (26) Bard, A. J.; Faulkner, L. R. *Electrochemical methods: fundamentals and applications*; 2nd ed.; John Wiley & Sons: New York, 2001.
- (27) He, Z.; Minteer, S. D.; Angenent, L. T. Electricity generation from artificial wastewater using an upflow microbial fuel cell. *Environ. Sci. Technol.* **2005**, *39*, 5262-5267.

- (28) Rabaey, K.; Clauwaert, P.; Aelterman, P.; Verstraete, W. Tubular microbial fuel cells for efficient electricity generation. *Environ. Sci. Technol.* **2005**, *39*, 8077-8082.
- (29) Rabaey, K.; Lissens, G.; Siciliano, S. D.; Verstraete, W. A microbial fuel cell capable of converting glucose to electricity at high rate and efficiency. *Biotechnol. Lett.* **2003**, *25*, 1531-1535.

Effect of the Type of Ion Exchange Membrane on Ion Transport and pH in Biocatalyzed Electrolysis of Wastewater

4



This chapter has been submitted for publication:

Rozendal, R. A.; Sleutels, T. H. J. A.; Hamelers, H. V. M.; Buisman, C. J. N. Effect of the type of ion exchange membrane on performance, ion transport, and pH in biocatalyzed electrolysis of wastewater. *Water Sci. Technol.* **2007**, Submitted.

Effect of the Type of Ion Exchange Membrane on Ion Transport and pH in Biocatalyzed Electrolysis of Wastewater

4

Previous studies have shown that the application of cation exchange membranes (CEMs) in bioelectrochemical systems running on wastewater can cause operational problems. In this chapter the effect of alternative types of ion exchange membrane is studied in biocatalyzed electrolysis cells. Four types of ion exchange membranes are used: (i) a CEM, (ii) an anion exchange membrane (AEM), (iii) a bipolar membrane (BPM), and (iv) a charge mosaic membrane (CMM). With respect to the electrochemical performance of the four biocatalyzed electrolysis configurations, the ion exchange membranes are rated in the order AEM > CEM > CMM > BPM. However, with respect to the transport numbers for protons and/or hydroxyl ions ($t_{H/OH}$) and the ability to prevent pH increase in the cathode chamber, the ion exchange membranes are rated in the order BPM > AEM > CMM > CEM.

4.1 Introduction

Energy production from wastewater by means of bioelectrochemical conversion has become a rapidly developing research field since the discovery of mediator-less microbial electron transfer to electrodes (1). Two types of technologies are currently being studied: (i) microbial fuel cells (MFCs) for electricity production (2), and (ii) biocatalyzed electrolysis (or BEAMR) for hydrogen production (3-5). With respect to these technologies much progress has been made in a relatively short timeframe. Extrapolating this progress to the future, it is expected that bioelectrochemical systems will eventually be limited by the capabilities of the electrochemically active microorganisms (6).

At the moment, however, bioelectrochemical systems are still limited by the non-biological part of the cell design. Within this scope, ion exchange membranes form an important challenge. Ion exchange membranes separate the biological anode from the cathode reactions, while at the same time facilitating the transport of ions through the membrane in order to maintain electroneutrality in the system. As the cathode reactions of both MFCs and biocatalyzed electrolysis consume protons in equal amounts with electrons, ideally only protons are transported through the ion exchange membrane. In this way electroneutrality is observed without pH changes taking place at the cathode. However, bioelectrochemical systems that are running on wastewater typically apply cation exchange membranes (CEMs) and various studies have shown that in that case mainly cation species other than protons are responsible for the transport of positive charge through the membrane (7,8). This results from the fact that in wastewater the concentrations of cations other than protons (e.g., Na^+ , K^+ , NH_4^+) are typically 10^5 times higher than the concentration of protons. This transport creates a membrane pH gradient between the anode and the cathode that can negatively affect cell performance (7).

The objective of this short study, therefore, was to investigate the effect of alternative ion exchange membranes on ion transport and pH in bioelectrochemical systems running on wastewater (9,10). This was tested in biocatalyzed electrolysis configurations with four different types of ion

exchange membranes (Figure 4.1): (i) a CEM, (ii) an anion exchange membrane (AEM), (iii) a bipolar membrane (BPM), and (iv) a charge mosaic membrane (CMM) (11).

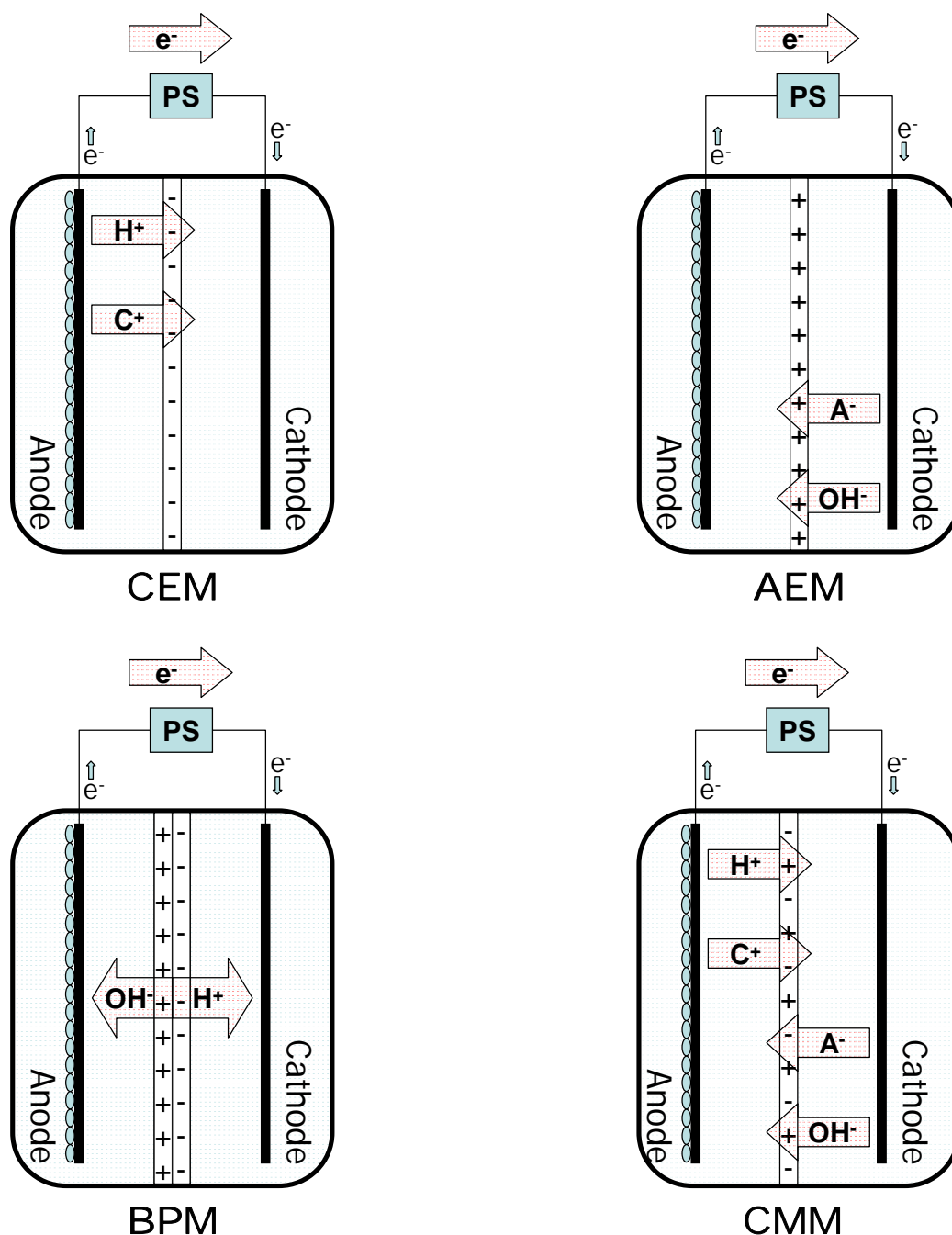


Figure 4.1. Theoretical working principle of membrane charge transport in four different types of ion exchange membranes used in biocatalyzed electrolysis: (A) CEM – through the transport of cations (ideally protons) from anode to cathode; (B) AEM – through the transport of anions (ideally hydroxyl ions) from cathode to anode; (C) BPM – through water splitting into protons and hydroxyl ions inside the membrane; (D) CMM – through the transport of cations (ideally protons) from anode to cathode AND/OR anions (ideally hydroxyl ions) from cathode to anode. PS = power supply, C^+ = Cations, A^- = Anions.

4.2 Materials and methods

4.2.1 Electrochemical cell

All experiments were performed in two-chamber electrochemical cells (total volume 6.6 liter; total liquid volume 6 L) as previously described in (7) with an anode of graphite felt (surface area: 400 cm², thickness: 3 mm – FMI Composites Ltd., Galashiels, Scotland) and a cathode of platinum coated (50 g/m²) titanium mesh (surface area: 400 cm², thickness: 1 mm, specific surface area: 1.7 m²/m² – Magneto special anodes bv, Schiedam, The Netherlands). The electrodes were electrically connected to an adjustable power supply (ES 030-5, Delta Elektronika bv, The Netherlands). Both the anode and the cathode chamber were equipped with an Ag/AgCl reference electrode for measuring potentials. The chambers were separated from each other by means of an ion exchange membrane. In the experiments four types of membranes (surface area 256 cm²) were tested for their ion transport properties: (i) a CEM (Nafion® 117), (ii) an AEM (Fumasep® FAB, FuMA-Tech GmbH), (iii) a BPM (Fumasep® FBM, FuMA-Tech GmbH), and (iv) a CMM (Dainichiseika Color & Chemicals, Co. Ltd., Japan). Conductivity and pH in the chambers were measured outside the electrochemical cells in a flow cell through which the anolyte/catholyte was continuously pumped at a rate of 340 mL/min.

4.2.2 Experimental procedures and calculations

All experiments were performed at 303 K. The anode chambers of the electrochemical cells were continuously fed (4 mL/min) with synthetic medium containing (in deionized water): 0.6 g/L CH₃COOH, 0.74 g/L KCl, 0.58 g/L NaCl, 0.68 g/L KH₂PO₄, 0.87 g/L K₂HPO₄, 0.28 g/L NH₄Cl, 0.1 g/L MgSO₄·7H₂O, 0.1 g/L CaCl₂·2H₂O, and 1 mL/L of a trace element mixture (12). Acetic acid was always available in excess and never limited current generation. The anode chamber was operated at pH 7 during all experiments by dosing 33% NaOH (Liquisys M CPM 253, Endress + Hauser). The electrochemical cells were started up by inoculating the anode chambers with 250 mL effluent taken from an active biocatalyzed electrolysis cell running on acetate (9). After stabilization at an applied

voltage of 1.0 V, membrane ion transport was studied in duplicate 48 h experimental runs at an applied voltage of 1.0 V. Prior to every run the cathode chamber was flushed 3 times with potassium phosphate buffer (10 mM, pH 7) and then filled with exactly 3 L of the same buffer. Subsequently, the cathode chambers were flushed with water saturated nitrogen gas (99.999% N₂, Air Products) until the experimental run was started by closing the electrical circuit. During the experimental runs hydrogen accumulated in the headspace of the cathode chamber and left the system through a gas flow meter (Milligascounter®, Ritter). A data logger (Ecograph T, Endress + Hauser) continuously logged the applied voltage, current, anode potential, cathode potential, cathode pH, cathode conductivity, and gas production. At the beginning and at the end of the experimental runs a 50 mL liquid sample was taken from the cathode chamber. The hydrogen fraction in the headspace of the cathode chamber and the ion content in liquid samples were analyzed according to Rozendal et al. (9). The amount of water still left in the cathode chamber after the experimental runs was measured to correct the ion transport data for osmotic loss of water from the cathode to the anode chamber (<3% for all membranes). Total charge production (Q_e) in Coulombs (C) after the 48 h experimental runs was calculated by integration of the current. Total charge production was compared to the transport of charge in the form of specific ions through the ion exchange membrane (Q_{ion}), which was calculated from the cathode chamber ion content data according to:

$$Q_{ion} = (x^{ion} - x^{ion,0}) \cdot V \cdot z^{ion} \cdot F \quad (1)$$

with Q_{ion} the transport of charge in the form of a specific ion through an ion exchange membrane after a 48 h experimental run in Coulombs (C), x^{ion} the molar concentration of a specific ion after a 48 h experimental run in moles per liter (M), $x^{ion,0}$ the molar concentration of a specific ion at start of a 48 h experimental run in moles per liter (M), V the cathode chamber liquid volume in liters (L), z^{ion} the valence of the specific ion and F the Faraday constant (96485.3 C/mol). Transport numbers for cation (t_c), anions (t_A), and protons and/or hydroxyl ions ($t_{H/OH}$) through the ion exchange

membranes were calculated according to Rozendal et al. (9). The transport of protons from anode to cathode and the transport of hydroxyl ions from cathode to anode were lumped together, because in practice no distinction can be made between them. Results are reported as means \pm standard deviation.

4.3 Results and discussion

Figure 4.2A shows the current generation of the four biocatalyzed electrolysis configurations during the 48 h experimental runs. As can be seen from this figure the CEM and the AEM configurations outperform the BPM and CMM configurations. As can be expected, this has a significant effect on the cumulative H_2 production during the 48 h experimental runs (Figure 4.2B). The average volumetric hydrogen production rates during the 48 h experimental runs were 0.13, 0.18, 0.04, 0.07 $Nm^3 H_2/m^3$ reactor liquid volume/day at cathodic hydrogen efficiencies (i.e., $e^- \rightarrow H_2$) of 78, 92, 71, and 83% for CEM, AEM, BPM, and CMM configurations respectively. With respect to the performance of the four biocatalyzed electrolysis configurations, therefore, the ion exchange membranes are rated in the order AEM > CEM > CMM > BPM.

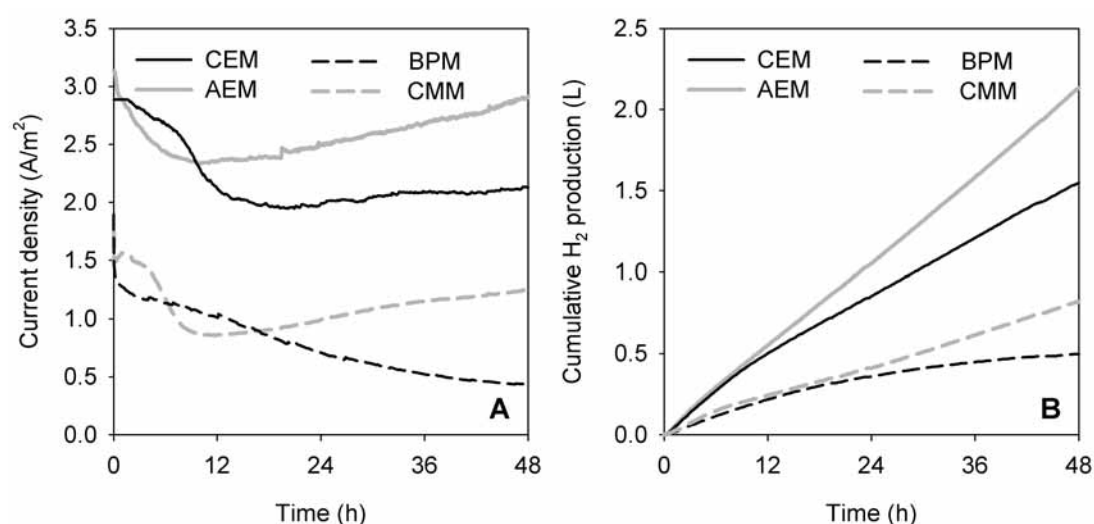


Figure 4.2. Performance of the four biocatalyzed electrolysis configurations with different types of ion exchange membranes: (A) current density and (B) cumulative H_2 production during duplicate 48 h experimental runs at an applied voltage of 1.0 V.

Potential measurements demonstrated that the difference in performance of the biocatalyzed electrolysis configurations was predominantly caused by the difference in voltage loss across the membrane. This voltage loss across the membrane is included in a measurement of the total voltage difference between the reference electrodes in the anode and cathode chambers (13). At the start of the experimental runs, i.e., when all other conditions in the cathode chamber were still identical, the voltage differences between the reference electrodes in the anode and cathode chambers were -0.27 ± 0.01 , -0.32 ± 0.02 , -0.71 ± 0.01 , and -0.45 ± 0.02 V for the CEM, AEM, BPM, and CMM configurations respectively. It seems unlikely that these differences are caused by the area resistance of the ion exchange membranes, which are typically in the order of $1\text{--}10 \text{ } \Omega\text{cm}^2$ (11). At the current densities as observed in the 48 h experimental runs ($<3.5 \text{ A/m}^2$) this area resistance of the ion exchange membranes can only account for a loss of several mV. The true causes of these differences in voltage loss across the membrane remain a topic of further investigation, but it is obvious that they have a significant effect on the overall electrochemical performance of the four biocatalyzed electrolysis configurations.

Another important membrane characteristic for application in bioelectrochemical systems is the ability to prevent pH increase in the cathode chamber. Figure 4.3 shows that the CEM, AEM, and CMM perform similar in this respect, especially when plotted against charge production (Figure 4.3C). The CEM, AEM, and CMM already show a rapid cathode pH increase after only little charge production. The BPM, on the other hand, demonstrated a more slowly increase of the cathode pH. Figure 4.3B and D indicate that the cathode pH increase for all membranes was related to the membrane transport of ion species other than protons and/or hydroxyl ions, as conductivity in the cathode chamber also gradually increases.

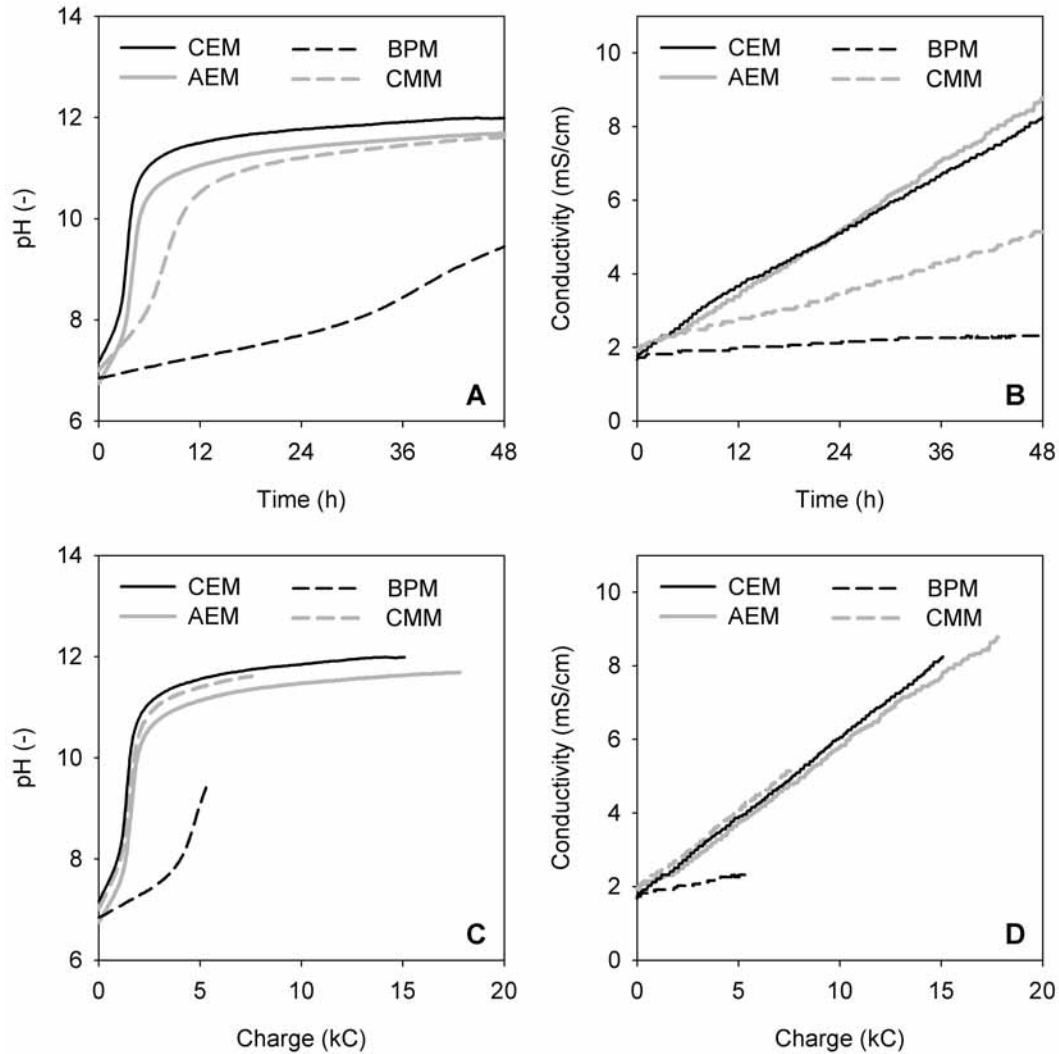


Figure 4.3. Ability of the ion exchange membranes to prevent pH and conductivity increase in the cathode chamber during duplicate 48 h experimental runs at an applied voltage of 1.0 V: (A) cathode chamber pH against time, (B) cathode chamber conductivity against time (C) cathode chamber pH against total charge production (D) cathode chamber conductivity against total charge production.

Furthermore, the pH and conductivity trends in Figure 4.3 give a good explanation for the large variations that were observed in the current density plots (Figure 4.2A). Current density is negatively affected by an increasing pH in the cathode chamber, but at the same time positively affected by an increase of cathode chamber conductivity. Again, the BPM shows deviating behavior, because the point of an increasing current density is not yet reached in the 48 h experimental run as a result of the slower cathode pH and conductivity increase.

Figure 4.4 compares the total charge production (Q_e) to the transport of charge in the form of specific ions through the ion exchange membrane

(Q_{ion}) after the duplicate 48 h experimental runs at an applied voltage of 1.0 V.

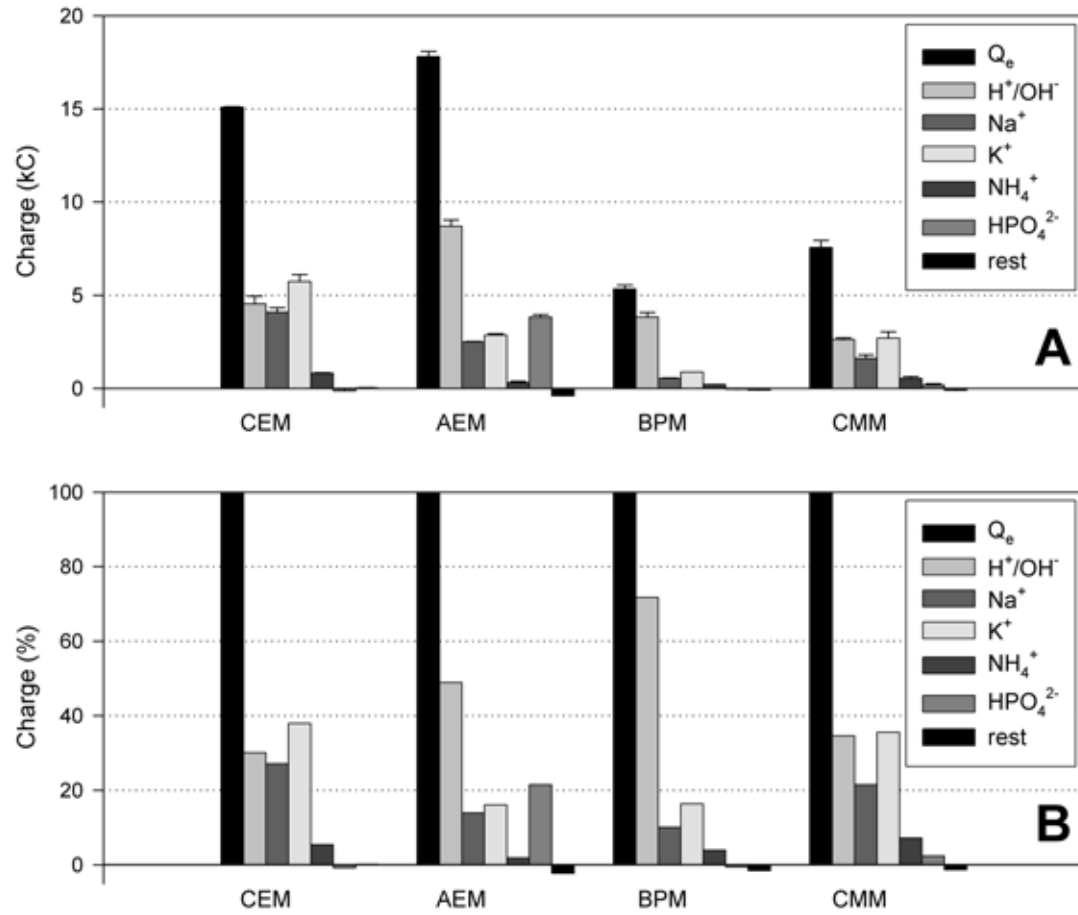


Figure 4.4. Comparison of the total charge production (Q_e) to the transport of charge in the form of specific ions through the ion exchange membrane (Q_{ion}) after the duplicate 48 h experimental runs at an applied voltage of 1.0 V: (A) absolute charge production, and (B) normalized to total charge production (Q_e). The sum of the categories H^+/OH^- , Na^+ , K^+ , NH_4^+ , HPO_4^{2-} , and rest accounts for 100% of the total charge transport through the ion exchange membrane.

As can be seen Figure 4, the CEM configuration behaved as expected. The membrane charge transport in the CEM configuration was predominantly in the form of cations ($t_c 0.71 \pm 0.04$) and H^+/OH^- ($t_{\text{H}/\text{OH}} 0.30 \pm 0.03$). The AEM configuration, on the other hand, did not behave completely as expected. The membrane charge transport in the AEM configuration was not only in the form of anions ($t_A 0.19 \pm 0.01$) and H^+/OH^- ($t_{\text{H}/\text{OH}} 0.49 \pm 0.01$), but also to a large extent in the form of cations ($t_c 0.32 \pm 0.00$). Next, the BPM configuration behaved according to the working principle of BPMs (Figure 4.1) as the membrane charge transport in the BPM configuration was predominantly in the form of H^+/OH^- ($t_{\text{H}/\text{OH}}$

0.72±0.02). However, also in the BPM configuration cations contributed (t_c 0.30±0.01) to the membrane charge transport, which explains the gradual increase of the cathode pH and conductivity (Figure 4.3). Finally, the membrane charge transport in the CMM configuration was predominantly in the form of cations (t_c 0.64±0.00) and H^+/OH^- ($t_{H/OH}$ 0.35±0.03). In contrast to what was expected based on the CMM working principle (Figure 4.1) anions (t_A 0.01±0.00) almost did not contribute to the membrane charge transport. Therefore, under the conditions of experimental runs, the CMM functioned more as a CEM than as a CMM.

On the basis of the results presented in Figure 4.3 and 4.4, the ion exchange membranes are rated in the order BPM > AEM > CMM > CEM with respect to the transport numbers for protons and/or hydroxyl ions ($t_{H/OH}$) and the ability to prevent pH increase in the cathode chamber.

4.4 Conclusions

The effect of the type of ion exchange membrane on ion transport and pH in bioelectrochemical systems running on wastewater was studied. Four types of ion exchange membranes were tested in a biocatalyzed electrolysis cell: (i) a CEM, (ii) an AEM, (iii) a BPM, and (iv) a CMM. With respect to the electrochemical performance of the four biocatalyzed electrolysis configurations, the ion exchange membranes are rated in the order AEM > CEM > CMM > BPM. However, with respect to the transport numbers for protons and/or hydroxyl ions ($t_{H/OH}$) and the ability to prevent pH increase in the cathode chamber, the ion exchange membranes are rated in the order BPM > AEM > CMM > CEM.

4.5 Acknowledgments

The authors especially thank Dr. Yasuyuki Isono of Dainichiseika Color & Chemicals, Co. Ltd., Japan for kindly providing us with charged mosaic membrane samples. This work was performed at Wetsus, Centre for Sustainable Water Technology. Wetsus is funded by the city of Leeuwarden, the Province of Fryslân, the European Union European Regional

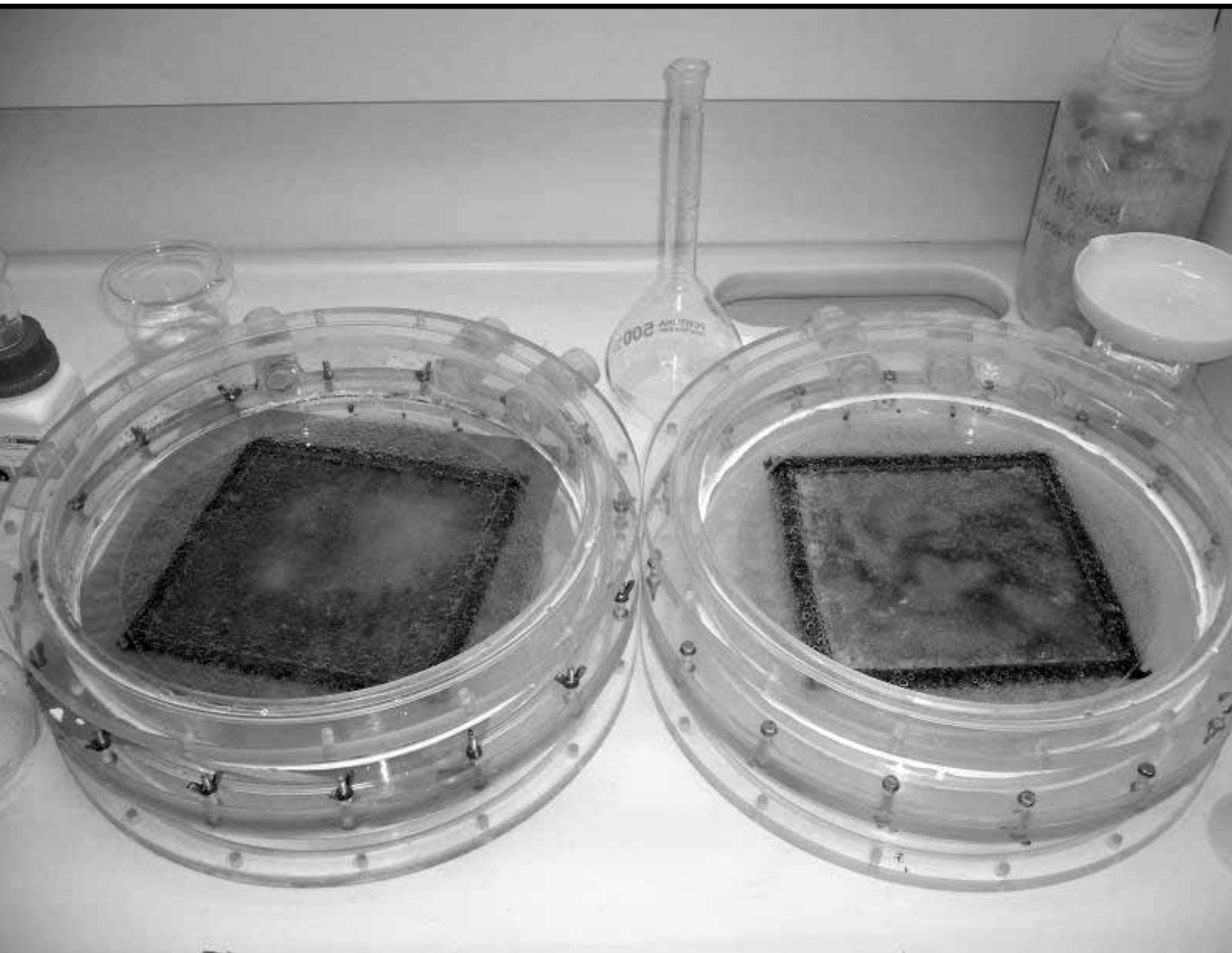
Development Fund and by the EZ/KOMPAS program of the “Samenwerkingsverband Noord-Nederland”. The authors like to thank the participants of the theme “Hydrogen” for their input and contributions: Shell, Paques bv, and Magneto Special Anodes bv.

4.6 References

- (1) Kim, B. H.; Kim, H. J.; Hyun, M. S.; Park, D. H. Direct electrode reaction of Fe(III)-reducing bacterium, *Shewanella putrefaciens*. *J. Microbiol. Biotechnol.* **1999**, *9*, 127-131.
- (2) Logan, B. E.; Hamelers, B.; Rozendal, R.; Schröder, U.; Keller, J.; Freguia, S.; Aelterman, P.; Verstraete, W.; Rabaey, K. Microbial fuel cells: methodology and technology. *Environ. Sci. Technol.* **2006**, *40*, 5181-5192.
- (3) Liu, H.; Grot, S.; Logan, B. E. Electrochemically assisted microbial production of hydrogen from acetate. *Environ. Sci. Technol.* **2005**, *39*, 4317-4320.
- (4) Rozendal, R. A.; Buisman, C. J. N. Process for producing hydrogen. **2005**, *Patent WO2005005981*.
- (5) Rozendal, R. A.; Hamelers, H. V. M.; Euverink, G. J. W.; Metz, S. J.; Buisman, C. J. N. Principle and perspectives of hydrogen production through biocatalyzed electrolysis. *Int. J. Hydrogen Energy* **2006**, *31*, 1632-1640.
- (6) Logan, B. E.; Regan, J. M. Electricity-producing bacterial communities in microbial fuel cells. *Trends Microbiol.* **2006**, *14*, 512-518.
- (7) Rozendal, R. A.; Hamelers, H. V. M.; Buisman, C. J. N. Effects of membrane cation transport on pH and microbial fuel cell performance. *Environ. Sci. Technol.* **2006**, *40*, 5206-5211.
- (8) Zhao, F.; Harnisch, F.; Schröder, U.; Scholz, F.; Bogdanoff, P.; Herrmann, I. Challenges and constraints of using oxygen cathodes in microbial fuel cells. *Environ. Sci. Technol.* **2006**, *40*, 5193-5199.
- (9) Rozendal, R. A.; Hamelers, H. V. M.; Molenkamp, R. J.; Buisman, C. J. N. Performance of single chamber biocatalyzed electrolysis with different types of ion exchange membranes. *Water Res.* **2007**, *41*, 1984-1994.
- (10) Kim, J. R.; Cheng, S.; Oh, S. E.; Logan, B. E. Power generation using different cation, anion, and ultrafiltration membranes in microbial fuel cells. *Environ. Sci. Technol.* **2007**, *41*, 1004-1009.
- (11) Xu, T. Ion exchange membranes: state of their development and perspective. *J. Membr. Sci.* **2005**, *263*, 1-29.
- (12) Zehnder, A. J. B.; Huser, B. A.; Brock, T. D.; Wuhrmann, K. Characterization of an acetate-decarboxylating, non-hydrogen-oxidizing methane bacterium. *Arch. Microbiol.* **1980**, *124*, 1-11.
- (13) Ter Heijne, A.; Hamelers, H. V. M.; De Wilde, V.; Rozendal, R. A.; Buisman, C. J. N. A bipolar membrane combined with ferric iron reduction as an efficient cathode system in microbial fuel cells. *Environ. Sci. Technol.* **2006**, *40*, 5200-5205.

*Performance of Single Chamber
Biocatalyzed Electrolysis
with Different Types of
Ion Exchange Membranes*

5



This chapter has been published as:

Rozendal, R. A.; Hamelers, H. V. M.; Molenkamp, R. J.; Buisman, C. J. N. Performance of single chamber biocatalyzed electrolysis with different types of ion exchange membranes. *Water Res.* **2007**, *41*, 1984-1994.

Performance of Single Chamber Biocatalyzed Electrolysis with Different Types of Ion Exchange Membranes

5

Hydrogen production through biocatalyzed electrolysis was studied for the first time in a single chamber setup. Single chamber biocatalyzed electrolysis was tested in two configurations: (i) with a cation exchange membrane (CEM) and (ii) with an anion exchange membrane (AEM). Both configurations performed comparably and produced over 0.3 Nm³ H₂/m³ reactor liquid volume/day at 1.0 V applied voltage (overall hydrogen efficiencies around 23%). Analysis of the water that permeated through the membrane revealed that a large part of potential losses in the system were associated with a pH gradient across the membrane (CEM $\Delta\text{pH}=6.4$; AEM $\Delta\text{pH}=4.4$). These pH gradient associated potential losses were lower in the AEM configuration (CEM 0.38 V; AEM 0.26 V) as a result of its alternative ion transport properties. This benefit of the AEM, however, was counteracted by the higher cathode overpotentials occurring in the AEM configuration (CEM 0.12 V at 2.39 A/m²; AEM 0.27 V at 2.15 A/m²) as a result of a less effective electroless plating method for the AEM membrane electrode assembly (MEA).

5.1 Introduction

5.1.1 *Biocatalyzed electrolysis*

Recently, it has been demonstrated that biocatalyzed electrolysis (or the bioelectrochemically assisted microbial reactor (BEAMR) process) is an interesting new technology for the production of hydrogen gas from wastewaters (1-3). Biocatalyzed electrolysis is related to microbial fuel cell (MFC) technology as it also applies electrochemically active microorganisms (4). Electrochemically active microorganisms are capable of using an electrode surface as an external electron acceptor for the oxidation of organic compounds. As a result, this electrode functions as a biological anode. At pH 7, electrochemically active microorganisms on the biological anode typically oxidize organic compounds at a potential of about -0.20 to -0.28 V (4). In biocatalyzed electrolysis, this biological anode is coupled to a hydrogen evolution reaction (HER; -0.42 V at pH 7) at the cathode, which results in an electromotive force (emf) of about -0.14 to -0.22 V (=cathode potential - anode potential) for the biocatalyzed electrolysis process. The negative value of the emf implies that a voltage of 0.14 to 0.22 V needs to be applied. Electrical energy, therefore, needs to be invested in order to generate hydrogen gas at the cathode. Compared to conventional water electrolysis, however, this energy investment is only low, as conventional water electrolysis theoretically requires applied voltages above 1.23 V (5).

5

5.1.2 *Performance*

Previously we studied the performance of a two-chamber biocatalyzed electrolysis setup at an applied voltage of 0.5 V (3). At this applied voltage the volumetric hydrogen production rate averaged 0.02 Nm³ H₂/m³ reactor liquid volume/day. Detailed analysis of the results revealed that the performance was to a large extent limited by inefficiencies occurring with the cathode reaction. In theory, however, HER cathodes should be able to outperform biological anodes up to 4 orders of magnitude. For example, at an overpotential of 0.025 V biological anodes can achieve current densities in the order of 1 A/m², while HER cathodes at the same overpotential are able to exceed 10000 A/m² (5). In our previous study, however, the cathode

overpotential was found to be already 0.28 V at a current density of 0.5 A/m², while the biological anode overpotential was 0.04 V. This clearly leaves room for improvement of the cathode performance. We estimate that if these improvements of the cathode performance can be realized, biocatalyzed electrolysis systems can be optimized to produce over 10 Nm³ H₂/m³ reactor liquid volume/day (3). These rates, however, also require an optimized geometrical design of the biocatalyzed electrolysis system.

5.1.3 Single chamber configuration

A better geometrical design of biocatalyzed electrolysis system can be achieved by changing the system from a configuration with two liquid chambers (i.e., two-chamber configuration) to a configuration with only one liquid chamber (i.e., single chamber configuration) by implementing a gas diffusion electrode. When this modification can be achieved without affecting the electrochemical performance, the volumetric hydrogen production rate theoretically doubles. Single chamber configurations have been tested successfully for the MFC (6,7). Interestingly, Liu and Logan demonstrated that the performance of single chamber MFCs can be significantly increased (494 versus 262 mW/m²) by removing the cation exchange membrane (CEM) from the system (8).

In biocatalyzed electrolysis, however, the presence of a membrane is essential for the purity of the hydrogen that is produced at the cathode. Without the membrane the produced hydrogen will be polluted with gaseous metabolic products from the anode chamber (e.g., CO₂, CH₄, H₂S). Furthermore, a significant amount of the produced hydrogen will be lost through diffusion to the anode chamber. A single chamber biocatalyzed electrolysis configuration, therefore, can only be successful if it functions optimally with a membrane included in the system.

5.1.4 Membrane ion transport

Previously it was shown in two-chamber MFCs that the performance loss associated with the CEM is caused by the transport of cation species other than protons (Na⁺, K⁺, NH₄⁺, Ca²⁺, and Mg²⁺) through the membrane (9,10). At a typical wastewater pH of 7, the proton concentration is about 10⁻⁴ mM.

The concentrations of cation species other than protons in wastewater, however, are typically 4–5 orders of magnitude higher. As a result, electroneutrality in the MFC is mainly observed by the transport of cation species other than protons through the CEM. Protons, however, are consumed equimolarly with electrons at the cathode in both the oxygen reduction reaction in MFCs ($\text{O}_2 + 4 \text{H}^+ + 4 \text{e}^- \rightarrow 2 \text{H}_2\text{O}$) as in the HER in biocatalyzed electrolysis ($2 \text{H}^+ + 2 \text{e}^- \rightarrow \text{H}_2$). The transport of cation species other than protons, therefore, causes a pH increase in the cathode chamber (9-11). This pH increase negatively affects the system performance, as the Nernst equation (12) states that for every pH unit difference between anode and cathode created in this way, an extra potential loss of about 0.06 V will occur in the system. Similar effects will also occur in single chamber configurations.

5.1.5 Anion exchange membrane

A possible solution to the pH gradient associated potential losses is the application of an anion exchange membrane (AEM) instead of a CEM (Figure 5.1). In the case of an AEM, electroneutrality is observed not by the transport of cations from the anode to the cathode, but by the transport of anions from the cathode to the anode. For biocatalyzed electrolysis this implies that hydrogen at the cathode is not produced from the reduction of protons, but from the reduction of water that diffuses through the membrane from anode to cathode. In this reaction hydroxyl ions are produced equimolarly with the consumed electrons ($2 \text{H}_2\text{O} + 2 \text{e}^- \rightarrow 2 \text{OH}^- + \text{H}_2$), which are then transported from cathode to anode through the AEM in order to observe electroneutrality. We predict that this has a neutralizing effect on the pH gradient across the membrane.

5.1.6 Objective

The objective of this study is twofold: (i) to study the performance of single chamber biocatalyzed electrolysis; and (ii) to study the influence of the type of ion exchange membrane on the performance. For this purpose we have operated two single chamber biocatalyzed electrolysis configurations in parallel, one with a CEM and one with an AEM.

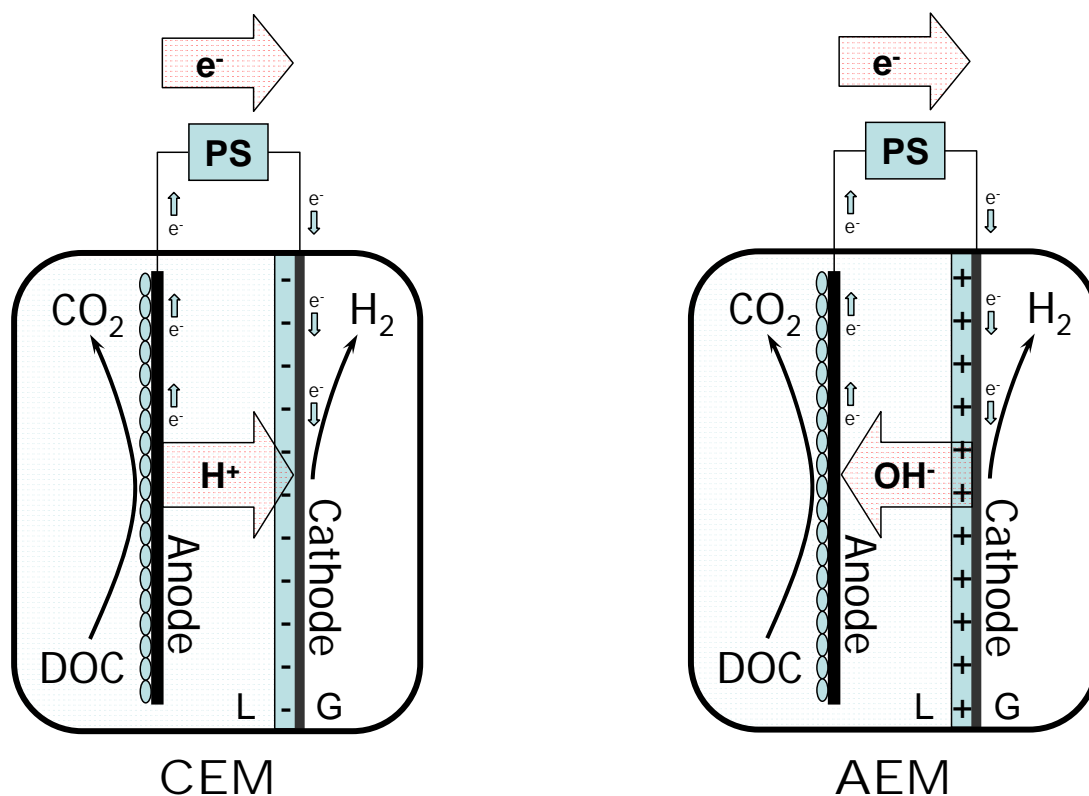


Figure 5.1. Schematic representation of single chamber biocatalyzed electrolysis with a cation exchange membrane (CEM) and an anion exchange membrane (AEM). DOC=dissolved organic compounds, PS=power supply, L=liquid phase, G=gas phase.

5.2 Materials and methods

5.2.1 Electrochemical cell

The experiments were performed in two identical electrochemical cells as previously described (3). Although the electrochemical cells had two chambers, they were operated in a single chamber configuration, in which only the anode chamber (liquid volume 3.3 L) was filled with medium (see below) and the cathode chamber (volume 3.3 L) functioned as a gas collection chamber. In one electrochemical cell the chambers were separated by a CEM (Nafion® 117, surface area 256 cm²); in the other by an AEM (Fumasep® FAB, FuMA-Tech GmbH, surface area 256 cm²). The anode consisted of graphite felt (surface area 400 cm², thickness 3 mm — FMI Composites Ltd., Galashiels, Scotland); the cathode consisted of platinum and was integrated with the membrane as a membrane electrode assembly (MEA; see below). The MEA was supported by a platinum coated (50 g/m²)

titanium mesh (surface area 400 cm², thickness 1 mm, specific surface area 1.7 m²/m² — Magneto special anodes bv, Schiedam, The Netherlands), which functioned both as part of the cathode and as the current collector. The anode and cathode were electrically connected to an adjustable power supply (ES 030-5, Delta Elektronika bv, The Netherlands). The current through the electrical circuit was determined (Ohm's law) by incorporating a high-precision shunt resistor (10 Ω) into the electrical circuit. The adjustable power supply was equipped with a sensing lead to automatically correct for the voltage loss across the shunt resistor. The anode chamber was equipped with an Ag/AgCl reference electrode (+0.2 V against NHE). A pH electrode was placed externally to the cell in a flow cell through which the anode medium was continuously pumped at a rate of 250 mL/min. The anode chamber was operated at pH 7 (Liquisys M CPM 253, Endress+Hauser). The electrochemical cells were connected to a data logger (Ecograph T, Endress+Hauser), which continuously logged the applied voltage, current, anode potential, cathode potential, pH, temperature, and gas production.

5.2.2 MEA preparation

5 The MEAs were prepared by means of electroless plating. The electroless plating method used for preparing the CEM MEA was based on a method developed by Millet et al. (13). One side of the membrane was subjected to two cycles of exposure for 15 min to 200 mL of an aqueous Pt(NH₃)₄Cl₂-solution (2 mg Pt/mL) and subsequent exposure for 2 h to 500 mL of an aqueous solution of sodium borohydride (NaBH₄; 15 g/L). This method is based on the diffusion of the positively charged platinum complex [Pt(NH₃)₄]²⁺ into the CEM and subsequently reducing this complex *in situ* to metallic platinum with sodium borohydride. This plating method results in a MEA with a conducting platinum layer outside the membrane in electrical contact with catalytic platinum microparticles inside the membrane. According to Millet et al. (13) this procedure results in a MEA with a platinum loading of about 1.0 mg Pt/cm².

For the AEM, the plating method was adapted by replacing the aqueous Pt(NH₃)₄Cl₂-solution with an aqueous K₂PtCl₆-solution (2 mg Pt/mL). This

solution contains the negatively charged complex $[\text{PtCl}_6]^{2-}$ that can diffuse into the AEM.

5.2.3 Experimental procedures and calculations

All experiments were performed at 303 K. The anode chambers of the electrochemical cells were filled and continuously fed (4 mL/min) with anode medium containing (in deionized water): 1.36 g/L $\text{NaCH}_3\text{COO} \cdot 3\text{H}_2\text{O}$, 0.74 g/L KCl, 0.58 g/L NaCl, 0.68 g/L KH_2PO_4 , 0.87 g/L K_2HPO_4 , 0.28 g/L NH_4Cl , 0.1 g/L $\text{MgSO}_4 \cdot 7\text{H}_2\text{O}$, 0.1 g/L $\text{CaCl}_2 \cdot 2\text{H}_2\text{O}$, and 1 mL/L of a trace element mixture (14). The electrochemical cells were started up by inoculation with 200 mL effluent taken from an active bioelectrochemical cell (9). In total the cells have been operated for about 100 days. After stabilization at an applied voltage of 1.0 V, the electrochemical cells were evaluated on the basis of three techniques: (i) applied voltage scans; (ii) electrochemical impedance spectroscopy (EIS); and (iii) hydrogen yield tests. During the applied voltage scans and EIS, the gas collection chamber was flushed continuously with water saturated nitrogen gas (99.999% N_2 , air products) in order to keep the experimental conditions constant. During the hydrogen yield tests the gas collection chamber was not flushed with nitrogen gas.

The applied voltage scans were obtained in triplicate by means of chronoamperometry. For this purpose, the electrochemical cells were connected to a potentiostat (Autolab PGSTAT12, Eco Chemie bv, The Netherlands). The applied voltage was increased stepwise from 0 to 1 V. The current generation was logged every 10 s for 1 h at 0, 0.1, 0.15, 0.2, 0.3, 0.4, 0.5, 0.6, 0.8, and 1.0 V. The last 10 data points of every applied voltage step were averaged and plotted in the applied voltage scan.

For the EIS the electrochemical cells were connected to a potentiostat equipped with a frequency response analyzer (Autolab PGSTAT30, Eco Chemie bv, The Netherlands). EIS was performed at an applied voltage of 1.0 V with an amplitude of 10 mV in the frequency range of 5 mHz to 100 kHz.

The hydrogen yield tests lasted for 48 h and were repeated in duplicate. In order to calculate the cumulative acetate consumption the anode was

regularly sampled and analyzed for acetate content using ion chromatography (Metrohm 761 Compact IC equipped with a conductivity detector and a Metrosep Organic Acids 6.1005.200 ion exclusion column). At the start of the hydrogen yield tests the gas collection chamber contained only nitrogen gas. During the hydrogen yield tests the gas collection chamber was connected to a gas flow meter (Milligascounter®, Ritter) for quantifying the total gas production. The gas collection chamber was sampled regularly and analyzed for its hydrogen fraction with a gas chromatograph (Shimadzu GC-2010 equipped with a thermal conductivity detector and a Varian molsieve 5A column). The actual hydrogen gas production was calculated from the total gas production and the measured hydrogen fractions by means of a mass balance equation adapted from (15):

$$V_{H,t} = V_{H,t-1} + (V_{T,t} - V_{T,t-1}) \frac{(C_{H,t} + C_{H,t-1})}{2} + V_{cat} (C_{H,t} - C_{H,t-1}) \quad (1)$$

with $V_{H,t}$ and $V_{H,t-1}$ the cumulative hydrogen gas production in liters (L) on sample time t and previous sample time $t-1$, respectively, $V_{T,t}$ and $V_{T,t-1}$ the total measured gas production in liters (L) on sample time t and previous sample time $t-1$, respectively, $C_{H,t}$ and $C_{H,t-1}$ the measured hydrogen fractions on sample time t and previous sample time $t-1$, respectively, and V_{cat} the gas collection chamber volume (3.3 L). The expected hydrogen production based on the cumulative charge production was calculated according to

$$V_{HC,t} = \frac{Q_t V_M}{2F} \quad (2)$$

with $V_{HC,t}$ the expected hydrogen production based on the cumulative charge production in liters (L) on sample time t , Q_t the cumulative charge production (equal to the integrated current over time) in coulombs (C) on sample time t , F Faraday's number (96485.3 C/mol), and V_M the molar gas volume (25.2 L/mol at 303 K).

During the hydrogen yield tests small amounts of water permeated through the membrane from the anode to the cathode side of the membrane into the gas collection chamber. This permeated water was collected from the gas collection chamber at the end of the hydrogen yield tests and analyzed for pH, conductivity, and ion content. Carbonate concentrations were determined using a total organic carbon analyzer (Shimadzu TOC-VCPH). Other anion concentrations (Cl^- , NO_2^- , NO_3^- , PO_4^{3-} , and SO_4^{2-}) were determined using an ion chromatograph (Metrohm 761 Compact IC) equipped with a conductivity detector and an anion column (Metrosep A Supp 5 6.1006.520). Ammonium concentrations were photometrically determined using standardized test kits (ammonium cuvette test LCK303, XION 500 spectrophotometer, Dr. Lange Nederland bv, The Netherlands). Other cation concentrations (Na^+ , K^+ , Ca^{2+} , and Mg^{2+}) were determined using inductively coupled plasma-optical emission spectroscopy (ICP-OES—Perkin Elmer Optima 3000XL). The ion content data of the permeated water were used to calculate transport numbers (t) for protons and hydroxyl ions through the ion exchange membranes. Because in practice no distinction can be made between the membrane transport of protons from anode to cathode and the membrane transport of hydroxyl ions from cathode to anode, the following transport number was defined:

$$t_{H/OH} = \frac{Q_{H/OH}}{Q_{total}} = \frac{Q_{total} - Q_{other}}{Q_{total}} \quad (3)$$

with $t_{H/OH}$ the transport number for the membrane transport of protons from anode to cathode and hydroxyl ions from cathode to anode, $Q_{H/OH}$ the membrane transport of positive charge from anode to cathode (or negative charge from cathode to anode) in the form of protons and hydroxyl ions in coulombs (C), Q_{other} the membrane transport of positive charge from anode to cathode (ϑ) (or negative charge from cathode to anode) in the form of ions other than proton and hydroxyl ions in coulombs (C), and Q_{total} the total membrane transport of positive charge from anode to cathode (or negative charge from cathode to anode) in coulombs (C). As the electroneutrality principle states that the total membrane transport of positive charge from

anode to cathode (or negative charge from cathode to anode) is equal to the total electron transport from anode to cathode through the electrical circuit, Q_{total} equals the integrated current over time.

After the experiments scanning electron microscope photos were taken of a cross-section of the MEAs. Prior to taking these scanning electron microscope photos, the plated membranes were submerged in liquid nitrogen to make them brittle. Subsequently, the membranes were broken and SEM photos were taken on the line of breakage. For the SEM photos a JEOL JSM-6480LV SEM was used (acceleration voltage 20 kV, LV-mode 60 Pa, BEI detector). The microscope was equipped with a NORAN System SIX Model 300 X-ray microanalysis system (Thermo Electron Corporation) for element analysis (linescan mode).

5.3 Results and discussion

5.3.1 Applied voltage scans

Figure 5.2A gives the applied voltage scans of the electrochemical cells taken after stabilization of the performance at 1.0 V. A comparison between the electrochemical cells shows that especially in the lower applied voltage range the CEM configuration outperforms the AEM configuration. The CEM configuration already starts to produce current at applied voltages above 0.2 V, while the AEM configuration only starts to produce current at applied voltages above 0.4 V. The theoretical applied voltage required for hydrogen production from acetate under the experimental conditions is around 0.17 V.

When the voltage comes above 0.6 V for both the CEM and the AEM configuration, the lines rapidly become steeper. The average slope of the applied voltage scan of the CEM configuration increases from 1.4 A/m²/V between 0.5 and 0.6 V to 5.9 A/m²/V between 0.8 and 1.0 V, while the average slope of the applied voltage scan of the AEM configuration even increases from 1.3 A/m²/V between 0.5 and 0.6 V to 6.6 A/m²/V between 0.8 and 1.0 V. As a result of this, the AEM configuration at 1.0 V even slightly outperforms CEM configuration, even though it was performing worse at the lower applied voltages.

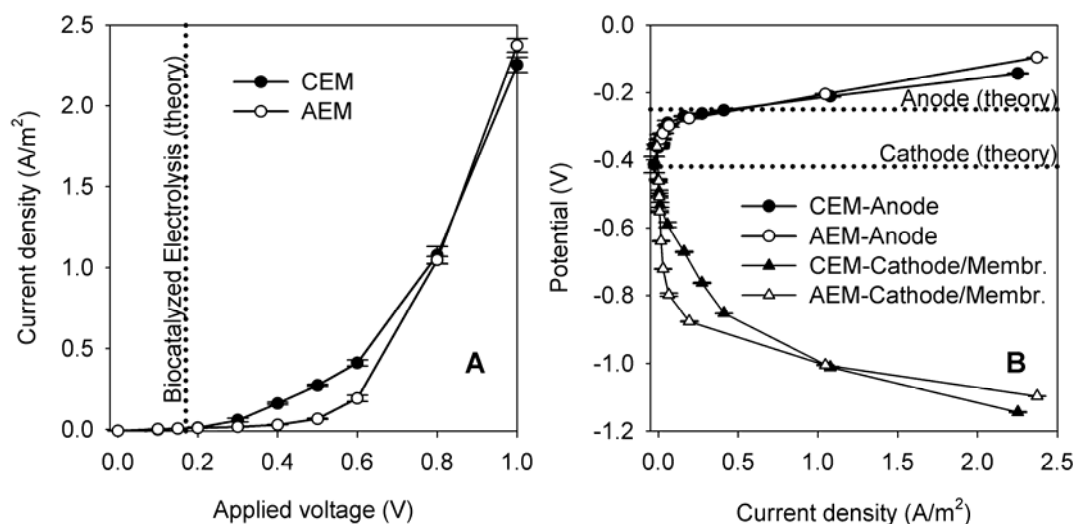


Figure 5.2. Evaluation of the performance of single chamber biocatalyzed electrolysis of acetate (10 mM) with a cation exchange membrane (CEM; Nafion® 117) and an anion exchange membrane (AEM; Fumasep® FAB): (A) applied voltage scans and (B) measured potentials during the applied voltage scans.

Figure 5.2B shows the electrode potentials measured during the applied voltage scans (Figure 5.2A). Because in a single chamber configuration only the anode chamber can be equipped with a reference electrode, only the anode potential can be measured as a true electrode potential. The cathode potential can only be measured through the membrane and therefore also includes the membrane potential.

Electrode overpotentials (i.e., potential losses) can be calculated by comparing the measured anode and cathode/membrane potentials with the theoretical potentials for acetate oxidation (-0.25 V) and proton reduction (-0.42 V). Figure 5.2B shows that the performance of both single chamber biocatalyzed electrolysis configurations to a large extent was limited by the combined cathode/membrane overpotential. At an applied voltage of 1.0 V (CEM 2.25 ± 0.05 A/m²; AEM 2.37 ± 0.04 A/m²) the anode overpotential was 0.12 ± 0.001 V for the CEM configuration and 0.16 ± 0.001 V for the AEM configuration, while the combined cathode/membrane overpotential was 0.72 ± 0.001 V for the CEM configuration and 0.68 ± 0.001 V for the AEM configuration. From Figure 5.2B it can be seen that a large part of the cathode/membrane overpotentials already occurred below 0.5 A/m². From the results it cannot unequivocally be determined which part of the cathode/membrane overpotential was caused by the cathode and which part

was caused by the membrane. However, it seems unlikely that these losses could have been caused by the ohmic resistance of the membrane as these types of membranes typically have ohmic resistances in the order of 1–10 Ωcm^2 (16). Below an applied voltage of 0.6 V the current densities in the cells were below 0.5 A/m². This results in a maximum ohmic loss across the membrane in the order of 0.0005 V ($=0.5 \times 10^{-4} \text{ A/cm}^2 \times 10 \text{ } \Omega\text{cm}^2$), which is too low to explain the cathode/membrane overpotentials that were observed.

5.3.2 Hydrogen yield tests

Hydrogen yield tests were done to assess the hydrogen production potential of both configurations (Figure 5.3). At first, the hydrogen production was tested at an applied voltage of 0.5 V, but the hydrogen production was too low to obtain reproducible results. Therefore, the applied voltage was increased to 1.0 V. At this applied voltage, the current density during the 48 h hydrogen yield tests averaged $2.39 \pm 0.15 \text{ A/m}^2$ for the CEM configuration and $2.15 \pm 0.26 \text{ A/m}^2$ for the AEM configuration. These values are in the same range as predicted by the applied voltage scans (Figure 5.2A), which shows that the applied voltage scans are indeed representative for predicting the performance of a biocatalyzed electrolysis configuration.

The measured values for the total gas production (Milligascounter®) and hydrogen fraction in the gas collection chambers were used to calculate the actual hydrogen production according to Equation 1. The expected hydrogen production based on the cumulative charge production was calculated according to Equation 2. The cumulative values after 48 h for acetate consumption, charge production, and hydrogen production were used to calculate three process efficiencies (Table 5.1): (i) coulombic efficiency; (ii) cathodic hydrogen efficiency; and (iii) overall hydrogen efficiency. The overall hydrogen efficiencies were comparable for both single chamber configurations in this study and were around 23%. These overall hydrogen efficiencies were the result of low coulombic efficiencies and high cathodic hydrogen efficiencies.

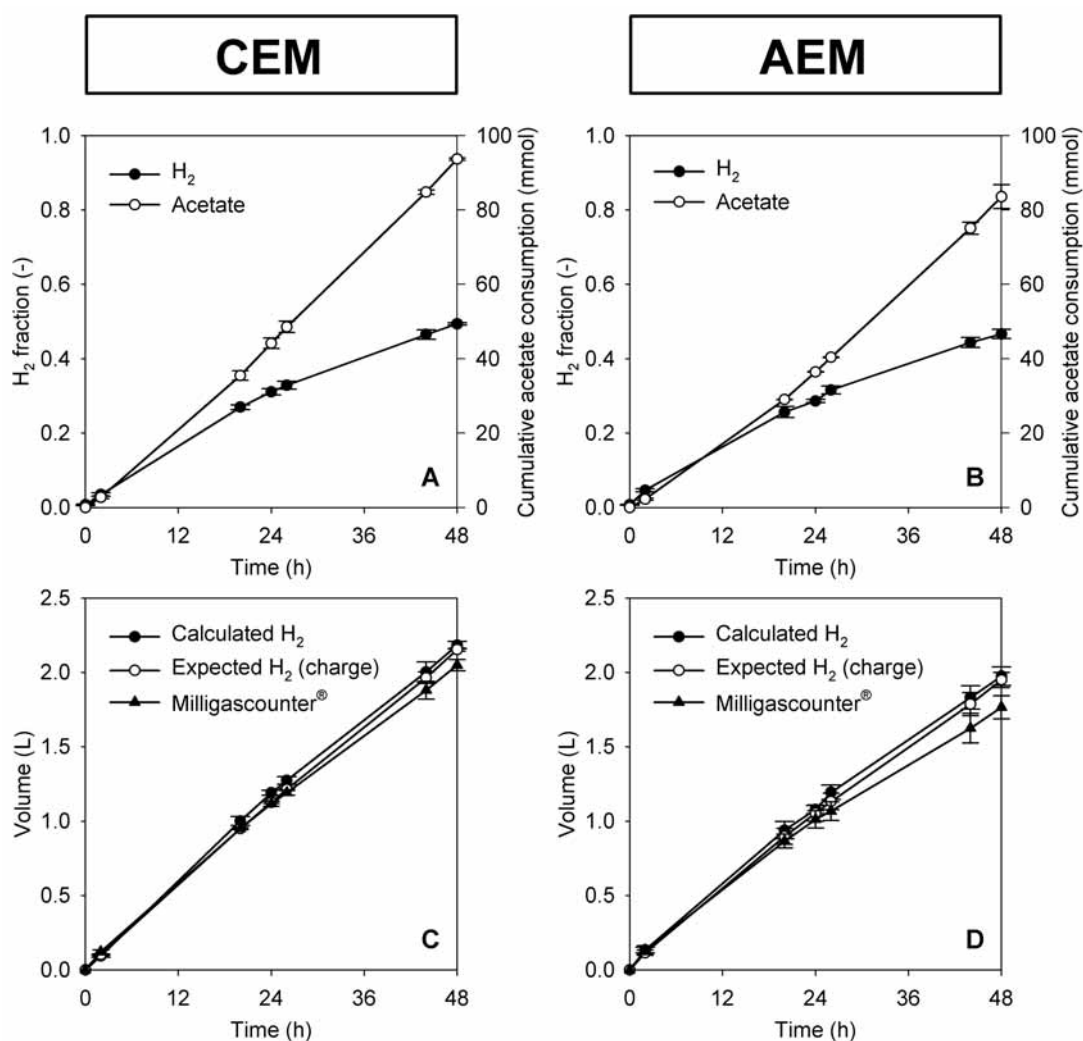


Figure 5.3. Experimental results of 48 h hydrogen yield tests of single chamber biocatalyzed electrolysis of acetate with a cation exchange membrane (CEM; Nafion® 117) and an anion exchange membrane (AEM; Fumasep® FAB): (A/B) hydrogen fraction in the gas collection chamber and cumulative acetate consumption; (C/D) calculated actual hydrogen production, expected hydrogen production based on the cumulative charge production, and the total gas production (Milligascounter®)

Table 5.1. Efficiencies^a of single chamber biocatalyzed electrolysis of acetate with a cation exchange membrane (CEM) and an anion exchange membrane (AEM)

	CEM	AEM
% Coulombic efficiency (acetate to e ⁻)	22.8 ± 0.2	23.2 ± 1.5
% Cathodic hydrogen efficiency (e ⁻ to H ₂)	101.4 ± 0.7	101.3 ± 0.6
% Overall hydrogen efficiency (acetate to H ₂)	23.1 ± 0.3	23.5 ± 1.7

a. Calculations based on: 1 acetate → 8 e⁻ → 4H₂.

Coulombic efficiency. In contrast to previous biocatalyzed electrolysis experiments, the coulombic efficiencies of both configurations were low. Liu et al. (1) achieved coulombic efficiencies of 60% to 78% and in our previous study in a similar electrochemical cell as used in this study we achieved a coulombic efficiency of $92 \pm 6.3\%$ (3). The significant difference with our previous study was most likely caused by the fact that the electrochemical cells in our previous study were operated in batch mode on autoclaved medium, while both electrochemical cells in this study had been operated in continuous mode on non-autoclaved medium for over two months prior to the hydrogen yield tests. This difference in operation of the cells might have resulted in the growth of methanogenic biomass inside the electrochemical cell (17), which was also suggested by the occurrence of dark spots of biomass on the walls of the reactor. This methanogenic biomass competes with the electrochemically active microorganisms for acetate, which decreases the coulombic efficiency. Limiting the growth of this biomass, therefore, needs to be a topic of further study to be able to increase the coulombic efficiency. Strategies to achieve this can be to increase the anode surface area to system volume ratio and to optimize the COD loading rate (18).

5

Cathodic hydrogen efficiency. The conversion of electrons to hydrogen (i.e., cathodic hydrogen efficiency) achieved in this study was practically complete in both configurations. This is in the same range as the 92% previously reported by Liu et al. (1) and much higher than the $57 \pm 0.1\%$ we achieved in our previous study in a similar electrochemical cell as used in this study (3). In our previous study calculations have shown that a large part of the produced hydrogen at the cathode was lost by diffusion of hydrogen from the cathode into the anode chamber through the ion exchange membrane. In the same study, however, we predicted that the importance of this diffusional hydrogen loss reduces at increasing current densities. At higher current densities, i.e., at higher hydrogen production rates, this diffusional hydrogen loss remains more or less constant in absolute sense, but becomes less important in relative sense. This prediction has now been confirmed by the results of the hydrogen yield tests presented in this study. In our previous study the current density was about 0.5 A/m^2

(at 0.5 V), while in this study the current density was between 2.0 and 2.5 A/m² (at 1.0 V). Indeed, at these higher current densities the cathodic hydrogen efficiencies have increased to about 100%. This is an important fact for future studies, which should focus on achieving these higher current densities at lower applied voltages.

Volumetric hydrogen production rates. The average volumetric hydrogen production rates were comparable for both configurations. The CEM configuration produced 0.33 Nm³ H₂/m³ reactor liquid volume/day and the AEM configuration produced 0.31±0.01 Nm³ H₂/m³ reactor liquid volume/day. This is much higher than the 0.02 Nm³ H₂/m³ reactor liquid volume/day that was achieved in our previous study in the two-chamber configuration (3). However, in our previous study the hydrogen was produced at an applied voltage of 0.5 V, while in this study the hydrogen was produced at 1.0 V, because the performance of both configurations at an applied voltage 0.5 V was too low to do reliable measurements. This low performance at an applied voltage 0.5 V was caused by various potential losses in the system (see below).

5.3.3 Electrochemical impedance spectroscopy

The electrochemical cells performing biocatalyzed electrolysis of acetate were subjected to EIS at 1.0 V (Figure 5.4). Interpretation of the Nyquist plots that were obtained through EIS was limited to the determination of the ohmic resistance of the system according to the methodology as applied by He et al. (19). As can be seen from the Nyquist plots both configurations show a comparable ohmic resistance in the order of 2 Ω. Although these values seem low compared to the values reported in other studies (19,20), it is actually already too high for practical application. The average currents during the 48 h hydrogen yield tests at 1.0 V were 95 mA (2.39 A/m²) for the CEM configuration and 86 mA (2.15 A/m²) for the AEM configuration, which means that the ohmic losses at these values already amount to 0.21 V (=95×10⁻³ A × 2.2 Ω) for the CEM configuration and 0.15 V (=86×10⁻³ A × 1.8 Ω) for the AEM configuration. This is a significant part of the total applied voltage of 1.0 V. In our system a substantial part of the ohmic resistance is caused by the anode itself. EIS of only the anode at a potential

of -0.25 V showed that the anode ohmic resistance was $0.64\ \Omega$ in the CEM configuration and $0.75\ \Omega$ in AEM configuration. This resistance is believed to be caused largely by the contact resistance of the graphite fibers in the graphite felt.

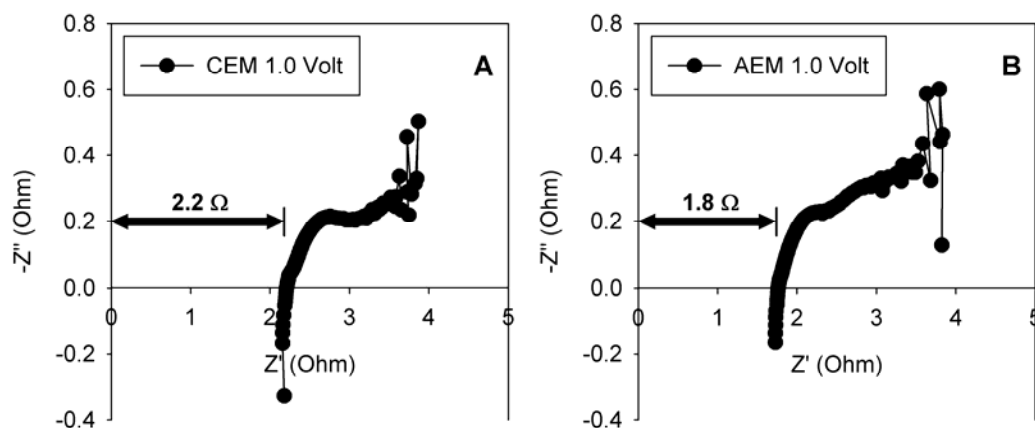


Figure 5.4. Electrochemical impedance spectroscopy (EIS): Nyquist plots of single chamber biocatalyzed electrolysis of acetate at an applied voltage of 1.0 V with: (A) a cation exchange membrane (CEM; Nafion® 117); and (B) an anion exchange membrane (AEM; Fumasep® FAB). The arrows indicate the ohmic resistance in the system.

5.3.4 Permeated water analysis

During the hydrogen yield tests small amounts of water permeated through the membrane from the anode to the cathode side of the membrane into the gas collection chamber. Ions that are transported through the membrane will accumulate in this permeated water. Table 5.2 shows that less water permeated through the AEM than through the CEM. In both configurations the permeated water had an increased pH as compared to the anode chamber (pH 6.8–7; conductivity: 5.22 mS/cm). As was predicted beforehand, the AEM is capable of significantly reducing the pH increase at the cathode, but the effect was smaller than anticipated. In both configurations the pH increase is caused by the membrane transport of ions other than protons and hydroxyl ions. Permeated water analysis showed that in both configurations others ions than protons and hydroxyl ions were transported through the membrane during the hydrogen yield test. However, this transport was much smaller in the AEM configuration as can be seen from the ion concentrations, the conductivity of the permeated water, and the calculated transport number $t_{H/OH}$. The transport of ions other than protons and hydroxyl ions is caused by the fact that ion exchange

membranes are never 100% selective for protons or hydroxyl ions and, moreover, not even for only cations or anions.

Table 5.2. Permeated water volume, composition and calculated H^+/OH^- transport number ($t_{H/OH}$) after the 48 h hydrogen yield tests.

	CEM	AEM
Volume (ml)	33.5	15.5
pH (-)	13.2	11.1
Conductivity (mS/cm)	73.05	3.06
Na ⁺ (mM)	125.7	7.1
K ⁺ (mM)	170.3	12.3
NH ₄ ⁺ (mM)	8.8	3.5
Cl ⁻ (mM)	0.6	0.2
HCO ₃ ⁻ /CO ₃ ²⁻ (mM)	4.8 ^a	11.9 ^b
Acetate (mM)	0.38	0.02
$t_{H/OH}$ (-)	0.94	1.00

a. At pH 13.2 HCO₃⁻:CO₃²⁻=0.001:1

b. At pH 11.1 HCO₃⁻:CO₃²⁻=0.17:1

The concentrations of ions other than protons and hydroxyl ions can be used to predict pH of the permeated water by assuming that for every net positive charge in the form of others ions than protons and hydroxyl ions transported into the permeated water, one hydroxyl ion accumulates in the permeated water. For the permeated water in the CEM configuration this predicts a pH of 13.5; for the permeated water in the AEM configuration a pH of 10.7. This prediction confirms the dramatic pH effects of the transport of only small amounts of ions other than protons and hydroxyl ions. This dramatic pH effect especially becomes clear when studying the composition of the permeated water of the AEM configuration. During the 48 h hydrogen yield tests, low amounts of ions other than protons and hydroxyl ions were transported to the permeated water and the transport number in the AEM configuration was almost equal to unity. Still, the pH effect was substantial.

Unfortunately, an extra 0.06 V potential loss occurs for every pH unit increase of the permeated water at the cathode as compared to the anode pH (CEM Δ pH=6.4; AEM Δ pH=4.4). A large part of the cathode/membrane overpotentials observed in the applied voltage scans, therefore, were likely caused by these pH gradient related potential losses. Furthermore, these

results also indicate how difficult it is to prevent the pH gradient related potential losses, especially in the case of single chamber configurations. The ion concentrations increase more rapidly in a small amount of permeated water in single chamber configurations than in the total liquid content of a cathode chamber in two-chamber configurations. Therefore, the pH increase at the cathode and the pH gradient related potential losses will occur more rapidly in single chamber configurations as compared to a two-chamber configurations (9). This also explains why the performance at an applied voltage of 0.5 V was so low in this study, as the applied voltage was too low to overcome the high pH gradient related potential losses of the single chamber configuration.

The obtained results suggest that the pH gradient related potential losses seem to be a fundamental problem associated with the use of ion exchange membranes in single chamber bioelectrochemical systems running on wastewater. In MFCs, omitting the membrane seems to be a solution, as was demonstrated by Liu and Logan in a single chamber MFC study (8). For biocatalyzed electrolysis, however, omitting the membrane would result in a contamination of the hydrogen product gas and in a reduction of the coulombic efficiency due to consumption of the hydrogen in the anode chamber.

5

5.3.5 Scanning electron microscopy

The MEAs that were used in the experiments were studied using scanning electron microscopy (SEM) combined with element analysis (Figure 5.5). The element analysis showed that the electroless plating procedure was more effective for the CEM than for the AEM, as the platinum profile is higher and can be found deeper into the CEM than into AEM. This has made the catalytic region larger in the CEM MEA than in the AEM MEA. Furthermore, the platinum peak close to the surface is much higher in the CEM platinum profile than in the AEM platinum profile. According to Millet et al. (13) this peak represents a conducting platinum layer outside the membrane, which is responsible for the electrical contact of the catalytic platinum microparticles inside the membrane with the electrical circuit. If this conducting platinum layer outside the membrane is

not well developed during the electroless plating procedure, the catalytic platinum microparticles become isolated and inactive for hydrogen production. The difference in visual appearance of the MEAs also was an indication for this. Whereas the outside of the CEM MEA developed a metallic appearance during the electroless plating procedure, the outside of the AEM MEA only turned black. The AEM MEA, therefore, might have lacked a well developed conducting platinum layer outside the membrane with inactive catalytic platinum microparticles inside the membrane as a result. A lower activity of catalytic platinum microparticles leads to increased cathode overpotentials (see below).

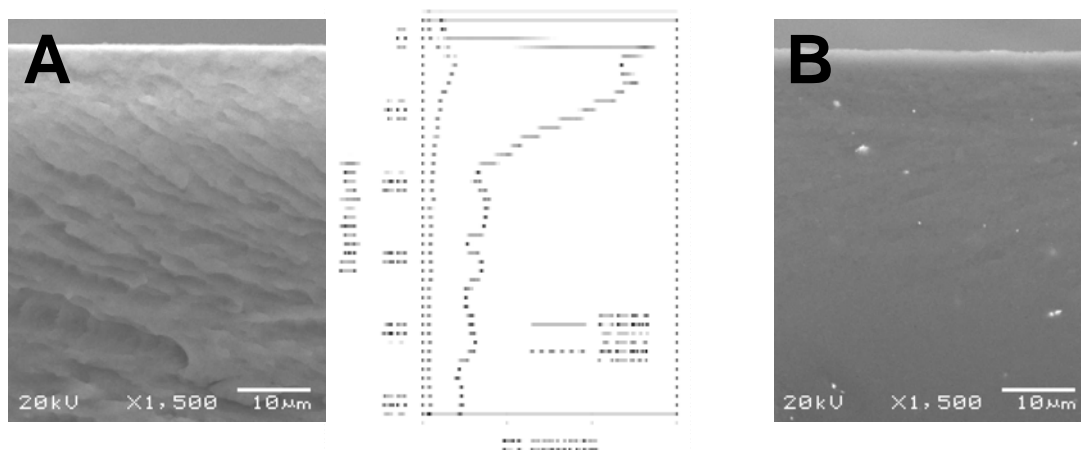


Figure 5.5. SEM photos of a cross section of the membrane electrode assemblies (MEAs) used in the single chamber biocatalyzed electrolysis experiments: (A) MEA with a cation exchange membrane (CEM; Nafion® 117); (B) MEA with an anion exchange membrane (AEM; Fumasep® FAB). The graph in the middle shows the platinum profiles inside the membranes resulting from the electroless plating procedure.

5.3.6 Potential losses

Table 5.3 gives an overview of the distribution of the applied voltage of 1.0 V during the 48 h hydrogen yield tests for both single chamber biocatalyzed electrolysis configurations. As was predicted by the analysis of the permeated water, the pH gradient associated potential loss, caused by the membrane charge transport of ions other than protons and hydroxyl ions, forms a significant part of the total potential losses in both configurations. However, Table 5.3 also shows that other potential losses are not insignificant either.

Table 5.3. Overview of the potential losses during the 48 h hydrogen yield tests at an applied voltage of 1.0 V

	CEM (at 2.39 A/m ²)	AEM (at 2.15 A/m ²)
Equilibrium voltage (V)	0.17 ^a	0.17 ^a
Ohmic loss (V)	0.21 ^b	0.15 ^b
Membrane pH gradient loss (V)	0.38 ^c	0.26 ^c
Anode overpotential (V)	0.12 ^d	0.15 ^d
Cathode overpotential (V)	0.12 ^e	0.27 ^e

a. Calculated for 1 mM acetate; 1 bar H₂.

b. Calculated from the ohmic resistances measured in the Nyquist plots (Figure 5.4).

c. pH gradient across the membrane (CEM $\Delta\text{pH}=6.4$; AEM $\Delta\text{pH}=4.4$) multiplied by 0.06 V.

d. Values corrected for the ohmic loss of the anode itself, as this was already included in the total ohmic loss (the ohmic resistance of the anode was determined with EIS: CEM 0.64 Ω ; AEM 0.75 Ω).

e. Cathode overpotential = applied voltage - equilibrium voltage - ohmic loss - membrane pH gradient loss - anode overpotential.

Even though the ohmic resistance is low compared to other studies (19,20), the ohmic potential loss is large. This paradox can be explained from the larger electrochemical cells that have been used in this study as compared to other studies. Consequently, the electrical currents that flow through the cells are larger and therefore size independent resistances (e.g., contact resistances) cause larger ohmic losses than the same resistances in smaller systems. This shows the importance of also studying larger systems in order to evaluate the consequences of scale-up (4).

The anode overpotentials are in the same range as those observed in other studies with acetate as the electron donor (21,22). They were similar in both configurations, which is not surprising as the conditions in the anode chambers were comparable. The anode overpotentials represent the smallest losses in the system, but at the relatively large current densities of around 2 A/m² they also have started to become significant. A possible reason for the increased anode overpotentials is the relatively low anode acetate concentration of around 1 mM during the hydrogen yield tests. Further, as the system was not stirred vigorously, concentration polarization could have started to occur (4). One of the effects that can take place as a result of concentration polarization is the occurrence of low pH near the anode due to

proton production. In future studies, the application of granular graphite (7,18) might help to lower the anode overpotentials.

The cathode overpotentials represent an important part of the total potential losses. In the AEM configuration the cathode overpotentials were higher than in the CEM configuration. One issue that needs to be examined further in this respect is the effectiveness of the MEA preparation method used for the AEM. SEM combined with element analysis showed that the penetration depth of the platinum was smaller in case of the AEM configuration and that the conducting platinum layer outside the membrane was less developed. This probably caused the difference in catalytic activity of MEAs and resulted in increased cathode overpotentials for the AEM MEA. The MEA preparation method was an adapted electroless plating method, originally developed for CEMs. In order to optimize the AEM MEA performance the influence of the plating parameters needs to be examined (e.g., increasing exposure time to the Pt-solution or the sodium borohydride). Also other MEA preparation methods can be examined in future studies.

5.3.7 Outlook

In this study the electrical energy requirement for hydrogen production through biocatalyzed electrolysis was about 2.2 kWh/Nm³ H₂ in both configurations. This is much lower than the 4.4–5.4 kWh/Nm³ H₂ required by commercial water electrolyzers (23). Our goal for future studies is to reduce the electrical energy requirement of biocatalyzed electrolysis to below 1.0 kWh/Nm³ H₂. This implies that the applied voltage needs to be lowered to at least 0.46 V. At the same time we aim at increasing the volumetric hydrogen production rate from 0.3 (this study) to about 10 Nm³ H₂/m³ reactor liquid volume/day. Increasing the volumetric hydrogen production rate means increasing the current density of the system. Based on recent results achieved in our laboratories (22), we estimate that an optimized biological anode is capable of achieving current densities of between 5 and 10 A/m². At these current densities we can afford only 0.29 V of potential losses (=applied voltage - equilibrium voltage=0.46 - 0.17 V). To

achieve these goals, major improvements of the electrochemical and geometrical design of the biocatalyzed electrolysis system are required.

This can only be achieved if the pH gradient associated potential losses as observed in this study can be eliminated completely in an optimized design of the biocatalyzed electrolysis system. For this purpose, the interesting characteristics of the AEM in this respect need to be further studied or other means of reducing the pH gradient associated potential loss need to be explored (e.g., other types of membranes).

Next, ohmic losses must be reduced by minimizing the electrode spacing and choosing better electrode materials (4). In order to reduce the ohmic loss of the system to 0.05–0.10 V at 5–10 A/m², the total ohmic resistance of the system needs to be reduced to between 50 and 200 Ωcm². For comparison, total ohmic resistances of water electrolyzers are typically in the order of 1 Ωcm² (5).

The overpotential of HER cathodes in water electrolyzers can be as low as 0.025 V at 10000 A/m² (5), which indicates that there is much room for optimization of HER cathodes in biocatalyzed electrolysis. Assuming that both the ohmic loss and the cathode overpotential can indeed be reduced to 0.05–0.10 V, anode overpotentials need to be reduced to 0.09–0.19 V. Extrapolating recent results achieved in our laboratories (22), we believe that achieving these kinds of anode overpotentials at current densities of 5–10 A/m² is realistic, but will require much fundamental research into the working principles of biological anodes.

Finally, an optimized system will also require an optimized geometrical design. The biocatalyzed electrolysis system that was used in this study, operating at a volumetric hydrogen production rate of 0.3 Nm³ H₂/m³ reactor liquid volume/day (at about 2 A/m²), has an anode surface area to system volume ratio of 12 m²/m³ reactor liquid volume. In order to reach the aimed volumetric production rate of 10 Nm³ H₂/m³ reactor liquid volume/day (at 5–10 A/m²), the anode surface area to system volume ratio will have to increase to about 80–160 m²/m³ reactor liquid volume. Similar anode surface area to system volume ratios have been demonstrated previously in MFC studies (24). Applying them also to biocatalyzed electrolysis brings the process another step closer to practical application.

5.4 Conclusions

This study has shown that it is possible to operate biocatalyzed electrolysis in single chamber configuration, although the performance at voltages below 0.6 V was limited. The performance of single chamber biocatalyzed electrolysis was comparable with a CEM and with an AEM in the configuration, producing over 0.3 Nm³ H₂/m³ reactor liquid volume/day at 1.0 V applied voltage. The coulombic efficiencies of both biocatalyzed electrolysis configurations were low (around 23%), which was most likely caused by the activity of methanogenic bacteria in the anode chamber. The cathodic hydrogen efficiencies, on the other hand, were high (close to 100%) in both configurations, which was the result of the high current densities (between 2.0 and 2.5 A/m²). The resulting overall hydrogen efficiencies for both single chamber configurations were around 23%.

Analysis of the water that permeated through the membrane revealed that a large part of potential losses in the system are associated with a pH gradient across the membrane. This pH gradient is caused by the membrane charge transport in the form of ions other than protons and hydroxyl ions. These pH gradient related potential losses are more problematic for single chamber configurations than for two-chamber configurations, as ion concentrations increase more rapidly in a small amount of permeated water in a single chamber configuration than in the total liquid content of a cathode chamber in a two-chamber configuration.

The AEM is better capable of preventing the pH gradient across the membrane than the CEM (CEM $\Delta\text{pH}=6.4$; AEM $\Delta\text{pH}=4.4$) as a result of its alternative ion transport properties. Consequently, the pH gradient associated potential losses were lower in the AEM configuration (CEM 0.38 V; AEM 0.26 V). In the AEM configuration, on the other hand, the reduced pH gradient associated potential losses were counteracted by the increased cathode overpotentials as compared to the CEM configuration (CEM 0.12 V at 2.39 A/m²; AEM 0.27 V at 2.15 A/m²). SEM combined with element analysis suggested that the increased cathode overpotentials in the AEM configuration were the result of a less effective electroless plating method for the AEM MEA.

5.5 Acknowledgments

This work was performed at Wetsus, Centre for Sustainable Water Technology. Wetsus is funded by the city of Leeuwarden, the Province of Fryslân, the European Union European Regional Development Fund and by the EZ/KOMPAS program of the “Samenwerkingsverband Noord-Nederland”. The authors like to thank the participants of the theme “Hydrogen” for their input and contributions: Shell, Paques bv, and Magneto Special Anodes bv. The authors further thank Dr. G.J.W. Euverink and Dr. S.J. Metz for critically reading of the manuscript.

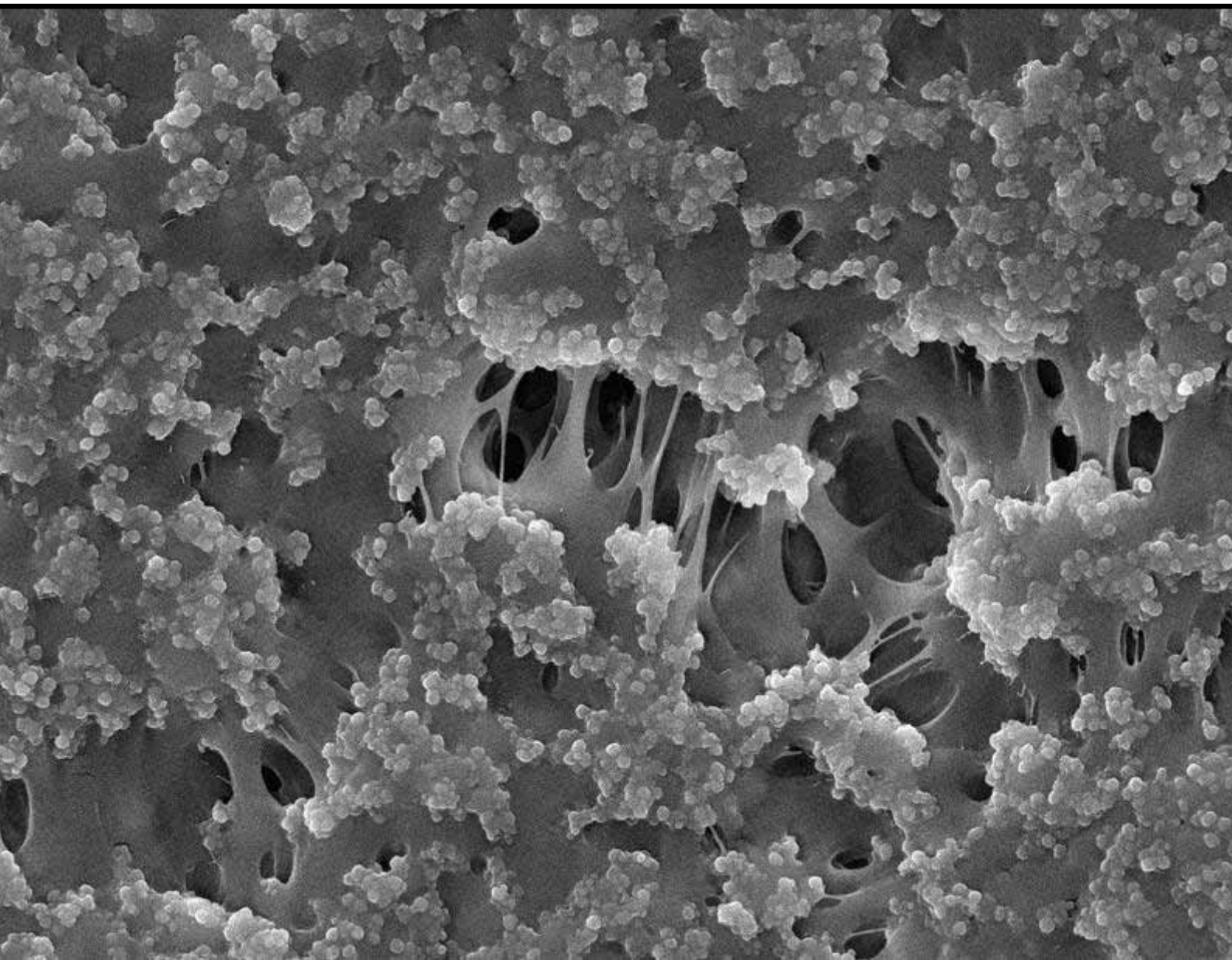
5.6 References

- (1) Liu, H.; Grot, S.; Logan, B. E. Electrochemically assisted microbial production of hydrogen from acetate. *Environ. Sci. Technol.* **2005**, *39*, 4317-4320.
- (2) Rozendal, R. A.; Buisman, C. J. N. Process for producing hydrogen. **2005**, *Patent WO2005005981*.
- (3) Rozendal, R. A.; Hamelers, H. V. M.; Euverink, G. J. W.; Metz, S. J.; Buisman, C. J. N. Principle and perspectives of hydrogen production through biocatalyzed electrolysis. *Int. J. Hydrogen Energy* **2006**, *31*, 1632-1640.
- (4) Logan, B. E.; Hamelers, B.; Rozendal, R.; Schröder, U.; Keller, J.; Freguia, S.; Aelterman, P.; Verstraete, W.; Rabaey, K. Microbial fuel cells: methodology and technology. *Environ. Sci. Technol.* **2006**, *40*, 5181-5192.
- (5) Kinoshita, K. *Electrochemical oxygen technology*; John Wiley & Sons, Inc.: New York, 1992.
- (6) Liu, H.; Ramnarayanan, R.; Logan, B. E. Production of electricity during wastewater treatment using a single chamber microbial fuel cell. *Environ. Sci. Technol.* **2004**, *38*, 2281-2285.
- (7) Sell, D.; Kramer, P.; Kreysa, G. Use of an oxygen gas diffusion cathode and a three-dimensional packed-bed anode in a bioelectrochemical fuel cell. *Appl. Microbiol. Biotechnol.* **1989**, *31*, 211-213.
- (8) Liu, H.; Logan, B. E. Electricity generation using an air-cathode single chamber microbial fuel cell in the presence and absence of a proton exchange membrane. *Environ. Sci. Technol.* **2004**, *38*, 4040-4046.
- (9) Rozendal, R. A.; Hamelers, H. V. M.; Buisman, C. J. N. Effects of membrane cation transport on pH and microbial fuel cell performance. *Environ. Sci. Technol.* **2006**, *40*, 5206-5211.
- (10) Zhao, F.; Harnisch, F.; Schröder, U.; Scholz, F.; Bogdanoff, P.; Herrmann, I. Challenges and constraints of using oxygen cathodes in microbial fuel cells. *Environ. Sci. Technol.* **2006**, *40*, 5193-5199.
- (11) Gil, G. C.; Chang, I. S.; Kim, B. H.; Kim, M.; Jang, J. K.; Park, H. S.; Kim, H. J. Operational parameters affecting the performance of a mediator-less microbial fuel cell. *Biosens. Bioelectron.* **2003**, *18*, 327-334.

- (12) Bard, A. J.; Faulkner, L. R. *Electrochemical methods: fundamentals and applications*; 2nd ed.; John Wiley & Sons: New York, 2001.
- (13) Millet, P.; Durand, R.; Pineri, M. Preparation of new solid polymer electrolyte composites for water electrolysis. *Int. J. Hydrogen Energy* **1990**, *15*, 245-253.
- (14) Zehnder, A. J. B.; Huser, B. A.; Brock, T. D.; Wuhrmann, K. Characterization of an acetate-decarboxylating, non-hydrogen-oxidizing methane bacterium. *Arch. Microbiol.* **1980**, *124*, 1-11.
- (15) Logan, B. E.; Oh, S. E.; Kim, I. S.; Van Ginkel, S. Biological hydrogen production measured in batch anaerobic respirometers. *Environ. Sci. Technol.* **2002**, *36*, 2530-2535.
- (16) Xu, T. Ion exchange membranes: state of their development and perspective. *J. Membr. Sci.* **2005**, *263*, 1-29.
- (17) Kim, J. R.; Min, B.; Logan, B. E. Evaluation of procedures to acclimate a microbial fuel cell for electricity production. *Appl. Microbiol. Biotechnol.* **2005**, *68*, 23-30.
- (18) Rabaey, K.; Clauwaert, P.; Aelterman, P.; Verstraete, W. Tubular microbial fuel cells for efficient electricity generation. *Environ. Sci. Technol.* **2005**, *39*, 8077-8082.
- (19) He, Z.; Wagner, N.; Minteer, S. D.; Angenent, L. T. An upflow microbial fuel cell with an interior cathode: assessment of the internal resistance by impedance spectroscopy. *Environ. Sci. Technol.* **2006**, *40*, 5212-5217.
- (20) Min, B.; Cheng, S.; Logan, B. E. Electricity generation using membrane and salt bridge microbial fuel cells. *Water Res.* **2005**, *39*, 1675-1686.
- (21) Liu, H.; Cheng, S. A.; Logan, B. E. Production of electricity from acetate or butyrate using a single-chamber microbial fuel cell. *Environ. Sci. Technol.* **2005**, *39*, 658-662.
- (22) Ter Heijne, A.; Hamelers, H. V. M.; De Wilde, V.; Rozendal, R. A.; Buisman, C. J. N. A bipolar membrane combined with ferric iron reduction as an efficient cathode system in microbial fuel cells. *Environ. Sci. Technol.* **2006**, *40*, 5200-5205.
- (23) Turner, J. A. Sustainable hydrogen production. *Science* **2004**, *305*, 972-974.
- (24) Kim, H. J.; Park, H. S.; Hyun, M. S.; Chang, I. S.; Kim, M.; Kim, B. H. A mediator-less microbial fuel cell using a metal reducing bacterium, *Shewanella putrefaciens*. *Enzyme Microb. Technol.* **2002**, *30*, 145-152.

*Intermezzo:
Understanding Cathode
pH Increase from the
Nernst-Planck Flux Equation*

I



Intermezzo: Understanding Cathode pH Increase from the Nernst-Planck Flux Equation



Chapter 3, 4, and 5 have shown that an increase of the cathode pH is commonly observed in bioelectrochemical systems that are running on wastewater and that these effect could not be eliminated by changing the type of membrane. This seems to imply that the observed pH effects are inherent to the use of membranes in bioelectrochemical systems that are running on wastewater. This hypothesis is qualitatively investigated in this short Intermezzo by approaching the problem of the cathode chamber pH increase with the Nernst-Planck flux equation. This equation is commonly used to describe the flux of an ion specie through a membrane as the sum of three contributions: (i) convection, (ii) diffusion, and (iii) migration. Without assuming anything about the type of ion exchange membrane, the Nernst-Planck flux equation indeed predicts the occurrence of cathode chamber pH increase. This cathode chamber pH increase can have a significant negative effect on the performance of bioelectrochemical systems and is an important issue to address in future research.

I.1 Nernst-Planck flux equation

The total flux of an ion specie through a membrane can be described as the sum of three contributions: (i) convection flux (J_{con}), (ii) diffusion flux (J_{dif}), and (iii) migration flux (J_{mig}). This is commonly described with the Nernst-Planck flux equation (1,2):

$$J_T = vC_i(x) - D_i \frac{d\bar{C}_i(x)}{dx} - D_i \frac{z_i F \bar{C}_i(x)}{RT} \cdot \frac{d\phi}{dx} \quad (1)$$

$$\left(= J_{conv}\right) \quad \left(= J_{dif}\right) \quad \left(= J_{mig}\right)$$

with J_T the total flux of ion specie i through a membrane (mol/dm²/s), v the velocity of the convective transport through the membrane (dm/s), $C_i(x)$ the concentration of ion specie i in the membrane (M) as a function of the coordinate x in the membrane (dm) (varies from 0 to δ , the thickness of the membrane), D_i the diffusion coefficient of ion specie i in the membrane (dm²/s), z_i the valence of ion specie i , F the Faraday constant (96485.3 C/mol), R the universal gas constant (8.3145 J/mol/K), T the temperature in K, ϕ the electrical potential (V),

$$\frac{d\bar{C}_i(x)}{dx} \quad \text{the concentration gradient across the membrane, and}$$

$$\frac{d\phi}{dx} \quad \text{the electric field across the membrane.}$$

The convection flux in the case of bioelectrochemical system (MFC or biocatalyzed electrolysis) with membranes is zero, as the applied membranes are typically non-porous and/or no pressure gradient exists across the membrane to support convection. Without convection Equation 1 reduces to:

$$J_i = -D_i \left[\frac{d\bar{C}_i(x)}{dx} + \frac{z_i F \bar{C}_i(x)}{RT} \frac{d\phi}{dx} \right] \quad (2)$$

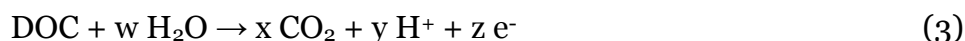
As can be seen from Equation 2 the membrane ion flux in a bioelectrochemical system is determined by (i) the diffusion flux, which is a function of the concentration gradient across the membrane, and (ii) the migration flux, which is a function of both the electric field across the membrane and the concentration of an ion specie in the membrane.

I.2 Why does pH increase?

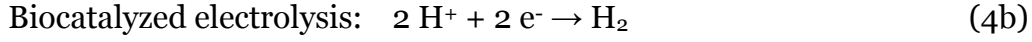
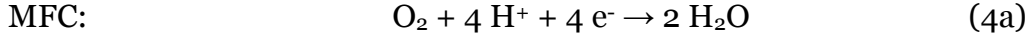
Consider the simple case of a two-chamber bioelectrochemical system (MFC or biocatalyzed electrolysis) with only 4 types of ions present: protons (H^+), hydroxyl ions (OH^-), univalent cations (C^+ , e.g., K^+) and univalent anions (A^- , e.g., Cl^-). In this system the anode and cathode chamber are separated by an ion permeable membrane.

Initially (Figure I.1; $t=0$), the cathode chamber ion composition is identical to that of the anode chamber with a concentration of n M of univalent cations and anions ($[C^+]=[A^-]=n \gg 10^{-7}$ M) and a pH of 7 (i.e., $[H^+]=[OH^-]=10^{-7}$ M ≈ 0 M). Furthermore, the anode chamber of this system is considered to be ideally mixed and is continuously fed with fresh medium (i.e., wastewater) at such a rate that the pH and composition in the anode chamber always remain constant. As the concentrations in the anode and cathode chamber are identical in the initial situation, the anode chamber is in physical/chemical equilibrium with the cathode chamber.

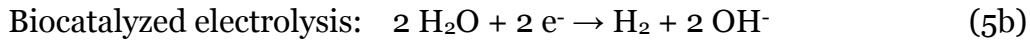
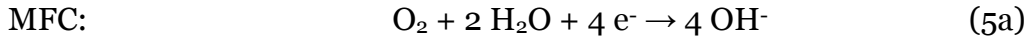
Once the electrical circuit of the bioelectrochemical system is closed, the electrode reactions start to take place and electrical current runs through the system. At the anode, dissolved organic compounds (DOC, e.g., glucose, acetic acid) are oxidized to form carbon dioxide, protons and electrons (Equation 3):



At the cathode, proton consumption takes place in the oxygen reduction reaction (MFC, Equation 4a) or hydrogen evolution reaction (biocatalyzed electrolysis, Equation 4b):



As protons and hydroxyl ions are always in equilibrium with each other through the water dissociation constant ($K_w=[\text{H}^+][\text{OH}^-]\approx 10^{-14}$), the proton consumption can also be described as hydroxyl ion production:



When electrical current flows, electrons are transported from the anode to the cathode chamber through the electrical circuit. In order to maintain electroneutrality, membrane ion flux compensates for this electron transport of negative charge from anode to cathode by the membrane transport of an identical amount of net positive charge from anode to cathode or net negative charge from cathode to anode. This driving force to observe electroneutrality is expressed by a built-up of an electric field across the membrane. As a result of this electric field cations migrate through the membrane from the anode into cathode chamber and anions migrate through the membrane from the cathode into anode chamber (Figure I.1/Table I.1; $t=0$). Initially, only migrational transport of ions takes place as the ion compositions of the anode and cathode chamber are still identical to each other (i.e., the concentration gradient=0). Furthermore, protons and hydroxyl are not considered to contribute substantially to this charge transport through the membrane as their initial concentrations are orders of magnitude lower than the other cation and anion concentrations in the system.

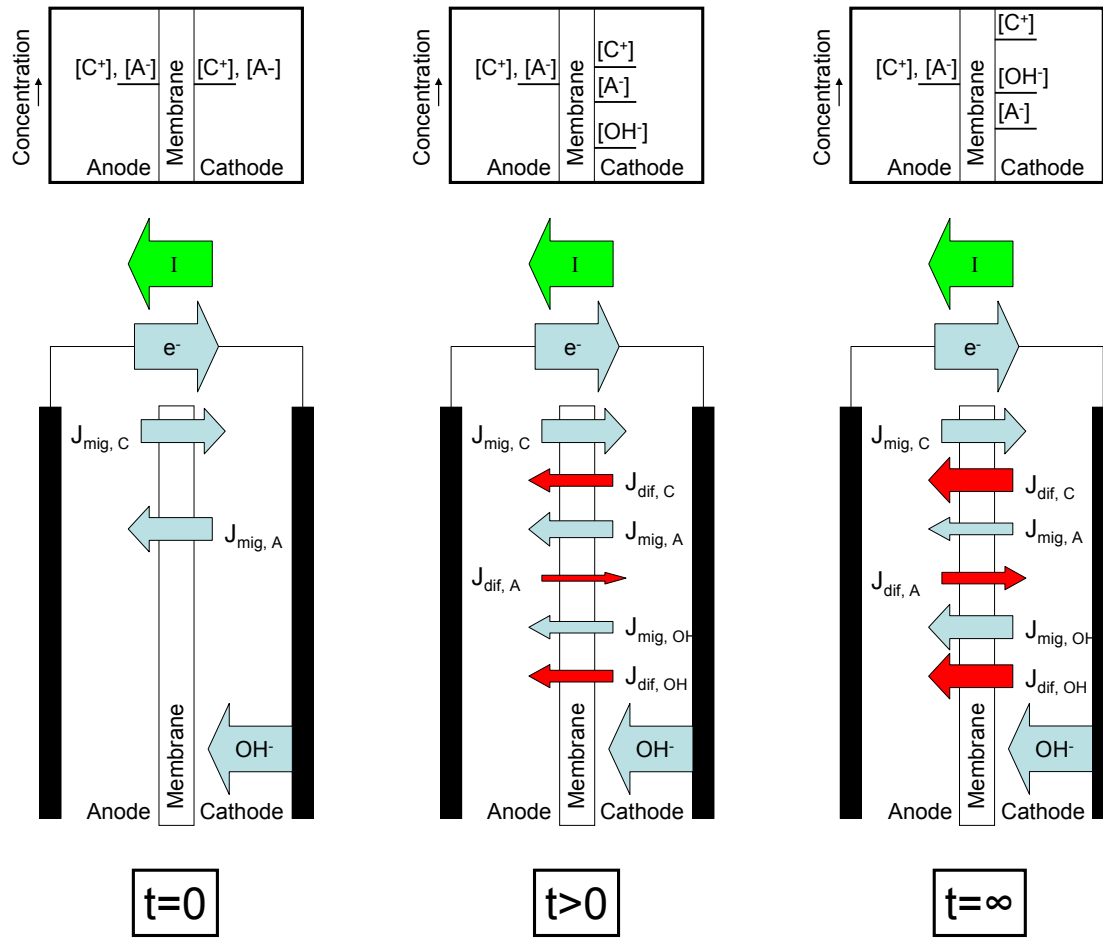


Figure I.1. Schematic representation of the anode/cathode chamber concentrations (above) and membrane ion flux (below) during operation of a bioelectrochemical system at $t=0$, $t>0$, and $t=\infty$. Initially, the cathode chamber ion composition is identical to that of the anode chamber with a concentration of n M of univalent cations and anions ($[C^+]=[A^-]=n>>10^{-7}$ M) and a pH of 7 (i.e., $[H^+]=[OH^-]=10^{-7}$ M ≈ 0 M). I =electrical current; mig=migration; dif=diffusion; C=cation; A= anion; OH=hydroxyl ion.

Table I.1. Parts of the membrane ion flux J contributing to the net membrane charge transport (j =current density). A flux in the direction from anode to cathode is defined positive; a flux in the direction from cathode to anode is defined negative.

	Remarks	$j=F\sum(Z_i J_i)$
$t=0$	$J_{dif,C}=J_{dif,A}=J_{mig,OH}=J_{dif,OH}=0$	$j=F\sum(J_{mig,C}-J_{mig,A})$
$t>0$	$J_{mig,C}+J_{dif,C}>0$; $-J_{mig,A}-J_{dif,A}>0$; $-J_{mig,OH}>0$; $-J_{dif,OH}>0$	$j=F\sum(J_{mig,C}+J_{dif,C}-J_{mig,A}-J_{dif,A}-J_{mig,OH}-J_{dif,OH})$
$t=\infty$	$J_{dif,C}+J_{mig,C}=0$; $-J_{dif,A}-J_{mig,A}=0$	$j=F\sum(-J_{mig,OH}-J_{dif,OH})$

As a result of the migration of cations and anions a concentration gradient of cation and anions is built up across the membrane, i.e., the cathode chamber cation concentration becomes higher than the anode chamber cation concentration and the cathode chamber anion concentration becomes lower than the anode chamber anion concentration. This built-up of concentration gradient across the membrane results in a diffusion flux of cations and anion in the opposite direction of the migration flux of cations and anion, i.e., cations diffuse through the membrane from the cathode into anode chamber and anions diffuse through the membrane from the anode into cathode chamber (Figure I.1/Table I.1; $t > 0$)).

A built-up of concentration gradient, however, also implies that a concentration imbalance between cations and anions is created in the cathode chamber. Whereas the cation and anion concentrations are identical in the anode chamber, the cathode chamber will show an increased cation concentration and a decreased anion concentration. In the cathode chamber this concentration imbalance can only be compensated by the increase of the concentration of hydroxyl ions, which are produced in the cathode reaction (Equation 5a/b). By definition, this increase of the concentration of hydroxyl ions implies that the pH has also increased. Furthermore, with the increased concentration of hydroxyl ions it becomes more likely that the hydroxyl ions also will start to contribute to the membrane ion flux.

The built-up of concentration gradient of cations and anions continues until the migration of cations and anions in one direction will exactly equal the diffusion of cations and anions in the opposite direction (Figure I.1/Table I.1; $t = \infty$). At this moment the contribution of these cations and anions to the net membrane ion flux has become zero and the only remaining ions in the system that can now substantially contribute to membrane ion flux are the hydroxyl ions. The hydroxyl ions diffuse and migrate from the cathode into the anode chamber, but are continuously replenished through the cathode reaction (Equation 5a/b). From that moment on, the flux of hydroxyl ions is exactly equal to the transport of electrons from anode to cathode. By then, however, it is likely that the pH in the cathode chamber has already increased substantially. This substantial increase in pH comes from the fact that the pH scale is defined as a

logarithmic scale and small concentration increases in the cathode chamber, therefore, cause a large increase of the cathode chamber pH. For example, at a hydroxyl ion concentration of only 1 mM ($[\text{OH}^-]=10^{-3}$) the pH has already increased to pH 11.

Furthermore, continuing this argumentation, it can also be expected that higher currents through the same system will result in a higher cathode pH as higher currents will cause higher electric fields. This will increase migration of cations and anions and will result in a higher cation and lower anion equilibrium concentration (i.e., when $J_{\text{dif, C}}+J_{\text{mig, C}}=0$ and $-J_{\text{dif, A}}-J_{\text{mig, A}}=0$). As a result, a higher concentration imbalance between cations and anions will be created and more hydroxyl ions will be present (i.e., higher pH) to compensate for this concentration imbalance.

I.3 What is the effect of membrane type?

The qualitative explanation of the cathode chamber pH increase given above did not yet assume any specific type of membrane. This explanation, therefore, is valid for any type of ion permeable membranes that is not 100% selective for cations, anions, protons, or hydroxyl ions. As 100% selective membranes do not exist, this means that all types of ion permeable membranes will show a cathode chamber pH increase. The severity of the cathode chamber pH increase, however, is influenced by the type of ion permeable membrane. In this perspective 5 types of ion permeable membranes can be discussed: (i) cation exchange membranes (CEMs), (ii) anion exchange membranes (AEMs), (iii) charge mosaic membranes (CMMs), (iv) neutral membranes, and (v) bipolar membranes (BPMs). The difference between these membrane types can be understood most easily by first looking at the first two categories of ion permeable membranes, i.e., CEMs and AEMs.

CEMs and AEMs typically consist of a polymer backbone to which charged functional groups are attached. In case of a CEM, the functional groups are negatively charged (e.g., sulfonate groups) and in the case of an AEM, the functional groups are positively charged (e.g., quaternary ammonium groups). Ions with a valence with a sign equal to that of the

charged functional groups of the ion exchange membranes (i.e., co-ions) will show a low concentration in the membrane. This is referred to a Donnan exclusion. Ions with a valence with a sign opposite to that to the charged functional groups (i.e., counter-ions), on the other hand, will show a high concentration in the membrane to compensate for the fixed charge density of the ion exchange membrane itself. As the fixed charge density of CEMs and AEMs is typically around 3 to 5 M, the counter-ion concentration in the membrane is often significantly higher than the concentration of the same ions in the solution of a (bio)electrochemical system.

At the membrane surface the membranes are in equilibrium with the solution according to the Donnan equilibrium (3). According to this equilibrium, the hydroxyl ion concentration in the membrane at the anode side of the membrane at $t=0$, $t>0$, and $t=\infty$, and in the membrane at the cathode side of the membrane at $t=0$ can be assumed to be zero, as the hydroxyl ion concentration in solution is also practically zero ($\text{pH } 7 \rightarrow [\text{OH}^-]=10^{-7} \text{ M} \approx 0 \text{ M}$). However, as explained above, at $t>0$ the hydroxyl ion concentration in solution in the cathode chamber will increase and, as a result, the hydroxyl ion concentration in the membrane at the cathode side of the membrane will also increase. From the difference in the properties of CEMs and AEMs with respect to their affinity for the negatively charged hydroxyl ions, it can be expected that these membranes will show different behavior. In contrast to an AEM, a CEM will show a high degree of Donnan exclusion of hydroxyl ions. Consequently, at an identical hydroxyl ion concentration in solution in the cathode chamber an AEM will show a much higher hydroxyl ion concentration in the membrane at the cathode side of the membrane than a CEM will show. This difference in hydroxyl ion concentration in the membrane at the cathode side of these membranes will have important consequences for the flux of hydroxyl ions (Equation 2).

As a result of the higher membrane hydroxyl ion concentration at the cathode side of an AEM, the concentration of hydroxyl ions throughout the complete membrane will be higher in an AEM than in a CEM. Furthermore, as the hydroxyl ion concentration at the anode side of the membrane will remain practically zero, also the concentration gradient of hydroxyl ions in an AEM will be higher than in a CEM under the same conditions.

Consequently, based on Equation 2, it can be expected that at a comparable hydroxyl ion concentration in solution in the cathode chamber, the flux of hydroxyl ions will be higher in case of an AEM than in case of a CEM. At $t=\infty$, therefore, when the flux of hydroxyl ions from cathode to anode is exactly equal to the transport of electrons from anode to cathode, the hydroxyl ion concentration in solution in the cathode chamber is expected to be lower in case of an AEM than in case of a CEM. Consequently, the cathode chamber pH at $t=\infty$ is expected to be lower in case of an AEM than in case of a CEM. This was indeed observed in the experiments that are described in Chapter 5¹.

CMMs contain both negatively charged and positively charged functional groups. From theory, the behavior of an ideal CMM with respect cathode chamber pH increase, therefore, is expected to be in between that of CEMs and AEMs, i.e., with an equilibrium pH ($t=\infty$) above that in the case of AEMs and below that in case of CEMs. This can also be expected for neutral membranes as they contain neither negatively charged nor positively charged functional groups.

Finally, BPMs, which are composed of a cation exchange layer on top of an anion exchange layer, should theoretically show no pH increase, as the working principle of BPMs is based on water splitting into protons and hydroxyl ions inside the membrane (1). Unfortunately, the water splitting efficiency of BPMs under the conditions valid for bioelectrochemical systems, is typically around 70% (4,5). This means that for the other 30% the BPM also transport cations and anions. Therefore, the cathode chamber pH will also increase in the case of a BPM, but the pH increase will be much slower. This was indeed observed for BPMs in the experiments as described in Chapter 4. How the equilibrium cathode chamber pH compares to that of the other ion permeable membranes is hard to predict, but judging from Figure 4.3 (Chapter 4) it is not expected to be much lower than that of the other membrane types.

¹ The cathode chamber pH increase for CEMs and AEMs can also be quantitatively assessed by modeling Equation 2. For this purpose, the Donnan equilibrium needs to be calculated and either the concentration gradient (Henderson approach) or the electrical field (Goldman approach) needs to be assumed constant (3). This quantitative modeling, however, goes beyond the scope of this PhD thesis.

I.4 What is the effect of cathode chamber pH increase?

As mentioned above, the pH scale is a logarithmic scale. Therefore, relatively small increases of the hydroxyl ion concentration relative to the hydroxyl ion concentration at pH 7 ($[OH^-]=10^{-7}$) already cause large pH increases. This has important consequences for the performance of the bioelectrochemical system. Hydroxyl ions (or protons) are involved in the cathode reaction of both the MFC and biocatalyzed electrolysis (Equation 5), and the concentration of hydroxyl ions (i.e., pH), therefore, influences the cathode potential. The influence of the concentration of hydroxyl ions on the cathode potential is described by the Nernst equation (Chapter 1):

$$E_{cat} = E_{cat}^0 - \frac{RT}{nF} \ln (\Pi) \quad (6)$$

Assuming other concentrations (e.g., O_2 and H_2) remain constant, the cathode potential is described as:

$$E_{cat}^{t>0} = E_{cat}^{t=0} - \frac{RT}{nF} \ln \left(\left(\frac{[OH^-]_{t>0}}{[OH^-]_{t=0}} \right)^a \right) \quad (7)$$

with $E_{cat}^{t=0}$ and $E_{cat}^{t>0}$ the cathode potential at $t=0$ and $t>0$ respectively.

In Equation 7 a denotes the reaction coordinate of the hydroxyl ions in the cathode reaction (Equation 5). As the hydroxyl ions are equimolarly produced with the electron consumption in the cathode reaction of both MFCs and biocatalyzed electrolysis a equals n and therefore:

$$E_{cat}^{t>0} = E_{cat}^{t=0} - \frac{RT}{F} \ln \left(\frac{[OH^-]_{t>0}}{[OH^-]_{t=0}} \right) \quad (8)$$

Because the pH scale is a logarithmic scale, a cathode chamber pH increase of 1 is a 10-fold increase of the hydroxyl ion concentration:

If $\Delta pH = 1 \rightarrow$

$$E_{cat}^{t>0} = E_{cat}^{t=0} - \frac{8.3145 \cdot 298.15}{96485.3} \ln(10) = E_{cat}^{t=0} - 0.059 \text{ V} \quad (9)$$

Every cathode chamber pH increase of 1 unit thus represents a cathode potential loss of 59 mV (Figure I.2A). At a constant anode chamber pH of 7, this can have significant consequences for the emf of bioelectrochemical systems (Figure I.2B).

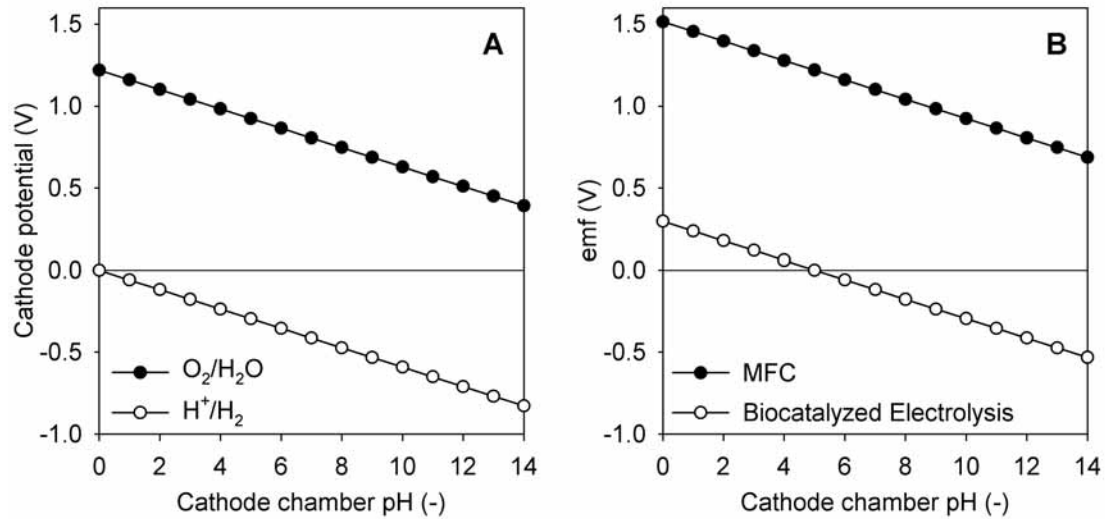


Figure I.2. Influence of the cathode chamber pH on (A) cathode potential and (B) electromotive force (emf) in bioelectrochemical systems (MFC and biocatalyzed electrolysis) with an anode chamber at a constant pH of 7. The anode potential at pH 7 is -0.296 V ($[HCO_3^-]=[CH_3COO^-]=5$ mM).

For example, at a cathode chamber pH of 12, the cathode potentials of both the oxygen reduction reaction and the hydrogen evolution reaction have decreased with 0.30 V relative to the value at pH 7 (Figure I.2A). At a constant anode pH of 7, this means that the electromotive force in the case of an MFC decreases from 1.10 V to 0.80 V and in the case of biocatalyzed electrolysis decreases from -0.12 V to -0.41 (Figure I.2B). In both cases this means that energy is lost, i.e., in case of an MFC less electrical energy is produced and in case of biocatalyzed electrolysis more electrical energy is

required to start the reaction (i.e., the theoretical energy requirement for hydrogen production increases from 0.26 to 0.89 kWh/Nm³ H₂).

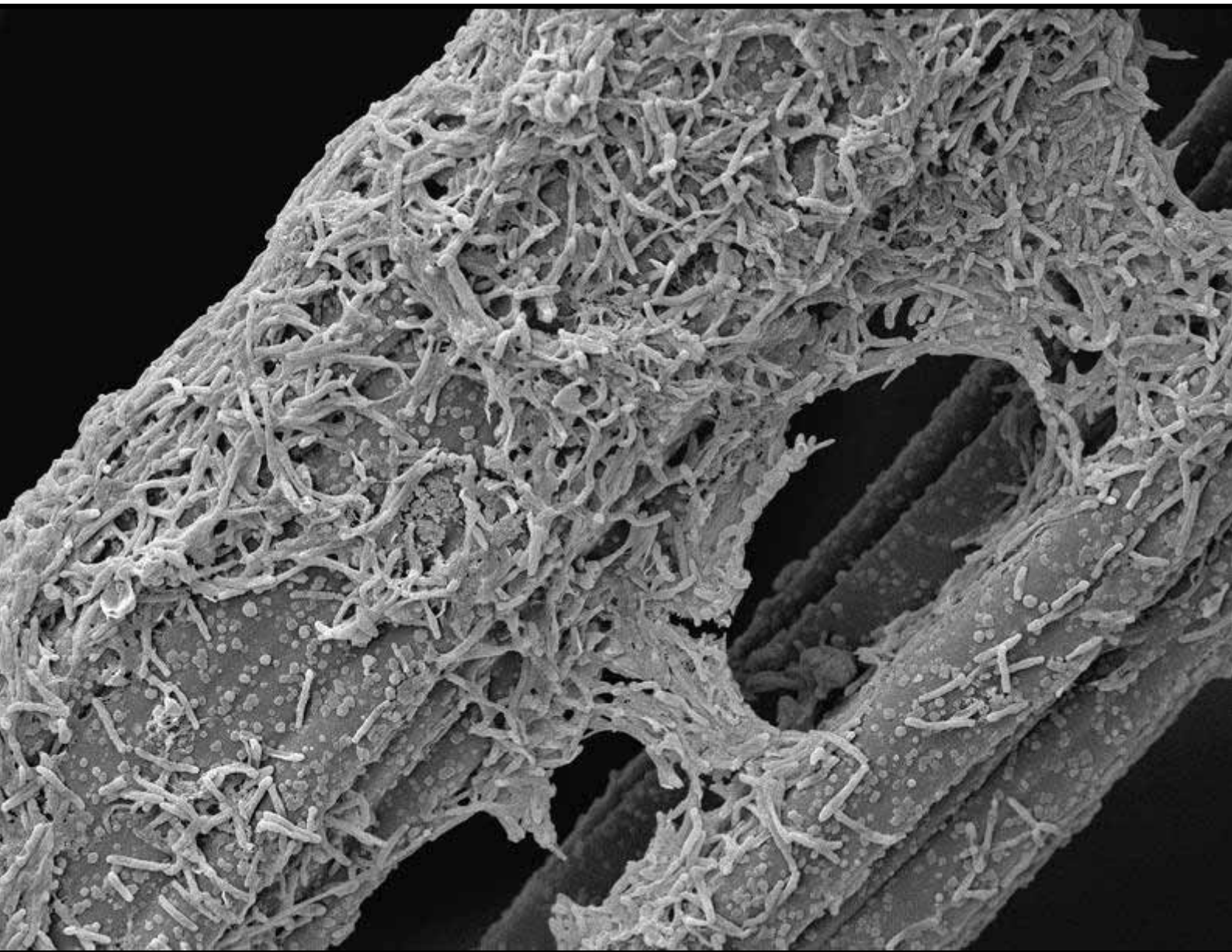
However, Figure I.2A also shows that this principle can work the other way around as well, i.e., cathode potentials increase with a decreasing cathode pH. If, for example, the cathode chamber pH decreases from 7 to 2, the cathode potentials of both the oxygen reduction reaction and the hydrogen evolution reaction increase with 0.30 V. At a constant anode chamber pH of 7, this means that the electromotive force in the case of an MFC increases from 1.10 V to 1.40 V and in the case of biocatalyzed electrolysis increases from -0.12 V to 0.18 V (Figure I.2B). In both cases this means that energy is gained, i.e., in case of an MFC more electrical energy can be produced and in case of biocatalyzed electrolysis less electrical energy is required to start the reaction (i.e., instead of theoretically requiring 0.26 kWh/Nm³ H₂ the system can theoretically even produce 0.39 kWh/Nm³ H₂ in addition to the hydrogen production).

I.5 References

- (1) Strathmann, H. *Ion-exchange membrane separation processes*; Elsevier: Amsterdam, 2004.
- (2) Bard, A. J.; Faulkner, L. R. *Electrochemical methods: fundamentals and applications*; 2nd ed.; John Wiley & Sons: New York, 2001.
- (3) Higa, M.; Tanioka, A.; Miyasaka, K. Simulation of the transport of ions against their concentration gradient across charged membranes. *J. Membr. Sci.* **1988**, *37*, 251-266.
- (4) Ter Heijne, A.; Hamelers, H. V. M.; Buisman, C. J. N. Microbial fuel cell operation with continuous biological ferrous iron oxidation of the catholyte. *Environ. Sci. Technol.* **2007**, *41*, 4130-4134.
- (5) Rozendal, R. A.; Sleutels, T. H. J. A.; Hamelers, H. V. M.; Buisman, C. J. N. Effect of the type of ion exchange membrane on performance, ion transport, and pH in biocatalyzed electrolysis of wastewater. *Water Sci. Technol.* **2007**, *Submitted*.

Hydrogen Production with a Microbial Biocathode

6



This chapter has been submitted for publication:

Rozendal, R. A.; Jeremiasse, A. W.; Hamelers, H. V. M.; Buisman, C. J. N. Hydrogen production with a microbial biocathode. *Environ. Sci. Technol.* **2007**, Submitted.

Hydrogen Production with a Microbial Biocathode

6

This chapter for the first time describes the development of a microbial biocathode for hydrogen production that is based on a naturally selected mixed culture of electrochemically active microorganisms. This is achieved through a three phase biocathode start up procedure that effectively turned an acetate and hydrogen oxidizing bioanode into a hydrogen producing biocathode by reversing the polarity of the electrode. The microbial biocathode that was obtained in this way had a current density of about -1.1 A/m^2 at a potential of -0.7 V . This was 3.6 times higher than that of a control electrode (-0.3 A/m^2). Furthermore, the microbial biocathode produced about $0.63 \text{ Nm}^3 \text{ H}_2/\text{m}^3$ cathode liquid volume/day at a cathodic hydrogen efficiency of 49% during hydrogen yield tests, whereas the control electrode produced $0.08 \text{ Nm}^3 \text{ H}_2/\text{m}^3$ cathode liquid volume/day at a cathodic hydrogen efficiency of 25%. The effluent of the biocathode chamber could be used to inoculate another electrochemical cell that subsequently also developed an identical hydrogen producing biocathode (-1.1 A/m^2 at a potential of -0.7 V). SEM photos were taken of both microbial biocathodes and showed a well developed biofilm on the electrode surface.

6.1 Introduction

Since the discovery of direct electron transfer by electrochemically active microorganisms on electrodes at the end of the last century (1), bioelectrochemical conversion of wastewaters has become a rapidly emerging research field (2). The most studied bioelectrochemical conversion technologies so far are: (i) microbial fuel cells (MFCs) for electricity production (3), and (ii) biocatalyzed electrolysis (or BEAMR process) for hydrogen production (4-6). Many research challenges, however, still remain before bioelectrochemical conversion of wastewater can be considered to be a mature wastewater treatment technology. One of the largest research challenges in this respect is the cathode catalyst.

Laboratory MFC or biocatalyzed electrolysis systems typically apply platinum as the cathode catalyst as platinum has proven to be an effective cathode catalyst in conventional fuel cells and electrolyzers. However, conventional fuel cells and electrolyzers typically operate at current densities ($\sim 10^3$ to 10^4 A/m²) that are orders of magnitude higher than those of MFCs and biocatalyzed electrolysis systems (~ 1 to 10 A/m²). In fact, as a result of the low current densities, MFCs and biocatalyzed electrolysis systems produce too little electricity or hydrogen per amount of platinum to justify the use of such an expensive material as the cathode catalyst. This has encouraged researchers to look for alternative cathode catalysts in MFCs and biocatalyzed electrolysis systems.

Microbial biocathodes hold great promise as an alternative cathode catalyst as they combine the advantage of an inexpensive electrode material (e.g., graphite) with the fact that they are self-regenerating (7). Several interesting microbial biocathode concepts have already been implemented successfully for catalyzing cathodic oxygen reduction in MFCs. These concepts include cathode systems that are based on redox cycling of transition metals (e.g., Mn and Fe) between the cathode and metal-oxidizing bacteria (8-10) and systems that are based on direct electron transfer by electrochemically active microorganisms (11). However, biocathode concepts that so far were developed for catalyzing cathodic hydrogen production have mostly been enzymatic (12,13) and not microbial. Enzymatic biocathodes

have the important drawback that they are relatively instable and that they are not self-regenerating (14).

The only microbial biocathode concept that was developed so far for catalyzing cathodic hydrogen production was based on an immobilized pure culture of *Desulfovibrio vulgaris* with methyl viologen as a redox mediator (15,16). However, a mixed culture, mediator-less microbial biocathode, especially when based on a naturally selected mixed culture, would be much more desirable with respect to the stability of operation of biocatalyzed electrolysis systems.

The objective of this study, therefore, was to develop a novel microbial biocathode system for hydrogen production that is based on a naturally selected mixed culture of electrochemically active microorganisms. Our strategy for achieving such a microbial biocathode system was based on the well-known reversibility of hydrogenases (17). Based on this hydrogenase reversibility we developed the following three phase biocathode start up procedure (Figure 6.1): (A) start up of an acetate and hydrogen oxidizing bioanode after inoculation with a mixed culture of electrochemically active microorganisms, (B) adaptation to hydrogen oxidation only, and (C) polarity reversal to a hydrogen producing biocathode and adaptation.

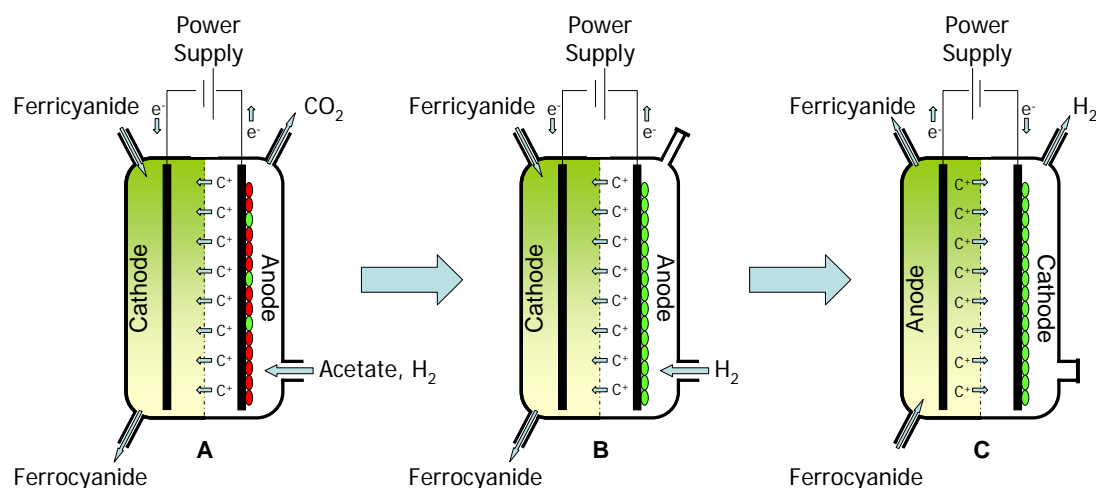


Figure 6.1. Overview of the three phase biocathode start up procedure (C^+ = cations): (A) start up of an acetate and hydrogen oxidizing bioanode after inoculation with a mixed culture of electrochemically active microorganisms, (B) adaptation to hydrogen oxidation only, and (C) polarity reversal to a hydrogen producing biocathode and adaptation.

6.2 Materials and methods

6.2.1 Biocatalyzed electrolysis cell

The experiments were performed in two identical electrochemical cells. The electrochemical cells consisted of 4 Plexiglas plates of 22 x 32 cm (Figure 6.2) of which the two outer plates served as the heating jacket for temperature control (303 K). The two inner plates served as the electrode chambers and were separated from each other by a cation selective membrane (Fumasep® FKE, FuMA-Tech GmbH). The electrode chambers consisted of vertically orientated channels (width 1.5 cm; depth 1 cm) for liquid transport (volume 0.25 L), and a headspace for gas collection (volume 0.03 L).

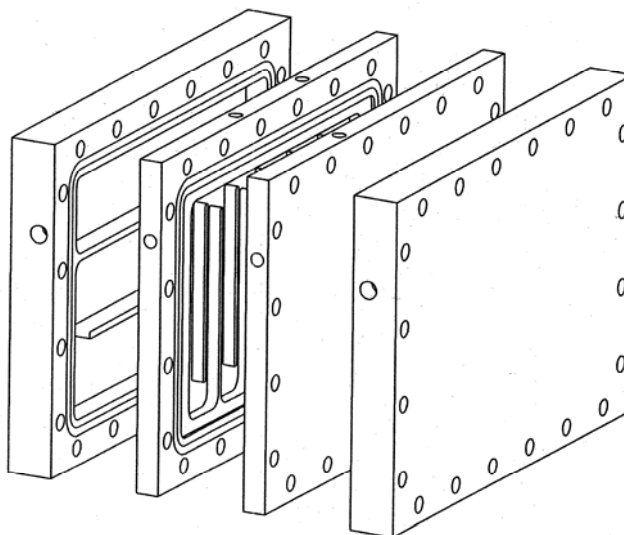


Figure 6.2. Design of the Plexiglas plates (22 x 32 cm) of the electrochemical cells. The two outer plates served as the heating jacket for temperature control; the two inner plates served as the electrode chambers and were separated from each other by a cation selective membrane (Fumasep® FKE, FuMA-Tech GmbH, Germany).

6

Both electrode chambers contained graphite felt (effective surface area 250 cm²; thickness 6.5 mm — National Electrical Carbon bv) as the electrode material. Three gold wires were pressed onto the graphite felt electrodes for current collection. Both electrode chambers were equipped with a Haber-Luggin capillary that was connected to an Ag/AgCl reference electrode (QM710X, ProSense bv). The electrochemical cells were each connected to a potentiostat (Wenking Potentiostat/Galvanostat KP5V3A,

Bank IC) and operated as a 3-electrode setup (18). The working electrode of one of the electrochemical cells was inoculated and subjected to the three phase biocathode start up procedure (see below). This electrode is referred to as the bioelectrode (during biocathode start up) or biocathode (after biocathode start up). The working electrode of the other electrochemical cell, which was not inoculated and not subjected to the three phase biocathode start up procedure, is referred to as the control electrode.

6.2.2 Experimental set-up

Figure 6.3 shows a schematic overview of the experimental set-up. The bioelectrode and the control electrode chamber were operated in continuous mode by supplying microbial nutrient medium (1.3 mL/min). Prior to entering the bioelectrode chamber the microbial nutrient medium was flushed with nitrogen from a nitrogen generator (purity >99.9%). The standard microbial nutrient medium was without carbon source and contained (in deionized water): 0.74 g/L KCl, 0.58 g/L NaCl, 0.68 g/L KH_2PO_4 , 0.87 g/L K_2HPO_4 , 0.28 g/L NH_4Cl , 0.1 g/L $\text{MgSO}_4 \cdot 7\text{H}_2\text{O}$, 0.1 g/L $\text{CaCl}_2 \cdot 2\text{H}_2\text{O}$, and 1 mL/L of a trace element mixture (19). During the biocathode start up, the standard microbial nutrient medium was supplemented with 10 mM sodium acetate or 10 mM sodium bicarbonate (Table 6.1). The counter electrode chamber contained a 100 mM potassium ferricyanide/ferrocyanide solution that was recycled (80 mL/min) over a 10 L buffer vessel.

The bioelectrode chamber solution was recycled (250 mL/min) over a gas washing bottle (640 ml). Liquid effluent left the gas washing bottle via a water lock to prevent diffusion of oxygen into the bioelectrode chamber. The headspace of the bioelectrode and control electrode chamber could be flushed with H_2 (>99.9992%), N_2 (>99.9992%), or CO (>99.997%) from a cylinder. Excess gas, either supplied or produced, left the system via the gas washing bottle and a gas flow meter (Milligascounter®, Ritter). The gas washing bottle contained a pH electrode for controlling the anode chamber at pH 7 by dosing with 1 M NaOH or 1 M HCl (Liquisys M CPM 253, Endress + Hauser). The electrochemical cells were connected to a data logger (Ecograph T, Endress + Hauser), which continuously logged the applied

voltage, current, anode potential, cathode potential, pH, temperature, and gas production. All potentials are reported against the normal hydrogen electrode (NHE).

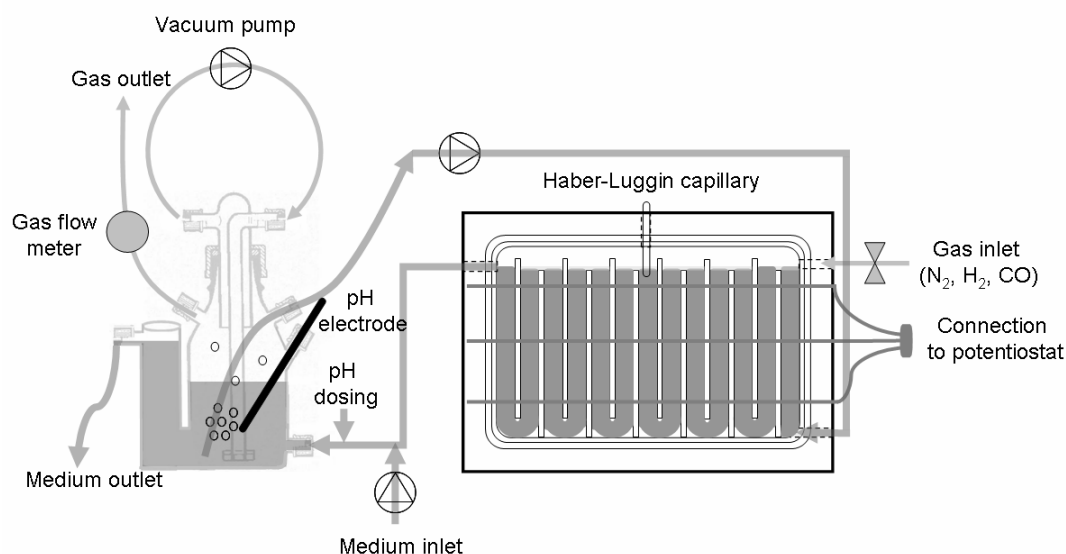


Figure 6.3. Schematic overview of the experimental set-up.

6.2.3 Experimental procedures

The bioelectrode chamber was inoculated with a mixed culture of electrochemically active microorganisms by adding 100 mL effluent taken from an active bioelectrochemical cell (20). Subsequently, the bioelectrode was subjected to the three phase biocathode start up procedure (Figure 6.1). Table 6.1 shows the differences in the experimental conditions during the three phases of the biocathode start up procedure.

After inoculation (phase A) the bioelectrode chamber was initially operated in batch mode (standard microbial nutrient medium supplemented with 17 mM sodium acetate). This was done to allow the electrochemically active microorganisms to adapt to the bioelectrode chamber without being washed out immediately. At $t=50$ h current generation started and the operation was switched from batch to continuous mode by starting the supply of microbial nutrient medium. When the headspace of the bioelectrode chamber was flushed with hydrogen gas (phase A and B), the gas phase of the gas washing bottle was recycled (10 L/min) over the liquid phase of the gas washing bottle using a vacuum pump to achieve a high level of hydrogen saturation in the recycled bioelectrode chamber solution.

Table 6.1. Experimental conditions during the three phase biocathode start up procedure

	Phase A	Phase B	Phase C
Medium supplement	10 mM NaCH ₃ COO	10 mM NaHCO ₃	10 mM NaHCO ₃
Headspace flushing	H ₂	H ₂	N ₂
Bioelectrode potential (V)	0.1/-0.2	-0.2	-0.7

In between phase B and C of the biocathode start up procedure the proper bioelectrode potential for biocathode operation was determined by means of a polarity reversal scan. During this scan the bioelectrode potential was lowered from -0.2 to -0.8 V at a scanrate of 0.025 mV/s using a potentiostat (Autolab PGSTAT12, Eco Chemie bv).

After start up the biocathode was compared to the control electrode on the basis of polarization curves, which were obtained by means of chronoamperometry. For this purpose current generation was logged every 5 minutes for 1 hour at -0.8, -0.75, -0.7, -0.65, -0.6, and -0.55 V. The last 5 data points at every potential were averaged and plotted in the polarization curve. Subsequently, the biocathode was compared to the control electrode on the basis of hydrogen yield tests. The hydrogen yield tests (duplicate) were performed in batch mode at -0.7 V and lasted for 48 hours. At the start of the experiment the headspace of the biocathode and the control electrode chamber contained only nitrogen. During the hydrogen yield tests the headspace of biocathode chamber was sampled 7 times and analyzed for its hydrogen fraction with a gas chromatograph (Shimadzu GC-2010 equipped with a thermal conductivity detector and a Varian molsieve 5A column). Due to the low gas production of the control electrode, the headspace of the control electrode chamber could only be sampled/analyzed twice (at the beginning and at the end of the hydrogen yield test). The hydrogen production was calculated from the total gas production and the measured hydrogen fractions by means of a mass balance equation as described in (21).

Next, both the biocathode and the control electrode were subjected to an inhibition test. During the inhibition test the biocathode and the control electrode chamber of both electrochemical cells were flushed with carbon monoxide. After a carbon monoxide exposure period of 20 hours, the

headspace of both reactors was flushed again with nitrogen to remove the carbon monoxide.

6.2.4 Scanning electron microscopy (SEM)

Electrode samples were fixed for 2 hours in 3% glutaraldehyde, twice washed for 15 minutes in PBS buffer (10 mM, pH 7.4), dehydrated in graded series of ethanol (10%, 25%, 50%, 75%, 90% and two times 100% with 20 minutes for each stage), and dried in a desiccator. The samples were coated with gold and observed with a JEOL JSM-6480LV SEM (acceleration voltage 6 kV, HV-mode, SEI detector).

6.3 Results and discussion

6.3.1 Biocathode start up

The bioelectrode was subjected to the three phase biocathode start up procedure (Figure 6.1; Table 6.1). The development of current generation during the three phases of the biocathode start up procedure is shown in Figure 6.4. During phase A the bioelectrode was first started up as an acetate and hydrogen oxidizing bioanode at a potential of 0.1 V (Figure 6.4A). During this phase the headspace of the bioelectrode chamber was continuously flushed with hydrogen gas. At $t=167$ h current generation stabilized (~ 7 A/m²) and the bioelectrode potential was lowered to -0.2 V.

Phase B of the biocathode start up procedure was started at $t=197$ h (current density: 5 A/m²) by removing the 10 mM sodium acetate from the microbial nutrient medium and replacing it with 10 mM sodium bicarbonate. Hydrogen gas remained as the only available electron donor for anodic current generation. Two tests were done to investigate whether the anode was indeed oxidizing hydrogen: (i) the supply of hydrogen to the bioelectrode chamber was twice increased by changing the liquid recycling rate over the gas washing bottle from 250 to 500 mL/min to see whether current generation would increase, and (ii) the hydrogen flushing was twice replaced by nitrogen flushing to see whether current generation would decrease (Figure 6.4B). This indeed confirmed that hydrogen was oxidized

and suggested that the electrochemically active microorganisms had an active hydrogen metabolism.

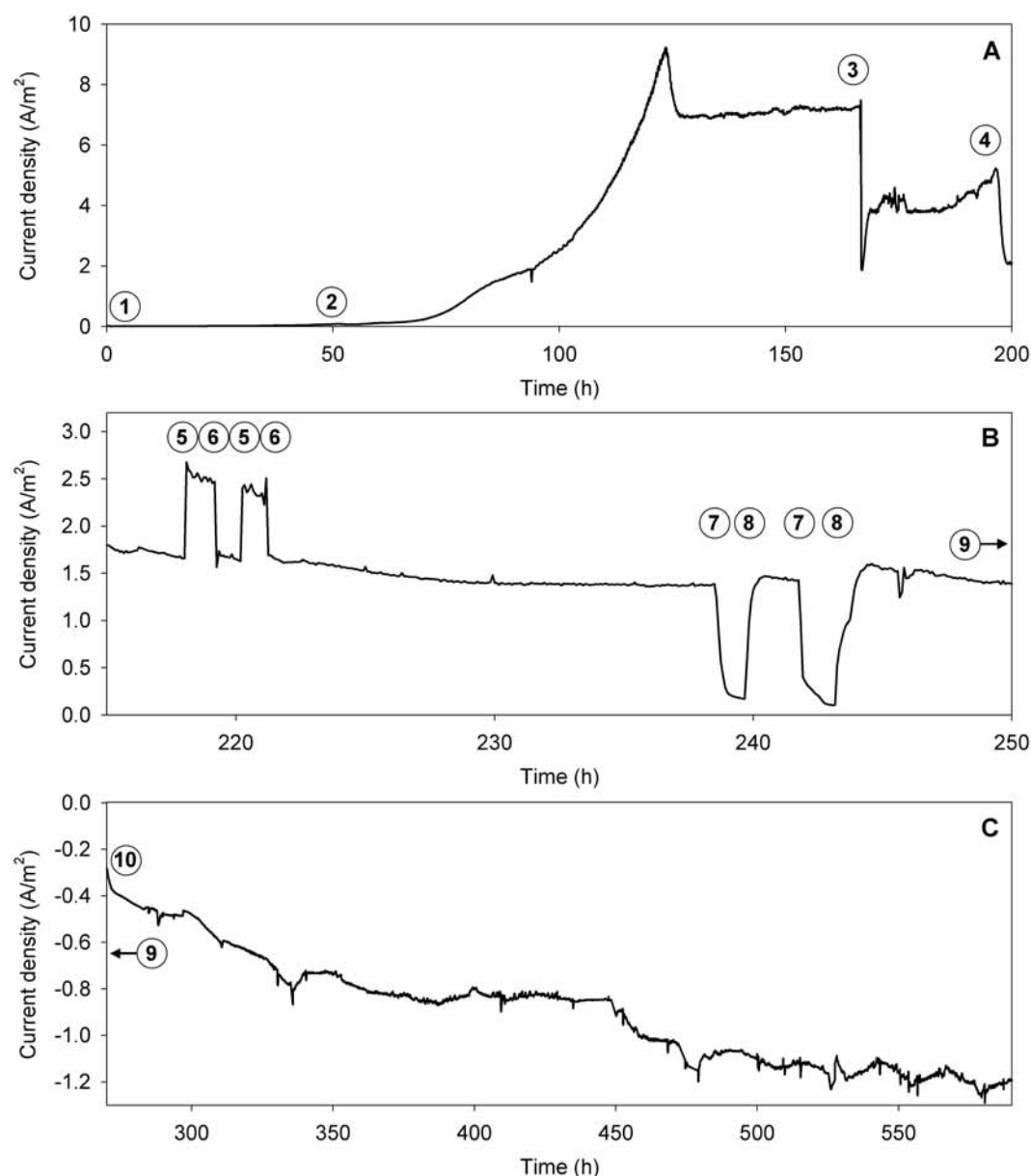


Figure 6.4. Development of current generation during the three phase biocathode start up procedure: (A) start up of an acetate and hydrogen oxidizing bioanode after inoculation with a mixed culture of electrochemically active microorganisms, (B) adaptation to hydrogen oxidation only, and (C) polarity reversal to a hydrogen producing biocathode and adaptation. (1) inoculation of the reactor at a bioelectrode potential of 0.1 V, (2) operation is switched from batch to continuous mode, (3) bioelectrode potential is lowered from 0.1 to -0.2 V, (4) sodium acetate is removed from the microbial nutrient medium and replaced by sodium bicarbonate, (5) liquid recycling rate over the gas washing bottle is increased from 250 to 500 mL/min, (6) liquid recycling rate over the gas washing bottle is decreased from 500 to 250 mL/min, (7) hydrogen flushing is replaced by nitrogen flushing, (8) nitrogen flushing is replaced by hydrogen flushing, (9) polarity reversal scan (Figure 6.5), and (10) bioelectrode operation is controlled at a potential of -0.7 V and hydrogen flushing is replaced by nitrogen flushing.

Next, in between phase B and C the proper bioelectrode potential for biocathode operation was determined by means of a polarity reversal scan (Figure 6.5). During the polarity reversal scan anodic current generation stopped at about -0.3 V, which is a typical open circuit potential for a bioanode (3). Cathodic current generation started at a bioelectrode potential of about -0.65 V, which is 0.23 V below the theoretical potential for hydrogen formation at pH 7 (-0.42 V).

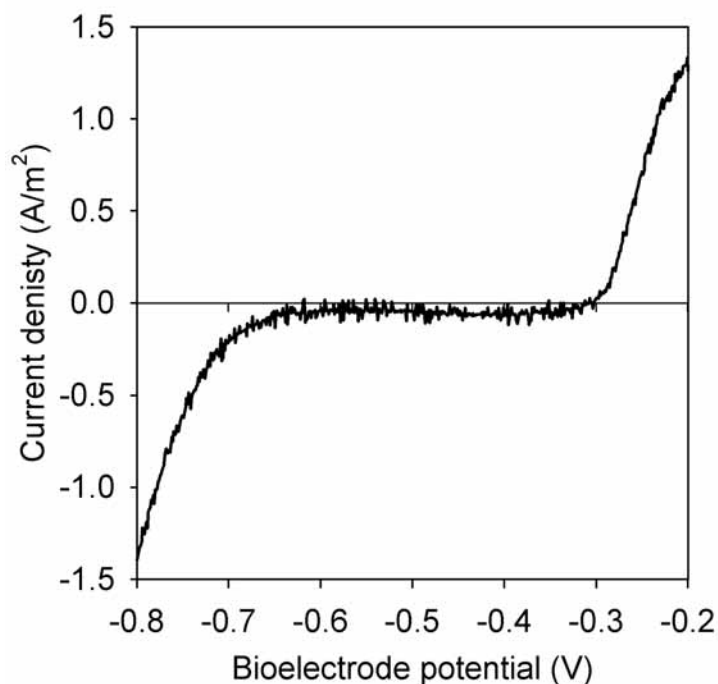


Figure 6.5. Polarity reversal scan of the bioelectrode from -0.2 to -0.8 V at a scanrate of 0.025 mV/s.

To stimulate the development of a hydrogen producing biocathode, the bioelectrode potential was controlled at -0.7 V during phase C of the biocathode start up procedure, i.e., at a slightly lower value than the value at which cathodic current generation had started during the polarity reversal scan. Hydrogen flushing was replaced by nitrogen flushing. From $t=270$ h until $t=590$ h the cathodic current increased from -0.3 to about -1.2 A/m² (Figure 6.4C), which suggested that the consortium of electrochemically active microorganisms was adapting to cathodic current generation.

6.3.2 Polarization curves

After the biocathode start up the performance of the biocathode was compared to that of a control electrode on the basis of polarization

curves (Figure 6.6). The biocathode outperformed the control electrode with respect to current generation over the complete measuring range of the polarization curves. Furthermore, at a potential of -0.7 V the biocathode even outperformed a platinum coated titanium electrode that was used in previous experiments under comparable conditions (6). At -0.7 V the current density of the biocathode was about -1.1 A/m², which was about 3.6 times that of the control electrode (-0.3 A/m²) and 2.4 times that of the platinum coated titanium electrode (-0.47 A/m²) used previously.

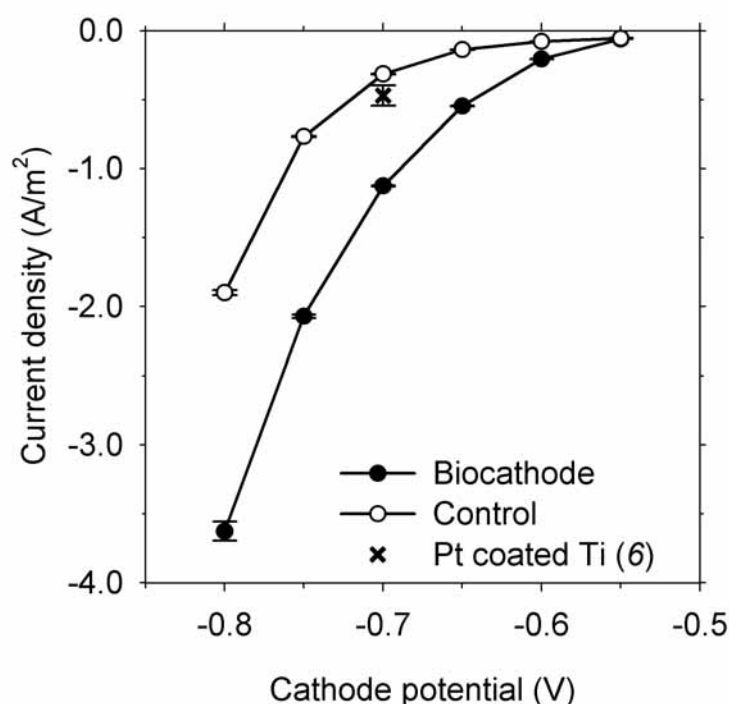


Figure 6.6. Polarization curves of the biocathode compared to a control electrode. The cross indicates the performance of a platinum coated titanium electrode that was used in previous experiments under comparable conditions (6).

6.3.3 Hydrogen yield tests

After the biocathode start up initially only methane was produced and no hydrogen could be detected. Presumably, the produced hydrogen was consumed directly by hydrogenotrophic methanogens that were naturally selected from the inoculum due to the presence of bicarbonate as a carbon source during the biocathode start up. Therefore, from about 150 hours prior to performing the hydrogen yield tests bicarbonate was removed from the microbial nutrient medium. This was a successful strategy to prevent hydrogenotrophic methanogenic consumption of hydrogen gas.

Remarkably, these carbon limited conditions have remained for over 1000 hours and did not influence cathodic current generation of the biocathode.

The results of the hydrogen yield tests are shown in Figure 6.7. During the hydrogen yield tests at a cathode potential of -0.7 V the average cathodic current generation of the biocathode was about -1.2 A/m², while that of the control electrode was about -0.3 A/m².

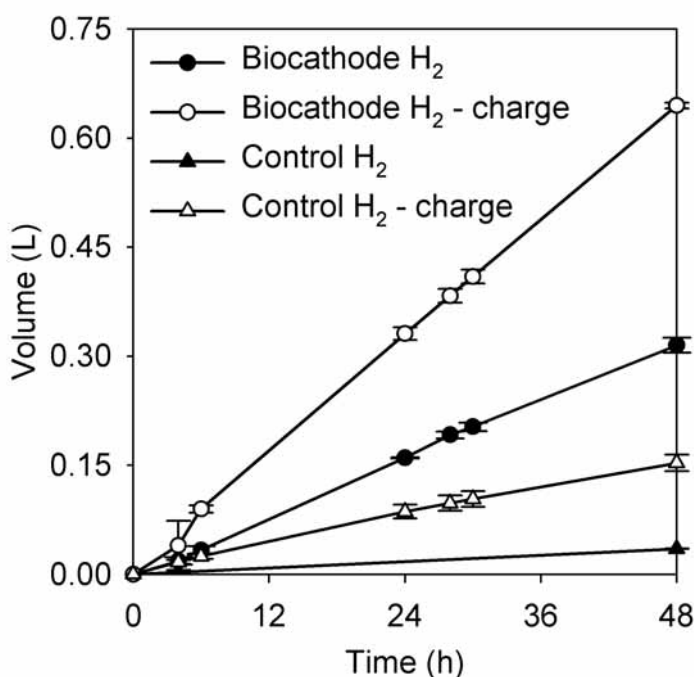


Figure 6.7. Measured hydrogen production (H₂) and expected hydrogen production based on the cumulative charge production (H₂ - charge) of the biocathode and the control electrode during 48 hour hydrogen yield tests at a cathode potential of -0.7 V.

During the hydrogen yield tests the biocathode produced about 0.31 L of hydrogen gas, which was over 8 times the hydrogen production of the control electrode (0.04 L). This corresponds to an average volumetric hydrogen production rate during the hydrogen yield tests of about 0.63 Nm³ H₂/m³ cathode liquid volume/day for the biocathode chamber and 0.08 Nm³ H₂/m³ cathode liquid volume/day for the control electrode chamber. Furthermore, the cathodic hydrogen efficiency (i.e., the measured hydrogen production compared to the expected hydrogen production based on the cumulative charge production) of the biocathode was about 49% (i.e., ~4 e⁻ → H₂), whereas that of the control electrode was 25% (i.e., ~8 e⁻ → H₂).

Most of the hydrogen loss in the electrochemical cell with the biocathode can be explained from the diffusional loss of hydrogen through the

membrane (4,6). The cation selective membrane (Fumasep® FKE) used in this experiment was over three times thinner than the Nafion® membrane we have used previously (6). Using the average hydrogen headspace concentration during the hydrogen yield tests of about 28.5% and assuming that the diffusion coefficient and solubility of hydrogen in the Fumasep® FKE membrane is similar to that in Nafion® (22), we estimate (23) that about 0.27 L of the produced hydrogen was lost through diffusion from the biocathode chamber into the anode chamber. This amount of hydrogen explains about 82% of the difference between the measured hydrogen production and the expected hydrogen production based on the cumulative charge production in Figure 6.7. As reported previously (6,21), the relative importance of this diffusional loss of hydrogen becomes smaller at higher current densities. Furthermore, the use of thicker membranes can reduce the absolute amount of this diffusional loss of hydrogen.

6.3.4 Indications for the microbial origin of the biocathode

The experiments so far gave a strong indication that the developed biocathode for hydrogen production was indeed of a microbial origin. During phase C of the biocathode start up procedure cathodic current generation (Figure 6.4C) increased to about -1.2 A/m^2 . This cathodic current generation was significantly higher than that of the control electrode (-0.3 A/m^2) and remained stable over long periods of time ($>2000 \text{ h}$). These observations are in line with what would be expected from a growing, adapting, and regenerating consortium of electrochemically active microorganisms. However, this indication does not yet unequivocally prove that the biocathode is of a microbial origin.

Therefore, a carbon monoxide inhibition test was performed (Figure 6.8). Carbon monoxide is a well known inhibitor for iron-hydrogenases, i.e., the type of hydrogenases that are most often associated with microbial hydrogen production (24,25). The carbon monoxide inhibition test showed that the performance of the biocathode was indeed negatively affected by the presence of carbon monoxide and that this effect could be completely reversed by removing the carbon monoxide through nitrogen flushing. This agrees with the expected behavior of a microbial biocathode.

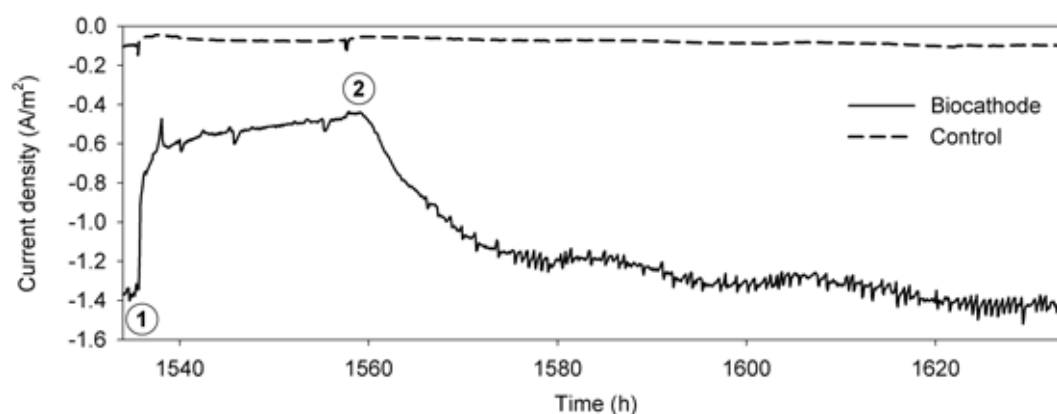


Figure 6.8. Current development of the biocathode and the control electrode in response to carbon monoxide flushing: (1) start of carbon monoxide flushing of the headspace of the biocathode chamber and the control electrode chamber, and (2) end of carbon monoxide flushing and start of nitrogen flushing of the headspace of the biocathode chamber and the control electrode chamber.

Subsequently, we investigated whether the effluent of the biocathode chamber could be used to inoculate and start up another biocathode. For this purpose we inoculated the control electrode chamber by connecting the medium outlet of the biocathode chamber to the medium inlet of the control electrode chamber for a period of about 100 hours (Figure 6.9). At first, no significant increase of the cathodic current generation of the control electrode could be observed, but after supplementing the microbial nutrient medium with a carbon source (10 mM sodium bicarbonate), cathodic current generation increased to about -1.1 A/m^2 , effectively turning the control electrode into another biocathode. After removal of the carbon source from the microbial nutrient medium, current generation remained stable and hydrogen production could be detected. The fact that the effluent of the biocathode could be used for the inoculation and start up of another biocathode is an extra indication that the biocathode is of a microbial origin.

6

Finally, the electrochemical cells were disassembled and samples of both biocathodes, i.e., original biocathode and former control electrode, were investigated with SEM (Figure 6.10). A well developed biofilm could be observed on all electrode samples. This again indicated that the biocathode was of a microbial origin. Furthermore, the original biocathode (Figure 6.10B) generally had a thicker biofilm layer than the former control electrode (Figure 6.10C). This was not unexpected as the original biocathode had also been operated as a bioanode during the biocathode start up and

had been operated as a biocathode for over 2000 hours, while the former control electrode had only been operated as a biocathode for less than 600 hours.

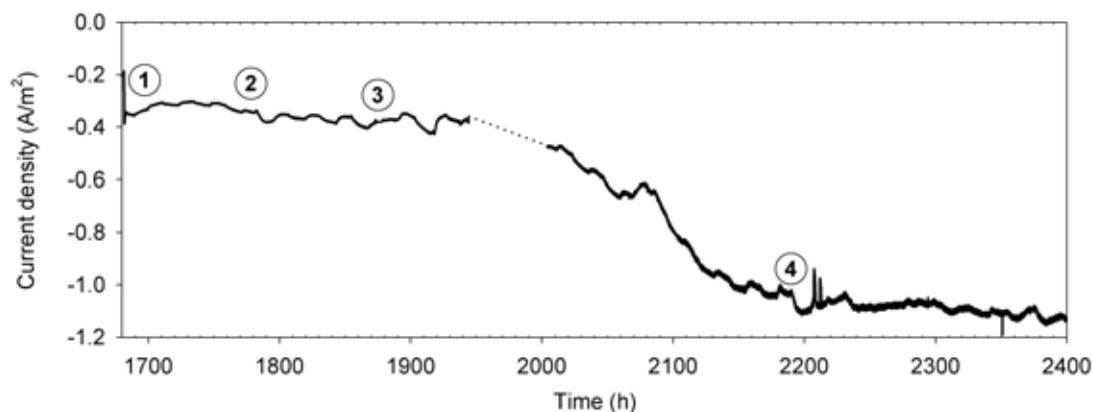


Figure 6.9. Current development of the control electrode after inoculation (dotted line = no data due to power cut): (1) inoculation of the control electrode chamber by connecting the medium outlet of the biocathode chamber to the medium inlet of the control electrode chamber, (2) disconnection of the medium outlet of the biocathode chamber from the medium inlet of the control electrode chamber and start of the supply of standard microbial nutrient medium (i.e. without carbon source), (3) start of the supply of standard microbial nutrient medium supplemented with 10 mM sodium bicarbonate, and (4) start of the supply of standard microbial nutrient medium (i.e., without carbon source).

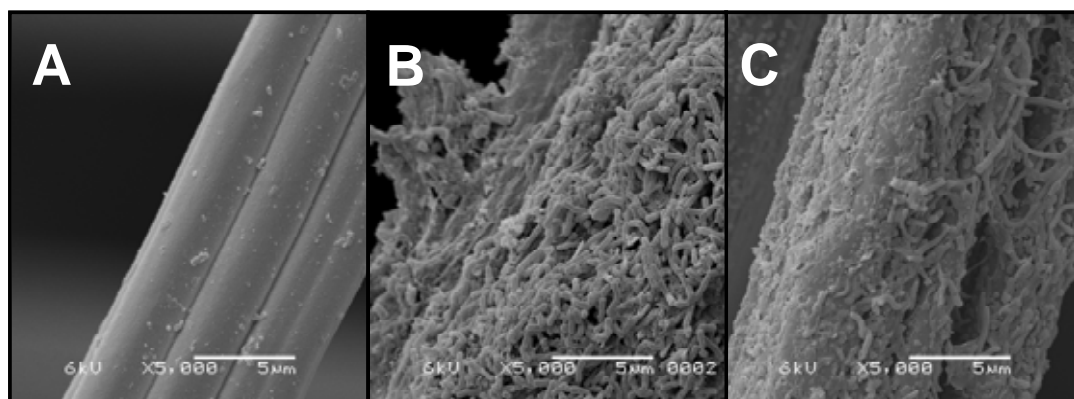


Figure 6.10. SEM photos of fibers of graphite felt electrode samples: (A) unused electrode, (B) original biocathode that had been operated as a biocathode for over 2000 h, and (C) former control electrode that had been operated as a biocathode for less than 600 h.

6.3.5 Future research and outlook

In a previous study (21), we estimated that the volumetric production rate of biocatalyzed electrolysis systems can be improved to about 10 Nm³ H₂/m³ reactor liquid volume/day at an energy input of below 1 kWh/Nm³ H₂. For the cathode performance this objective implies that the cathode overpotential needs to be reduced to about 0.05 to 0.10 V at a current

density of -5 to -10 A/m², which means that at pH 7 the cathode potential needs to be in the range -0.47 to -0.52 V at a current density of -5 to -10 A/m². The microbial biocathode of this study had a current density of about -1.2 A/m² at a potential of -0.7 V (i.e., cathode overpotential $-0.42 - (-0.7) = 0.28$ V), which shows that the performance of microbial cathode needs to be improved in order to reach the above objective. Nevertheless, the performance of the microbial biocathode of this study is already a significant improvement compared to our previous study with a platinum coated titanium electrode as the cathode, which showed less than half of this current density (i.e., -0.47 A/m²) at an identical overpotential and under comparable conditions (6). Furthermore, there is no reason to assume that the microbial biocathode cannot be improved much further. In the last decade power production of MFCs has increased by several orders of magnitude (26), partly due to a better understanding of the bioanode. To get a better understanding of the microbial biocathode, future research work amongst others should focus on identifying the responsible microbial species that catalyze cathodic hydrogen production, elucidating their electron transfer mechanisms, and understanding their ATP generation mechanisms.

Another important topic that needs a better understanding is the role and the effects of the carbon limited conditions that were applied in this study to prevent hydrogenotrophic methanogenic consumption of the produced hydrogen gas. These carbon limited conditions were maintained for over 1000 hours without any significant loss of performance. As it seems unlikely that microorganisms survive that long without any carbon source, it is probable there has been an alternative carbon source present in the system. The electrochemically active microorganisms might have used decaying biomass as a carbon source that was likely present after the biocathode start up. Furthermore, some carbon dioxide might still have been present in the influent (although it was flushed with nitrogen) or diffused through the membrane from the counter electrode chamber. It is important to investigate what the optimal carbon source availability should be for maintaining a well-performing microbial biocathode as the removal of the bicarbonate from the microbial nutrient medium was a successful

strategy to prevent hydrogenotrophic methanogenic consumption of hydrogen.

Nevertheless, the results described in this chapter comply with the objective of a microbial biocathode system for hydrogen production that is based on a naturally selected mixed culture of electrochemically active microorganisms. This is an important finding as it allows for the use of inexpensive electrode materials and holds great promise for the cost-effective production of hydrogen gas from wastewaters through biocatalyzed electrolysis.

6.4 Acknowledgments

This work was performed at Wetsus, Centre for Sustainable Water Technology. Wetsus is funded by the city of Leeuwarden, the Province of Fryslân, the European Union European Regional Development Fund and by the EZ/KOMPAS program of the “Samenwerkingsverband Noord-Nederland”. The authors like to thank the participants of the theme “Hydrogen” for their input and contributions: Shell, Paques bv, and Magneto Special Anodes bv. The authors further thank A. van Aelst, Dr. M.A. Pereira, and Dr. A. Zwijnenburg for their assistance with the SEM photos.

6.5 References

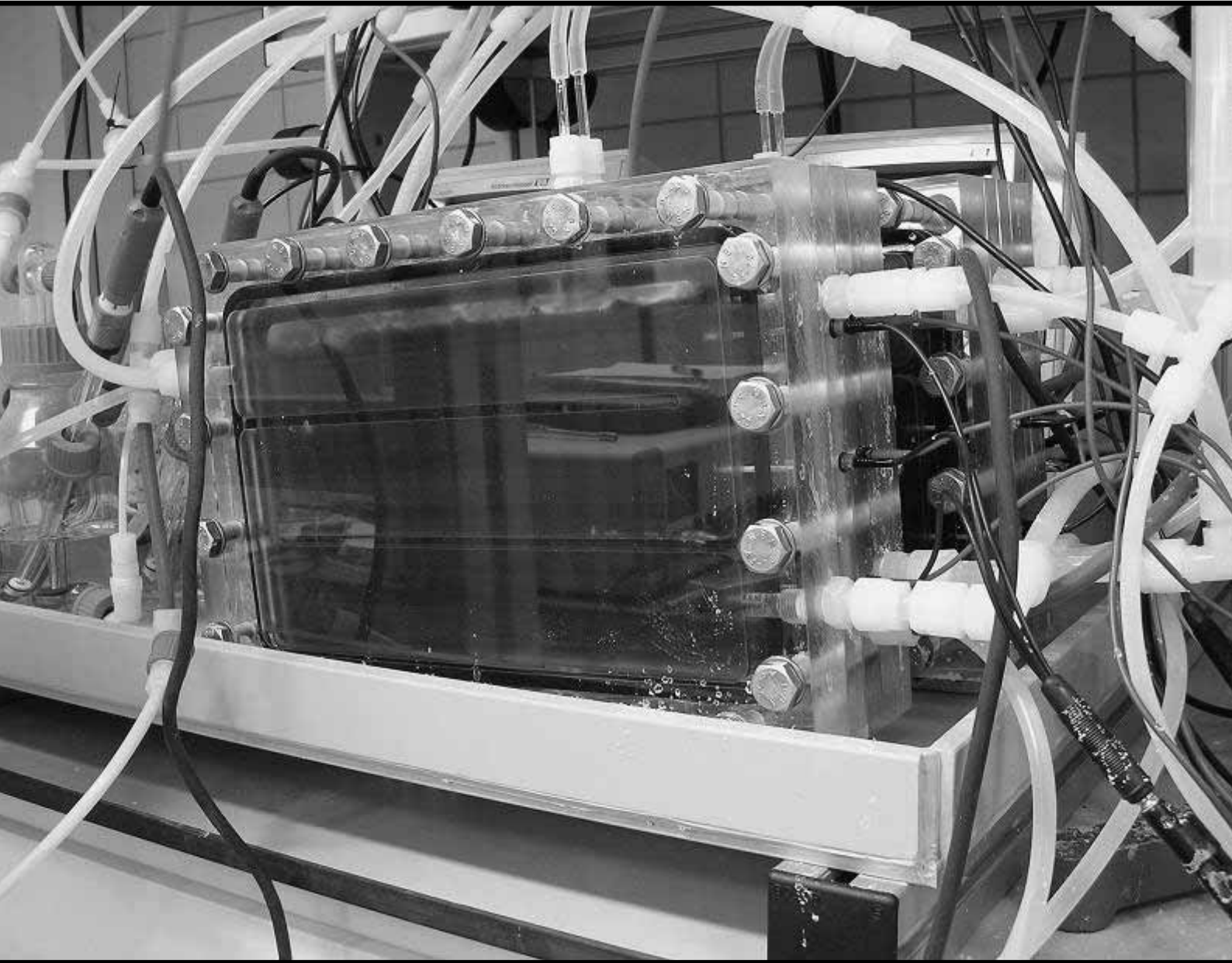
- (1) Kim, B. H.; Kim, H. J.; Hyun, M. S.; Park, D. H. Direct electrode reaction of Fe(III)-reducing bacterium, *Shewanella putrefaciens*. *J. Microbiol. Biotechnol.* **1999**, *9*, 127-131.
- (2) Rabaey, K.; Rodriguez, J.; Blackall, L. L.; Keller, J.; Gross, P.; Batstone, D.; Verstraete, W.; Nealson, K. H. Microbial ecology meets electrochemistry: electricity-driven and driving communities. *ISME J.* **2007**, *1*, 9.
- (3) Logan, B. E.; Hamelers, B.; Rozendal, R.; Schröder, U.; Keller, J.; Freguia, S.; Aelterman, P.; Verstraete, W.; Rabaey, K. Microbial fuel cells: methodology and technology. *Environ. Sci. Technol.* **2006**, *40*, 5181-5192.
- (4) Liu, H.; Grot, S.; Logan, B. E. Electrochemically assisted microbial production of hydrogen from acetate. *Environ. Sci. Technol.* **2005**, *39*, 4317-4320.
- (5) Rozendal, R. A.; Buisman, C. J. N. Process for producing hydrogen. **2005**, *Patent WO2005005981*.

- (6) Rozendal, R. A.; Hamelers, H. V. M.; Euverink, G. J. W.; Metz, S. J.; Buisman, C. J. N. Principle and perspectives of hydrogen production through biocatalyzed electrolysis. *Int. J. Hydrogen Energy* **2006**, *31*, 1632-1640.
- (7) He, Z.; Angenent, L. T. Application of bacterial biocathodes in microbial fuel cells. *Electroanalysis* **2006**, *18*, 2009-2015.
- (8) Rhoads, A.; Beyenal, H.; Lewandowski, Z. Microbial fuel cell using anaerobic respiration as an anodic reaction and biomineralized manganese as a cathodic reactant. *Environ. Sci. Technol.* **2005**, *39*, 4666-4671.
- (9) Ter Heijne, A.; Hamelers, H. V. M.; Buisman, C. J. N. Microbial fuel cell operation with continuous biological ferrous iron oxidation of the catholyte. *Environ. Sci. Technol.* **2007**, *41*, 4130-4134.
- (10) Ter Heijne, A.; Hamelers, H. V. M.; De Wilde, V.; Rozendal, R. A.; Buisman, C. J. N. A bipolar membrane combined with ferric iron reduction as an efficient cathode system in microbial fuel cells. *Environ. Sci. Technol.* **2006**, *40*, 5200-5205.
- (11) Bergel, A.; Feron, D.; Mollica, A. Catalysis of oxygen reduction in PEM fuel cell by seawater biofilm. *Electrochem. Commun.* **2005**, *7*, 900-904.
- (12) Morozov, S. V.; Vignais, P. M.; Cournac, V. L.; Zorin, N. A.; Karyakina, E. E.; Karyakin, A. A.; Cosnier, S. Bioelectrocatalytic hydrogen production by hydrogenase electrodes. *Int. J. Hydrogen Energy* **2002**, *27*, 1501-1505.
- (13) Pershad, H. R.; Duff, J. L. C.; Heering, H. A.; Duin, E. C.; Albracht, S. P. J.; Armstrong, F. A. Catalytic electron transport in *Chromatium vinosum* [NiFe]-hydrogenase: Application of voltammetry in detecting redox-active centers and establishing that hydrogen oxidation is very fast even at potentials close to the reversible H^+/H_2 value. *Biochemistry* **1999**, *38*, 8992-8999.
- (14) Lojou, E.; Bianco, P. Electrocatalytic reactions at hydrogenase-modified electrodes and their applications to biosensors: From the isolated enzymes to the whole cells. *Electroanalysis* **2004**, *16*, 1093-1100.
- (15) Lojou, E.; Durand, M. C.; Dolla, A.; Bianco, P. Hydrogenase activity control at *Desulfovibrio vulgaris* cell-coated carbon electrodes: Biochemical and chemical factors influencing the mediated bioelectrocatalysis. *Electroanalysis* **2002**, *14*, 913-922.
- (16) Tatsumi, H.; Takagi, K.; Fujita, M.; Kano, K.; Ikeda, T. Electrochemical study of reversible hydrogenase reaction of *Desulfovibrio vulgaris* cells with methyl viologen as an electron carrier. *Anal. Chem.* **1999**, *71*, 1753-1759.
- (17) Vignais, P. M.; Colbeau, A. Molecular biology of microbial hydrogenases. *Curr. Issues Mol. Biol.* **2004**, *6*, 159-188.
- (18) Bard, A. J.; Faulkner, L. R. *Electrochemical methods: fundamentals and applications*; 2nd ed.; John Wiley & Sons: New York, 2001.
- (19) Zehnder, A. J. B.; Huser, B. A.; Brock, T. D.; Wuhrmann, K. Characterization of an acetate-decarboxylating, non-hydrogen-oxidizing methane bacterium. *Arch. Microbiol.* **1980**, *124*, 1-11.
- (20) Rozendal, R. A.; Sleutels, T. H. J. A.; Hamelers, H. V. M.; Buisman, C. J. N. Effect of the type of ion exchange membrane on performance, ion transport, and pH in biocatalyzed electrolysis of wastewater. *Water Sci. Technol.* **2007**, Submitted.

- (21) Rozendal, R. A.; Hamelers, H. V. M.; Molenkamp, R. J.; Buisman, C. J. N. Performance of single chamber biocatalyzed electrolysis with different types of ion exchange membranes. *Water Res.* **2007**, *41*, 1984-1994.
- (22) Jiang, J. H.; Kucernak, A. Investigations of fuel cell reactions at the composite microelectrode|solid polymer electrolyte interface. I. Hydrogen oxidation at the nanostructured Pt|Nafion® membrane interface. *J. Electroanal. Chem.* **2004**, *567*, 123-137.
- (23) Liu, H.; Logan, B. E. Electricity generation using an air-cathode single chamber microbial fuel cell in the presence and absence of a proton exchange membrane. *Environ. Sci. Technol.* **2004**, *38*, 4040-4046.
- (24) Adams, M. W. W.; Stiefel, E. I. Organometallic iron: the key to biological hydrogen metabolism. *Curr. Opin. Chem. Biol.* **2000**, *4*, 214-220.
- (25) Adams, M. W. W.; Stiefel, E. I. Biochemistry - Biological hydrogen production: Not so elementary. *Science* **1998**, *282*, 1842-1843.
- (26) Logan, B. E.; Regan, J. M. Electricity-producing bacterial communities in microbial fuel cells. *Trends Microbiol.* **2006**, *14*, 512-518.

Concluding Remarks and Outlook

7



Concluding Remarks and Outlook

7

This final chapter discusses the status and future potential of hydrogen production through biocatalyzed electrolysis. This is done by summarizing the insights that were gained in this PhD thesis, by evaluating the possible applications of biocatalyzed electrolysis, and by critically assessing which scale-up and research issues need to be addressed before biocatalyzed electrolysis can be referred to as a mature technology for hydrogen production from wastewaters.

It is expected that volumetric hydrogen production rates can be improved to over 10 Nm³ H₂/m³ reactor volume/day at an energy input of below 1 kWh/Nm³ H₂ by improving the performance of the critical biocatalyzed electrolysis system components (bioanode, membrane, and cathode). However, to get to a mature hydrogen production technology, it is also important to realize a cost-effective scale-up that considers ohmic losses and material costs.

7.1 General conclusion

This PhD thesis describes the first steps in the development of biocatalyzed electrolysis, a promising new technology for hydrogen production from wastewaters. Biocatalyzed electrolysis makes a much wider variety of wastewaters than before suitable for hydrogen production as it found a novel means of dealing with the endothermic reactions that are inherent to hydrogen production from wastewaters. Technologies that are currently regarded as “state of the art” for hydrogen production from wastewaters are not able to deal with these endothermic reactions (i.e., dark fermentation) or deal with them in an impractical way by using sunlight (i.e., photoheterotrophic fermentations). Biocatalyzed electrolysis, on the other hand, deals with these endothermic reactions in a practical way by using small amounts electrical energy to overcome thermodynamic barriers.

The innovative step of the biocatalyzed electrolysis process is the application of electrochemically active microorganisms for hydrogen production. Electrochemically active microorganisms are capable of exocellular electron transfer, which enables them to grow on an electrode surface while using the electrode as an electron acceptor for the oxidation of dissolved organic compounds (e.g., in wastewater). This creates a bioanode that can be coupled to a hydrogen producing (bio)cathode by means of an electrical circuit. Subsequently, the required energy input to overcome thermodynamic barriers can be supplied electrically by including a power supply in the electrical circuit.

Electrochemically active microorganisms can be naturally selected from a wide range of inocula (1) and have proven to be capable of utilizing a wide range of dissolved organic compounds that commonly occur in wastewaters, such as sugars (2-4), fatty acids (5), and proteins (6). This makes biocatalyzed electrolysis technology an interesting hydrogen production process for a wide range of applications.

7.2 Applications

7.2.1 Wastewater treatment

From a wastewater treatment perspective biocatalyzed electrolysis can be seen as a method to produce a high quality COD stream (i.e., hydrogen rich gas) from a diluted COD stream (e.g., domestic wastewater) at the cost of a small energy input. In terms of COD loading rates future biocatalyzed electrolysis systems are expected to perform in between high rate aerobic systems (up to 5 kg COD/m³ reactor volume/day) and high rate anaerobic systems (more than 10 kg COD/m³ reactor volume/day) (7). For example, a biocatalyzed electrolysis system that produces 10 Nm³ H₂/m³ reactor volume/day at 90% cathodic hydrogen efficiency (Paragraph 7.4.1) converts about 7 kg COD/m³ reactor volume/day.

There are many kinds of reduction processes used on wastewater treatment plants that require large amounts of electron donor. These reduction processes include denitrification (e.g., for production of drinking water or effluent polishing in a sand filter), sulfate reduction (e.g., for metal precipitation), and metal reduction (e.g., for metal precipitation) (7). Often it is impractical to use COD-containing wastewaters as the electron donor for these reduction processes as this would dilute or contaminate the effluent of the reduction process. Alternatively, methane can theoretically be used as an electron donor for these reduction processes (8). However, due the low growth rate of anaerobic methanotrophic microorganisms the application of methane as an electron donor for reduction processes has not yet led to practical processes. Anaerobic hydrogenotrophic microorganisms, on the other hand, grow much faster, and hydrogen, therefore, is an ideal electron donor for reduction processes at wastewater treatment plants. The oxidation of hydrogen only yields water and, consequently, does not contaminate the effluent. Biocatalyzed electrolysis could be a cost-effective method to produce the hydrogen required for reduction processes, as the hydrogen can be produced from a COD-containing wastewater elsewhere in the wastewater treatment plant.

7.2.2 Transportation

Transportation fuels are responsible for about 20 to 25% of the global fossil fuel consumption (9). However, due to the threat of climate change and instabilities in the fossil fuel market (Chapter 1), society is currently considering alternative fuels for transportation. To replace fossil fuels in a sensible way, these alternative fuels need to be produced renewably and without carbon dioxide emission. Besides biodiesel, bioethanol, and biogas, also hydrogen is currently considered to be one of the possible alternatives for fossil fuels (i.e., hydrogen economy). Biocatalyzed electrolysis could produce a significant part of the required hydrogen for transportation from wastewaters. This could effectively turn wastewater treatment systems into fuelling stations. For example, an average sized industrial wastewater treatment, which treats 10 ton COD/day (estimated reactor volume: ~1500-2000 m³), could produce about 1.25 ton H₂/day. Assuming a fuel efficiency of 0.5 to 1 kg hydrogen per 100 km for a fuel cell powered passenger car (10), this is enough for driving 46 to 91 million car kilometers per year. Furthermore, in the case of the Netherlands (2002), all domestic wastewater could theoretically provide enough biodegradable material for the production of about 240 ton H₂/day, which is enough for driving 9.4–19% of the total car km in the Netherlands (11).

An important advantage of hydrogen as a transportation fuel is the fact that it can be produced from practically any kind of renewable energy, whereas most other alternative fuels can only be produced from biomass (Chapter 1). Furthermore, hydrogen can be converted to electrical energy efficiently and directly in a hydrogen fuel cell, which occurs practically emission-less with water as the only byproduct. Last, in a transition towards a renewable society, hydrogen can be deployed for “clean” utilization of fossil fuels, i.e., hydrogen production from fossil fuels in combination with carbon dioxide sequestration.

Disadvantages with respect to hydrogen as a transportation fuel, on the other hand, include the problems around hydrogen distribution (12) and onboard hydrogen storage (10). Obviously, these problems need to be solved before hydrogen can be considered to be a practical transportation fuel for long range vehicles, such as passenger cars. However, already on a short

term hydrogen fuel can offer opportunities for short range vehicles, such as city busses (13). City busses require only limited fuel storage capacity as they can be refueled each “round”. Nowadays, city busses are often powered by diesel combustion, which creates particulate matter that negatively affects air quality in urban regions (14). Hydrogen fuel cell technology solves this problem.

7.2.3 Industry

In 2000, the global annual hydrogen demand was estimated to be about 50 million tons of which about two thirds was consumed by the petrochemical industry (15). Most hydrogen that is used in the petrochemical industry is consumed for upgrading of fossil fuels (e.g., hydrodesulfurization and hydrocracking). This demand is expected to increase significantly in the coming years as oil consumption is also expected to increase (9). Furthermore, as most of the lighter crude oils with low sulfur content have already been extracted from the wells, more and more heavy oils with high sulfur content will be processed in the future. These heavy oils with high sulfur content need much more upgrading and, therefore, will require much more hydrogen.

Other large-scale uses of hydrogen in the petrochemical industry include ammonia synthesis, methanol synthesis, and hydrochloric acid synthesis. Furthermore, besides the petrochemical industry, also other industries consume significant amount of hydrogen. These industries include the food industry, which uses hydrogen for the saturation of unsaturated fats and oils (e.g., for margarine production), and the metal industry, which uses hydrogen as a reducing agent for metallic ores.

To integrate biocatalyzed electrolysis with large industrial sites, biocatalyzed electrolysis could treat the industrial wastewaters of the industrial sites and deliver hydrogen back to a hydrogen distribution network, which is commonly available at large industrial sites. An example of such an industrial site is the Rijnmond region (The Netherlands) with a total hydrogen throughput of more than 1000 ton H₂/day (16). Depending on the availability of wastewater on this site, biocatalyzed electrolysis could

deliver a modest contribution to the hydrogen production, while closing material cycles and adding value to the wastewater.

7.3 Performance – status & objective

The working principle of biocatalyzed electrolysis is interesting, but performance has to be improved significantly to become a mature technology for hydrogen production. Table 7.1 gives an overview of the performance of published biocatalyzed electrolysis studies and the objective for biocatalyzed electrolysis as a mature technology. This objective is based on an extrapolation of results achieved with bioanodes in MFC studies and on a realistic design for full scale bioelectrochemical reactors (Paragraph 7.4).

Table 7.1. Performance of published biocatalyzed electrolysis studies and the objective for biocatalyzed electrolysis as a mature technology.

Study	System Volume (L)	Substrate	Vol. H ₂ prod. rate (m ³ /m ³ /day)	Overall H ₂ efficiency (%)	Energy input (kWh/m ³)
Liu et al. (17)	0.03	Acetate	0.36 ^a	61 ^b	~1 ^a
Rozendal et al. (18)	6.6	Acetate	0.02	53	1.9
Rozendal et al. (19)	3.3 ^c	Acetate	0.30	23	2.2
Ditzig et al. (20)	0.58	Wastewater	0.01 ^d	9.8	2.5
Objective	10 ⁴ -10 ⁶	Wastewater	>10 ^e	>90 ^e	<1 ^e

- Calculated at an applied voltage of 0.45 V (cathodic H₂ efficiency 94%; current density 1.4 A/m² – from Figure 4 in (17)).
- From (21)
- Excluding the gas collection chamber.
- Calculated at an applied voltage of 0.5 V (cathodic H₂ efficiency 42.7%; current density ~0.37 A/m² – from Figure 3A in (20)).
- Based on a current density of 5 to 10 A/m² at an applied voltage of below 0.42 V at a cathodic H₂ efficiency of above 90%.

Table 7.1 shows that the biocatalyzed electrolysis systems that have been used so far are relatively small (mL to L scale) and that the performance decreases with increasing system volume. This illustrates the enormous challenges of scaling up biocatalyzed electrolysis to a full scale system while at the same time improving the performance (Paragraph 7.4). However, when the objective of 10 Nm³ H₂/m³ reactor volume/day at an energy input

of below 1 kWh/Nm³ H₂ (Table 7.1) is indeed accomplished in a full scale biocatalyzed electrolysis system, the performance will compare well with that of other biological hydrogen production technologies, such as dark fermentation (22,23). Biocatalyzed electrolysis, however, is suitable for treating a much wider variety of wastewaters, which makes the process more suitable for practical application.

The required energy input of 1 kWh/Nm³ H₂ (~1.5-1.7 kWh/kg COD) is not high for a wastewater treatment system as on a COD basis it is in the same order as the energy input required by the aerators in aerobic treatment (0.7-1.4 kWh/kg COD (24)). Moreover, with about the same energy input biocatalyzed electrolysis produces a valuable product, while aerobic wastewater treatment systems just produce carbon dioxide. Furthermore, future biocatalyzed electrolysis systems are expected to exhibit higher volumetric loading rates (Paragraph 7.2.1) and lower sludge production (*I*) than aerobic systems.

Compared to anaerobic wastewater treatment systems, biocatalyzed electrolysis will typically show lower COD loading rates (Paragraph 7.2.1). Biocatalyzed electrolysis, however, has the advantage that from the same amount of COD it produces a 7 times more valuable product (0.75 \$/kg H₂-COD vs. 0.11 \$/kg CH₄-COD - calculated from (25)).

Also compared to water electrolysis biocatalyzed electrolysis is an interesting process for hydrogen production. Biocatalyzed electrolysis has an exergetic efficiency (i.e Gibbs free energy efficiency) of about 266% (at 1 kWh/Nm³ H₂) on the basis of electricity input and hydrogen output (i.e., excluding the exergy content of the wastewater). This means that the Gibbs energy content of the hydrogen output is 2.66 times that of the electricity input. By comparison, water electrolysis has an exergetic efficiency of only 49 to 60% (at 4.4 to 5.4 kWh/Nm³ H₂ (26)).

7.4 Outlook – scale up & future research

7.4.1 Scale up issues

Scale-up is one of the most important issues along the way of commercialization of biocatalyzed electrolysis. The volumes of biocatalyzed

electrolysis systems that are published in literature do not yet go beyond the mL to L scale (Table 7.1). Future systems, however, have to be designed on the m³ scale and at the same time will have to comply with the objective to produce over 10 Nm³ H₂/m³ reactor volume/day at an energy input of below 1 kWh/Nm³ H₂ (Table 7.1). This will require a much more fundamental understanding of the biocatalyzed electrolysis system. This paragraph outlines the challenges with respect to scale up of biocatalyzed electrolysis systems.

Process design. One of the most challenging aspects of a full scale design is the fact that small electrical resistances that do not matter in a laboratory cell, become important in a full scale bioelectrochemical reactor. For example, an electrical resistance in the order of 0.1-1 Ω (e.g., a contact resistance) at a current of only 1 A already causes a potential loss of 0.1-1 V, which is a lot compared to theoretical voltage of 0.12 V (Chapter 1). Therefore, in a full scale bioelectrochemical reactor operating at about 900-1000 A/m³ (=~10 Nm³ H₂/m³ of reactor volume/day), the ohmic losses can be enormous if the system is not properly designed. To eliminate ohmic losses one would like to apply materials with high conductivity. However, due to the relatively low production rates, full scale bioelectrochemical reactors can only become economically feasible if they apply inexpensive materials (see below), which generally show lower conductivities and thus higher ohmic losses.

A stack design with bipolar plates (Figure 7.1) is one of the most viable designs capable to deal with this trade-off between material costs and conductivity (27,28). The advantage of stack designs with bipolar plates compared to (stack) designs without bipolar plates (1,29,30) is that the ohmic loss due to the conductivity of the electrodes is minimized. The reason for this is that bipolar plates connect anodes and cathodes across the complete surface so that the electrons travel only short distances through the electrode material. Consequently, inexpensive electrode materials (such as graphite) can be used as the electrode materials are not required to have extremely high conductivities (such as metals).

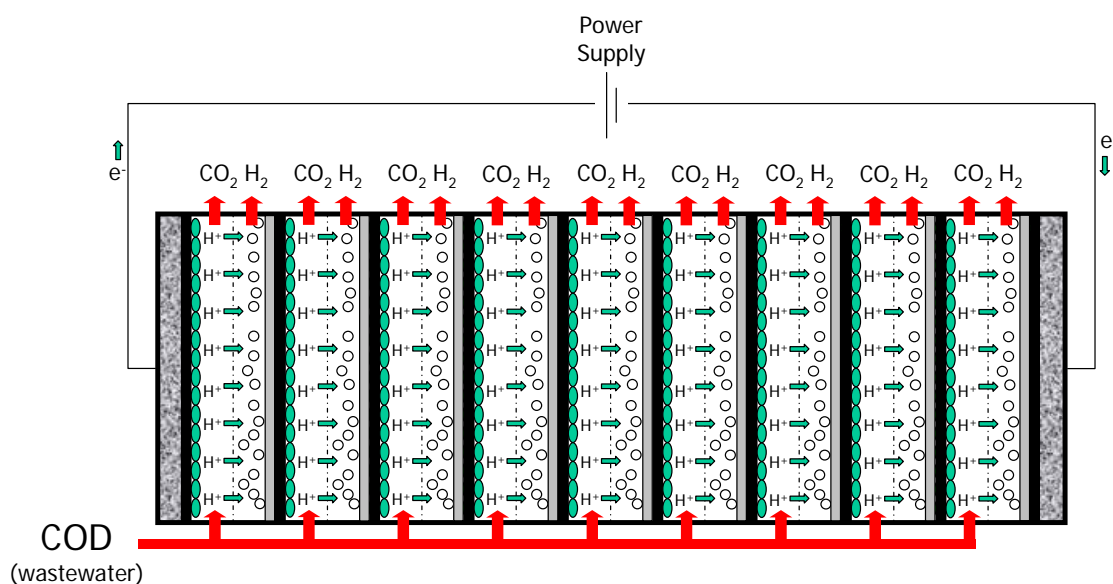


Figure 7.1. Schematic representation of a stack design with bipolar plates for hydrogen production through biocatalyzed electrolysis.

A drawback of stack designs with bipolar plates compared to (stack) designs without bipolar plates, however, is that the ohmic loss due to ion transport will play much more important role. This is caused by the fact that the ions have to travel significant distances through the wastewater in between the electrodes. As a result, the feasibility of a stack design with bipolar plates will highly depend on wastewater conductivity.

For example, an energy consumption of below 1 kwh/Nm³ H₂ implies that the applied voltage has to be below 0.42 V (at 90% cathodic hydrogen efficiency). When subtracting the equilibrium voltage of 0.12 V, this means that the sum of all potential losses (i.e., ohmic and electrode potential losses) has to be below 0.3 V. To minimize the energy required for pumping, the anode to cathode distance should not be much lower than 0.5 cm. Assuming an electrode thickness of 1 mm, this means that the single cell thickness in a stack design will be in the order of 0.7 cm. At a single cell thickness of 0.7 cm the current density has to be at least 7 A/m² (assuming 90% cathodic hydrogen efficiency) to be able to achieve the objective of 10 Nm³ H₂/m³ of reactor volume/day. Figure 7.2 shows what this means for the ohmic loss due to ion transport in relation to the wastewater conductivity.

At a wastewater conductivity of below 1.2 mS/cm more than the available 0.3 V is already consumed by the ohmic loss due to ion transport. This leaves nothing for the electrode overpotentials and, therefore, a stack design

with bipolar plates at a wastewater conductivity of below 1.2 mS/cm that complies with the objective is impossible. At a wastewater conductivity of above 3.5 mS/cm, on the other hand, the ohmic loss decreases to below 0.1 V, which leaves over 0.2 V for the electrode overpotentials. Such electrode overpotentials are attainable (Paragraph 7.4.2) and, therefore, a stack design with bipolar plates at a wastewater conductivity of above 3.5 mS/cm that complies with the objective is realistic.

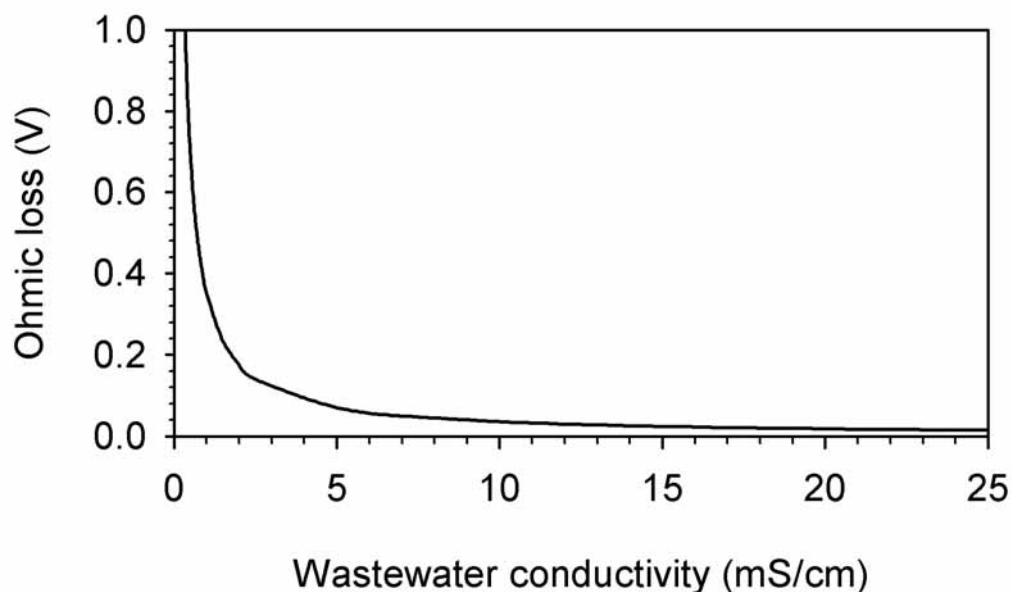


Figure 7.2. Ohmic loss due to ion transport in relation to the wastewater conductivity (current density 7 A/m²; anode to cathode distance 0.5 cm)

Production costs. Besides process design also production costs have to be taken into account in a full scale biocatalyzed electrolysis system. As biocatalyzed electrolysis systems exhibit current densities that are typically 3 to 5 orders of magnitude smaller than those in other electrochemical systems (e.g., water electrolyzers), material costs have a much stronger influence on the hydrogen production costs in biocatalyzed electrolysis systems than in other electrochemical systems. For example, at the moment all biocatalyzed electrolysis laboratory systems apply platinum as the cathode electrocatalyst (17-20). Assuming a cost of 500 €/m² for a platinum catalyzed electrode, an electrode lifetime of 5 years, and a current density of 7 A/m², the cathode costs already account for almost 4 €/Nm³ H₂ (at 90% cathodic hydrogen efficiency), which is already more than 10 times the market price (2004) of hydrogen (~0.38 €/Nm³ H₂ (1)).

Figure 7.3 gives an overview of the estimated production costs of hydrogen produced through biocatalyzed electrolysis in an optimized design based on laboratory materials (including a platinum catalyzed cathode) compared to an optimized design based on inexpensive substitutes.

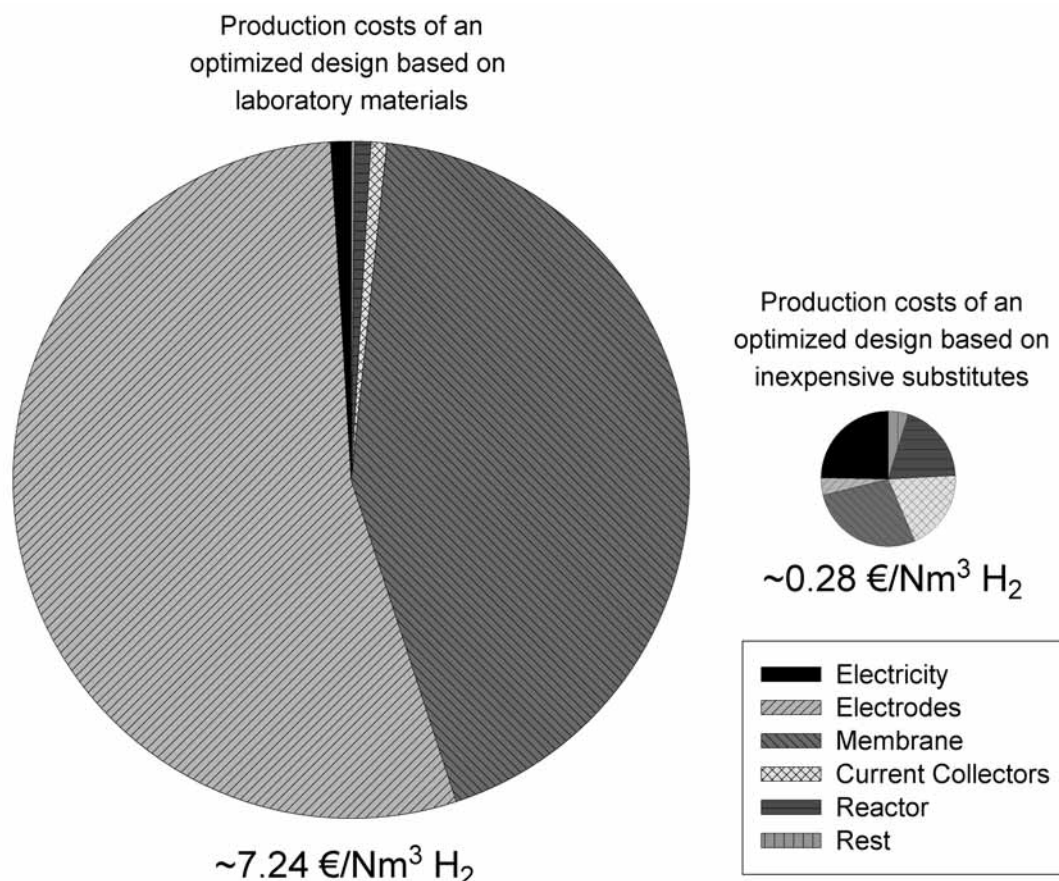


Figure 7.3. Estimated production costs for hydrogen produced through biocatalyzed electrolysis in an optimized design based on laboratory materials compared to an optimized design based on inexpensive substitutes. (Assumptions: 90% cathodic hydrogen efficiency, 10 Nm³ H₂/m³/day, 1 kWh/Nm³ H₂, lifetime electrodes/membrane/current collectors: 5 yr, lifetime reactor/rest: 20 yr; Costs: electricity: 0.07 €/kWh, single sided platinum catalyzed electrode: 500 €/m², inexpensive substitute electrode (graphite paper): 1.5 €/m², Nafion® membrane: 400 €/m², inexpensive substitute membrane: 10 €/m², current collectors: 500 €/m², reactor: 4000 €/m³ (3I), rest: 1000 €/m³ reactor).

As can be seen from Figure 7.3 the most expensive components in the current laboratory biocatalyzed electrolysis systems are the electrodes and the membranes. To commercialize biocatalyzed electrolysis it is important, therefore, to replace these components by inexpensive substitutes. Only then the production costs of hydrogen through biocatalyzed electrolysis can go below the market price (2004) of 0.38 €/Nm³ H₂ (25).

In the example of Figure 7.3 the estimated production costs of hydrogen through biocatalyzed electrolysis go as low as 0.28 €/Nm³ H₂. Although this number does not include all costs (e.g., operator costs), it does illustrate the potential of biocatalyzed electrolysis as a mature hydrogen production technology. Even more so, as the number also does not yet include the fact that wastewater often represents a negative market value (31).

7.4.2 Critical biocatalyzed electrolysis system components

To achieve the objective of 10 Nm³ H₂/m³ reactor volume/day at an energy input of below 1 kWh/Nm³ H₂ in full scale bioelectrochemical reactors, it is important that also the critical biocatalyzed electrolysis system components comply with this objective. This paragraph, therefore, discusses the current status of the performance the bioanode, the membrane, and the cathode. Furthermore, this paragraph points out for each critical biocatalyzed electrolysis system component which research challenges need to be solved to be able to comply with the objective.

Bioanode. Bioanode performance will have to improve to about 5 to 10 A/m² at reasonable overpotentials ($\sim <0.10$ V) to be able to achieve the objective of 10 Nm³ H₂/m³ reactor volume/day at an energy input of below 1 kWh/Nm³ H₂. Moreover, this performance has to be achieved on real wastewaters. Table 7.1 shows that not many biocatalyzed electrolysis studies have dealt yet with hydrogen production from real wastewaters and the only study that did so far showed that it is not straightforward (20). Therefore, much more experience with real wastewaters is required before biocatalyzed electrolysis can be implemented in practice.

Still, based on the current density of about 4.4 A/m² at a potential loss of about 0.05 V recently achieved with MFCs in our laboratories on acetate medium (32), and based on the current density of about 5 A/m² at a potential loss of about 0.06 V on hydrogen and acetate medium achieved in Chapter 6, we believe that achieving current densities of 5 to 10 A/m² at potential loss of below 0.10 V is realistic. However, further improving anode performance will require a more fundamental understanding of the working principles of electrochemically active biofilms. One of the most interesting topics to study with respect to bioanode performance is the occurrence of

multilayered biofilms on the bioanode, as multilayered biofilms could significantly improve bioanode performance (33). Initial MFC studies only discussed the occurrence of monolayered biofilms, but more recent studies suggest that also multilayered biofilms are possible that still rely on electron transfer through direct contact (33) by means of electrically conductive pili or nanowires (34,35). Stimulation of these multilayered biofilm could be an interesting strategy to boost bioanode performance.

Besides the electrochemically active biofilm, also methanogenesis is an important microbiological aspect to consider with respect to the performance of the anode chamber. As methanogens consume the same substrates as electrochemically active microorganisms, methanogenic activity in the anode chamber can reduce electron and hydrogen recoveries. Recently, an interesting MFC study was published in this respect by Freguia and co-workers (4). They found that electrochemically active microorganisms in a bioanode chamber can outcompete methanogens when acetate (non-fermentable) was used as the substrate. However, when glucose (fermentable) was used as the substrate, a significant amount of methanogenic activity was also observed. It was suggested that methane was produced through hydrogenotrophic methanogenesis from the hydrogen that is formed through the fermentation of glucose. This implies that in this study the electrochemically active microorganisms in the anode chamber were not able to outcompete hydrogenotrophic methanogens when hydrogen was the substrate. It is not unlikely, however, that future research will be able to completely eliminate methanogenesis in the bioanode chamber. A strategy that could be investigated in this respect is to increase the anode potential in such a way that the electrochemically active microorganisms in the bioanode chamber get the competitive advantage with respect to the hydrogen oxidation.

Membrane. As described in Chapter 3, 4, 5 and the Intermezzo, there is a fundamental problem associated with the use of membranes in bioelectrochemical systems running on wastewater. Under the conditions for wastewater treatment (~pH 7) these membranes predominantly transport other ion species than protons and hydroxyl ions to maintain electroneutrality. As the cathode reaction is a proton consuming (or

hydroxyl ion producing) reaction, this transport of other ion species than protons and hydroxyl ions, causes a pH increase in the cathode chamber, which negatively affects the performance of the bioelectrochemical system.

The experiments have shown that in general the cathode pH rapidly increases to over 12. Unfortunately, every pH unit difference created in this way between anode and cathode chamber causes a potential loss of about 59 mV (i.e., an additional energy requirement of about 0.13 kWh/Nm³ H₂). This means that at an anode chamber pH of 7 and a cathode chamber pH of 12, an extra voltage of about 0.30 needs to be applied in order to compensate for the potential losses associated with the membrane pH gradient. As this increases the theoretical energy requirement of biocatalyzed electrolysis to about 0.9 kWh/Nm³ H₂, not much energy credit is left within the objective to compensate for other potential losses. Therefore, membrane pH gradients make it practically impossible to achieve the objective of 10 Nm³ H₂/m³ reactor volume/day at an energy input of below 1 kWh/Nm³ H₂ in full scale bioelectrochemical reactors and are important to address in future biocatalyzed electrolysis research.

In Chapter 4, 5 and the Intermezzo it was shown that the choice of membrane type influences the severity of membrane pH gradients to some extent, but never completely solves the problem of the membrane pH gradients. From a theoretical point of view, the only true solution to completely eliminate the membrane pH gradients increase in a conventional configuration is the application of an ion exchange membrane that is 100% permselective for protons or hydroxyl ions. However, these types of membranes do not exist (yet) for application in bioelectrochemical systems.

At some industrial sites a more practical solution to the membrane pH gradients would be to use onsite acidic wastewater streams that need neutralization. This wastewater could first pass the cathode chamber of a bioelectrochemical treatment system before discharge or further treatment. If this wastewater stream is very acidic, the membrane pH gradient could even go the other way around (i.e., lower pH at the cathode than at the anode), which would even lower the theoretically applied voltage by utilizing the chemical energy stored in the acidic stream (Intermezzo). Unfortunately,

this solution has only a limited applicability as it only works when acidic wastewater streams are indeed available.

Membrane-less operation, on the other hand, might be solution for the membrane pH gradients with broader applicability. In the Intermezzo we have seen that without convection (Intermezzo - Equation 2), cathode chamber pH increase is inevitable. Membrane-less operation, however, makes it possible to introduce convection into the system (Intermezzo - Equation 1). With convection (e.g., mixing) it is possible to eliminate (part of) the pH increase due to proton consumption (or hydroxyl ion production) at the cathode by using pH decrease due to proton production (or hydroxyl ion consumption) at the anode. Electrolytic processes, such as biocatalyzed electrolysis, are particularly suitable for membrane-less operation as the difference between an anode and a cathode in a biocatalyzed electrolysis system is determined by the direction of the applied voltage. This is in contrast with MFC systems, where the local conditions determine which electrode is the anode (anaerobic) and which electrode is the cathode (aerobic).

Membrane-less operation would also offer a cost advantage by eliminating one of the most expensive parts of the biocatalyzed electrolysis system (Paragraph 7.4.1). In principle, membrane-less operation should therefore be feasible. However, there are three important drawbacks that could limit the applicability of membrane-less operation: (i) the advantage of a pure product gas is lost as the hydrogen can become polluted with gaseous metabolic products from the anode chamber (e.g., CO₂, CH₄, H₂S), (ii) the risk of current cycling, i.e., hydrogen is produced at the cathode and subsequently oxidized again at the anode, and (iii) the risk of hydrogen loss through hydrogenotrophic methanogenesis. The impact of these drawbacks needs to be investigated in membrane-less configurations and compared to the negative effects of membrane pH gradients in conventional configurations. It is possible that with proper design and operation the impact of these drawbacks can be reduced to acceptable levels.

Cathode. Most biocatalyzed electrolysis studies up till now have applied platinum as the electrocatalyst for cathodic hydrogen production. Theoretically, platinum is one of most efficient electrocatalysts for cathodic

hydrogen production. Nonetheless, the experiments presented in Chapter 2 (Figure 2.3) showed that the platinum catalyzed cathode in the biocatalyzed electrolysis system suffered more potential losses than the bioanode (graphite felt). This was unexpected as cathodic hydrogen production is theoretically a much simpler electrochemical reaction than acetate oxidation. The cathode potential loss in Chapter 2 was found to be already 0.28 V at a current density of only 0.5 A/m². However, to achieve the objective of 10 Nm³ H₂/m³ reactor volume/day at an energy input of below 1 kWh/Nm³ H₂, the performance of the cathode will have to improve to about 5 to 10 A/m² at much lower overpotentials ($\sim < 0.10$ V).

Furthermore, as platinum is already expensive for application in conventional electrochemical systems (e.g., water electrolyzers) with current densities about 3 to 5 orders of magnitude higher than those in biocatalyzed electrolysis systems, application of platinum for biocatalyzed electrolysis is not likely to result in an economically feasible process design (Paragraph 7.4.1). To improve the performance and economic feasibility of biocatalyzed electrolysis, therefore, platinum needs to be replaced by alternative electrocatalysts for cathodic hydrogen production. Two strategies can be explored in this perspective: (i) alternative inexpensive chemical electrocatalysts, and (ii) microbial biocathodes (Chapter 6).

With respect to the first strategy many alternative inexpensive chemical electrocatalysts need to be investigated as not much is currently known about cathodic hydrogen production at near neutral pH (36). It seems most likely that at near neutral pH, hydrogen is not produced through proton reduction, but through water reduction (36). According to literature the transition metals Fe and Ni are interesting electrocatalysts for catalyzing water reduction under alkaline conditions and are much less expensive than platinum (37). These metals (and many other materials), therefore, might prove to be interesting alternatives to platinum for the cathode of biocatalyzed electrolysis. Further, as single chamber operation offers possible advantages with respect to the optimization of the volumetric hydrogen production (Chapter 5), it would be interesting to also investigate whether these alternatives are suitable for application into membrane electrode assemblies (MEAs).

The second strategy for improvement of the cathode performance, i.e. microbial biocathodes, can be even more interesting than the development of alternative inexpensive chemical electrocatalysts as it implies that also the cathode can consist of inexpensive graphite. The feasibility of microbial biocathodes for hydrogen production was recently demonstrated in our laboratories (Chapter 6). The preliminary results with these microbial biocathodes are promising as they exhibit lower overpotentials than a platinum coated titanium electrode that was used in previous experiments (18). More research will be required to improve the performance of the microbial biocathode to the level that it can be incorporated into a system that is able to meet the objective to produce over 10 Nm³ H₂/m³ reactor volume/day at an energy input of below 1 kWh/Nm³ H₂. At this stage, however, there is no reason to assume that future microbial biocathodes will not be able to perform as well as bioanodes with respect to current densities and overpotentials.

As the hydrogen producing microbial biocathode is a completely new development within biocatalyzed electrolysis research, not much is known yet about the involved electrochemically active microorganisms. To further improve the performance of microbial biocathodes it is interesting, therefore, to investigate which species of microorganisms are present, which electron transfer mechanisms are involved, how these microorganisms generate metabolic energy, etc. Furthermore, it is important to take into account the risk of hydrogenotrophic methanogenesis when working with microbial biocathodes. By consuming the hydrogen product in the cathode chamber hydrogenotrophic methanogenesis can significantly reduce the overall hydrogen yield of biocatalyzed electrolysis. Therefore, research to develop strategies for preventing hydrogenotrophic methanogenesis in microbial biocathode chambers will be important for achieving high hydrogen recoveries. Such strategies could include operation under carbon dioxide limited conditions (Chapter 6), operation at short solid retention times, or operation at low pH (38,39).

7.5 To summarize, ...

Biocatalyzed electrolysis is a promising technology for hydrogen production from wastewaters with a wide range of possible applications in wastewater treatment, transportation, and industry. The principle of the biocatalyzed electrolysis concept is proven, but performance needs to be improved. It is expected that volumetric hydrogen production rates can be improved to over 10 Nm³ H₂/m³ reactor volume/day at an energy input of below 1 kWh/Nm³ H₂ by improving the performance of the critical biocatalyzed electrolysis system components (bioanode, membrane, and cathode). However, to get to a mature hydrogen production technology, it is also important to realize a cost-effective scale-up that considers ohmic losses and material costs.

7.6 References

- (1) Logan, B. E.; Hamelers, B.; Rozendal, R.; Schröder, U.; Keller, J.; Freguia, S.; Aelterman, P.; Verstraete, W.; Rabaey, K. Microbial fuel cells: methodology and technology. *Environ. Sci. Technol.* **2006**, *40*, 5181-5192.
- (2) Rabaey, K.; Lissens, G.; Siciliano, S. D.; Verstraete, W. A microbial fuel cell capable of converting glucose to electricity at high rate and efficiency. *Biotechnol. Lett.* **2003**, *25*, 1531-1535.
- (3) Rabaey, K.; Ossieur, W.; Verhaege, M.; Verstraete, W. Continuous microbial fuel cells convert carbohydrates to electricity. *Water Sci. Technol.* **2005**, *52*, 515-523.
- (4) Freguia, S.; Rabaey, K.; Yuan, Z. G.; Keller, J. Electron and carbon balances in microbial fuel cells reveal temporary bacterial storage behavior during electricity generation. *Environ. Sci. Technol.* **2007**, *41*, 2915-2921.
- (5) Liu, H.; Cheng, S. A.; Logan, B. E. Production of electricity from acetate or butyrate using a single-chamber microbial fuel cell. *Environ. Sci. Technol.* **2005**, *39*, 658-662.
- (6) Heilmann, J.; Logan, B. E. Production of electricity from proteins using a single chamber microbial fuel cell. *Water Environ. Res.* **2006**, *78*, 531-537.
- (7) Paques bv. <http://www.paques.nl/>.
- (8) Thauer, R. K.; Shima, S. Biogeochemistry - Methane and microbes. *Nature* **2006**, *440*, 878-879.
- (9) International Energy Agency, 2004. World Energy Outlook 2004. Paris, France.
- (10) Schlappbach, L.; Zuttel, A. Hydrogen-storage materials for mobile applications. *Nature* **2001**, *414*, 353-358.
- (11) Statistics Netherlands (CBS). <http://www.cbs.nl/en/>.

- (12) Mulder, G.; Hetland, J.; Lenaers, G. Towards a sustainable hydrogen economy: Hydrogen pathways and infrastructure. *Int. J. Hydrogen Energy* **2007**, *32*, 1324.
- (13) Christen, K. Europe's CUTE project for hydrogen-fuel-cell buses deemed a success. *Environ. Sci. Technol.* **2006**, *40*, 4541-U4541.
- (14) Jacobson, M. Z.; Colella, W. G.; Golden, D. M. Cleaning the air and improving health with hydrogen fuel-cell vehicles. *Science* **2005**, *308*, 1901-1905.
- (15) Stoll, R. E.; von Linde, F. Hydrogen - what are the costs? *Hydrocarb. Process.* **2000**, *79*, 42-46.
- (16) Platform Nieuw Gas, 2006. Waterstof: brandstof voor transitie. The Netherlands.
- (17) Liu, H.; Grot, S.; Logan, B. E. Electrochemically assisted microbial production of hydrogen from acetate. *Environ. Sci. Technol.* **2005**, *39*, 4317-4320.
- (18) Rozendal, R. A.; Hamelers, H. V. M.; Euverink, G. J. W.; Metz, S. J.; Buisman, C. J. N. Principle and perspectives of hydrogen production through biocatalyzed electrolysis. *Int. J. Hydrogen Energy* **2006**, *31*, 1632-1640.
- (19) Rozendal, R. A.; Hamelers, H. V. M.; Molenkamp, R. J.; Buisman, C. J. N. Performance of single chamber biocatalyzed electrolysis with different types of ion exchange membranes. *Water Res.* **2007**, *41*, 1984-1994.
- (20) Ditzig, J.; Liu, H.; Logan, B. E. Production of hydrogen from domestic wastewater using a bioelectrochemically assisted microbial reactor (BEAMR). *Int. J. Hydrogen Energy* **2007**, *32*, 2296-2304.
- (21) Logan, B. E.; Liu, H., Pennsylvania State University (Dept. of Civil and Environmental Engineering), USA. Personal communication, **2007**.
- (22) Hawkes, F. R.; Hussy, I.; Kyazze, G.; Dinsdale, R.; Hawkes, D. L. Continuous dark fermentative hydrogen production by mesophilic microflora: Principles and progress. *Int. J. Hydrogen Energy* **2007**, *32*, 172-184.
- (23) Li, C. L.; Fang, H. H. P. Fermentative hydrogen production from wastewater and solid wastes by mixed cultures. *Crit. Rev. Environ. Sci. Technol.* **2007**, *37*, 1-39.
- (24) Tchobanoglous, G.; Burton, F. L.; Stensel, H. D. *Wastewater engineering: treatment and reuse*; 3rd ed.; Metcalf & Eddy, McGraw-Hill: New York, 2003.
- (25) Logan, B. E. Extracting hydrogen and electricity from renewable resources. *Environ. Sci. Technol.* **2004**, *38*, 160a-167a.
- (26) Turner, J. A. Sustainable hydrogen production. *Science* **2004**, *305*, 972-974.
- (27) Larminie, J.; Dicks, A. *Fuel cell systems explained*; John Wiley & Sons: Chichester, 2000.
- (28) Hoogers, G., Ed. *Fuel cell technology handbook*; CRC Press: Boca Raton, FL, 2003.
- (29) Aelterman, P.; Rabaey, K.; Pham, T. H.; Boon, N.; Verstraete, W. Continuous electricity generation at high voltages and currents using stacked microbial fuel cells. *Environ. Sci. Technol.* **2006**, *40*, 3388-3394.
- (30) Tayhas, G.; Palmore, R. Bioelectric power generation. *Trends Biotechnol.* **2004**, *22*, 99-100.

- (31) Rabaey, K.; Verstraete, W. Microbial fuel cells: novel biotechnology for energy generation. *Trends Biotechnol.* **2005**, *23*, 291-298.
- (32) Ter Heijne, A.; Hamelers, H. V. M.; Buisman, C. J. N. Microbial fuel cell operation with continuous biological ferrous iron oxidation of the catholyte. *Environ. Sci. Technol.* **2007**, *41*, 4130-4134.
- (33) Logan, B. E.; Regan, J. M. Electricity-producing bacterial communities in microbial fuel cells. *Trends Microbiol.* **2006**, *14*, 512-518.
- (34) Gorby, Y. A.; Yanina, S.; McLean, J. S.; Rosso, K. M.; Moyles, D.; Dohnalkova, A.; Beveridge, T. J.; Chang, I. S.; Kim, B. H.; Kim, K. S.; Culley, D. E.; Reed, S. B.; Romine, M. F.; Saffarini, D. A.; Hill, E. A.; Shi, L.; Elias, D. A.; Kennedy, D. W.; Pinchuk, G.; Watanabe, K.; Ishii, S.; Logan, B.; Nealson, K. H.; Fredrickson, J. K. Electrically conductive bacterial nanowires produced by *Shewanella oneidensis* strain MR-1 and other microorganisms. *PNAS* **2006**, *103*, 11358-11363.
- (35) Reguera, G.; McCarthy, K. D.; Mehta, T.; Nicoll, J. S.; Tuominen, M. T.; Lovley, D. R. Extracellular electron transfer via microbial nanowires. *Nature* **2005**, *435*, 1098-1101.
- (36) Andersen, T. N.; Dandapani, B. S.; Berry, J. M. Hydrogen evolution studies in neutral media. *J. Electroanal. Chem.* **1993**, *357*, 77-89.
- (37) Tilak, B. V.; Ramamurthy, A. C.; Conway, B. E. High performance electrode materials for the hydrogen evolution reaction from alkaline media. *Proc. Indian Acad. Sci. (Chem. Sci.)* **1986**, *97*, 359-393.
- (38) Hawkes, F. R.; Dinsdale, R.; Hawkes, D. L.; Hussy, I. Sustainable fermentative hydrogen production: challenges for process optimisation. *Int. J. Hydrogen Energy* **2002**, *27*, 1339-1347.
- (39) Kim, I. S.; Hwang, M. H.; Jang, N. J.; Hyun, S. H.; Lee, S. T. Effect of low pH on the activity of hydrogen utilizing methanogen in bio-hydrogen process. *Int. J. Hydrogen Energy* **2004**, *29*, 1133-1140.

*Summary/
Samenvatting*

S



Summary

Hydrogen production through biocatalyzed electrolysis

S

This PhD thesis describes the first steps in the development of a promising new technology for hydrogen production from wastewaters. This bioelectrochemical technology, referred to as biocatalyzed electrolysis, was invented and developed within this PhD project.

Up till now, many wastewaters were unsuitable for biological hydrogen production due to the slightly endothermic nature of many of the involved reactions. Biocatalyzed electrolysis, however, is capable of overcoming this thermodynamic barrier through the application of electrochemically active microorganisms in combination with a small input of electrical energy. Electrochemically active microorganisms are capable of using an electrode as an electron acceptor for the oxidation of organic matter. This turns the electrode into a bioanode. Biocatalyzed electrolysis couples this bioanode to a conventional proton reducing cathode by means of a power supply. Consequently, the organic matter is electrolyzed and hydrogen is generated.

The theoretically required applied voltage for biocatalyzed electrolysis of organic material is about 0.12 V, which equals a theoretical energy requirement of about 0.26 kWh/Nm³ H₂. Microbial metabolic losses and other potential losses (e.g., ohmic loss and electrode overpotentials) will increase this energy requirement under practical conditions, but the energy requirement of biocatalyzed electrolysis is expected to remain far below that of commercial water electrolysis (4.4 to 5.4 kWh/Nm³ H₂).

As biocatalyzed electrolysis is a new technology, **Chapter 2** describes the “proof of principle” of biocatalyzed electrolysis by demonstrating the process with acetate as a model substrate. At an applied voltage of 0.5 V about 0.02 Nm³ H₂/m³ reactor liquid volume/day is produced from acetate at an overall hydrogen efficiency of 53±3.5%. The most important bottlenecks that have limited this performance are cell design, diffusional

loss of hydrogen from the cathode to the anode chamber, and potential losses associated with the cathode reaction.

Another bottleneck of the system has been identified in **Chapter 3**. This chapter discusses the operational problems associated with the application of cation exchange membranes in bioelectrochemical systems operated on wastewater. This is illustrated in an microbial fuel cell system with Nafion® as an example membrane. In contrast to what was generally assumed by most researchers, the experiments show that cation exchange membranes in bioelectrochemical systems operated on wastewater transport significant amounts of other cation species (Na^+ , K^+ , NH_4^+ , Ca^{2+} , and Mg^{2+}) than protons, because the concentrations of these other cation species are typically 10^5 times higher than the proton concentration. As the cathode reactions of both microbial fuel cell and biocatalyzed electrolysis systems consume protons equimolarly with electrons, the transport of cation species other than protons causes a significant pH increase in the cathode chamber. This pH increase in the cathode chamber creates a pH gradient across the membrane, which negatively affects the performance of bioelectrochemical systems. For every pH unit difference created in this way between the anode and the cathode chamber a potential loss of about 59 mV is suffered. For biocatalyzed electrolysis this causes an additional energy requirement of about 0.13 kWh/Nm³ H₂ per pH unit.

To prevent these membrane pH gradient associated potential losses, therefore, we have evaluated the possibilities of using alternative types of ion exchange membranes in **Chapter 4**. Four types of ion exchange membranes have been tested in a biocatalyzed electrolysis configuration: (i) a cation exchange membrane (CEM), (ii) an anion exchange membrane (AEM), (iii) a bipolar membrane (BPM), and (iv) a charge mosaic membrane (CMM). With respect to the electrochemical performance of the four biocatalyzed electrolysis configurations, the ion exchange membranes are rated in the order AEM > CEM > CMM > BPM. However, with respect to the transport numbers for protons and/or hydroxyl ions ($t_{\text{H/OH}}$) and the ability to prevent pH increase in the cathode chamber, the ion exchange membranes are rated in the order BPM > AEM > CMM > CEM. Unfortunately, none of the alternative types of ion exchange membranes are

capable of completely eliminating the pH increase in the cathode chamber. Typically, the cathode pH increases to above 12, which increases the theoretical energy requirement of biocatalyzed electrolysis from 0.26 to above 0.89 kWh/Nm³ H₂ (at an anode pH of 7).

Chapter 5 shows that biocatalyzed electrolysis can also be operated with one liquid chamber instead of two by producing hydrogen gas directly in the gas phase. This single chamber operation has possible advantages with respect to system volume, which can improve volumetric hydrogen production. Single chamber biocatalyzed electrolysis was tested in two configurations: (i) with a cation exchange membrane (CEM) and (ii) with an anion exchange membrane (AEM). Both configurations performed comparably and produced over 0.3 Nm³ H₂/m³ reactor liquid volume/day at 1.0 V applied voltage (overall hydrogen efficiencies around 23%). Analysis of the water that permeated through the membrane during operation of the configurations revealed that a large part of potential losses in the system were associated with a pH gradient across the membrane (CEM $\Delta\text{pH}=6.4$; AEM $\Delta\text{pH}=4.4$). These pH gradient associated potential losses were lower in the AEM than in the CEM configuration (CEM 0.38 V; AEM 0.26 V) as a result of its alternative ion transport properties. This benefit of the AEM, however, was counteracted by the higher cathode overpotentials occurring in the AEM configuration (CEM 0.12 V at 2.39 A/m²; AEM 0.27 V at 2.15 A/m²) as a result of a lower effectiveness of the electroless plating method that was used for the AEM membrane electrode assembly (MEA).

Cathode pH effects were observed in all the experiments of **Chapter 3, 4, and 5**, which seems to imply that the observed pH effects are inherent to the use of membranes in bioelectrochemical systems that are running on wastewater. This hypothesis has been investigated in the **Intermezzo** on the basis of the Nernst-Planck flux equation. Without assuming anything about the type of membrane, the Nernst-Planck flux equation indeed predicts that the observed pH effects are inherent to the use of membranes in bioelectrochemical systems that are running on wastewater.

Chapter 6 for the first time describes the development of a microbial biocathode for hydrogen production that is based on a naturally selected mixed culture of electrochemically active microorganisms. Microbial

biocathodes are interesting for application in biocatalyzed electrolysis systems as they are based on inexpensive electrode materials (e.g., graphite) and a self-regenerating catalyst (i.e., the microorganisms). Our microbial biocathode system was established through a three phase biocathode start up procedure that effectively turned an acetate and hydrogen oxidizing bioanode into a hydrogen producing biocathode by reversing the polarity of the electrode. The microbial biocathode that was obtained in this way had a current density of about -1.1 A/m^2 at a potential of -0.7 V . This was 3.6 times higher than that of a graphite control electrode (-0.3 A/m^2) and 2.4 times higher than that of the platinum coated titanium electrode (-0.47 A/m^2) used in **Chapter 2**. Furthermore, the microbial biocathode produced about $0.63 \text{ Nm}^3 \text{ H}_2/\text{m}^3 \text{ cathode liquid volume/day}$ at a cathodic hydrogen efficiency of 49% during hydrogen yield tests, whereas the graphite control electrode produced $0.08 \text{ Nm}^3 \text{ H}_2/\text{m}^3 \text{ cathode liquid volume/day}$ at a cathodic hydrogen efficiency of 25%.

Finally, **Chapter 7** discusses the status and the future potential of biocatalyzed electrolysis. Biocatalyzed electrolysis is a promising technology for hydrogen production from wastewater with a wide range of possible applications in wastewater treatment, transportation, and industry. The principle of the biocatalyzed electrolysis concept is proven, but performance needs to be improved. It is expected that volumetric hydrogen production rates can be improved to over $10 \text{ Nm}^3 \text{ H}_2/\text{m}^3 \text{ reactor volume/day}$ at an energy input of below $1 \text{ kWh/Nm}^3 \text{ H}_2$ by improving the performance of the critical biocatalyzed electrolysis system components (bioanode, membrane, and cathode). However, to get to a mature hydrogen production technology, it is also important to realize a cost-effective scale-up that considers ohmic losses and material costs.

Samenvatting

Waterstof productie d.m.v. biogekatalyseerde elektrolyse



Dit proefschrift beschrijft de eerste stappen in de ontwikkeling van een veelbelovende technologie voor de productie van waterstof uit afvalwater. Deze bio-elektrochemische technologie, biogekatalyseerde elektrolyse genaamd, is uitgevonden en ontwikkeld binnen dit promotieproject.

Tot nu toe waren veel soorten afvalwater ongeschikt voor de biologische waterstofproductie door het licht endothermische karakter van veel van de betrokken reacties. Biogekatalyseerde elektrolyse is echter in staat deze thermodynamische barrières te overwinnen door het toepassen van elektrochemisch actieve micro-organismen gecombineerd met het toevoeren van een kleine hoeveelheid elektrische energie. Elektrochemisch actieve micro-organismen zijn in staat om een elektrode te gebruiken als elektronenacceptor voor het oxideren van organisch materiaal. Dit maakt van deze elektrode een bioanode. Door middel van een vermogensbron koppelt biogekatalyseerde elektrolyse deze bioanode aan een conventionele protonreducerende kathode. Hierdoor wordt het organisch materiaal geëlektrolyseerd en waterstof gegenereerd.

Het theoretisch benodigde voltage voor biogekatalyseerde elektrolyse is ongeveer 0.12 V. Dit komt overeen met een theoretisch energieverbruik van ongeveer 0.26 kWh/Nm³ H₂. Onder praktische omstandigheden zullen microbiële metabolische verliezen en andere potentiaalverliezen (bijv. ohmse verliezen en elektrode overpotentialen) dit energieverbruik enigszins verhogen, maar het is de verwachting dat het energieverbruik van biogekatalyseerde elektrolyse ver onder dat van commerciële waterelektrolyse zal blijven (4.4. tot 5.4 kWh/Nm³ H₂).

Omdat biogekatalyseerde elektrolyse een nieuwe technologie is, beschrijft **Hoofdstuk 2** de “proof of principle” van biogekatalyseerde elektrolyse door het proces te demonstreren met acetaat als modelsubstraat.

Bij een aangelegd voltage van 0.5 V werd vanuit acetaat ongeveer 0.02 Nm³ H₂/m³ reactor vloeistofvolume/dag geproduceerd met een overall waterstofefficiency van 53±3.5%. De meest belangrijk knelpunten die deze prestatie limiteerden, zijn het celontwerp, diffusioneel verlies van waterstof vanuit het kathode- naar het anodecompartiment en potentiaalverliezen in de kathodereactie.

Nog een ander knelpunt van het systeem werd geïdentificeerd in **Hoofdstuk 3**. Dit hoofdstuk bediscussieert de operationele problemen die voortkomen uit het gebruik van kation uitwisselingsmembranen in bio-elektrochemische systemen die op afvalwater werken. Dit werd geïllustreerd aan de hand van een microbiële brandstofcel met Nafion® als voorbeeldmembraan. In tegenstelling tot wat algemeen werd aangenomen door de meeste onderzoekers, lieten de experimenten zien dat kation uitwisselingsmembranen in bio-elektrochemische systemen die op afvalwater werken significante hoeveelheden andere soorten kationen (Na⁺, K⁺, NH₄⁺, Ca²⁺ en Mg²⁺) dan protonen transporteren, doordat de concentraties van deze andere soorten kationen typisch 10⁵ keer hoger zijn dan de protonconcentratie. Omdat de kathodereacties van zowel de microbiële brandstofcel als biogekatalyseerde elektrolyse protonen equimolair consumeren met elektronen, veroorzaakt het transport van andere soorten kationen dan protonen een significante pH verhoging in het kathodecompartiment. Deze pH verhoging in het kathodecompartiment veroorzaakt een pH gradiënt over het membraan, die de prestatie van bio-elektrochemische systemen negatief beïnvloedt. Voor elke pH eenheid verschil tussen het anode- en het kathodecompartiment die op deze manier tot stand komt, wordt een verlies van ongeveer 59 mV geleden. Voor biogekatalyseerde elektrolyse veroorzaakt dit een additioneel energieverbruik van ongeveer 0.13 kWh/Nm³ H₂ per pH eenheid.

Om deze, aan de membraan pH gradiënt gerelateerde, potentiaalverliezen te voorkomen, hebben we de mogelijkheden van alternatieve soorten ion uitwisselingsmembranen onderzocht in **Hoofdstuk 4**. Vier soorten ion uitwisselingsmembranen zijn getest in een biogekatalyseerde elektrolyse configuratie: (i) een kation uitwisselingsmembraan (CEM), (ii) een anion uitwisselingsmembraan

(AEM), (iii) een bipolair membraan (BPM) en (iv) een “charge mosaic” membraan (CMM). Met betrekking tot de elektrochemische prestatie van de vier biogekatalyseerde elektrolyse configuraties, kunnen de ion uitwisselingsmembranen worden gerangschikt in de volgorde AEM > CEM > CMM > BPM. Echter, met betrekking tot de transportgetallen van protonen en/of hydroxyl ionen ($t_{H/OH}$) en het vermogen van de membranen om pH verhoging in het kathodecompartiment te voorkomen, kunnen de ion uitwisselingsmembranen worden gerangschikt in de volgorde BPM > AEM > CMM > CEM. Helaas was geen van de alternatieve soorten ion uitwisselingsmembranen in staat om de pH verhoging in het kathodecompartiment compleet te elimineren. De kathode pH stijgt typisch tot boven de pH 12. Dit betekent dat het theoretisch energieverbruik van biogekatalyseerde elektrolyse stijgt van 0.26 naar boven de 0.89 kWh/Nm³ H₂ (bij een anode pH van 7).

Hoofdstuk 5 toont aan dat biogekatalyseerde elektrolyse ook bedreven kan worden met één i.p.v. twee vloeistofcompartimenten door de waterstof direct in de gasfase te produceren. Deze manier van bedrijven heeft mogelijke voordelen met betrekking tot het systeemvolume, zodat de volumetrische waterstofproductie verbeterd kan worden. Biogekatalyseerde elektrolyse met één vloeistofcompartiment is getest in twee configuraties: (i) met een kation uitwisselingsmembraan (CEM) en (ii) met een anion uitwisselingsmembraan (AEM). Beide configuraties presteerden vergelijkbaar en produceerden meer dan 0.3 Nm³ H₂/m³ reactor vloeistofvolume/dag (overall waterstofefficiency 23%) bij een aangelegd voltage van 1.0 V. Analyse van het water dat gedurende het bedrijf van de configuraties door het membraan heen drong, wees uit dat een groot gedeelte van de potentiaalverliezen in het systeem verband hielden met een pH gradiënt over het membraan (CEM $\Delta pH=6.4$; AEM $\Delta pH=4.4$). Deze, aan de membraan pH gradiënt gerelateerde, potentiaalverliezen waren lager in de AEM dan in de CEM configuratie (CEM 0.38 V; AEM 0.26 V) vanwege de alternatieve ion transporteigenschappen. Dit voordeel van de AEM werd echter teniet gedaan door de hogere kathode overpotentialen die voorkwamen in de AEM configuratie (CEM 0.12 V bij 2.39 A/m²; AEM 0.27 V bij 2.15 A/m²). Deze hogere kathode overpotentialen werden veroorzaakt

door een lagere effectiviteit van de “electroless plating” procedure die gebruikt was voor de AEM “membrane electrode assembly” (MEA).

Kathode pH effecten werden waargenomen in alle experimenten van **Hoofdstuk 3, 4 en 5**. Dit lijkt te impliceren dat deze waargenomen pH effecten inherent zijn aan het gebruik van membranen in bio-elektrochemische systemen die op afvalwater werken. In het **Intermezzo** is deze hypothese onderzocht op basis van de Nernst-Planck flux vergelijking. Zonder enige aanname te doen over het type membraan voorspelt de Nernst-Planck flux vergelijking inderdaad dat de waargenomen pH effecten inherent zijn aan het gebruik van membranen in bio-elektrochemische systemen die op afvalwater werken.

Hoofdstuk 6 beschrijft voor de eerste keer de ontwikkeling van een microbiële biokathode voor waterstofproductie die werkt op basis van natuurlijk geselecteerde mengcultures van elektrochemisch actieve micro-organismen. Microbiële biokathodes zijn interessant voor toepassing in biogekatalyseerde elektrolyse systemen, omdat ze gebaseerd zijn op goedkope elektrodematerialen (bijv. grafiet) en een zichzelf regenerende katalysator (d.w.z. de micro-organismen). Ons microbiële biokathode systeem werd bewerkstelligd door een drie-fase biokathode opstartprocedure, die op effectieve wijze een acetaat en waterstof oxiderende bioanode veranderde in een waterstofproducerende biokathode door de polariteit van de elektrode om te keren. De microbiële biokathode die op deze manier verkregen werd, had een stroomdichtheid van ongeveer -1.1 A/m^2 bij een potentiaal van -0.7 V . Dit was 3.6 maal hoger dan die van een grafiet controle-elektrode (-0.3 A/m^2) en 2.4 maal hoger dan die van de platina gecoate titanium elektrode (-0.47 A/m^2) die gebruikt is in **Hoofdstuk 2**. Verder produceerde de microbiële biokathode gedurende waterstof opbrengstproeven ongeveer $0.63 \text{ Nm}^3 \text{ H}_2/\text{m}^3 \text{ kathode vloeistofvolume/dag}$ bij een kathodische waterstofefficiency van 49%, terwijl de grafiet controle-elektrode $0.08 \text{ Nm}^3 \text{ H}_2/\text{m}^3 \text{ kathode vloeistofvolume/dag}$ produceerde bij een kathodische waterstofefficiency van 25%.

Ten slotte is in **Hoofdstuk 7** de status en het toekomstige potentieel van biogekatalyseerde elektrolyse bediscussieerd. Biogekatalyseerde elektrolyse is een veelbelovende technologie voor de productie van waterstof

uit afvalwater met een breed scala aan mogelijke toepassingen op gebied van afvalwaterzuivering, transport en industrie. Het principe van biogekatalyseerde elektrolyse is bewezen, maar de prestatie moet nog worden verbeterd. Het is de verwachting dat de volumetrische waterstofproductie kan worden verbeterd naar meer dan $10 \text{ Nm}^3 \text{ H}_2/\text{m}^3$ reactor vloeistofvolume/dag bij een energieverbruik van minder dan $1 \text{ kWh}/\text{Nm}^3 \text{ H}_2$ door de prestatie van de essentiële biogekatalyseerde elektrolyse systeemonderdelen (bioanode, membraan en kathode) te verbeteren. Echter, om inderdaad tot een volwassen waterstofproductie technologie te kunnen komen, dient ook een kosteneffectieve opschaling van de technologie gerealiseerd te worden die rekening houdt met zowel de ohmse verliezen als de materiaalkosten.

Dankwoord/Acknowledgments

Daar staan we dan vier jaar later met alleen nog het dankwoord te schrijven. Het gevaarlijkste stukje schrijfwerk van het hele proefschrift, want stel dat je iemand vergeet... En er zijn zoveel mensen te bedanken dat ik haast wel mensen moet gaan vergeten. Om zo weinig mogelijk mensen daadwerkelijk te vergeten, zal ik proberen chronologisch door de afgelopen vier jaar heen te gaan, te beginnen bij Cees Buisman. Zonder jouw inspirerende gesprek tijdens een lunchwandeling bij Paques bv ergens in de eerste helft van 2003, was ik überhaupt nooit aan promotieonderzoek begonnen. Gedurende dat kleine halfuurtje is de kiem gelegd voor dit proefschrift. Kort na dit gesprek kwam het biogekatalyseerde elektrolyse proces tot mij in een soort “*Eureka!*” moment. Vanaf dat allereerste begin heb je mij de ruimte gegeven en mij gestimuleerd dit nieuwe, nog onbekende proces te onderzoeken. Bedankt daarvoor!

Zelfs nog voordat ik echt begonnen was op de vakgroep, maakte ik al kennis met Bert Hamelers toen hij mij hielp bij het aanvragen van subsidies voor biogekatalyseerde elektrolyse. Sindsdien is hij betrokken gebleven als dagelijks begeleider. Bert, mede door jou als continue, kritische sparringpartner heeft dit proefschrift de kwaliteit gekregen waar ik naar streefde. Verder waardeer ik in jou de eigenschap dat jij, hoe druk je het ook hebt, altijd ook tijd maakt voor een goed gesprek over andere dan strikt werkgerelateerde zaken. Ook deze gesprekken heb ik altijd als zeer inspirerend ervaren.

Toen ik uiteindelijk daadwerkelijk aan het onderzoek begon, heb ik eerst ruim een half jaar op de Milieutechnologie vakgroep in Wageningen rondgelopen. Dit was een aangename tijd voor mij en daarvoor wil ik iedereen van de vakgroep bedanken. Van al deze mensen wil ik speciaal Pim nog even noemen. In ons studentenappartement in Sneek hebben we elkaar uiteindelijk overtuigd te gaan promoveren; een beslissing waar ik (en ik hoop ook jij) geen spijt van heb gekregen. En natuurlijk bedank ik in het bijzonder nog Liesbeth, Anita en Gusta, die ik vanuit Leeuwarden regelmatig bestookte met “vraagjes”. Als laatste zou ik de Wageningse leden van de Bio-energie groep nog even apart willen noemen. Naast Bert zijn dat Annemiek, David, Kirsten en Vinnie. Bedankt voor de inspirerende bijeenkomsten!

Na mijn Wageningse periode vertrok ik naar Leeuwarden om het onderzoek voort te zetten bij het kersverse onderzoeksinstituut Wetsus. Daar is het werk eigenlijk pas echt goed van start gegaan. Dit werk was zonder de hulp van vele Wetsianen niet mogelijk geweest, te beginnen met Johannes, die samen met Cees het instituut gebracht heeft tot waar het nu staat: een onderzoeksinstituut van wereldklasse! In het bijzonder bedank ik in deze context natuurlijk ook de groep mensen die onmisbaar zijn (of zijn

geweest) voor de opbouw van Wetsus en het optimaal functioneren van de experimenteerhal, het analytisch laboratorium, microscopie en de kantoren: Alcina, Arie, Bob, Janneke, Jelmer, Harm, Harrie, Helena, Marijke, Naomi, Trienke en Wim. Bedankt, zonder jullie hulp was dit allemaal echt onmogelijk geweest!

Verder bedank ik nog: Ellen, Guillo en Ronald voor het warme welkom en het wegwijs maken in het allereerste begin in Leeuwarden; Natasja en Petra voor de gezellige ritjes en de leerzame *Tips & Tricks* dineetjes; Perry en Maxime voor de incidentele slaapplek; Elsemiek, Gert-Jan, Jan (P.), Joost, Michel, Nienke, Piotr, Sybrand, Tom en Urania voor hun gedeelde interesse in energie zaken en Onder hen mijn kamergenoten voor de gezelligheid in de meest “Energieke” kamer van Wetsus; Heleen, Helena en Nelleke voor de uitzoekerij rondom het organiseren van een eerste verdediging in Leeuwarden; en alle hiervoor genoemde Wetsianen plus Agata, Albert, Aleid, Bart, Carien, Gerrit, Hans, Hardy, Geo, Hellen, Ingo, Jan (de G.), Kamuran, Loes, Lucia, Ludmila, Maarten, Manon, Marco, Marthe, Mateo, Nathalie, Nina, Nynke, Paula, Sandra, Tim en Walter voor hun ondersteuning, koffiepraatje, gezelligheid en vriendschap.

Dan bedank ik natuurlijk ook nog “mijn” studenten: Joel, Pei, Redmar, Emily en Adriaan, die mij veel werk uit handen namen en waarvan ik veel geleerd heb! Adriaan zal samen met Tom en Elsemiek het biogekatalyseerde elektrolyse onderzoek in het waterstof thema verder voort gaan zetten. Bizar om na al die tijd het biogekatalyseerde elektrolyse onderzoek uit handen te geven en los te laten... Gelukkig is dat aan deze drie zeer zeker toevertrouwd! Omdat Adriaan mij qua tijdsplanning zo’n beetje aflost (hij neemt zelfs mijn bureau over), vond ik het wel symbolisch om hem te vragen als mijn paranimf samen met Natasja. Hierbij bedank ik hen voor hun steun in voorbereiding van en tijdens de verdediging.

Verder zou ik graag alle aan Wetsus gelieerde bedrijven willen bedanken zonder welke Wetsus niet geworden zou zijn wat het nu is. In het bijzonder zou ik de bedrijven willen bedanken die het waterstof thema hebben mogelijk gemaakt: Shell (m.n. Leo Petrus† en Paul Ayoub), Magneto (m.n. Pieter Hack) en Paques (m.n. Ronald Mulder). Paques bedank ik ook voor het vertrouwen dat ze in mij getoond hebben door mij in de laatste acht maanden al voor één dag per week in dienst te nemen, zodat ik het bedrijfsleven alvast kon verkennen.

Wetenschappelijk gezien ben ik ook aan een aantal mensen dank verschuldigd. Allereerst aan Jan Gerritse en Jaap Koppejan van TNO, die mij in de pre-Wetsus periode binnen een EET project de fijne kneepjes van de MFC bijbrachten. Daarnaast zou ik Korneel Rabaey graag willen bedanken voor het feit dat hij ons introduceerde in de “MFC community” (www.microbialfuelcell.org). Via Korneel heb ik ook Bruce Logan voor het

eerst mogen ontmoeten, onze “concullega” die gelijktijdig met biogekatalyseerde elektrolyse het BEAMR proces ontwikkelde. Bruce, I guess we are tuned into the same wavelength as we keep getting the same ideas at the same time... Thanks for coming to my PhD defense and thanks for all the scientific discussions! Naast Bruce Logan zou ik ook de andere leden van mijn promotiecommissie willen bedanken: Ronald Mulder, Matthias Wessling en Fons Stams. De laatste bedank ik (samen met Jeanine Geelhoed) ook voor zijn betrokkenheid en wetenschappelijk inbreng in het waterstof thema.

Als laatste bedank ik vrienden en familieleden, die mij altijd door dik en dun gesteund hebben. Speciaal bedank ik nog mijn neef Henk-Jan, die de geweldige cover van dit proefschrift ontworpen heeft.

Als aller-laatste bedank ik in het bijzonder nog mijn ouders en mijn zusje Laura. Ik hou zielsveel van jullie en ik ben me er zeer van bewust dat jullie opvoeding, vertrouwen en liefde dit allemaal voor mij mogelijk hebben gemaakt.

Als aller-aller-laatste bedank ik Maartje, omdat ze er altijd voor me is. Ik hou onbeschrijfelijk veel van jou en samen kunnen we de hele wereld aan!

Curriculum Vitae



René Alexander Rozendal was born on December 18, 1978 in Utrecht (The Netherlands). In 1997 he finished his pre-university education (VWO) at the Cals College in Nieuwegein (The Netherlands). From 1997 until 2003 he studied (bio)chemical engineering at the Delft University of Technology (The Netherlands) and specialized in Environmental Biotechnology. He did his graduation work at Paques bv on a topic related to the Anammox process. After finishing his MSc (with honors) he started a PhD on microbial fuel cell technology at the Sub-Department of Environmental Technology of Wageningen University (The Netherlands). During this PhD research he invented and patented biocatalyzed electrolysis, a new bioelectrochemical technology for the production of hydrogen from wastewaters. The results of this PhD research are presented in this PhD thesis. During the last 10 months of his PhD he was employed one day per week as a process technologist at Paques bv.

List of publications

- (1) Rozendal, R. A.; Hamelers, H. V. M.; Euverink, G. J. W.; Metz, S. J.; Buisman, C. J. N. Principle and perspectives of hydrogen production through biocatalyzed electrolysis. *Int. J. Hydrogen Energy* **2006**, *31*, 1632-1640.
- (2) Rozendal, R. A.; Hamelers, H. V. M.; Buisman, C. J. N. Effects of membrane cation transport on pH and microbial fuel cell performance. *Environ. Sci. Technol.* **2006**, *40*, 5206-5211.
- (3) Ter Heijne, A.; Hamelers, H. V. M.; De Wilde, V.; Rozendal, R. A.; Buisman, C. J. N. A bipolar membrane combined with ferric iron reduction as an efficient cathode system in microbial fuel cells. *Environ. Sci. Technol.* **2006**, *40*, 5200-5205.
- (4) Logan, B. E.; Hamelers, B.; Rozendal, R.; Schröder, U.; Keller, J.; Freguia, S.; Aelterman, P.; Verstraete, W.; Rabaey, K. Microbial fuel cells: methodology and technology. *Environ. Sci. Technol.* **2006**, *40*, 5181-5192.
- (5) Rozendal, R. A.; Hamelers, H. V. M.; Molenkamp, R. J.; Buisman, C. J. N. Performance of single chamber biocatalyzed electrolysis with different types of ion exchange membranes. *Water Res.* **2007**, *41*, 1984-1994.
- (6) Rozendal, R. A.; Sleutels, T. H. J. A.; Hamelers, H. V. M.; Buisman, C. J. N. Effect of the type of ion exchange membrane on performance, ion transport, and pH in biocatalyzed electrolysis of wastewater. In: Proceedings of the 10th IWA World Congress on Anaerobic Digestion (AD11), Brisbane, Australia, September 23 - 27, 2007.
- (7) Rozendal, R. A.; Sleutels, T. H. J. A.; Hamelers, H. V. M.; Buisman, C. J. N. Effect of the type of ion exchange membrane on performance, ion transport, and pH in biocatalyzed electrolysis of wastewater. *Water Sci. Technol.* **2007**, *Submitted*.
- (8) Rozendal, R. A.; Jeremiasse, A. W.; Hamelers, H. V. M.; Buisman, C. J. N. Hydrogen production with a microbial biocathode. *Environ. Sci. Technol.* **2007**, *Submitted*.

List of patents

- (1) Rozendal, R. A.; Buisman, C. J. N. Process for producing hydrogen. **2005**, *Patent WO2005005981*.
- (2) Rozendal, R. A.; Hamelers, H.V.M.; Buisman, C. J. N.; Jeremiasse, A.W. Werkwijze voor het verkrijgen van een kathodofiele, waterstof producerende microbiële cultuur, microbiële cultuur verkregen met deze werkwijze en gebruik van deze microbiële cultuur. *Dutch patent application 1034123 (Filing date: July 12, 2007)*.



Netherlands Research School for the
Socio-Economic and Natural Sciences of the Environment

CERTIFICATE

The Netherlands Research School for the
Socio-Economic and Natural Sciences of the Environment
(SENSE), declares that

René Rozendal

Born on: *18 December 1978* at: *Utrecht, The Netherlands*

has successfully fulfilled all requirements of the
Educational Programme of SENSE.

Place: *Wageningen* Date: *24 October 2007*

the Chairman of the
SENSE board

Prof. dr. R. Leemans

the SENSE Director
of Education

Dr. C. Kroeze



The SENSE Research School declares that Mr. René Rozendal has successfully fulfilled all requirements of the Educational PhD Programme of SENSE with a work load of 30 ECTS, including the following activities:

SENSE PhD courses:

- Environmental Research in Context
- Research Context Activity: "Organizing an international expert meeting on 'Microbial Fuel Cells' (25 July 2006)"
- Dynamic Energy Budgets

Other PhD courses and activities:

- Techniques for Writing and Presenting a Scientific Paper
- Teaching and Supervising Thesis Students
- Site Specific Training: Labview Basic I, National Instruments B.V., January 2004, Woerden, The Netherlands
- Site Specific Training: Electroanalytical Techniques: Principles and Applications, June 2004, University of Bath, Bath, UK.

Oral Presentations:

- SENSE Summer Symposium "Kyoto and Beyond: A Good Climate for Responding to Climate Change?", Biocatalyzed Electrolysis: A new route for sustainable hydrogen production from wastewaters, 23 June 2005, Ede, The Netherlands.
- International Bio-hydrogen Production Technology Forum, Biocatalyzed Electrolysis: A breakthrough technology for hydrogen production from wastewaters, 14 - 15 January 2006, Harbin, China.
- Workshop on Mixed Culture Biotechnology (MCB) for production of chemicals and energy, Biocatalyzed Electrolysis: A breakthrough technology for hydrogen production from wastewaters, 12 - 13 June 2006, Delft, The Netherlands.
- European Symposium on Environmental Biotechnology (ESEB), Biocatalyzed Electrolysis: A breakthrough technology for hydrogen production from wastewaters, 9 - 13 July 2006, Leipzig, Germany.

Deputy director SENSE
Dr. A. van Dommelen

Cover design by Henk-Jan Berkhoff, A36, Amsterdam.
Printed by PrintPartners Ipskamp bv, Enschede.
